THE CONTRIBUTION OF THE INTRACELLULAR DOMAINS TO P2X$_1$ RECEPTOR REGULATION

**Thesis submitted for the degree of
Doctor of Philosophy
at the University of Leicester**

Hairuo Wen

January 2009

Abstract

The contribution of the intracellular domains to P2X$_1$ receptor regulation

Hairuo Wen

P2X$_1$ receptors are expressed throughout the body and contribute to a range of physiological process, e.g. thrombosis and smooth muscle tone. The intracellular terminals of the P2X$_1$ receptor have been shown to be involved in channel regulation. The aim of this thesis was to explore the contribution of the intracellular amino and carboxy termini to channel regulation, using concatenation, site-directed mutagenesis and biochemical methods. Trimeric concatenated P2X$_1$ receptors were non-functional.The interactions between the intracellular termini were revealed to be essential for subunit aggregation and channel expression. Subsequently, over 30 cysteine point mutations at both the amino and carboxy domains of the P2X$_1$ receptors were generated and examined by electrophysiological studies with methanethiosulfonate modifications. The conserved TXTXK/R at the amino terminal and the residues around the YXXXK motif at the carboxy terminal were highlighted to be important for channel gating and protein trafficking. Residues close to the P2X$_1$ channel pore were shown to be essential in ion conduction and implied interactions between the conserved regulatory motifs and the channel pore of adjacent residues. Roles of the intracellular domains of P2X$_1$ receptor in regulation by protein kinase were revealed by co-expression of minigenes encoding the sequences of amino/carboxy terminus with WT receptors. The results indicated both amino and carboxy termini contribute to the phorbol ester PMA and GPCR mediated response regulations, and demonstrated the important roles of the conserved TXTXK/R motif and the residues around the YXXXK motif. This research sheds light on the possible interactions between the amino and carboxy termini to P2X$_1$ receptor function. The results will be useful for understanding the intracellular topology and signaling modulation mechanism of P2X$_1$ receptor.

Acknowledgement

It was a completely coincident for me to do a research project in P2X receptor. When I completed my lecture-based modules of the Master course in Molecular Genetics, I had little prior lab experience and no knowledge to the purinergic receptors at all. At that time, I was looking for a project while Richard's research proposal was left unattended in the mailbox of my course convenor. However, being a project student in Richard's lab turned out to be an amazing turning point in my life and became the beginning of my PhD study in Pharmacology. This invaluable lab experience and thesis writing practices enabled me to be confident with all kinds of trouble-shooting in research and daily life, and discovered my potential as an independent researcher. It also allowed me a memorable and pleasurable working experience with such kind scientists. I would express my gratitude to all the support I received from following people; I would have never finished this thesis without their generous help.

First of all, I would like to thank my supervisor Prof. Richard Evans, who was always encouraging me throughout these years. Thank Richard for his logical writing methods and smart presentation skills, the well-planned working schedule, "thinking-before-doing" methodology as well as the mysterious electrophysiological techniques those not only emphasized my capability but also the confidence to future career.

Special thanks go to Dr. Catherine Vial, for all of the molecular biological techniques and all kinds of support since my first day in laboratory, for the diligent working attitude, for her care and consideration to my personal life, for her encouragement and also the enjoyable sharing in manga and French learning.

I would deeply thank Dr. Jonathan Roberts for always being patient, clear and effective in all kinds of technical and non-technical problem solving.

Thanks to Dr. Ulya Lalo for her sense of humor and the hands in cell culture and patch clamp recording.

Thanks to Dr. Rebecca Allsopp for her kindness and creating a pleasant lab atmosphere.

Thanks to Ms Amelia Atterbury-Thomas and Miss Marie Valente for making everything convenient and organized.

And everyone else for enjoying me from details.

Finally, I am indebted to my parents Di Wen and Yamei Xu too much, and therefore devote this thesis to them for everything.

Abbreviations

5-HT	5-hyroxytryptamine
ABC transporter	ATP-binding cassette transporters
ADP	Adenosine diphosphate
AFM	Atomic force microscope
AMP	Adenosine monophosphate
ApnA	Diadenosine polyphosphates
ASICs	Acid-sensing ion channels
ATP	Adenosine-5'-triphosphate
BAPTA/AM	Bis(*o*-aminophenoxy)ethane-*N,N,N′,N′*-tetra-acetic acid tetrakis-(acetoxymethyl ester)
BN-PAGE	Blue native polyacrylamide gel electrophoresis
BzATP	3'-O-(4-benzoyl)benzoyl adenosine 5'-triphosphate
CDK5	Cyclin-dependent protein kinase 5
CIAP	Calf intestinal alkaline phosphatase
CMV	Cytomegalovirus
CNS	Central nervous system
DAG	Diacylglycerol
DDS	Disuccinimidyl suberate
DMSO	Dimethyl sulfoxide
DNA	Deoxyribonucleic acid
DSS	Disuccinimidyl suberate
DTT	Dithiothreitol
EC$_{50}$	Half maximal effective concentration
ECL	Electrogenerated chemiluminescence
EDTA	Ethylenediaminetetraacetic Acid
ENaC	Epithelial sodium channel
ER	Endoplasmic reticulum
FRET	Fluorescence resonance energy transfer
GDP	Guanosine-5'-diphosphate
GPCRs	G-protein coupled receptors
G-protein	Guanosine nucleotide binding protein

GTP	Guanosine 5'-triphosphate
HEK	Human embryonic kidney
IC$_{50}$	Half maximal inhibitory concentration
IL-1β	Interleukin-1β
Kir	Inward retifying potassium channel
KO	Knockout
LGICs	Ligand-gated ion channels
mGluRIα	Metabotropic glutamate receptor Iα
MRS2220	Cyclic pyridoxine-α4,5-monophosphate-6-azo-phenyl-2',5'disulfonate
MTS	Methanethiosulfonate
MTSB	Butyl methanethiosulfonate
MTSEA	(2-aminoethyl)methanethiosulfonate
MTSES	Sodium (2-sulfonatoethyl) methanethiosulfonate
MTSET	(2-(Trimethylammonium)ethyl methanethiosulfonate, Bromide)
MTSM	Methyl methanethiolsulfonate
nAChR	Nicotinic acetylcholine receptors
NF023	8,8′-(Carbonylbis(imino-3,1-phenylene carbonylimino)bis(1,3,5-naphthalenetrisulfonic) acid)
NF279	8,8'-(Carbonylbis(imino-4, 1-phenylenecarbonylimino-4,1-phenylenecarbonylimino)) bis(1,3,5-naphthalenetrisul fonic acid)
NF449	4,4',4'',4'''-(Carbonylbis(imino-5,1,3-benzenetriylbis(carbonylimino)))
NMDA	N-methyl-D-aspartic acid
NMDG$^+$	N-methyl- D-glucamine
OD	Optical density
P2X	Purinoceptors 2X
P2Y	Purinoceptors 2Y
PCR	Polymerase chain reactions
PI(4,5)P2	Inositol phospholipid phosphatidylinositol 4,5-bisphosphate
PKA	Protein kinase A
PKC	Protein kinase C
PLC	Phospholipase C
PMA	Phorbol-12-myristate-13-acetate
PPADS	Pyridoxal-phosphate-6-azophenyl-2', 4'-disulfonate
PSIPRED	Protein Structure Prediction Server
PTK	Protein tyrosine kinase

RNA	Ribonucleic acid
SCAM	Substituted cysteine accessibility method
SDS-PAGE	Sodium dodecyl sulfate polyacrylamide gel electrophoresis
TMA-Cl	N-[2-(trimethylammonium) ethyl] maleimide chloride
TMs	Transmembrane segments/domains
TNP-ATP	[2'(3')-O-(2,4,6-Trinitrophenyl)adenosine 5'-triphosphate]
TRPV1	Transient receptor potential cation channel, subfamily V, member 1
UDP	Uridine diphosphate
UTP	Uridine 5'- triphosphate
Vrev	Reversal potential
WT	Wild type
α,β-meATP	α,β-methylene ATP

Table of contents

Chapter 1. Introduction

General introduction

Receptors are proteins inside or on the surface of cells that bind to specific molecules and initiate physiological effects (Rang, 1999). The concept of receptors had been envisaged earlier than 1900. A mutual antagonism between pilocarpine and atropine was shown by Langley in experiments on cat salivary gland in 1878 (Langley, 1878). He subsequently proposed a physiological substance that can help these two chemicals combine with each other, and the action of these chemicals depend on their affinity to the cell (Langley, 1878). It was the first evidence for the existence of receptors. Nowadays, a large number of receptors have been identified, and they can be divided into four major types: ligand-gated ion channels, G protein-coupled receptors, kinase-linked receptors and intracellular receptors that regulate DNA transcription (Rang, 1999).

It was Burnstock who first suggested the novel concept of purinoceptors for nucleotide molecules in 1972 (Burnstock, 1972). The purinoceptors are divided into P1 receptors for adenosine and P2 receptors for nucleotides, and P2X receptors are one of the subtypes of the P2 family (Burnstock, 1978). The P2X receptor family is involved in a wide range of physiological roles including smooth muscle contraction, blood clotting, bone formation, pain as well as irritable bowel syndrome, and the receptors may provide novel therapeutic targets. Studies on P2X receptors will enable a better understanding of the structure and channel regulation of these receptors.

1.1 History of adenosine triphosphate (ATP)

Adenosine 5'-triphosphate (ATP) was first isolated from muscle and liver extracts in 1929 (Lohmann, 1929; Fiske *et al*, 1929), and its structure was confirmed 20 years later by chemical synthesis (Baddiley *et al*, 1949). ATP, is made of an adenine base, a ribose sugar and a chain of three phosphate groups (Figure 1.1)

.
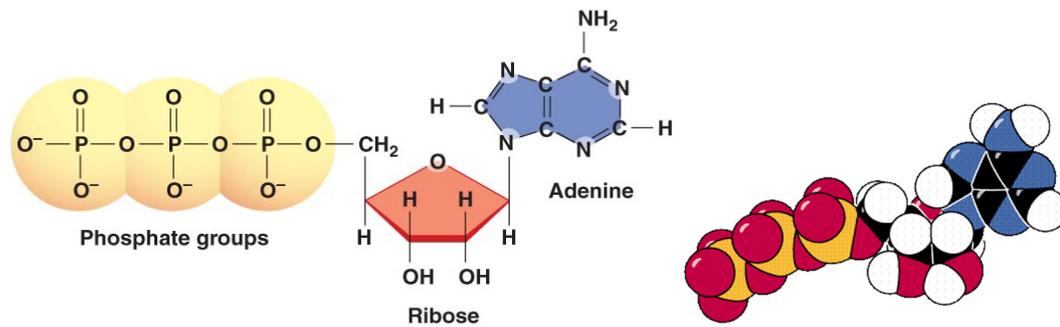
Figure 1.1 Structure of ATP molecule
ATP is composed of one adenine molecule (blue), joined with one ribose molecule (red) and three phosphate groups (yellow). The high energy covalent bonds are between the second and third phosphates.

ATP is most commonly considered as an energy reservoir, which releases energy during the hydrolysis of its high energy covalent bonds. It was in 1929, that Drury and Szent-Gyorgyi first described the physiological roles of extracellular adenine compounds in muscular contraction in the heart, blood vessels and intestinal smooth muscle (Drury *et al*, 1929). Subsequently, a number of non-cardiovascular effects were revealed in bladder, vagina, gut and other visceral organs (Burnstock, 1970; Burnstock, 1972). Holton *et al* first suggested that ATP may play a neurotransmitter role for the vasodilator action of spinal root extracts (Holton *et al*, 1954). An absorbance spectrum study indicated the existence of ATP in the nervous system, and when ATP or adenosine diphosphate (ADP) was injected, prolonged vasodilatation was observed. In 1959, Holton further suggested that nerves were the source of the ATP, and ATP can be liberated from the nerve terminal of great auricular nerve in response to both mechanical and electrical stimulation (Holton, 1959). The functions of ATP in a range of nervous tissues were subsequently reported. The roles of ATP had been first suggested as a chemical energy supply for membrane permeability maintenance (Caldwell *et al*, 1957) and binding to noradrenaline in sympathetic nerves (Schumann, 1958). It has been accepted that ATP acts on many different types of receptors and plays important roles as a transmitter or co-transmitter in both the central and peripheral nervous system (Unsworth *et al*, 1990; Salgado *et al*, 2000).

Storage and action of cellular ATP
ATP can be synthesised in nerve terminals by glycolysis and stored in the cytoplasm (Sperlagh *et al*, 1996). The cellular ATP is stored in types of synaptic vesicles as well as the cytoplasmic and mitochondrial stores. ATP as a source of chemical energy can act

as a co-factor in a range of physiological processes, including muscle contraction (Davies, 1963). In addition, it has been shown to be a neurotransmitter in the nervous sytem and can be co-released with acetylcholine (Salgado et al, 2000), GABA (Jo et al, 1999) and substance P (Sladek et al, 2001). Furthermore, ATP is an essential energy source for the Na^+/K^+ ATPase, H^+ ATPase and the Ca^{2+} ATPase for maintaining the resting potential of the cell membrane, proton gradient and Ca^{2+} balancing (Sperlágh et al, 1996). Other uses include exocytosis, providing a phosphate source for protein kinases, guanosine 5'-triphosphate (GTP) synthesis and G-protein activity.

Sources of extracellular ATP

Sylvester Vizi made a profound contribution to establish the ATP release mechanism from both neuronal (Vizi et al, 1988; Sperlagh et al, 1991; Vizi et al, 1997) and non-neuronal cells (Vizi et al, 1992), and abundant evidence suggests the ATP is synthesised, stored by central and peripheral nervous systems and released in response to depolarisation. A rise in extracellular ATP can be accomplished by three mechanisms (Bodin et al, 2001): (i) Cell death or membrane damage leading to millimolar levels of ATP release from cells, (ii) Released through vesicles from nerve terminals or non-neuronal cells upon stimulation, (iii) Activation of ATP-binding cassette transporters (ABC transporters) proteins. Hence, the ATP molecules can be released from neurons, platelets, broken cells or cells under sheer stress. However, once it is released into the extracellular environment, it can be broken down to ADP by ectoATPase.

1.2 Purinergic receptors

The concept of purinoceptors for ATP was proposed by Burnstock in 1972 to describe a group of non-adrenergic and non-cholinergic responses (Burnstock, 1972). Burnstock found the existence of an unidentified resistant response, when the adrenergic and cholinergic responses were blocked by guanethidine and atropine respectively during the investigation of nerve evoked responses of the taenia coli of the guinea pig (Burnstock, 1972). Since this response can be mimicked following ATP stimulation, he suggested the term purinergic to describe the transmission via nucleotide molecules. Burnstock subsequently proposed purinoceptors could be divided into two classes (Burnstock, 1978). This division was based on their relative potencies of ATP, ADP, adenosine monophosphate (AMP) and adenosine, the selective antagonism by

methylxanthines, the activation of adenylate cyclase and the stimulation of prostaglandin synthesis by ATP and ADP (Burnstock *et al*, 1985). However, the current characterization was accorded to their molecular structures, effector systems, pharmacological profiles and tissue distributions (Abbracchio *et al*, 1994) (Figure 1.2). Adenosine receptors (A_1, A_{2A}, A_{2B} and A_3) which are sensitive to adenosine and AMP mediate their effects by adenylyl cyclase and constitute the P1 group; while the P2 group refers to those that tend to be activated by ATP and ADP. Furthermore, the P2 group can be subdivided into two main subtypes P2X and P2Y receptors (Abbracchio *et al*., 1994).
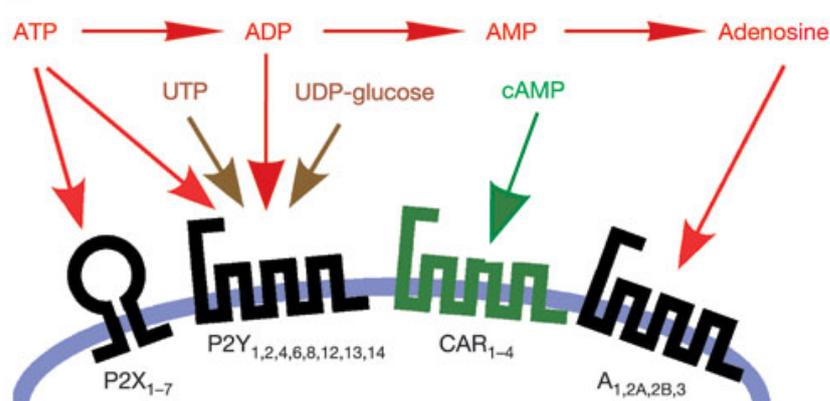
Figure 1.2 The purinocepter family
There are four members of the purinoceptors family shown in the figure above. ATP can be converted to ADP, AMP and adenosine. Nucleotides including UTP and UTPs act on the receptors for cell signalling. P2X receptors are ATP gated ion-channels, whereas the others are G protein- coupled receptors. There are four well known subtypes of P1 receptors(A_1,A_{2A},A_{2B},A_3), seven subtypes of P2X receptors ($P2X_{1-7}$), eight P2Y subtypes($P2Y_{1,2,4,6,8,12,13,14}$) in vertebrates (in black) and four cAMP receptor subtypes (CAR_{1-4}) that expressed in *Dictyostelium* (in green) (taken from Khakh *et al*, 2006).

1.3 P2Y receptors

The P2Y receptors with seven transmembrane domains belong to the G protein-coupled receptor superfamily. They are sensitive to a range of agonists including ATP, ADP, uridine 5'- triphosphate (UTP) and uridine diphosphate (UDP). The first two P2Y receptors $P2Y_1$ from embryonic chick brain and $P2Y_2$ from mouse neuroblastoma cells were cloned in 1993 (Webb *et al*, 1993; Lustig *et al*, 1993). Subsequently, $P2Y_4$, $P2Y_6$ and $P2Y_{11}$ were isolated by homology cloning. The G_i-coupled $P2Y_{12}$ receptor was not identified until 2001 by expression cloning (Hollopeter *et al*, 2001), and the $P2Y_{13}$, and $P2Y_{14}$ were isolated during a systematic study of orphan receptors (Chambers *et al*, 2000; Communi *et al*, 2001). Currently, eight human P2Y receptors ($P2Y_{1,2,4,6,11,12,13 \text{ and } 14}$) have been identified, and the missing numbers refer to the ones either having no function to nucleotides or non-mammalian orthologs.

The P2Y receptors range from 308 to 377 amino acids long with a mass of ~41 to 53 kDa following glycosylation. As members of the G protein-coupled receptor family, the P2Y receptors share a topology of seven transmembrane domains with an extracellular N-terminus and an intracellular C-terminus (See figure 1.3). Studies to identify the agonist binding site have shown that transmembrane regions 6 and 7 act as a binding dock for the phosphate groups of purines and pyrimidines (Erb *et al*, 1995), while important residues in the transmembrane domains 3 and 7 are considered for ATP binding on human $P2Y_1$ receptors (Jiang *et al*, 1997). The conserved binding motif H-X-X-R/K in the eight subtypes is located in the sixth transmembrane domain, while the $P2Y_{1,2,4,6 \text{ and } 11}$ share a Y-Q/K-X-X-R motif in the seventh transmembrane domain, the $P2Y_{12,13 \text{ and } 14}$ share another K-E-X-X-L motif (Abbracchio *et al*, 2003).

P2Y receptors are widely distributed in the heart, vascular system, brain and the immune system. The $P2Y_1$ receptor was studied by selective antagonists and knockout mice and was suggested to be involved in platelet aggregation (Hechler, 2005).The $P2Y_{12}$ receptor is mostly expressed in platelets and considered as a therapeutic target of the active metabolite in anti-thrombotic treatment (Savi *et al*, 2005). Functional $P2Y_2$ receptors are expressed in smooth muscle, epithelial, leukocytes, osteoblasts, cardiomyocytes and nervous system, and several lines of evidence have implied roles of the $P2Y_2$ receptor in the regulation of epithelial transmembrane transport, bone formation and neuroprotection (Abbracchio *et al*, 2003).
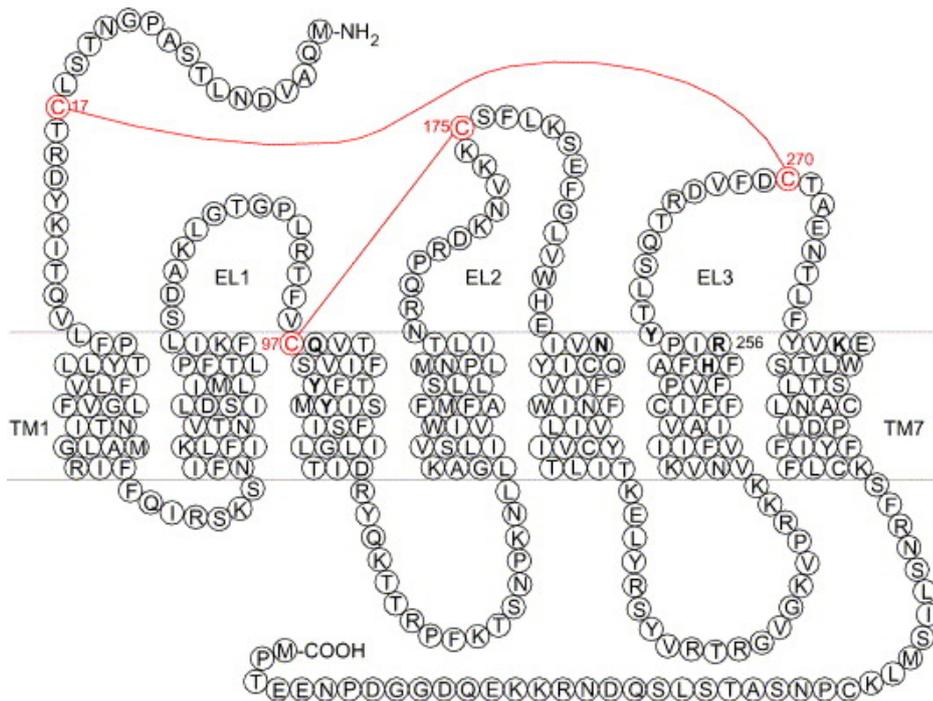
Figure 1.3 Topology of P2Y receptors
This figure is showing a predicted amino acid sequence and topology of the human P2Y$_{12}$ receptor. It is a G-protein coupled receptor with seven transmembrane domains, an extracellular amino terminus and an intracellular carboxy terminus. The nucleotide binding sites are shown in bold circles with highlighted letters. The red lines show predicted disulfide bridges (taken from von Kugelgen, 2005).

1.4 P2X receptors

By contrast to other purinergic receptors, the P2X receptors are ligand-gated ion channels and open in the millisecond range in response to the binding of extracellular ATP (Burnstock, 1996a; North, 2002). Initial research indicated that the P2X receptors are ligand-gated ion channels based on the receptor kinetics. P2X receptors activated by ATP and show a preferable permeability to calcium. The activation of P2X receptors on rabbit arterial smooth muscle can induce the influx of Na$^+$ and Ca^{2+} (Benham, 1987). Another study on rat vas deferens smooth muscle also demonstrated an ATP-induced current when voltage-gated Ca^{2+} and K$^+$ currents were eliminated, and this conductance was cation selective (Nakazawa *et al*, 1987).

The P2X ligand-gated channels were cloned since 1994, the P2X$_1$ and P2X$_2$ subunits were the first ones of the P2X family isolated by expression cloning. The cDNA encoding the P2X$_1$ receptor sequence was cloned from rat vas deferens (Valera *et al*, 1994), and the P2X$_2$ receptor sequence was obtained from the PC12 rat pheochromocytoma cells (Brake *et al*, 1994). Subsequently, five other subtypes of the P2X receptors were identified by homology and PCR strategies. The P2X$_3$ receptor was

isolated from dorsal root ganglia and it was the first one found to be expressed in sensory neurons (Chen *et al*, 1995). The cDNA of the rat $P2X_4$ subunit was first extracted from hippocampus (Bo *et al*, 1995), the rat $P2X_5$ subunit was isolated from celiac ganglia (Collo *et al*, 1996), and the rat $P2X_6$ subunit was cloned from superior cervical ganglia (Collo *et al*, 1996). The $P2X_7$ subunit was the last one identified, and the cDNA was cloned from the rat superior cervical ganglia (Surprenant *et al*, 1996).

Seven subtypes of the P2X receptors have been identified. The cDNAs vary from 40 kb for the largest one (mouse $P2X_3$ subunit) to 1.2 kb of the smallest (human $P2X_6$ subunit) and share 26 to 47 percent homology at the gene level. The sequence of $P2X_7$ is the longest one with the least similarity to the other P2X subunits (North, 2002). The proteins of the P2X family range from 384 ($P2X_4$) to 595 ($P2X_7$) amino acids long and share 40 to 55% identity (North, 2002). $P2X_4$ and $P2X_7$ subunits share the most number of conserved amino acids ($\sim$49%). These genes are next to each other on the chromosome (North *et al*, 2002). In addition, a range of mammalian P2X receptor splice variant sequences were identified (North, 2002). For example, there is a rat $P2X_2$ receptor splice variant with shortened carboxy terminus where 69 amino acids from Val^{370} to Gln^{438} are missing (Brandle *et al*, 1997). In a recent published study, a truncated $P2X_7$ receptor variant missing the entire intracellular carboxy terminus was found to be expressed in cervical cancer cells (Feng *et al*, 2006).

1.5 Basic structure of P2X receptors
1.5.1 Topology

The membrane topology model of P2X receptors was initially predicted from hydrophobicity plots (North, 1996). These use a computer algorithm to quantitatively analyze primary amino acid sequences, the hydrophobic and hydrophilic region of the sequences can be predicted based on the nature of the amino acids. For a transmembrane domain with an alpha-helix, 20-25 hydrophobic amino acids are required. The two hydrophobic regions of P2X receptors are about 20 amino acids long, and this indicates that two regions could form transmembrane domains across the lipid bilayer. Analysis of the sequence also showed that there is no leader signal peptide sequence found on the N-terminal sequence. This taken together with the two transmembrane domains indicated that both the amino and carboxy termini of the P2X receptor are intracellular (Brake *et al*, 1994; Soto *et al*, 1997). This suggests a topology

of P2X receptors with two tramsmembrane segments (TMs) which are separated by an extracellular loop and the amino and carboxy termini are located intracellularly (Figure 1.4).The distribution of hydrophilic and hydrophobic domains are similar among the seven subtypes (North, 2002). Subsequent studies suggested three other major lines of evidence that have confirmed the membrane topology.
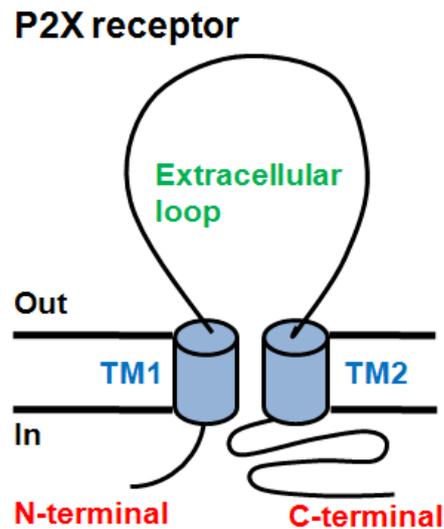
Figure1. 4 The topology model of P2X receptors
P2X receptors as novel cation selective channels have been defined with a large extracellular loop (green) for ligand binding, two transmembrane domains (blue) and intracellular amino and carboxy termini (red).

(i). An antibody against the C-terminus of the P2X receptor was developed (Vulchanova *et al*, 1997; Torres *et al*, 1998a). Successful immunohistochemical detection of the receptor was only seen when tissues were permeabilized demonstrating that the C-terminal epitope was intracellular.

(ii). Mutagenesis studies of the proposed extracellular loop showed residues involved in drug action consistent with its binding "outside" the cell. For instance, point mutations at Lys^{68} and Lys^{309} in the extracellular domain affect ATP potency (Ennion *et al*, 2000). In addition, Buell suggested that the substitution of Glu^{249} to lysine influenced the binding of the extracellular antagonist pyridoxal-phosphate-6-azophenyl-2', 4'-disulfonate (PPADS), and this result further indicated the loop is related to the extracellular binding (Buell *et al*, 1996).

(iii). During the post-translational modification process, a sugar chain can be attached to the N-X-S/T sequence within the endoplasmic reticulum. The N-glycosylation of proteins only happens on the surface of extracellular domains and relates to protein folding. Newbolt and colleagues pretreated the $P2X_2$ receptor with endoglycosidase H to remove glycoslation, and a reduction of molecular mass was observed (Newbolt *et al*, 1998).The sites of glycosylation were identified by mutagenesis and shown at the asparagines Asn^{182}, Asn^{239} and Asn^{298} of $P2X_2$ receptor, this indicated that the region that can be glycoslyated is located in the central domain. Hence, the loop in the middle of P2X receptor protein sequences should be extracellular.

In addition, N-glycosylation modification is associated with maintaining channel properties. As described previously, all of the subtypes have consensus sequences for Asn-linked glycosylation, for example, there are four in the $P2X_1$ receptor and three such sites in the $P2X_2$ receptor (North, 2002). Rettinger *et al* tried to remove individual N-glycosylation sites by mutagenesis at the $P2X_1$ receptor. These experiments not only influenced the glycosylation, but also disrupted the function of the $P2X_1$ receptor. It was shown that at least one N-glycosylation per subunit is necessary for the assembly of $P2X_1$ receptors and elimination of residue Asn^{210} reduced ATP potency by 3 fold (Rettinger *et al*, 2000). The mutations on the consensus sites of glycosylation Asn^{153}, Asn^{242} and Asn^{300} of human $P2X_1$ receptors showed no obvious effects to the channel properties (Roberts *et al*, 2005), which is consistent with the finding at rat $P2X_1$ and $P2X_2$ receptors (Rettinger *et al*, 2000; Newbolt *et al*, 1998). Whereas, the alanine mutation on the most conserved glycosylation site Asn^{184} produced a decrease in ATP potency (Roberts *et al*, 2005).

1.5.2 Contribution of defined regions to P2X receptor function
Molecular studies have highlighted the roles of important domains for channel properties, these functional regions will be described in detail.

1.5.2.1 Intracellular domains
N-terminus
Among the different P2X subtypes, the length of the amino termini are less than 30 amino acids. Although the lengths are similar, there are some variations in the sequence (Dunn *et al*, 2001; North, 2002). There is a conserved protein kinase motif (Thr^{18}-Xaa^{19}-Arg/Lys^{20}) on the N-terminus. Mutations at this site suggested it is

involved in regulation of the time-course, as mutation of this sequence leads to the speeding of channel desensitization (Boue-Grabot et al, 2000 and Ennion et al, 2002a) (See figure 1.4). The T18A mutant of the $P2X_1$ receptor resulted in approximately 10 fold faster desensitization to ATP. This mutation also provided fast desensitization in heteromeric $P2X_1$ channels with wild type or the K68A mutant which is slowly desensitizing and suggested a dominant role of T18A in control of the desensitizing phenotype. For the $P2X_1$ receptor, the mutations T18N and K20T also exhibited quick desensitization (Ennion et al, 2002a). Hence, the N-terminal of P2X receptors was considered associated with desensitization. Furthermore, once the C-terminal was truncated, the slow desensitization pattern at $P2X_2$ receptor was removed. However, this was recovered by phorbol ester which acts on the PKC sites at the amino terminal (Boue-Grabot et al, 2000). Combining the results of the $P2X_1$ and $P2X_2$ receptors, it suggested that channel regulation may be facilitated by intracellular phosphorylation or dephosphorylation. Vial et al showed the $P2X_1$ receptor can be potentiated by phorbol ester and GPCRs, and it is interesting that the potentiation was still shown when the consensus PKC site was disrupted (Vial et al, 2004a). However, no direct phosphorylation can be observed in the intracellular domains, and this regulation may be associated with accessory proteins rather than in a direct way. Similar results have been shown on the $P2X_3$ receptor as well (Paukert et al, 2001). (See chapter 7 for more details).

The amino terminal of the $P2X_2$ receptor was studied by the substituted cysteine accessibility method (SCAM, refer to chapter 4 for details) and suggested to contribute to channel gating properties (Jiang et al, 2001). The cysteine mutation affected the basic properties on residues Asp^{15}, Pro^{19}, Val^{23} and Val^{24} where the disruptions led to a shift in ATP potency (from 1 to 3-10 μM for EC_{50}) (Jiang et al, 2001). In addition, methyl methanethiolsulfonate (MTSM) application blocked the currents at P19C, V23C and V24C and suggested these residues have roles in channel permeation (Jiang et al, 2001). For more details see chapter 5 about the roles of amino terminus residues.

C-terminus

Although the lengths of the carboxy termini differ greatly from 25 amino acids in $P2X_6$ to 240 amino acids in $P2X_7$, there are still a number of conserved serine, threonine and tyrosine residues in this region (Dunn et al, 2001; North, 2002). The hydroxyl group of

these residues can be potential phosphorylation sites on the $P2X_1$ receptor (Vial *et al*, 2004a).   In addition, there is a completely conserved YXXXK motif on the C-termini, which relates to protein trafficking and facilitates the stabilization of the $P2X_2$ receptor (Chaumont *et al*, 2004). Mutation in this motif resulted in a great reduction in receptor expression at the plasma membrane because of rapid internalization. The C-terminal may also regulate channel pore dilation at the P2X receptor. Take the $P2X_2$ receptor for example, splicing variants and mutants (residue 401-439) of the C-termini can vary the diameter of the channel pore from 11 Å to at least 14 Å during the Na^+-selective state transition (Eickhorst *et al*, 2002). For more details on C-terminus refer to chapter 6.

1.5.2.2 Transmembrane segments

There are two transmembrane segments in the P2X receptor; they are the hydrophobic regions that are close to each other in the plasma membrane (Jiang *et al*, 2003).   Take the $P2X_2$ receptor for example, its first transmembrane segment extends from amino acid 30 to 50 and the second one extends from residues 330 to 353. There is no significant difference among the lengths of the transmembrane domains of the different subtypes (North, 1996) (Figure 1.5).

The TMs were considered to play an important role in the time-course of response. Chimeric $P2X_1$ and $P2X_2$ subunits were produced by swapping the transmembrane domains (Werner *et al*, 1996). The $P2X_1$ receptors exhibit fast desensitization, while the $P2X_2$ receptors desensitize slowly. The chimeras revealed that both of the transmembrane domains of the $P2X_1$ receptor were necessary for the fast desensitization in the $P2X_2$ subunit chimera. In contrast, either of the $P2X_2$ receptor transmembrane domains could confer slow desensitization to the $P2X_1$ receptor. These results suggest the essential role of the transmembrane domains of the response to ATP. Another study on $P2X_{1/2}$ chimeras suggested that the TM1 is important for agonist operations (Haines *et al*, 2001). It was shown that the α,β-methylene ATP (α,β-meATP) sensitivity can be conferred to the rat $P2X_2$ receptor after the replacement of the TM1 from the α,β-meATP sensitive $P2X_1$ or $P2X_3$ subunit. However, these chimeras' antagonist sensitivities remained the same as the wild type rat $P2X_2$ receptor. In addition, the transmembrane segments of P2X receptors were predicted to contribute to pore formation. Contribution of the transmembrane segments to channel pore lining of P2X

receptors was determined by substituted cysteine accessibility method (SCAM, refer to chapter 4 for details) or other mutagenesis approaches.

SCAM has been a powerful approach to determine the pore forming regions of the transmembrane domains. Take the Kv2.1 channel for instance (Pascual *et al*, 1995), the carboxy half of the pore-forming region was substituted by individual cysteines. Residues 374 and 378 were identified at the inner and outer mouths of the channel. The residues throughout the TM2 region of P2X$_2$ receptor were replaced individually by cysteine and studied by SCAM. Methanethiosulfonate (MTS) reagents can introduce different sizes of side groups to estimate the accessibility at narrow locations (See chapter 4 for details). ATP evoked currents at the mutants I328C, N333C, T336C were inhibited by MTS compounds, which indicated the binding of MTS at these locations and blocked the ion influx. These residues may line the outer vestibule of the pore (Egan *et al*, 1998) (Figure 1.5). The I328C mutant can be modulated in the absence of ATP and was suggested to be at the outer layer of the channel pore. Whereas, the mutations L334C, S345C, L352C and L353C fail to react with MTS reagents were suggested to be inside of the vestibule (Egan *et al*, 1998) (Figure 1.5). Two other substitutions L338C and D349C on the TM2 segments showed inhibition only when the smaller ethylamine derivative was applied. The L338C mutant currents can be inhibited by MTS reagents whether or not the channel was opened by ATP, while the D349C was inhibited by MTS reagents only when the ATP was applied. Therefore the residues Lys^{338} and Asp^{349} are likely to be either side of the ionic gate (Egan *et al*, 1998; Rassendren *et al*, 1997). This suggested that the TM2 formed part of pore of the P2X$_2$ receptor.
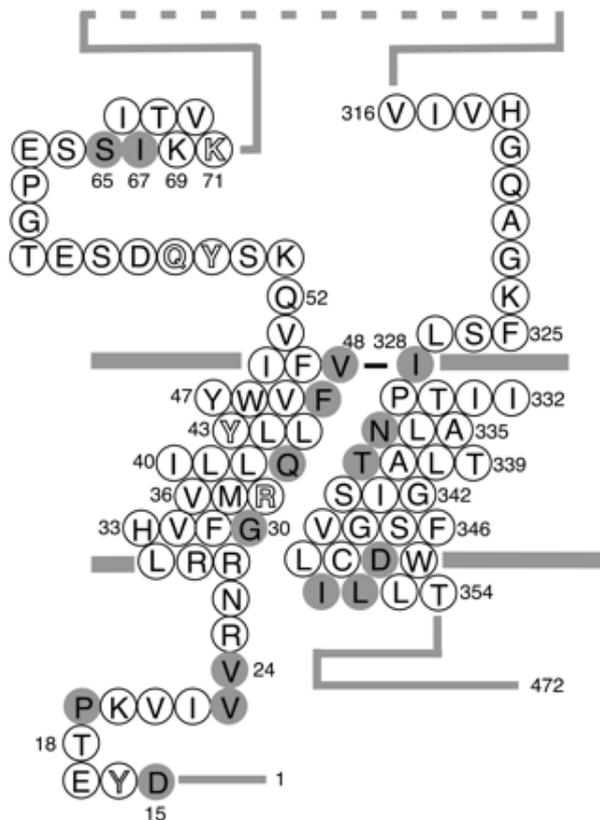
Figure 1.5 Schematic summary of mutagenesis on residues of P2X$_2$ receptor transmembrane domains.
Both of the transmembrane domains were studied by cysteine substitutions on rat P2X$_2$ receptors. Outline letters (Y^{16}, R^{34}, Y^{43}, Q^{56} and K^{71}) indicate those positions where no functional channels were expressed. Solid gray circles indicate those positions where a MTS inhibited the current (including membrane-permeable MTS). The line between V^{48} and I^{328} indicates the disulfide bond that forms when both residues are substituted by cysteine (Taken from North, 2002).

Alanine is a neutral small amino acid and suitable for investigating the transmembrane domains and the 24 residues in TM2 of P2X$_2$ receptor were studied by alanine scanning. Nine mutants in this segment (I328A, P328A, N333A, L338A, T339A, S340A, G342A, G344A and S345A) resulted in changes in potency, and the results further confirmed TM2 was involved in the formation of the channel pore (Li *et al*, 2004).

The first transmembrane segment (TM1) of the P2X$_2$ receptor was studied by alanine mutagenesis. Seven (H22A, Q37A, I40A, L41A, Y43A, F44A and I50A) out of the 22 mutants in the TM1 produced channels with altered agonist potencies (Li *et al*, 2004), and these seven mutated residues may be part of the channel pore. In addition, these sensitive residues were separated by two inaccessible residues and suggested a helical secondary structure of this region. The mutants V45A, Y47A and V51A of P2X$_2$ receptors failed to respond to ATP, while Y43A and F44A were active without the

agonist (Li *et al*, 2004). These five residues may relate to channel gating. Moreover, Jiang studied TM1 by cysteine scanning mutagensis and found the residue Val[48] at the outer end of the first hydrophobic segment was an essential component of channel gating and residue Phe[44] seems associated with channel conformation (Jiang *et al*, 2001).

In a recent study, cysteines were introduced to the two transmembrane segments at P2X$_2$ receptors to look at the rates of modification by MTS reagents (Li *et al*, 2008). At TM1, only V48C showed accessibility to 2-(trimethylammonium) ethyl methanethiosulfonate bromide (MTSET), and the modification of MTSET resulted in a reduction in current and marked slowing of channel closing. However, this modification rate was rather modest and implied the residue is not readily accessible to MTSET. By contrast, the eight mutants at TM2 showed significant changes to MTSET for T336C and this was suggested to be a gate in the external region of TM2. The TM2 therefore showed a central role in ion-conduction pathway, whereas TM1 did not make substantial contributions.

1.5.2.3 Extracellular domain

The extracellular loop that is responsible for agonist binding of the P2X receptor connects the two transmembrane domains and is about 280 amino acids long. Although the modifications of the binding loop are diverse among different subtypes, 93 out of these residues are conserved in at least six P2X family members (Vial *et al*, 2004b) (See figure 1.6). As P2X receptors have little structural similarity to other ATP binding proteins (e.g. ABC transporter family) and the absence of the common nucleotide binding sequences such as the Walker motif A (GXXXXGKT/S) (Walker *et al*, 1982), site-directed mutagenesis was used to investigate the structure and function of P2X receptors. The replacement of key conserved or important residues may cause changes in the properties of the receptors, and some critical regions involved in specific roles have been probed. In the cases where the modifications had no effects, suggested the corresponding residues are not important for maintaining the receptor function. The residues that contribute to the ATP binding model will be described in the following section, as well as the structural residues and ones involved in ionic regulation and subunit interactions will be described subsequently. At the end, the currently proposed ATP binding pocket of P2X receptors will be briefly summarized.

Figure 1.6 Summary of mutagenesis studies on the P2X₁ receptor
The extracellular domain and parts of the adjacent transmembrane domains of human P2X₁ receptor is shown above. The mutations on residues that had no or less than 10-fold effect on ATP potency are shown as dashed lines. Conserved residues involved in ATP potency are shown in orange and underlined. Conserved aromatic residues involved in the binding of adenine group are shown in blue. Purple residues may be responsible for the differential ATP and BzATP agonist sensitivity at P2X₇ receptor.Ten conserved cystienes are shown in bold black. The yellow residues indicate the ones are responsible for the channel regulations by ions or pH on other subunits (From Evans, 2008).

ATP binding pocket identification

Conserved positively charged residues and aromatic residues are considered to comprise the ATP binding pocket by capturing the phosphate chain and adenine group respectively. Polar residues adjacent may also contribute to the conformation changes.

Positively charged residues

The conserved positively charged amino acids in the extracellular region of P2X₁ and P2X₂ receptors have been investigated by site-directed mutagenesis (Ennion *et al*, 2000; Jiang *et al*, 2000). 11 conserved positive charges in the extracellular loop of the human P2X₁ receptor were converted to neutral (Lys to Ala, Arg to Ala) or positive residues (Lys to Arg, Arg to Lys). Modest changes in ATP potency were found on mutants K70R (20-fold decrease) and R292K/A (100-fold decrease), and a striking reduction in ATP potency was observed at K68A and K309A with an over 1400-fold decrease indicating their contribution to ATP potency (Ennion *et al*, 2000). A prolonged decay time of the P2X₁ current to ATP was also observed at the mutants K68A and K309A. However, these mutations had no effect on suramin sensitivity. The changes in decay time reflected the channel opening mechanism was influenced. Positively charged amino acids would attract the negatively charged phosphate chain of ATP, similar to the conserved lysine in the Walker A motif (GXXXXGKT/S) contributes to the phosphate chain attraction of ADP or ATP. These findings suggested that the lysine and arginine

residues close to the channel pore were considered to act in agonist binding or gating (Ennion et al, 2000). At P2X$_2$ receptors, alanine substitution mutagenesis was performed on 30 polar residues of the extracellular domain, and the residue Lys^{69} and Lys^{71} were found to be critical for ATP action (Jiang et al, 2000). Mutations resulted in no detectable current for Lys^{68}, and a 1000-fold right shift in ATP concentration-response for Lys^{71}. Thus, it was predicted that the residues Lys^{68}, Lys^{70}, Lys ^{309} and Arg ^{292} (P2X$_1$ numbering) which are close to the TM1 and TM2 respectively were essential for ATP action.

Aromatic residues

Aromatic residues can coordinate the binding of the adenine group in many ATP-binding proteins. For example, the residue Tyr^{11} in the ABC transporter was suggested to have stacking interactions with the adenine base of ATP (Smith et al, 2002). There are 20 conserved aromatic amino acids within at least six subtypes of the P2X receptors, and individual alanine replacement mutagenesis was done at the human P2X$_1$ receptor (Roberts et al, 2004). Most of the mutants had less than a six fold change in ATP potency. The ATP potency was decreased by 10-160 fold in mutants F185A and F291A. Since previous mutagenesis studies on the residues close to Phe^{185} (Lys^{190} at P2X$_1$: 5 fold; Thr^{184} and Lys^{188} at P2X$_2$: 100 fold) exhibited significant decrease in ATP potency as well, the region from residues 185 to 190 at P2X$_1$ receptor was proposed to be a FT(L/I/V)X(I/V)K ATP action motif. However, whether the shifts in ATP potency are due to the changes in agonist binding affinity or channel opening is still an issue. Ap5A and BzATP are partial agonists and also bind to and activate the P2X$_1$ receptor, but have only partial efficacy. Studies on ionotropic glutamate receptors indicated that partial agonists can control the open probability of the channel and may be able to differentiate agonist binding from channel opening (Armstrong et al, 2003). Leu^{650} was suggested to be a binding cleft residue that was conserved among AMPA receptors, however AMPA, a high-affinity full agonist to WT receptors, only acted as a partial agonist for the L650T mutant and gave partial closure of the "clamshell-shaped" ligand binding core (Armstrong et al, 2003). BzATP was an antagonist and Ap5A at the F185A mutant. The decreased activities of BzATP and Ap5A supported Phe^{185} as an important residue in ligand binding. The aromatic Phe^{291} is located within a conserved triplet Asn^{290}-Phe^{291}-Arg^{292} and is likely to have a role in ATP action (Roberts et al, 2004).

Polar residues

Polar residues are able to play important roles in hydrogen bonding and conformational stabilization. Studies have shown that the polar asparagine side chain can provide a strong thermodynamic driving force for membrane helix association (Choma *et al*, 2000). The conserved extracellular polar non-charged glutamine, asparagine and threonine residues at the $P2X_1$ receptors were substituted to alanines, and the majority of mutants had no effect on ATP potency. Mutants T186A, N204A and N290A exhibited 6-fold, 3-fold and 60-fold reductions in ATP potency respectively (Roberts *et al*, 2006). The partial agonists BzATP and Ap_5A still bind to the mutants T186A and N290A, but they cannot activate the channel anymore. Thus these polar residues may combine with the aromatic residues to contribute a pocket of Phe^{185}-Thr^{186} and Asn^{290}-Phe^{291}-Arg^{292} triplet for ATP adenine ring binding. In addition, the mutants Q95A, Q112A, Q114A and T158A showed changes in partial agonist efficacy and the corresponding residues were suggested to contribute in channel gating of $P2X_1$ receptor.

Intersubunit ATP binding site

The location of nicotinic agonists and competitive antagonist binding site for nAChR (nicotinic acetylcholine receptor) was revealed to be at the neighbouring $\alpha1/\gamma$ and $\alpha1/\delta$ subunits interfaces, and charged aromatic and acidic amino acids are involved in the nicotinic binding (Martinez *et al*, 2000). Recently a study using the cysteine cross-linking suggested that ATP binds to the receptor in between two neighbouring P2X subunits rather than intrasubunit binding (Marquez-Klaka *et al*, 2007)(See figure 1.8). The potential residues involved in ATP binding were substituted with cysteines respectively, and co-expressed in *Xenopus* oocytes in pairs. Mutants of K68C and F291C can form dimers on the non-reducing SDS-PAGE gel (sodium dodecyl sulfate polyacrylamide gel electrophoresis), and the double mutants with K68C and F291C readily forms trimers. The cross-linked subunits were able to exhibit small ATP-activated currents, and over 60 fold increased amplitudes were obtained after the application of the reducing agent dithiothreitol (DTT). Under reducing conditions, the intersubunit disulfide bridges can be dissociated and ATP can bind to activate the channel. Disulphide bond formation between the introduced cysteines was prevented in the presence of ATP, which suggested these residues are involved in ATP binding. The above results implied these two residues must be close to each other to participate in an intersubunit ATP binding site.

P2X receptor binding model

Based on the above mutagenesis study and the similarity to the ATP binding environment of rat synapsin II, an ATP binding model was proposed combining the positively charged lysine residue Lys[68], Lys[70] (involved in ATP action and contribute to the inter subunit binding site) and Lys[309] (interact with the negatively charged ATP phosphate groups), and polar and aromatic residues Phe[185], Asn[290], Phe[291] and Arg[292] (involved in adenine ring binding) (Roberts *et al*, 2007). It is likely that the ATP binding site is located between two adjacent subunits (Marquez-Klaka *et al*, 2007). The assumed P2X receptor binding model was shown as in figure 1.7.
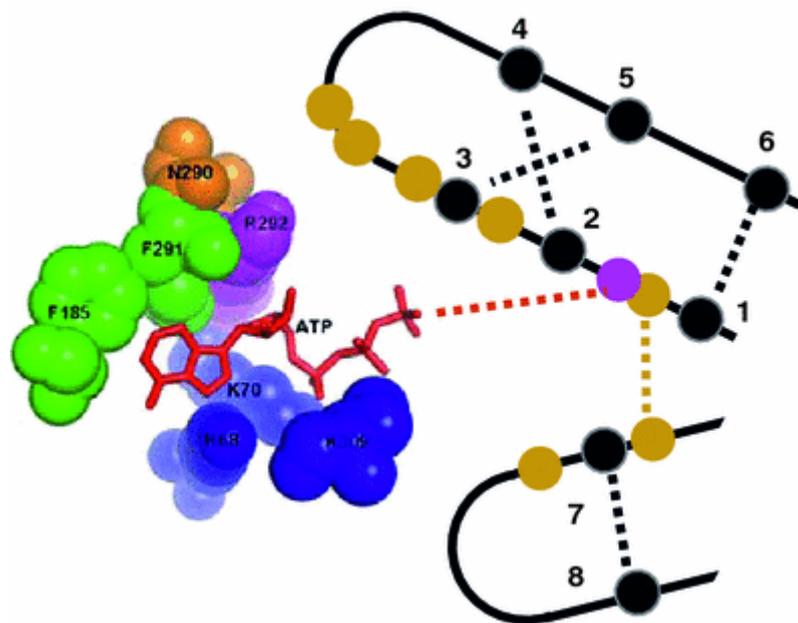
Figure 1.7 Model of ATP action at P2X$_1$ receptor
The ATP binding model was proposed from mutagenesis data and crystal structures. Positively charged lysine residues (Lys[68], Lys[70] and Lys[309]) are thought to interact with the negatively charged phosphates of ATP in the P2X$_1$ receptor, and the aromatic residue Phe[185],Phe[291]and polar residues Asn[290], Arg[292] may be involved with coordinating the binding of the adenine ring of ATP (Roberts *et al*, 2007). The residues K68 and K70 participate in the binding site (Marquez-Klakaet *et al*, 2007). The conserved cysteines are shown in black circles and the numbers are corresponding to the order in the extracellular loop. The predicated disulphide bonds are shown as black dotted lines in the pairings 1–6, 2–4, 3–5 and 7–8. The residues His[120] and His[213] are close enough to be cross-linked with cysteine substitutions (Nagaya *et al*. 2005) were shown as yellow dotted line. Other residues that are involved in allosteric regulation were shown as yellow cycles (From Evans, 2008).

Conserved structural residues

The extracellular cysteine, glycine and proline residues could also play essential roles in maintaining the tertiary structure and the protein folding of P2X receptor. These conserved residues at the extracellular binding loop of the P2X$_1$ receptor will be described as follows.

Conserved cysteine resiudes

Cysteine residues with a highly reactive sulfur group are able to form disulphide bonds spontaneously (Figure 1.8). These disulfide bonds are single covalent bonds derived from the thiol groups coupling, and connecting the two cysteines together. They may stabilize the protein folding by pulling two segments of the protein in close vicinity.
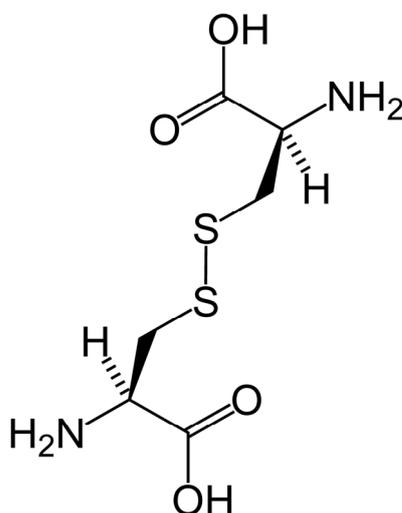
Figure 1.8 Disulfide bond forms between two cysteine residues.
The disulfide bond forms by the covalent coupling of thiol groups between cysteines (C-S-S-C). It is important for protein folding and stability and cannot tolerate a reducing environment.

The roles of extracellular cysteines have been shown to be important for secondary structure maintenance, and also protein trafficking. Cho studied two conserved cysteines in the Kir2.1 channel by replacement to either alanine or serine (Cho *et al*, 2000). The cysteine residues Cys^{122} and Cys^{143} (Kir2.1 numbering) are completely conserved in the inward rectifier potassium channels (Kir). Proper expression can still be observed after the removal of cysteine residues, while the currents in *Xenopus* oocytes were absent. Co-expression studies further suggested a single mutated subunit is enough to eliminate the normal current of Kir2.1 channels. It implied these cysteines are essential for channel function. The existence of a disulfide bond was studied by combining V8 protease digestion and western blotting under reducing condition. There

are glutamate residues present between the two cysteines, and V8 protease can specifically recognize the glutamate residues and cleave the subunit to smaller pieces. However, if the disulfide bond is present, it will link the major two fragments together and prevent digestion. After the V8 protease treatment, the wild type receptor exhibited a band with a similar size as before and indicated the presence of the disulfide linkage. This linkage can be removed by reducing reagent DTT and suggested there was a covalent bridge, and this bond did not form with the presence of mutants C122S and C154S. The overall finding indicated an intramolecular disulfide bond exists between the conserved cysteine residues which are essential in channel folding of Kir2.1.

In addition to intrasubunit linkage, disulfide bonds may also form between adjacent subunits (Lesage *et al*, 1996). The P domain (containing two pore-forming regions) of the potassium channel TWIK-1 has been studied and the size of a single subunit was estimated to be 37 kDa. However, without the presence of reducing reagents, the molecular weight of it was shown as 65 kDa which suggested that TWIK-1 can self-associate to form a dimer via a disulfide bond formation. The Cys^{69} that is situated in the extracellular loop between M1 (first transmembrane domain) and P1 (first pore-forming region) was suspected to be involved in the formation of an interchain disulfide bond. When the mutant C69S was generated and analyzed by SDS-PAGE, the usual band of 65 kDa indicating the dimer was no long detected. This indicated the contribution of Cys^{69} in the intermolecular disulfide bond formation. The function of C69S mutant was examined by electrophysiological methods and the channel activity was lost for the C69S mutant. These results clearly indicated the disulfide bridge between subunits is necessary for the stable formation of functional TWIK-1 channel.

Extracellular cysteines at P2X receptors also contribute to the channel regulation. There are ten conserved cysteines present among all known P2X mammalian subtypes as well as in *Schistosome* (Agboh *et al*, 2004). Previous studies (Nicke *et al*, 1998) demonstrated that P2X receptors can be dissociated into monomers under a variety of non-reducing conditions. Therefore, the $P2X_1$ subunits should be assembled by non-covalent interactions and the disulfide bonds, if present, should be within a single subunit.

Ennion first suggested the existence of disulfide bonds between paired cysteines at P2X$_1$ receptors by making alanine substitutions. The existence of disulfide bonds were probed by using MTSEA-biotin which specifically recognizes and forms stable bonds to any free cysteines. Since no WT P2X$_1$ receptor protein can be pulled down by MTSEA-biotin ((2-aminoethyl) methanethiosulfonate-biotin) on the SDS-PAGE gel, the cysteines at the extracellular loop of P2X receptor should form disulfide bonds in pairs, or be inaccessible. To test if the adjacent cysteine residues form disulfide bonds spontaneously, a series of double mutants were generated. When the correct pair of the disulfide linked cysteines was mutated, the MTSEA-biotinylation would be lost due to the breaking of the cysteine linkage. Surface MTSEA-biotinylation was hardly detected in all of the double mutants, and the cysteine pairs were proposed as Cys^{117}/Cys^{165}, Cys^{126}/Cys^{149}, Cys^{132}/Cys^{159}, Cys^{217}/Cys^{227} and Cys^{261}/Cys^{270} by combining the results with the ATP potency studies (See figure 1.9). The C261A and C270A mutants caused over 90% decrease in current peak amplitude and their cell-surface expressions were revealed at low level. The reduction of molecular mass from 57kDa to 54kDa of P2X$_1$ subunits were also observed on these mutants. Glycoslation at P2X$_1$ receptor increases its molecular mass (Rettinger *et al*, 2000) and is involved in the protein trafficking from ER to cell membrane. Thus, point mutations at the cysteine residues Cys^{261} and Cys^{270} could impair membrane trafficking by affecting the subunit glycoslation. Double mutations at Cys^{117} and Cys^{165} did not produce functional responses and exhibited low surface expression. This indicated the disulfide bond between Cys^{117} and Cys^{165} is essential for maintaining the protein trafficking.
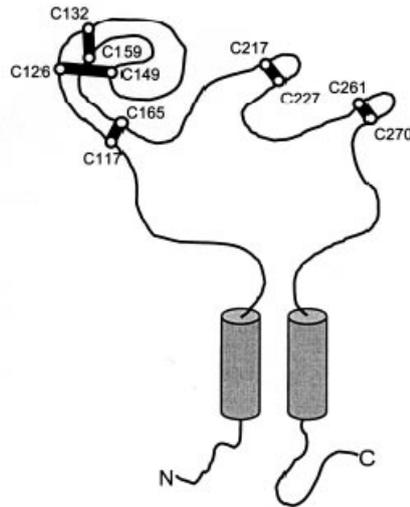
Figure 1.9 Proposed disulfide bonds between paired cysteines at P2X$_1$ receptor
There are ten conserved cysteines present on the extracellular loop of the P2X$_1$ receptor. They form five pairs of disulfide bridges and play important roles in maintaining channel function and protein glycoslation. The proposed cysteine pairs are Cys^{117}/Cys^{165}, Cys^{126}/Cys^{149}, Cys^{132}/Cys^{159}, Cys^{217}/Cys^{227} and Cys^{261}/Cys^{270} respectively (Taken from Ennion *et al*, 2002b).

The conserved cysteines at P2X$_2$ receptors were investigated by Hume's group (Clyne *et al*, 2002a), and nine out of ten alanine replacements produced functional channels. P2X$_2$ receptors are known for their sensitivity to zinc allosteric regulation. The disulfide bond model was established on the agonist and zinc binding potency studies, and residues Cys^{113}/Cys^{164}, Cys^{258}/Cys^{267} and Cys^{214}/Cys^{224} were proposed to be the candidates for disulfide bonds. The residues Cys^{124}, Cys^{130}, Cys^{147} and Cys^{158} are possible to form two more pairs, while there is no basis for specific pairing. This model is essentially according to the results at P2X$_1$ receptor (Ennion *et al*, 2002b). In addition, seven of these mutants decreased the zinc potentiations and lower ATP potency at P2X$_2$ receptors. If these residues take part in zinc binding directly, only the zinc potentiation would be eliminated, just as the results have been shown at histidine residues His^{120} and His^{213} (Clyne *et al*, 2002b). It further suggested the cysteine residues may play roles in maintaining the structure of the zinc binding pocket, rather than located in the zinc binding sites.

Conserved glycine residues
Glycine can introduce flexibility to proteins by giving rise to turns and breaks in secondary structure, it can also be considered as an essential component of an ATP binding motifs, for example the Walker motif (GXXXGKXXXXXXI/V) (Walker *et al*, 1982) and the GXGXG motif which is conserved in over 95% known human protein

kinases (Okkeri *et al*, 2004). Nakazawa made site directed mutations on the glycine-rich region in $P2X_2$ receptors, the sensitivity to ATP in the G237A or G251A mutants had no difference to the wild type channel (Nakazawa *et al*, 1999). By contrast, the ATP sensitivity was reduced in G248A and completely abolished in the G247A mutant. The ATP sensitivity was also lost in the G248V mutant with a larger side chain than alaine. These results suggested the neighboring residues Gly^{247} and Gly^{248} are essential for channel function (Nakazawa *et al*, 1999). The 16 conserved extracellular glycine residues on the $P2X_1$ receptor were substituted individually by Digby *et al*, and most of the substitutions had little effect on receptor function (Digby *et al*, 2005). By contrast, when Gly^{250} was replaced with a range of amino acids this resulted in non-functional channels except for G250S. Therefore the Gly^{250} was implied to be essential in determining the function of P2X receptors. They further pointed out the residue Gly^{250} is located at a C-terminal end of an α-helix based on structural predictions and this lack of function is likely to result from a reduced receptor expression level at the cell surface. Interestingly, the glycine to alanine substitutions (G251A and G254A) in the GGXXG motif (250-254 of $P2X_1$ receptor numbering) resulted in normal or increased sensitivity to ATP, which suggested that Gly^{250} may contribute to channel function with neighboring glycine residues. In addition, the Gly^{71} may also be involved in ATP action together with the neighboring Lys^{68} and Lys^{70}.

Conserved proline residues

Proline is another important residue in maintaining the secondary structure of proteins. Proline residues can introduce kinks to the α-helices due to its unique structure and also have significant effects on channel function. Seven conserved proline residues (at least across five isoforms) in the extracellular ATP binding loop were studied in the $P2X_1$ receptors, and four of them (Pro^{93}, Pro^{166}, Pro^{228} and Pro^{272}) are totally conserved. Most of the alanine mutants had similar ATP potency to the wild type receptor, while a 4 fold reduction of ATP potency was observed at P93A mutant. Either alanine, aspartate or lysine replacement at Pro^{272} abolished the channel function completely, while the isoleucine substitution had no effects, increased ATP potency was observed with glycine or phenylalanine substitutions. Thus, the residue Pro^{272} which may associate with the conformation of the ATP binding site was shown to be dependent to the substituted amino acids, and none of these conserved prolines are fundamental for P2X receptor function. (Roberts *et al*, 2005).
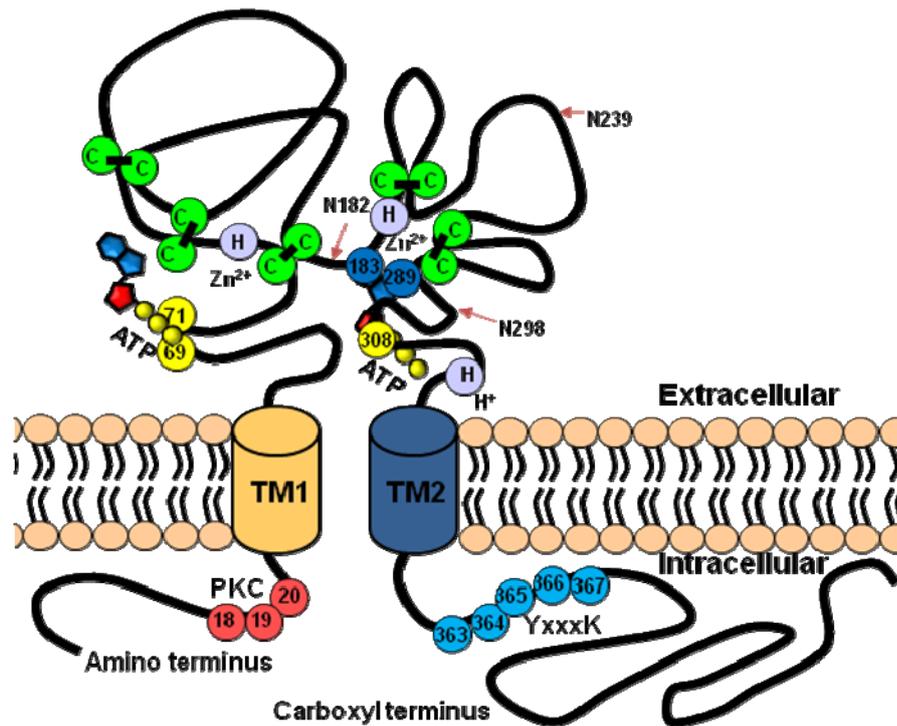
Figure 1.10 Model of ATP-binding loop and intracellular domains of human P2X₁ receptor. Each subunit of P2X receptors comprises two transmembrane domains (TMs), a large extracelluar loop and intracellular NH$_2$- and COOH-termini. N-glycosylation modification, positively charged amino acids, aromatic acids and cysteines which are involved in the binding mechanisms of the ligand loop are shown.There are 10 conserved cysteines which maintains a secondary structure by 5 disulfide bonds. There is a conserved protein kinase C site on N-terminus. The length of C-termini varies from 25 amino residue of P2X$_6$ to 240 residue of P2X$_7$, and there is a completely conserved intracellular YXXXK motif near the TM2.

1.5.3 Comparison of P2X receptors with other ligand-gated ion channels

The extracelluarly activated ligand-gated ion channels (LGICs) are transmembrane proteins which require the binding of specific ligands to induce the gating of the channel pore, and result in a subsequent increase of ion permeability to the cell.

They are subdivided into three families based on their structures: the glutamate activated cationic channel family (*eg.* NMDA receptors), the cys-loop superfamily (*eg.* nicotinic receptors and 5-HT$_3$ receptors) and ATP gated channels (*eg.* P2X receptors) (Golan *et al*, 2005). It can be concluded that the primary features of P2X receptors are the two transmembrane domains, one large extracellular binding loop for ATP molecules and two intracellular termini which will be discussed in following chapters respectively (See figure 1.4). Surprisingly, this distinct topology has no evident similarity to other ligand-gated ion channel families, while the receptor subunits in the cys-loop family contain extracellular N and C termini with four transmembrane segments, and the glutamate cationic receptor subunit contain the extracellular

N-terminal and intracellular C-terminal with three transmembrane segments (See figure 1.11). The inward rectifying potassium (Kir) channel, mechanosesitive channel of *E.coli*, epithelial sodium channel (ENaC) and acid-sensing ionic channels (ASICs) share the topological similarity to P2X receptor with two transmembrane segments (See figure 1.12). However, there is no homology at the protein sequence level.
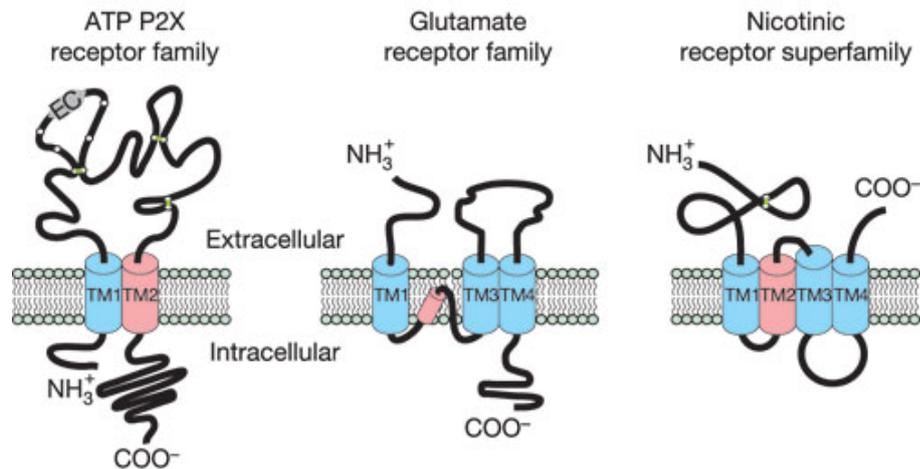
Figure 1.11 Topology of ligand-gated ion channel families.
The extracelluarly activated ligand-gated ion channels are divided into three families based on their distinct structures: the glutamate activated cationic channel families with three transmembrane domains for each subunit; the cys-loop superfamily contain four transmembrane domains for each subunit; and ATP gated P2X channels containing two transmembrane domains for each subunits (from Khakh *et al, 2006).
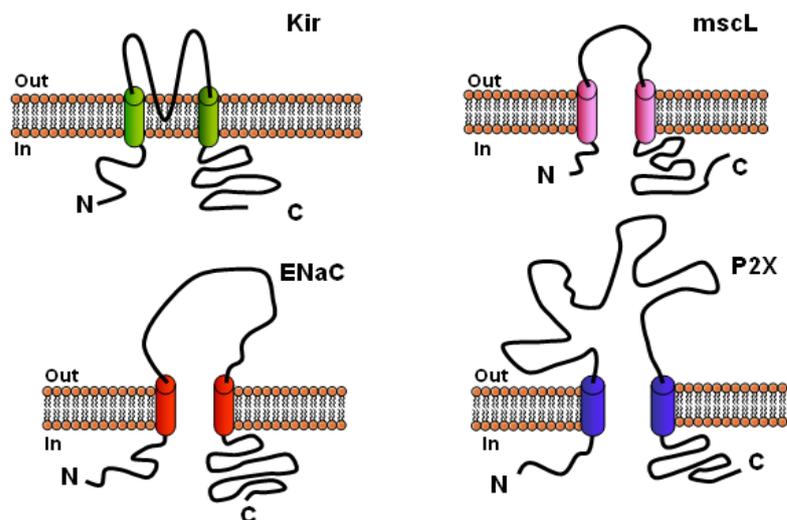
Figure 1.12Schematic of four types of channel with two hydrophobic domains.
The channels have two hydrophobic domains above are Kir (inward rectifier potassium channel), mscL (mechanosesitive channel of *E.coli.*), P2X (ATP-gated cation channel) and ENaC (Epithelial sodium channel family). The hydrophobic domains are represented by parallel slanted lines. Although inward rectifying potassium (Kir) and epithelial sodium channels (ENaC) share the similar topologies with the P2X receptor, they do not share the similarity in protein sequences.

1.6 Subunit assembly

All of the known ligand-gated channels are multimers. For example, the nicotinic acetylcholine receptors (nAChR) at the neuromuscular junction are heteromeric glycoprotein complexes composed of five subunits in a stoichiometry of $\alpha_2\beta\gamma\delta$ (Rang *et al*, 1999) , while the ionotropic glutamate receptors tend to be homo or hetero-tetramers (Rosenmund *et al*, 1998)(Figure 1.13). Currently, several lines of evidence support that functional P2X channels are assembled by three subunits and these will be explained as follows.

Trimeric   Tetrameric   Pentameric

$P2X_{1-7}$ AMPARs,   nAChRs, 5-HT$_3$Rs,
                      NMDARs,   GABA$_A$Rs, GlyRs,
                      KARs   GluCl, MOD-1
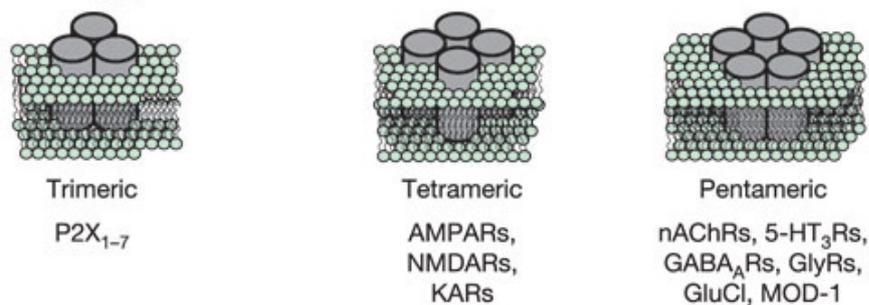
Figure 1.13The topology of ligand-gated ion channel families.
The extracelluarly activated ligand-gated ion channels are divided in to three families based on their distinct structures: the glutamate activated cationic channel families with four subunits within one channel and three transmembrane domains for each subunit ; the cys-loop superfamily require five subunits and four transmembrane domains for each subunit; and ATP gated P2X channels containing three subunits in each channel and two transmembrane domains for each subunits (from Khakh *et al*, 2006).

1.6.1 P2X receptors are multimeric channels

As more than two transmembrane domains are required for channel pore formation, the P2X receptor was originally predicted to be a multimeric channel based on its topological similarity with Kir and ENaC. The three major lines of evidence indicating the multimeric assembly are described as follows. (i) The Hill slope of the ATP concentration- response curve for recombinant P2X receptors is greater than one, which indicated that there is more than one binding site for each channel (Evans *et al*, 1995). (ii) Lewis showed that the co-expression of $P2X_2$ and $P2X_3$ subunits gave a P2X channel with novel properties that were not simply the addition of the two types of subunits (Lewis *et al*, 1995). This indicated the new channel should be formed by subunit hetero-polymerization. (iii)Two $P2X_2$ receptor subunits tagged with epitopes on the carboxy termini can be detected by immunoprecipitation and western blotting after co-transfection into human embryonic kidney 293 (HEK293) cells. It was found that the interaction between the subunits was strong enough to withstand high detergent levels, implying that the interaction is highly specific (Torres *et al*, 1998a).

1.6.2 Trimer is the basic form

In order to investigate the number of subunits required to form a stable functional multimeric P2X channel, chemical cross-linking and blue native polyacrylamide gel electrophoresis (BN-PAGE) were used. The cross-linking makes use of small reactive reagents which target primary amines, and can from covalent bonds. The $P2X_1$ and $P2X_3$ subunits can be cross-linked either in intact oocytes or after solubilization with digitonin, and run as trimers on the gel (Nicke *et al*, 1998). The $P2X_2$ subunits were also used in cross-linking and higher order complexes were produced, which supports the presence of trimers as well (Barrera *et al*, 2005). The other approach is BN-PAGE, this can be used for isolation of large multi-protein complexes, and the molecular masses of the complexes can be measured. The $P2X_7$ receptor was run in this way and the size was estimated to be a trimer (Kim *et al*, 2001). Stoop *et al* used the concatamer approach and suggested that trimeric complexes are the crucial elements in the construction of P2X ion channels (Stoop *et al*, 1999). Significant current amplitudes were recorded in oocytes with trimer constructed $P2X_2$ receptor, not dimers, tetramers or hexamers (Stoop *et al*, 1999).

The trimer form has been confirmed by atomic force microscopy (AFM). This technique allows single isolated uncrystalised proteins to be studied. The mean molecular volume of the $P2X_2$ receptor was determined to be 409 nm^3 by AFM, which is close to the expected value of a trimer (473 nm^3). For receptors with two bound antibodies, the mean angle detected between the antibodies was about 123°, which is very close to 120° and implicates the trimer form again (Barrera *et al*, 2005). In addition, Mio applied electron microscopy to study the recombinant $P2X_2$ receptors. They revealed the 3D image of $P2X_2$ receptor like a crown-capped inverted three-sided pyramid (Mio *et al*, 2005). A recent published study used fluorescence resonance energy transfer (FRET) and electron microscopy methods to look at the architecture of human $P2X_4$ receptors. The C-terminal tails were labeled with gold particles, and the estimated molecular volume of 270 nm^3 was corresponding to the trimer masses of 165 kDa for $P2X_4$ receptors (Young *et al*, 2008).

1.6.3 Co-assembly of P2X receptor subunit

P2X receptors could exist as either homomeric or heteromeric assemblies. The $P2X_2/P2X_3$ hetero-oligomeric receptors were observed in dorsal root sensory neurons

(Lewis *et al*, 1995). In addition, Radford *et al* used the epitope tags to label the C-terminal of $P2X_2$ and $P2X_3$ subunits and interactions between the subtypes were detected (Radford *et al*, 1997), indicating the forming of heteromeric channels. When $P2X_2$ and $P2X_3$ subunits were co-expressed, the heteromeric assembled channels gave rise to a composite phenotype that came from both constituent subunits (Lewis *et al*, 1995, see 1.6.4 for details). It implies the possibility of other subunit combinations. To explore the possible subunits combinations, Torres analysed the co-assembly possibilities of the seven P2X subunits by pairwise expression of tagged subunits and co-immunoprecipitation and the results is summarised in table 1.1 (Torres *et al*, 1999). This table also includes the findings contributed by the co-immunoprecipitation studies of others: the $P2X_{2/3}$ (Radford *et al*, 1997), $P2X_{4/6}$ (Le *et al*, 1998), $P2X_{1/5}$ (Le *et al*, 1999), $P2X_{1/4}$ (Nicke *et al*, 2005) and $P2X_{4/7}$ (Guo *et al*, 2007). These results provide direct biochemical evidence for the preferential association between different subtypes.

	$P2X_1$	$P2X_2$	$P2X_3$	$P2X_4$	$P2X_5$	$P2X_6$	$P2X_7$
$P2X_1$	+	+	+	+	+	+	-
$P2X_2$		+	+	-	+	+	-
$P2X_3$			+	-	+	-	-
$P2X_4$				+	+	+	+
$P2X_5$					+	+	-
$P2X_6$						-	-
$P2X_7$							+

Table 1.1 Summary of co-assembly possibilities among different P2X subunits.
The interactions between two subunits were detected by immunprecipitation approach using epitope tags. The specific and detergent-stable associations of a number of P2X subunit combinations are shown.

The subunit stoichiometry in heteromers was investigated at $P2X_{2/3}$ channels. The $P2X_2/P2X_3$ hetro-oligomeric channel was generated by co-expression with double cysteine substituted subunits (Jiang *et al*, 2003). When the Val^{48} and Ile^{328} at the outer end of the transmembrane domains were replaced by cysteines at $P2X_2$ and $P2X_3$ subunits respectively, disulfide bonds can be formed between the neighboring subunits. This disulfide bond was further confirmed by the application of agonists, and the reduction in amplitude was reversed by reducing reagents. Furthermore, co-expression of a double cysteine substituted $P2X_3$ subunit and WT $P2X_2$ receptors can make up channels with reduced response to α,β-me ATP, and these can be potentiated greatly with the presence of reducing reagents. Therefore the subunit composition in the heteromeric channel was found to be preferable as 1:2 for $P2X_2$ and $P2X_3$ subunits. The distribution of the $P2X_4$ and $P2X_6$ subunits in the heteromeric $P2X_{4/6}$ were revealed by AFM.

However, when P2X$_4$ and P2X$_6$ subunits were mixed for expression, the expression level was suggested to be dependent on their RNA levels (Bobanovic *et al*, 2002). Hence, the unbalanced subunits contribution pattern in heteromeric channel may not be a consensus.

The pairwise subunit arrangement pattern was also studied by co-expressing P2X$_2$ and P2X$_3$ subunits bearing cysteine substitutions in the intersubunit region, where disulfide bonds were formed between each subunit in the trimeric channel. Since the reducing reagent can only recover the responses to the heteromeric channels with cysteine substitutions at different transmembrane domains for P2X$_2$ and P2X$_3$ subunits, this study also indicated a head-to-tail arranged manner for functional channels which is linking the TM1 from one subunit and the TM2 from another subunit together (Jiang *et al*, 2003) (See figure 1.14).
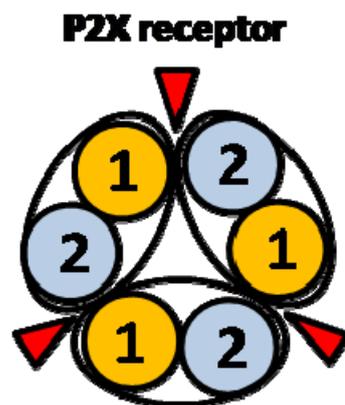
Figure 1.14 Subunits arrangement of P2X receptors
The subunit arrangement of P2X receptors were revealed as a head-to-tail pattern. The first (1) and second (2) transmembrane domains are shown in yellow and blue colors. The intersubunit ATP binding site that located between two subunits is indicated by the red arrows.

1.6.4 Heteromeric P2X channels with composite properties

Novel phenotypes can be seen often after the co-expression of different P2X subunits. The composite phenotypes with properties derived from the constituent subunits were initially found in P2X$_{2/3}$ heteromeric channels. P2X$_2$ homomers have relatively sustained responses to ATP and are insensitive to α, β-meATP, while P2X$_3$ homomers desensitize to ATP quickly and are sensitive to α, β-meATP (Refer to 1.7 for properties of P2X receptors). However, the P2X$_2$/P2X$_3$ channels possessed the properties of non-desensitizing time-course of P2X$_2$ and α,β-meATP sensitivity of P2X$_3$ (Lewis *et al*, 1995) (See figure 1.15). There is another example, the P2X$_1$/P2X$_5$ heteromeric channel. When P2X$_1$ and P2X$_5$ receptors were expressed in human embryonic kidney 293 cells, resultant P2X$_1$/P2X$_5$ channels showed properties of non-desensitizing time-course of

P2X$_5$ and the α,β-meATP sensitivity of P2X$_1$. Heteromeric assembly was confirmed using a co-immunoprecipitation assay (Torres *et al*, 1998b). Unique heteromeric properties were also observed in P2X$_{4/6}$ channels. P2X$_6$ subunits fail to assemble as homomeric channel into surface receptors, while the P2X$_4$ homomeric channels assemble into ATP-gated channels and exhibit weak sensitivity to α,β-meATP and insensitive to the suramin. However, the heteromeric P2X$_{4/6}$ channel is much more sensitive to α,β-meATP and the suramin than the constituent subunits (Bobanovic *et al*, 2002).
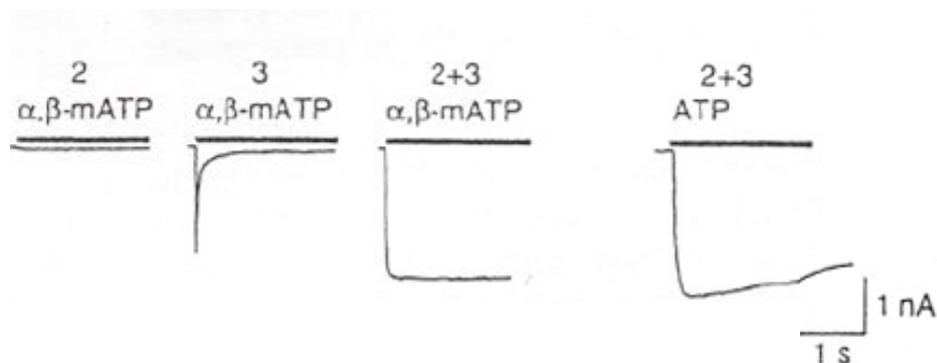
Figure 1.15: Heteromeric P2X$_{2/3}$ channels can have a composite phenotype with properties derived from constructed subunits
P2X$_2$ homomers are non- desensitizing to ATP and insensitive to α,β-me ATP. In contrast, P2X$_3$ homomers desensitize to ATP and sensitive to α,β-me ATP. And the P2X$_2$/P2X$_3$ channels possess the properties of non-desensitizing time-course of P2X$_2$ and α,β-me ATP sensitivity of P2X$_3$(taken from Lewis *et al*, 1995).

The heteromeric P2X$_{1/2}$ channel showed composite properties of P2X$_1$ and P2X$_2$ subunits. The P2X$_1$ receptor produces fast desensitizing changes in the membrane currents after the activation by ATP, whereas the P2X$_2$ receptor can maintain the response for a long time application of agonist. When these two subunits were co-expressed together, the resultant P2X$_{1/2}$ receptor demonstrated a biphasic inward current with P2X$_1$-like fast inactivation and followed by a P2X$_2$-like slow desensitizing current and changed pH sensitivity (Brown *et al*, 2002). In general, these findings suggest subunit heteromerization provides a way of increasing functional diversity of P2X receptor responses.

1.7 Properties of P2X receptors
P2X receptors on the cell membrane can be activated by the binding of extracellular adenosine 5'-triphosphate (ATP) (Burnstock *et al*, 1996b; North, 2002). Following stimulation with ATP, the cation-conducting pathway of the ligand-gated receptor opens

almost simultaneously. The characteristics of the currents will be discussed in the following sections.

1.7.1 Time-course of response

Desensitization which can be measured by the time-course of response describes the decay rate of the inward currents elicited by the ion channel during the continuous application of agonist. $P2X_1$ and $P2X_3$ receptors are fast desensitizing receptors, and the desensitization takes place within 10 milliseconds after the application of ATP (Figure 1.16). For example, the $P2X_1$ receptors produce fast desensitizing (~300 ms as measured for time of 50% decay response) changes in membrane currents (Valera *et al*, 1994) after the binding by ATP, and they require five minute washout to recover. The mechanism of channel recovery was suggested by Rettinger's group (Rettinger *et al*, 2003). They found that unlike the nicotinic superfamily, the $P2X_1$ channel must first open to desensitize even at low ATP concentrations and activation as predominantly determined by the receptor desensitization status. By contrast, relatively sustained responses were observed at the $P2X_2$, $P2X_4$ and $P2X_7$ receptors (Ralevic *et al*, 1998) (Figure 1.16). There is no more than 15% desensitization observed in $P2X_2$ receptors after two minutes of the ATP application (Evans *et al*, 1996).
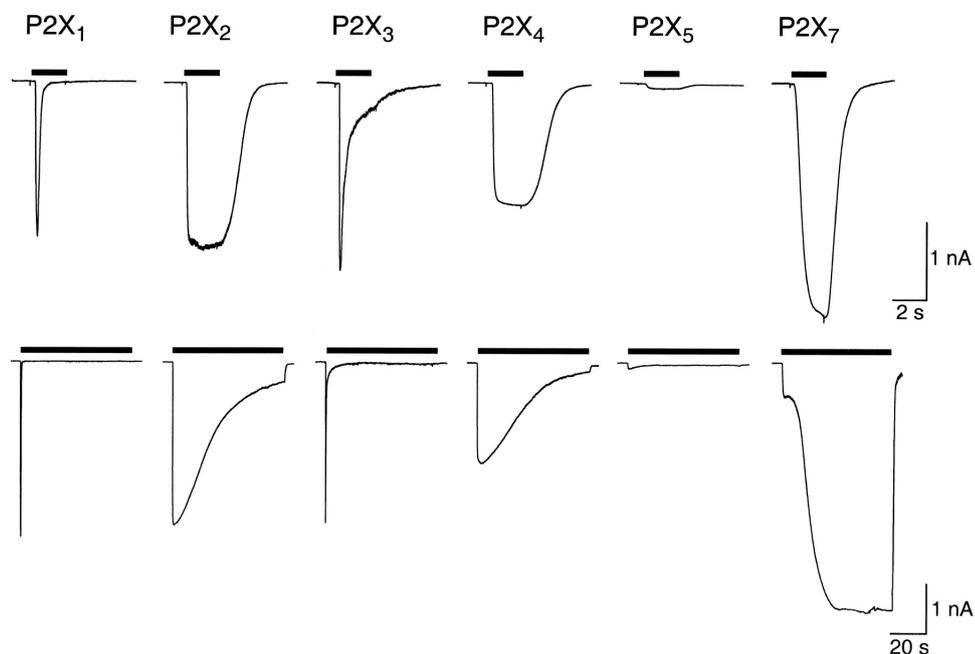
Figure 1.16 Fast and slow desensitization patterns of homomeric rat P2X receptors.
$P2X_1$ and $P2X_3$ receptors are fast desensitization to the application of 30 µM ATP (1 mM ATP for $P2X_7$), while $P2X_2$ and $P2X_4$ receptors are slow desensitization. The $P2X_5$ and $P2X_7$ receptors show little desensitizing with the presence of the agonists. When the agonists are applied for a longer time, biphasic effect is observed at $P2X_7$ receptor with a small current at first and followed by a larger response. (Adapted from North, 2002)

1.7.2 Permeability

The activation of the P2X receptors can lead to the movement of the ions and cause fast inward currents. It was Nakazawa who first suggested that the P2X receptors are cation channels non-selective to Ca^{2+} and K^+ (Nakazawa, 1987). Subsequent studies further suggested that they are equally permeable to the monovalent Na^+ and K^+ (Brake *et al*,1994; Soto *et al*.1996), and Valera suggested a relatively high permeability to Ca^{2+} (Valera *et al*,1994). The cation permeability is usually quantified by comparing the relative permeability of cations to Na^+ using changes in reversal potential. Liu studied the relative permeability of the native P2X receptor to monovalent and divalent cations in parasympathetic neurons using the patch clamp technique (Liu *et al*, 2001). The results indicated that the P2X receptors had weak selectivity among the monovalent cations, the selectivity sequence is $Na^+>Li^+>Cs^+>Rb^+>K^+$, there is also no strong selectivity among the divalent cations and the selectivity order is $Ca^{2+} > Sr^{2+} > Ba^{2+} > Mn^{2+} > Mg^{2+}$ (Liu *et al*, 2001). However, P2X channels were suggested to be more calcium conductive than other channels and it could be a large source of transmitter-activated calcium influx at resting membrane potential (Egan *et al*, 2004). The permeability ratio for Ca^{2+} relative to sodium was approximately 4 for $P2X_1$ receptor (Evans *et al*, 1996), but only 2.5 for $P2X_2$ receptor (Virginio *et al*, 1998). Besides, the range of cations of the $P2X_2$ receptors was probed as guanidinium > potassium = sodium > methylamine > caesium > dimethylamine. Since the channel permeability is dependent on the size of channel pore, this study is useful to investigate the diameter of the estimated channel pore at the P2X receptor (Evans *et al*, 1996).

Interesting permeability feature of channel pore dilation was demonstrated at the $P2X_7$ receptor during continued or prolonged application of agonist. The $P2X_7$ channel became non-selective and allowed large molecules to pass through the channel pore, such as YO-PRO-1(Surprenant *et al*, 1996). However, when the long C-terminal of the $P2X_7$ subunit was shortened, the YO-PRO-1 uptake was abolished, which indicated its pore formation is associated with the intracellular carboxy domain. Pannexin-1 was considered to be involved in $P2X_7$ receptor pore dilation, as the blockage of the pannexin-1 removed the $P2X_7$ receptor dye up-take (Pelegrin *et al*, 2007). Thus, it may act as a hemichannel and provide the dye uptake signalling via the activation of $P2X_7$ receptor.

A similar pore dilation phenomenon was observed in the $P2X_2$ receptor. For $P2X_2$ receptors, the time-dependent decrease in ionic selectivity was probed by voltage-clamp recording and fluorescence dye YO-PRO-1 uptake. After 2 to 5 minutes application of the agonist, the permeability to N- methyl-D-glucamine ($NMDG^+$) of $P2X_2$ ion channel could be increased by 6 fold in rat superior cervical ganglia neurons (Khakh *et al*, 1999). The underlying mechanism was possibly related to protein conformation changes in TM2 (Khakh *et al*, 1999). Furthermore, Virginio's research pointed out that the continued applications of ATP may lead to pore dilation of the $P2X_2$ receptors and the dilation could be a concentration-dependent progressive course (Virginio *et al*, 1999). Individual residues in the $P2X_2$ receptor C-terminal are also relevant to the permeability. Eickhorst and colleagues suggested that when the two most distal residues Ser^{432} and Asp^{444} were modified, the size of the pore can be increased (Eickhorst *et al*, 2002).

1.7.3 Pharmacological properties

Extracellular ATP has been recognised as a physiological transmitter or co-transmitter in the nervous system since 1959 (Holton, 1959). Besides ATP, many other agonists such as αβ-meATP and antagonists, such as suramin and 2'3'-O-(2',4',6')-trinitrophenyl-ATP (TNP-ATP), are available and have been widely used in the functional studies of the P2X receptors (Khakh *et al*, 2001). The sensitivity of agonists and antagonists, together with the ion permeabilities are important criteria for P2X receptor characterization. Each receptor has a different "signature" of pharmacological profile and sensitivity to drugs (Summarized in table 1.2 and table 1.3) that can help to differentiate the P2X subtypes in tissues.

P2X₁ subunits

Agonists refer to the drugs that activate the receptors when they occupy it, while antagonists are those that inhibit the normal physiology receptor function with high binding-site specificity (Rang *et al*, 1999). Both agonists and antagonists are useful tools to study the channel properties and are widely used in receptor classification.

ATP is a potent agonist at homomeric $P2X_1$ receptors with a half effective concentration (EC_{50}) at 1 μM (Khakh *et al*, 2001). Rapid desensitization begins during the continuous agonist application. One defining features of homomeric $P2X_1$ receptors is the high

sensitivity to L-β,γ-meATP which exhibit 30 fold more sensitive to P2X$_1$ than P2X$_3$ receptor (Trezise *et al*, 1995).

The α,β-meATP has resistance to enzymatic degradation which is a useful feature to distinguish the P2X$_1$ subunit in multicellular preparations (Khakh *et al*, 1995). Moreover, the length of phosphate tail is related to the agonist efficacy. In rat homomeric P2X$_1$, an interesting phenomenon was observed that the agonist diadenosine polyphosphates (ApnA) shows an increasing activity with the increasing number of phosphate groups (Wildman *et al*, 1999). Only the Ap6A was found to be a full agonist with two to three folds less potent than ATP, while the Ap5A, Ap4A were partial agonists. A previous study also suggested that Ap5A could only produce a maximal response near 65% of the response of ATP at the P2X$_1$ receptor (Evans *et al*, 1995).

Some potent antagonists for homomeric P2X$_1$ receptors have been identified and include TNP-ATP and cyclic pyridoxine-α4,5-monophosphate-6-azo-phenyl-2',5'disulfonate (MRS2220). TNP-ATP is 1000-fold more effective on P2X$_1$ subunits than at P2X$_2$, P2X$_4$ and P2X$_7$ subunits, and its half inhibitory concentration (IC$_{50}$) is about 1nM (Virginio *et al*, 1998). TNP-ADP and TNP-AMP also had similar effects. TNP-ADP could block the effects of α,β-meATP with an IC$_{50}$ of 2 nM at P2X$_1$ receptors (Virginio *et al*, 1998). MRS2220 blocks the ATP-induced current at the P2X$_1$ receptor with an inhibitory concentration of 10 μM, whereas its parent analog cyclic pyridoxine-α4, 5-monophosphate can potentiate the response under a similar concentration (Jacobson *et al*, 1998).

Although suramin is not specific to the P2X$_1$ receptor, one of its analogs 8,8'-(carbonylbis (imino-3,1-phenylene carbonylimno) bis (1,3,5-naphthalenetrisulfonic acid) (NF023) demonstrates high selectivity (Soto *et al*,1999). Remarkably, NF023 is 200-fold more potent for P2X$_1$ than P2X$_2$. In addition, the research suggested that a novel suramin analog 4, 4', 4", 4'''- (carbonylbis (imino-5, 1, 3-benzenetriylbis (carbonylimino))) tetrakis – benzene -1, 3 - disulfonic acid (NF449) is a potent selective antagonist to P2X$_1$ receptor with IC$_{50}$ of 0.3nM (Rettinger *et al*, 2005). Furthermore, P2X$_1$ homomeric receptors are also sensitive to non-selective antagonists like pyridoxal-phosphate-6-azophenyl-2', 4'-disulfonate (PPADS) and suramin (Khakh *et al*, 2001).

Extracellular ions bind to the receptor and can act as allosteric modulators. The concentration of protons effects the peak current amplitudes of $P2X_1$ receptors. The current at $P2X_1$ receptors can be decreased by acidification to pH 6.3 by nearly 50%, but are little changed by alkalinization to pH 8.3 (Stoop *et al*, 1997). The extracellular Zn^{2+} ions (0.1-1000 μM) could potentiate firstly and inhibit ATP-evoked responses at $P2X_1$ receptor in a concentration-dependent manner (Wildman *et al*, 2002), whereas the extracellular calcium concentration had little effect on ATP-evoked responses (Evans *et al*, 1996).

P2X_2 subunits

There are no specific selective agonist or antagonists for homomeric $P2X_2$ receptors, however, the properties of $P2X_2$ can be modulated by ions. Previous studies found that the EC_{50} of $P2X_2$ receptor to ATP ranges from 5 to 60 μM (Brake *et al*, 1994; Soto *et al*, 1997). The $P2X_2$ receptor has quite weak sensitivity and efficacy to αβ-meATP (Brake *et al*, 1994), but it still can be antagonized by suramin and PPADS with the IC_{50} at 10 μM and 1 μM respectively.

$P2X_2$ receptors demonstrated striking features in ion modulation and sensitivity, and the responses of $P2X_2$ receptor can be potentiated by protons and low concentrations of copper and zinc. Compared to the $P2X_1$ receptor, H^+ ions have different effect to the $P2X_2$ receptor. Following the acidification, the response of $P2X_2$ homomeric channel can be dramatically potentiated, while alkalinization attenuated the responses (Stoop *et al*, 1997). It was suggested that the $P2X_2$ receptor may have a single titratable site for the amplitude changing with pKa of 7.3. Since $P2X_2$ can be potentiated by increasing the concentration of protons, the protons may increase the affinity of the ATP for $P2X_2$ receptor. Both Cu^{2+} and Zn^{2+} can potentiate the response of $P2X_2$ ion channel, and this potentiation is independent of the membrane potential between -80 and +20 mv (Xiong *et al*, 1999). It was suggested that the affinity of the receptor for ATP can be increased by both of Cu^{2+} and Zn^{2+}. In addition, since the Cu^{2+} can not further enhance ATP-activated response when Zn^{2+} reached to its maximal effect, there could be a common site or mechanism for these two ions on the $P2X_2$ receptors (Xiong *et al*, 1999). The sensitivity to Cu^{2+} can also distinguish it from the $P2X_4$ receptors.

In contrast, extracellular calcium can act on the $P2X_2$ receptor as a blocker. In excised outside-out patches, the evoked current declines during the continued application of ATP and this decline was found to be regulated by the concentration of extracellular calcium (Ding *et al*, 1999). If there is no calcium in the external solution, no decline will be detected (Ding *et al*, 2000). This result indicated that extracellular calcium plays an important role in maintaining the activation status of the $P2X_2$ homomeric channel.

$P2X_{1/2}$ *heteromeric channel*

$P2X_1$/ $P2X_2$ heteromeric receptors were generated by co-expressing the rat $P2X_1$ and $P2X_2$ subunits in *Xenopus* oocytes (Brown *et al*, 2002). The sensitivity to Ap6A of the heteromeric channel was much greater than the homomeric $P2X_1$ receptor. Since Ap6A is inactive at $P2X_2$ receptors, this suggested a $P2X_1$ subunit dominant agonist sensitivity pattern. In addition, a high sensitivity to α,β-meATP of the heteromeric phenotype was also conferred from the $P2X_1$ subunit. However, the agonist potency order for $P2X_1$/$P2X_2$ heteromeric channel was α,β-meATP > ATP > Ap_6A, which was unrelated to both homomeric $rP2X_1$ receptors (ATP > Ap_6A >α,β-meATP) and homomeric $rP2X_2$ receptors (ATP: active; α,β –meATP: weak agonist; Ap_6A inactive) (Brown *et al*, 2002). In addition, the heteromeric receptor can be potentiated in both acidic and alkaline conditions and suggested a $P2X_2$-like ion modulation pattern (Brown *et al*, 2002).

$P2X_3$ *subunits*

Similar to the $P2X_1$ receptor, the $P2X_3$ receptor also exhibits fast desensitizing currents in the presence of agonist (100 μM ATP, -80 mV) (Chen *et al*, 1995). Its EC_{50} was evaluated as 1.2 μM for ATP, and a longer recovery time of a minimum 15 minutes may be required which is dependent on tissues. A range of ATP-related compounds are able to activate this channel, such as α,β-meATP. However, it is not sensitive to L-β,γ-meATP, and this feature can be used to differentiate it from the $P2X_1$ receptor (Trezise *et al*, 1995). Suramin and PPADS are potent antagonists at $P2X_3$ and TNP-ATP was identified as a nanomolar blocker of $P2X_3$ and $P2X_{2/3}$ heteromeric channels (Virginio *et al*, 1998). In addition, a potent and selective $P2X_3$ subunit blocker A-317491 was identified recently (Jarvis *et al*, 2002). Both Zinc and acidic extracellular environment to pH 6.3 can induce potentiated response on $P2X_3$ receptor as well (Stoop *et al*, 1997).

$P2X_4$ subunits

The responses of $P2X_4$ to ATP and its analogs resemble to the $P2X_2$ receptors with slow desensitizing inward currents (Buell *et al*, 1996). Maximum responses were evoked with 100 μM ATP with an EC_{50} at about 10 μM. The methylene substituted ATP, UTP, GTP and adenosine had no effect to the $P2X_4$ receptor at high concentration (up to 300 μM), suramin and PPADS are also not effective antagonists. Similar to $P2X_2$ receptors, the responses of $P2X_4$ receptors can be attenuated by H^+ at pH6.3 and potentiated by Zn^{2+} (Stoop *et al* , 1997).

$P2X_5$ subunits

The ATP induced $P2X_5$ receptor currents showed little desensitization to the presence of ATP (Collo *et al*, 1996). The EC_{50} for ATP is about 15 μM, and it can be antagonized by both suramin and PPADS .The peak current of $P2X_5$ receptor was initially thought to be smaller (only 5-10%) than other subtypes. For the ionic effects, Wildman's group discovered the current of $P2X_5$ receptor were desensitized by the continued presence of extracellular Ca^{2+} (Wildman *et al*, 2002). The response of $P2X_5$ receptor can be inhibited under acidic but not an alkaline extracellular environment, and zinc again was an extracellular allosteric modulator that can potentiate the response (Wildman *et al*, 2002).

$P2X_6$ subunits

$P2X_6$ subunit failed to form efficient trimers unless it was correctly glycosylated (Jones *et al*, 2004). However the properties for homomeric $P2X_6$ channel have been reported in HEK293 cell line (Collo *et al*, 1996; Jones *et al*, 2004). A range of full agonists including ATP, 2-methylthio-ATP, 2-chloro ATP and ADP and partial agonist ATP-γ-S have been identified (Collo *et al*, 1996). The attenuation caused by suramin and PPADS can be only observed when they were applied at high concentration (over 100 μM) to $P2X_6$ receptors.

Receptor	Agonist	Antagonist	ATP EC_{50}	Desensitizing	pH	Calcium	Zinc
Homomeric							
P2X$_1$	2-meSATP>ATP>Ap6A >α,β-meATP>βγ-L-meATP	Suramin PPADS,TNP-ATP, MRS2220,NF023, NF449	1	Fast	pH6.3: increase pH8.0: no effect	Increase: no effect	1-300µM: decrease amplitude
P2X$_2$	ATP>2-meSATP >ATPγS	Suramin, PPADS, reactive blue 2	5-60	Slow	pH6.5:increase pH8.0:decrease	Increase: reduced amplitude	0.3-30µM: 2-20 fold increasing
P2X$_3$	2-meSATP>ATP >α,β-meATP >ATPγS>Ap3A,	A-317491 Suramin, PPADS,TNP-ATP	1	Fast, concentration dependent	pH6.5:increase pH8.3:no effect	Increase: no effect	_
P2X$_4$	ATP>ATPγS >2-meSATP	Suramin, PPADS at high concentration	10	Slow	pH6.5:increase pH8.3:decrease	_	10µM: increase amplitude
P2X$_5$	ATP=2-meSATP >ATPγS>2-CIATP	Suramin, PPADS	15	Little desensitizing	pH6.5:decrease pH8.0:no effect	1.8 mM: reduced amplitude	1-100µM: increase amplitude
P2X$_6$	ATP>α,β-meATP >2-CIATP>2-meSATP	Suramin, PPADS	12	Slow	_	_	
P2X$_7$	BzATP>ATP >2-meSATP	KN62, NF279, Suramin, TNP-ATP,PPADS	115	Little desensitizing	_	_	Low concentration: Increase amplitude

Table 1.2 Summary of the pharmacological profile of P2X homomeric channels
The properties of P2X homomeric channels (P2X$_{1-7}$) to agonists, antagonists, EC_{50} to ATP, desensitizing time, pH changes and effects of ions and were summarised in the table.

Receptor	Agonist	Antagonist	ATP EC$_{50}$	Desensitizing	pH	Calcium	Zinc
Heteromeric							
P2X$_{1/2}$	ATP>Ap6A >α,β-meATP	_	3.3	Fast and slow	pH6.5:increase pH8.0:increase	_	_
P2X$_{1/4}$	ATP, α,β-meATP	Suramin, TNP-ATP, PPADS	_	Slow	_	_	_
P2X$_{1/5}$	ATP>2-meSATP >α,β-meATP>ADP	Suramin, TNP-ATP.PPADS	0.7	Fast and slow	pH6.5:increase pH8.0:no effect	Increase: no effect	10µM: decrease amplitude
P2X$_{2/3}$	ATP>α,β-meATP	Suramin, PPADS,TNP-ATP	0.4	Slow	pH6.3:increase pH8.0:decrease	Increase: reduced amplitude	_
P2X$_{2/6}$	ATP=ATPγS >2-meSATP	Suramin	32	Fast and slow	pH5.5:decrease pH6.3:increase pH8.0:increase	_	1-10µM: increase amplitude
P2X$_{4/6}$	ATP>2-meSATP> α,β-meATP	Suramin, PPADS, reactive blue 2	6	Slow	pH6.3:increase pH8.0:no effect	_	10µM: increase amplitude
P2X$_{4/7}$	BzATP, ATP[4]	TNP-ATP, BBG	_	Little desensitizing	_	_	_

Table 1.3 Summary of the pharmacological profile of P2X heteromeric channels
The properties of P2X heteromeric channels (P2X $_{1/2, 1/4, 1/5, 2/3, 2/6, 4/6 \text{ and } 4/7}$) to agonists, antagonists, EC$_{50}$ to ATP, desensitizing time, pH changes and effects of ions and were summarised in the table above.

P2X₇ subunits

The activation of P2X$_7$ receptors normally requires over 100 μM ATP, and 3'-O-(4-benzoyl) benzoyl adenosine 5'-triphosphate (BzATP) (EC$_{50}$ of 7 μM) is 10 to 30 times more sensitive than ATP (Surprenant *et al*, 1996). With repeated application of the agonist, the time-course of P2X$_7$ receptor currents can be significantly pro-longed. An interesting observation was that ATP or BzATP currents can be attenuated by extracellular calcium and magnesium. The most potent antagonist is 8, 8'-(carbonylbis (imino-4, 1-phenylenecarbonylimino-4, 1-phenylenecarbonylimino)) bis (1, 3, 5-naphthalenetrisul fonic acid) (NF279) with an IC$_{50}$ of 10 μM. PPADS and suramin were less effective at the P2X$_7$ receptor.

1.8 Distribution and physiological roles of P2X receptors

Distribution

The P2X receptors are distributed in a wide variety of tissues, including brain, sensory neurons, heart muscles, vasculature, urinary bladder and blood platelets (Valera *et al*,1994; Chen *et al*,1995; Scase *et al*,1998; Bo *et al*,1995; Collo *et al*,1996). It is well-known that the P2X$_1$ subunit has high expression in smooth muscle, such as vas deferens, arteries and bladder (Valera *et al*, 1994; Sage *et al*, 2000; Scase *et al*, 1998). However, most of the cells, such as sympathetic neurons, sensory neurons, were dominated by more than two subtypes. For example the P2X$_2$ and P2X$_3$ subunits are often co-expressed in sensory neurons in the form of P2X$_{2/3}$ heteromeric channel (Vulchanova *et al*, 1997). The expressions of different P2X subtypes are summarized in Table 1.4.

Subtypes	Localisation	References
$P2X_1$	Smooth muscle, Sensory ganglia, Cerebellum, Heart, Platelet	Valera,1994;Kidd,1995; Collo,1996;Scase,1998
$P2X_2$	Autonomic ganglia, Brain, Pituitary, Sensory ganglia, Smooth muscle, Retina	Brake,1994;Chen,1995; Kidd,1995;Collo,1996; Vulchanova,1996
$P2X_3$	Sensory ganglia, Solitary tract neurons, Sympathetic neurons	Chen,1995;Collo,1996
$P2X_4$	Brain, Pancreas, Testes, Colon, Smooth muscle	Bo,1995;Buell,1996; Collo,1996;Soto,1996;Wang,1996
$P2X_5$	Heart, Gut, Bladder, Autonomic ganglia, Skin, Thymus, Spinal cord	Collo,1996
$P2X_6$	Skeletal muscle, Brain, Spinal motor neurons, Autonomic ganglia	Collo,1996;Soto,1996
$P2X_7$	Apoptotic cells, Marcophages, Lymphocytes, Microglia, Skin	Surprenant,1996

Table 1.4 Distribution of different P2X subtypes.
The tissues from which the P2X subunits were first cloned are listed. P2X receptors are widespread expressed in many tissues, and different subtype tends to distribute in specific tissue.

Knockout mice studies

Due to the lack of subtype selective drugs, the physiological roles of specific subtypes are difficult to assess. To date, knockout mice models of $P2X_1$, $P2X_2$, $P2X_3$, $P2X_4$ and $P2X_7$ subunits have been constructed and the associated physiological properties were studied. In brief, these results indicated the P2X receptors are essential in maintaining the normal functions of several tissues, and the roles of $P2X_1$ receptor will be focused in this section. For instance, the contractile P2X phenotype in large mesenteric arteries was characterized by its pharmacological profile (Gitterman *et al*, 2000). The rapidly desensitizing response to agonists demonstrated the characteristic feature of $P2X_1$ and $P2X_3$ subtypes. However, they were also insensitive to α,β-meATP as seen in the $P2X_{2,4,5,6,7}$ subtypes and lack of effect of suramin as in the $P2X_{4\&6}$ subtypes. This study suggested no single subtype could account for the phenotype of the P2X receptor in large mesenteric artery, and more than one isoforms were deduced to contribute to the contractile response in large mesenteric arterial vasculature.

$P2X_1$

The $P2X_1$ KO mice have been used to investigate functions of $P2X_1$ receptors in the vas deferens, platelet, bladder and also the CNS.

The roles of the $P2X_1$ receptor in the vas deferens was studied using the $P2X_1$ null mice and a reduction of fertility was observed (Mulryan *et al*, 2000). The non-functional

P2X$_1$ receptor gene was generated by deleting the first 45 amino acids of the P2X$_1$ receptor exon1, and both male and female P2X$_1$ KO mice were produced. The interbreeding of mutant mice results suggested the reduced fertility is exclusive to the male P2X$_1$ receptor deficient mice. The measurement of the fluids secreted from the accessory sexual glands indicated the contraction and function of these glands were unaffected, and the association between P2X$_1$ receptor and spermatogenesis and the sperm dysfunction was ruled out by the immunohistochemistry. Further observation suggested the reduced amount of sperm in the uterus lavage from matings with P2X$_1$ deficient mice, which showed that the reduction in male fertility results from the reduced sperm ejaculated. This reduction was related to the reduction of sympathetic nerve mediated contraction of the vas deferens.

P2X$_1$ receptors have been cloned from human platelets (Scase et al, 1998; Vial et al, 1997). Megakaryocytes were focused on as progenitor cells of platelet, and their principal role is maintaining the normal blood platelet count. P2X$_1$ receptor deficient mice were generated and the spleen and bone marrow were dissected and studied by immunohistochemical methods. The P2X$_1$ receptor deficiency had no effect on the number or size distribution of magakaryocytes in bone marrow from adult mice, and suggested the P2X$_1$ receptor is not essential for the megakaryocyte formation (Vial et al, 2002a). However, the initial transient inward current and calcium influx triggered by ATP was absent in megakaryocytes form the P2X$_1$ receptor knockout mice. Additionally, the calcium rise in megakaryocytes and platelet can be accelerated and amplified remarkably by co-stimulation of P2X$_1$ and P2Y$_1$ receptors. This suggested the synergistic interaction between the P2X$_1$ and P2Y$_1$ receptors and the P2X$_1$ receptor may have a role in the priming activation of P2Y receptors. Due to the large amount of ATP release from the damaged cells in vascular injury, the P2X$_1$ receptor could accelerate the platelet activation during the hemostasis or thrombosis. Subsequently, another investigation to the roles of P2X$_1$ receptor in the hemostasis and thrombosis procedure was carried out by using the knockout mice as well. The bleeding time observed for P2X$_1$ deficient mice was normal and suggested the P2X$_1$ receptor has little impact to primary hemostasis (Hechler et al, 2003), however, they showed resistance to the acute thromboembolism due to the collagen-induced platelet aggregation and secretion. In $vivo$, compared to the control group, the mortality of the P2X$_1$ null mice because of the thromboembolism was reduced, and the time to remove the thrombus reduced too. Thus,

it was concluded that the $P2X_1$ receptor contributes to the formation of platelet thrombi. The $P2X_1$ subtype demonstrated a range of important roles in platelet formation, and therefore the $P2X_1$ subtype KO mice can be a model for further investigation of thrombosis.

The involvement of the $P2X_1$ subtype in the vasoconstriction of mesenteric arteries was also identified using the KO mice (Vial *et al*, 2002b). ATP, α,β-meATP and PPADS as the selective agonist and antagonist for $P2X_1$ receptor failed to act in the arteries of KO mice from a range of vascular beds. This indicated the homomeric $P2X_1$ receptors is a dominant phenotype in the artery smooth muscle and contributes to sympathetic neurogenic vasoconstriction.

The distribution of P2X receptor subunits in bladder was revealed by using the $P2X_{1-7}$ selective antibodies, and the immunoreactivity of $P2X_1$ receptor was strongly detected in the detrusor and blood vessels. In the bladder of $P2X_1$ deficient mice, the abolition of contractions and inward currents mediated by $P2X_1$ receptors were also observed. The peak amplitude of response for $P2X_1$ deficient mice was only about 30% of the WT mice to 10Hz nerve stimulation. These findings underlined it as an essential subtype in the bladder smooth muscle (Vial *et al*, 2000).

$P2X_1$ subunits also contribute to the nervous system. The $P2X_1$ receptor was shown as the isoform that was responsible for 80% of the α,β-meATP sensitivity in superior cervical ganglia neurons. Together with the time-course, antagonist and pH sensitivity exhibited in the $P2X_1$ knockout neuron, the $P2X_1$ receptor subunits were suggested to make up a $P2X_1/P2X_2$ heteromeric channel. The distribution of P2X receptor in the auditory brainstem synapse was characterised by the pharmacological profiles and the KO mice studies, and for the first time that the functional role of $P2X_1$ receptors was demonstrated in the CNS (Watano *et al*, 2004). The sensitivity to L-β, γ-meATP and the abolition response in the $P2X_1$ receptor deficient mice suggested the involvement of $P2X_1$ receptor in these neurones. Thus, the presynaptic $P2X_1$-containing receptors may be located on the inhibitory neurones and act to facilitate the transmitter release in the superior olivary complex.

Other P2X subtypes

KO mice models of other P2X subtypes including the P2X$_{2, 3, 4 \& 7}$ receptor were generated to investigate the distributions and physiological roles of the P2X receptors in CNS, sensory neurones, vessel endothelial and immune cells.

The roles of P2X$_2$ subunit were studied by P2X$_2$ receptor deficient mice, and patch-clamping recording suggested that the P2X receptors on sympathetic ganglion neurones involve almost exclusively P2X$_2$ subunits (Cockayne *et al*, 2000). The sympathetic neurones had barely detectable responses in the P2X$_2$ subunit KO mice. Lacking of the P2X$_2$ receptor leads to the reduction of urinary bladder reflexes and pelvic afferent nerve activity in response to bladder distension. Interestingly, the P2X$_2$ subunit is not crucial in the central nerve system (CNS). There is no deficit in CNS behavioural tests observed in the P2X$_2$ receptor deficient mice.

By contrast, the P2X$_3$ subunit has limited distribution, and functional P2X$_3$ channels can only be detected in sensory neurons. Souslova *et al* suggested that ablation of the P2X$_3$ deficient tissue inhibited the normal sensor motor function (Souslova *et al*, 2000). The pain behaviour was suppressed and the termal hyperalgesia in chronic inflammation was enhanced. Interestingly, although the dorsal-horn neuron has normal responses to the mechanical and noxious heat, the P2X$_3$-null mice were not able to respond to the non-noxious warming stimuli.

P2X$_2$/P2X$_3$ double KO mice were studied by Cockayne and colleagues (Cockayne *et al*, 2000). It was found that the sympathetic and sensory neurones from the KO mice had almost no response to ATP, and the reflexes of urinary bladder was reduced as well. These data revealed the P2X$_2$ and P2X$_3$ subunits incorporate in sensory and sympathetic ganglia, and P2X$_{2/3}$ heteromeric channel is an important component to nocieptive responses and mechanosensory transduction within the urinary bladder.

The most recent published KO mice model of P2X receptor is P2X$_4$ subunit deficient mice (Yamamoto *et al*, 2006).The P2X$_4$ deficient mice exhibit abnormal endothelial cell responses. In addition, the vessel dilation caused by acute increase of blood flow was reduced significantly, and a decrease in vessel size was observed in response to a chronic decreasing blood flow. Take these data together, the endothelial P2X$_4$ channel

showed essential roles in flow-sensitive mechanisms to regulate the blood pressure and vascular remodelling.

The $P2X_7$ subunit only tends to form homomeric channels and exhibits high expression in macrophages, monocytes and lymphocytes. $P2X_7$ deficient mice have been generated, and the roles of the $P2X_7$ subunit to the haemopoietic cells were revealed (Solle *et al*, 2001; Labasi *et al*, 2002). It was found that the *in vivo* cytokine signalling cascades were impaired in the $P2X_7$ deficient model, since it failed to produce mature interleukin-1β (IL-1β).This results suggested that the activation of $P2X_7$ receptor related to the process of cytokines signalling (Solle *et al*, 2001). The leukocytes from $P2X_7$ KO mice were found having abolished responses to ATP, such as the expressions of L-selectin and IL-1β. Additionally, compared to the wild type under the same treatment, the $P2X_7$ deficient mice were markedly less affected by the responses to induced monoclonal anti-collagen-induced arthritis. These indicated the $P2X_7$ receptor can be seen as a crucial component of an *in vivo* inflammatory response (Labasi *et al*, 2002).

1.9 Thesis aim

In this thesis, the contribution of the intracellular amino and carboxy termini of $P2X_1$ receptor to channel regulation will be studied. A combination of concatenated channels, site-directed mutagenesis and other molecular biological, biochemical and electrophysiological methods will be used to establish the regulation mechanism of $P2X_1$ receptor. This research will provide better insights into the physiological roles of $P2X_1$ receptors and their regulation.

Chapter 2. Materials and Methods

2.1 Molecular biology

2.1.1 pcDNA3.0 vectors and P2X receptor sequences.

The pcDNA3.0 plasmid (Invitrogen, Paisley, U.K.) was used as a vector for containing the $P2X_1$ cDNA which was isolated from human bladder (Ennion *et al*, 2000). Ampicillin and Neomycin resistance genes indicated in the plasmid map (See figure 2.1) are for selection and maintenance in *E.coli*. CMV (cytomegalovirus), T7 and Sp6 promoters give efficient protein expression and were located before or after the multiple restriction sites for $P2X_1$ cDNA sequence cloning. A poly (A) tail sequence was inserted to the 3' non-translated region of the $P2X_1$ cDNA sequence to aid in protecting the translated mRNA from degradation by exonucleases. The *MluI* site was present and used to linearise the plasmid to make the mRNA.
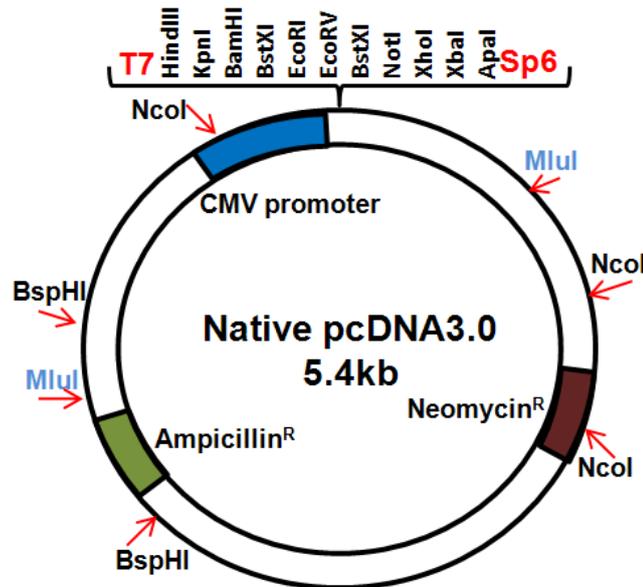
Figure 2.1 Plasmid map of pcDNA 3.0 vector

The features of the pcDNA3.0 vector are shown in the map. The human cytomegalovirus (CMV) promoter (Blue), T7 and Sp6 promoters enable high-level expression of the recombinant $P2X_1$ receptor, T7 and Sp6 promoters are also used in the sequencing of the insert. Multiple cloning sites between the T7 and Sp6 promoter facilitate cloning of the $P2X_1$ receptor sequence. Neomycin (Brown) and Ampicillin (Green) resistance genes allow selection of transformation in both mammalian and bacterial cells. The locations of the endogenous *MluI* (for linearization of P2X sequence in mRNA production), *NcoI* and *BspHI* sites are indicated with red arrows.

2.1.2 Site-directed mutagenesis

Point mutations were introduced into the human $P2X_1$ plasmid using the Quick Change^{TM} mutagenesis kit (Stratagene, Amsterdam, Netherlands).

Setting up the reactions:

DNA template (human P2X$_1$ receptor cDNA in pcDNA 3.0)	50 ng
Reaction buffer for *pFu* Turbo DNA polymerase	1X
dNTPs (each)	200 μM
Forward primer	125 ng
Reverse primer	125 ng
PfuTurbo® DNA polymerase (Stratagene)	2.5 u

Reactions were performed in a final volume of 50 μl in a Techne Genius thermocycler using the following cycling parameters for the site-directed mutagenesis methods:

Denaturation	95ºC	for 3 minutes

Denaturation	95ºC	for 30 seconds	
Annealing	55ºC	for 60 seconds	16 cycles
Extension	68ºC	for 16 minutes	

Final hold	4ºC	

The DNA templates were eliminated by digestion with 10 units of the DpnI restriction enzyme (New England Biolabs® Inc.) for 1 hour at 37 ºC. The DpnI enzyme cleaves only when its recognition site (5'-GA^TC-3') is methylated. In this case, the DNA template was purified from dam$^+$ strains bacteria and the plasmid was methylated. Since the new synthetic DNA from the site-directed mutagenesis was not methylated, it was not cut by the DpnI enzyme and only the plasmid template from the bacteria was degraded.

2.1.3 PCR amplification

PCR was performed on the vector pcDNA3.0 containing the human P2X$_1$ receptor cDNA sequences.

Setting up the reaction conditions:

DNA template	50 ng
Reaction buffer for pFuTurbo DNA polymerase	1X
dNTPs (each)	200 μM
Forward primer	100 μM
Reverse primer	100 μM
PfuTurbo DNA polymerase (Stratagene)	2.5 u

Reactions were performed in a final volume of 50 μl in a Techne Genius thermocycler using the following program:

Denaturation	94ºC	for 3 minutes
Denaturation	94ºC	for 45 seconds
Annealing	55ºC	for 45 seconds
Extension	72ºC	for 90 seconds

30 cycles

Final extension	72ºC	for 10 minutes
	4ºC	on hold

2.1.4 Gel extraction for PCR products

After addition of 12.5 μl of 5X loading buffer (Bioline Ltd.U.K.), PCR products were loaded on a 1% agarose gel with TAE buffer 1X (0.4M Tris-acetate, 0.01M EDTA, pH 8.3 ± 0.1) and ethidium bromide (0.5 μg/ml) and run at 100 V for 25 minutes. The gel was visualized on a UV light box and the PCR product was removed with a sterile blade.

The PCR products were extracted from the agarose gel using the QIAquick Extraction kit (Qiagen®, U.S.A) and eluted in 30 μl H_2O.The purified PCR products were double digested with the corresponding restriction enzyme (New England Biolabs® Inc.) for 2 hours at 37 ºC. The digested PCR products were run again on a 1% agarose gel, extracted using the QIAquick Extraction kit (Qiagen®, U.S.A) and eluted in 30 μl H_2O. In order to quantify the digested PCR products corresponding to each P2X receptor sequence, an aliquot of 1μl of the eluted 30 μl DNA was run on a 1% agarose gel.

Quantification was established by comparing the intensity to the bands to the quantitative DNA ladder Hyperladder ^{TM} I (Bioline Ltd, U.K.)

2.1.5 Dephosphorylation and ligation

Native pcDNA 3.0 (1.5μg) was digested with the corresponding restriction enzymes (New England Biolabs® Inc.) for 2 hours at 37 ºC. The digested vector was then run on a 1% agarose gel. The band of linearized pcDNA3.0 plasmid was cut and extracted and dephosphorylated as follows.

Dephosphorylation:

(i)   The vector was dephosphorylated in a final volume of 60 μl as follows:

pcDNA3.0 linearized with enzyme   30 μl (eluted)

Calf Intestinal Alkaline Phosphatase Buffer (Promega® U.S.A)   1X

Calf Intestinal Alkaline Phosphatase (CIAP) (Promega®U.S.A)   1 unit

Dephosphorylation was carried out for 20 minutes at 37 ºC and stopped by the addition of 300 μl of CIAP Stop Solution (Tris-HCl (pH 7.5) 10mM, EDTA (pH 5) 1mM, NaCl 200 mM, 0.5% SDS.)

(ii)CIAP was then removed by a Phenol/Chloroform/ Isoamyl Alcohol (25:24:1) (1:1) extraction. One volume of phenol/chloroform/ Isoamyl Alcohol was added to the dephosphorylated vector and votexed before centrifugation 5min at 13000rpm. The aqueous top phase was then transferred to a new tube and precipitated overnight at -20 ºC with 0.5 volume of Ammonium Acetate 7.5 M (pH 5.5) and 2.5 volume of 100% ethanol.

(iii)The DNA was pelleted by centrifuging at 13000 rpm for 20 min at 4 ºC and washed once with 70% ethanol.

(iv)The pellet was dried at 58 ºC for few minutes before reconstitution in 20 μl H_2O

To quantify the precipitated vector pcDNA 3.0, an aliquot of 1μl of the reconstituted 20 μl DNA was run on a 1% agarose gel. Quantification was established by comparing the

intensity to the bands to the quantitative DNA ladder Hyperladder ^{TM} I (Bioline, Ltd,U.K.)

The sequences from PCR amplification were then cloned into the pcDNA3.0 vector by ligation to construct the linker vector. In order to use the right quantity of insert and vector, the following equation was used:

(50 ng vector X size of insert (kb) X 3)/size of vector (kb) = Quantity of insert to use (ng).

Ligation was performed at 14 ºC overnight in the presence of 400 units of T4 DNA ligase (New England Biolabs® Inc.), 1X T4 DNA ligase buffer and H_2O to reach a final volume of 10 μl.

2.1.6 Transformation

50 μl of Library Efficient DH5α ^{TM} Competent cells (Invitrogen®) were transferred to a pre-cooled tube (Falcon 2059) and 1μl of the mutation reaction (e.g. from section 3.4) was added to the cells on ice. The tube was kept on ice for 30 minutes and then the transformation was performed with a heat shock for 45 seconds at 42 ºC before being placed again on ice for 2 min. 500 μl of SOC medium (Super optimal broth with catabolite repression) (Invitrogen®)   was added to the tube before shaking at 250 rpm in the 37 ºC shaker for 1 hour. 100μl of cells were plated on LB agar Petri dishes complemented with 100 μg/ml Ampicillin and left in a 37 ºC incubator overnight.

Colonies grown on Petri dishes were picked with sterile toothpicks and transfered to tubes containing 6 ml LB Broth and 100 μg/ml Ampicillin. These minicultures were left overnight on a 37 ºC shaker at 250 rpm. The plasmid DNA was then extracted from these minicultures by using the Promega® wizard plus SV minipreps DNA purification system (Promega, U.S.A). Plasmid DNA was recovered in 100 μl nuclease free water (H_2O).

2.1.7 Sequencing

The sequences were confirmed by DNA sequencing (PNACL sequencing service, Leicester University). To analyze the result of my sequencing reactions, programme Chromas 2.3 (Technelysium) and Seqman^{TM} II (DNASTAR) were used.

2.1.8 RNA synthesis and quantification

Synthesis of concatenated channel mRNA

(i) For each of the concatenated constructs, 38 μl of plasmid DNA (from miniprep) was linearized with 50 units of *MluI* restriction enzyme for 4 hours at 37 ºC. In order to denature the enzyme, *MluI* restriction enzyme was incubated at 50 ºC for 1 hour in presence of proteinase K (190 μg/ml) and 0.5% SDS.

(ii) This was followed by a Phenol/Chloroform/ Isoamyl Alcohol (25:24:1) extraction (1:1 volume) and precipitation by addition of 2.5 volume 100% ethanol at -20 ºC overnight.

(iii)The precipitate was centrifuged at 13000 rpm for 20 minutes at 4 ºC and washed twice with 70% ethanol. The pellet was dried at 58 ºC for five minutes before reconstitution in 6 μl RNAase free H_2O.

(iv)To synthesise mRNA for each construct, I used the High Yield Capped RNA transcription Kits for Sp6 T7 and T3 promoter: mMessage mMachine™, Ambion (Europe).

* DNA template (*MluI* linearized plasmid pcDNA3.0 with concatenated constructs)

	6μl
* T7 enzyme mix buffer	1 X
* ATP/CTP/	7.5 mM each
* GTP	1.5 mM
* CTP analog	6 mM
*T7 enzyme mix (RNA polymerase/SUPERase·In.)	2 μl

And the reaction was brought to 20 μl by addition of RNAase free H_2O.

RNA synthesis was carried out for 2 hours at 37 ºC. In order to remove the DNA template, 2 u of DNase I was added and the reaction was incubated for 15 min at 37 ºC.

(v) To stop the reaction and precipitate the RNA, 30μl of RNAase free H_2O and 25 μl of LiCl (7.5 M lithium chloride, 50mM EDTA) were added and the mixture was stored at -20 ºC overnight.

(vi)The sample was centrifuged 20 min at 13000 rpm 4ºC and the mRNA pellets were washed twice with 70% ethanol. The pellets were dried at 58 ºC for a few minutes and reconstituted by adding 23 μl of nuclease free water.

RNA quantification

(i) 2.5 μl of the RNA was used for optical density quantification: prepared tubes with 1ml H_2O + 2.5 μl of the RNA and quantified at 260 nm wave length.

(ii) In addition, to check the RNA quality, 0.5μl of the RNA was run on a RNA gel (0.5 g of agar, 10ml 1X MOPS, 5% formaldehyde in DEPC treated H_2O). 0.5μl RNA sample was mixed with 3.5μl loading bufferII (mMessage mMachine^{TM} kit), 3 μl H_2O and 2 μl Ethidium Bromide (200 μg/ml) in tube and denatured at 85 ºC for 3 min and loaded on the RNA gel. Run at 100 V in RNA electrophoresis buffer (1X MOPS).

2.2 Expression in *Xenopus laevis* oocytes

The human mGluR1α receptor was a gift from Professor S. R. Nahorski (University of Leicester, Leicester, U.K.). pcDNA3.0 vectors (Invitrogen, Paisley, U.K.) containing either P2X$_1$ mutant or wild-type P2X$_1$, mGluR1α receptors and N-termini minigenes were linearized. Sense-strand cRNAs were generated from these linearized plasmids with the T7 mMessage mMachine^{TM} kit (Ambion (Europe), Huntingdon, Cambs., U.K.).

Xenopus laevis oocytes stage V were prepared by enzymatic treatment followed by manual defolicolation as described previously (Hall *et al*, 2004). 50nl of mRNA (1 μg/μl) was injected into isolated *Xenopus* oocytes using Inject+Matic microinjector (J.Alejandro Gaby, Geneva, Switzerland). For co-injections with the minigene, the RNA was mixed to give 5 ng WT P2X$_1$ + 10 ng mGluR1α + 35 ng minigene (or appropriate volume of water was added in the absence of minigene) and injected in a 50 nl volume. Cells were maintained at 18 ºC in ND96 buffer (NaCl 96 mM, KCl 2 mM, CaCl$_2$ 1.8 mM, MgCl$_2$ 1 mM, sodium pyruvate 5 mM and Hepes 5 mM, pH 7.5) adding 50 μg/ml gentamycin and were used for recording after 24-72 hours.

2.3. Electrophysiological recordings

2.3.1 Two-electrode voltage clamping

The two-electrode voltage clamp technique was used on cRNA-injected oocytes to record responses to applied ATP (Mg^{2+} salt; Sigma, Poole, UK). Microelectrodes were pulled from filamented borosilicate glass using an automatic two stage puller (Narishige, Japan), so that the diameter of the tip was about 1 to 2 μm. The microelectrodes were filled with potassium chloride (3 M) solution and had resistances of 0.2 MΩ to 0.5 MΩ. Oocytes were placed in a 2ml volume chamber and perfused with buffer ND96 (NaCl 96 mM, KCl 2 mM, $BaCl_2$ 1.8 mM, $MgCl_2$ 1 mM, sodium pyruvate 5 mM and Hepes 5 mM, pH 7.5) at the flow speed of 2 ml/min. The oocytes were voltage clamped at a holding potential of -60mV using a GeneClamp 500B recording amplifier (Axon Instruments, Union City, CA, U.S.A). The data were digitized by Digidata 1322 analogue-to-digital converter and collected with pClamp 9.0 acquisition software (Molecular Devices, Menlo Park, CA) on a personal computer. The ATP with different concentrations was applied with the fast-flow U-tube perfusion system.

Measurement of EC$_{50}$

To estimate the EC_{50} value of the receptor, ATP (0.01 μM to 10 mM) was applied at 5 min intervals and reproducible ATP-evoked responses were recorded. Individual concentration–response curves were fitted with the Hill equation: $Y = [(X)^H \times M]/[(X)^H + (EC_{50})^H]$, where Y is the response, X is the agonist concentration, H is the Hill coefficient, M is the maximum response, and EC_{50} is the concentration of agonist evoking 50% of the maximum response. In the figures, concentration–response curves are fitted to the mean normalized data.

Characterization of the effects of MTS compounds

To study the effect of MTS compounds on ATP activation at WT and cysteine mutants, ATP at EC_{50} was applied. MTS reagents (1 mM) were made in ND96 solution immediately before use. The MTS compounds including MTSM(methyl methanethiolsulfonate), MTSB(butyl methanethiosulfonate), MTSEA (2-aminoethyl methanethiosulfonate hydrobromide), MTSET (2-(trimethylammonium)ethyl methanethiosulfonate bromide) and TMA-Cl(N-[2-(trimethylammonium) ethyl] maleimide chloride) (Toronto Research Chemicals, Toronto, Ontario, Canada) were bath perfused (for at least 5 min, the recovery time required between applications to see

reproducible responses) before co-application with ATP via the U-tube. This procedure should allow MTS reagents to bind to free cysteine residues in either the nonactivated (absence of ATP) or ligand-bound activated (presence of ATP) state. ATP was applied to the P2X receptors every 5 minutes for obtaining reproducible current up to 45 minutes. The MTS compounds were perfused into the bath between the 4th to 8th ATP applications, and thus the maximum effects exhibited during the 5th to the 8th ATP applications were compared to the ATP evoked response before the treatments (Figure 2.2). To determine if these effects are irreversible, the oocytes were washed in the bath for extra 5 to 10 minutes. Alternatively, oocytes were pre-incubated in 1 mM MTSEA solution for 60 minutes at room temperature immediately before recording.
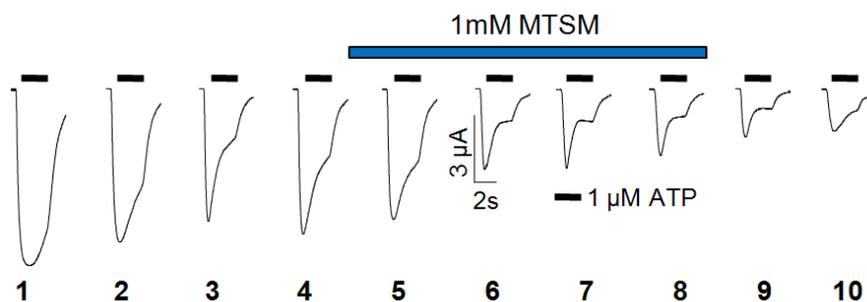
Figure 2.2 Protocol for characterising the effects of MTS compounds

The effect of MTSM to the WT P2X$_1$ receptors was studied by two-electrode voltage clamping methods on *Xenopus* oocytes. Reproducible currents of WT P2X$_1$ receptors were evoked by ATP (1 µM for EC50 level, as indicated in black bar) in 5 minutes intervals up to 45 minutes. After the first ATP application, the about 70% of the peak current amplitudes was maintained. MTSM (1 mM, indicated in blue bar) was perfused in bath immediately after the fourth ATP application and continued for 20 minutes. The maximum effects of MTSM were compared with the mean responses. Oocytes were washed in ND96 bath for extra 5 to 10 minutes after the MTSM treatment.

Apyrase treatment

To determine whether the channel opening by ATP binding was required for the action of MTSEA on cysteine mutants, the oocytes were treated for at least 30 minutes at room temperature before the recording in the presence of MTSEA (1 mM) and 3.2 units/ml of apyrase to break down any endogenous ATP.

Pharmacological treatment

For oocytes pre-treated with PMA, 100 nM PMA was made in ND96 solution and the oocytes were pre-incubated in the PMA solution for 10 minutes at room temperature immediately before recording. Comparisons were made between groups of control untreated oocytes and those exposed to PMA. The protein kinase inhibitors Calphostin

C(1 μM) (Sigma C6303), K252a (100 nM) (Sigma 05288), Gö6983(200 nM) (Sigma G1918) or Gö6976 (200 nM) (Sigma G1171) were incubated with the oocytes for 1 hour at room temperature before recording. When looking at the potentiation of the P2X$_1$ receptor, glutamate (100 μM) with or without the protein kinase inhibitors was bath-perfused for 5 min between the stimulations of the P2X$_1$ receptor by ATP via the U-tube as described previously. The glutamate was applied to the oocytes when stable responses were observed (Vial *et al*, 2004a).

Reversal potential

The reversal potential (Vrev) for the currents under different ionic conditions was obtained using a step and ramp protocol that changed the holding potential of the cell either under control conditions (no drug application) or during the desensitising phase of the P2X current.

For example, two ramps for 200 ms were run immediately after the peak current had been reached (as showed in figure 2.3). Each ramp increased or decreased the holding potential by 20 mV around the predicted reversal potential for each ionic solution (obtained from Evans *et al*, 1996). The ramp was preceded by a 200 ms step change in holding potential to the potential at the beginning of the ramp. If the channel is not cation selective, the predicted reversal potential for ND96 is approximately 0 mV. The reversal potential of the P2X receptor current was calculated from the intersection of the currents evoked in control conditions and during the application of agonist. The mean of the two reversal potentials obtained for each cell was calculated to give the reversal potential for each ion.
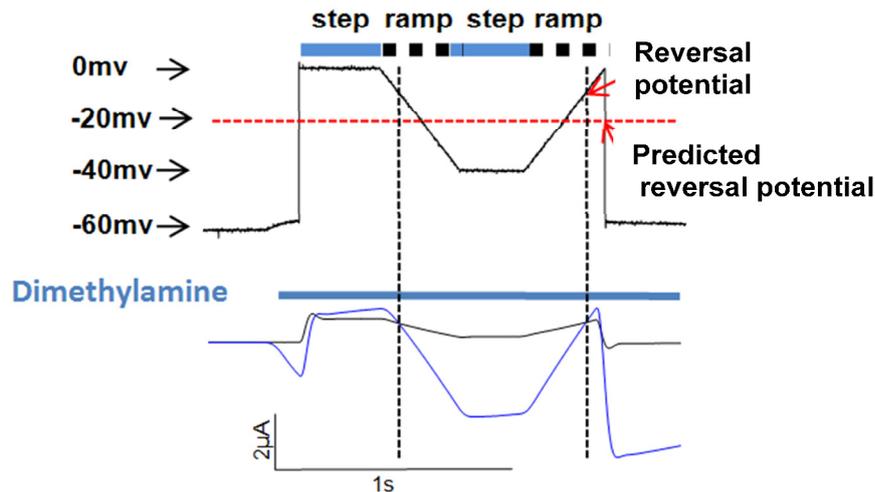
Figure 2.3 Step and ramp protocol for reversal potential
In this example, -20 mV was assumed to be the reversal potential (red dashed line) for dimethylamine based on previous study (Evans *et al*, 1996), and two ramps jump from 0 mV to -40 mV were given. A step period was inserted between the two ramps and allowed a recovery time of the evoked current. The periods for steps (blue line) and ramps (black dashed line) were continued for 200 ms each. The currents evoked on $P2X_1$ receptor with (blue) or without (black) the presence of 100 μM ATP in dimethylamine bath solution were overlapped, and the intersections to the corresponding potential were estimated as real reversal potential for dimethylamine.

2.3.2 Cell culture and whole cell patch clamping

Cell culture

Human embryonic kidney 293 (HEK293) cells stably expressing the human $P2X_1$ receptor were maintained in minimal essential medium with Earle's salts (with GlutaMAX I) medium supplemented with 10% fetal bovine serum, 1% nonessential amino acids (Invitrogen, Paisley, UK) at 37°C in a humidified atmosphere of 5% CO_2 and 95% air. For transfection, wild type HEK293 cells were plated at 10 cm^2 culture dish the day before transfection. cDNAs (4 μg) of WT and mutant $P2X_1$ receptors transiently dissolved in LipofectAMINE 2000 reagent/Opti-MEM (Invitrogen, Paisley, UK) were placed in the dish. Cells were maintained in normal culture medium at 37°C. The fluorescent pEGFP-N1 (Clontech, Cambridge, UK) vector (10% of total plasmid transfected) was co-transfected with $P2X_1$ plasmids as a control for identifying the transfection efficiency. When required for study, cells were attached to glass coverslips (13 mm) and used for experiments 24 + 72 hours after transfection.

Whole cell patch clamping

Currents from HEK293 cells were recorded 1–3 days after transfection. Patch pipettes were made with a two stage vertical pipette puller (PP-83, Narishige, Japan) from standard walled filamented borosilicate glass (Clark Electromedical, GC150F-7.5)

Pipette resistances were between 4-6 MΩ when filled with intracellular solution (potassium gluconate 140 mM, NaCl 5 mM, HEPES 10 mM, EGTA 9 mM, (pH adjusted to 7.3 with KOH). Cells were continuously perfused with an E_{total} solution (NaCl 150 mM, KCl 2.5 mM, HEPES 10 mM, $CaCl_2$ 2.5 mM and $MgCl_2$ 1 mM (pH adjusted to 7.3 with NaOH)), and agonists were applied rapidly using a U-tube perfusion system (Evans *et al*, 1994) for 200 or 500 ms at 5 min intervals. Whole-cell currents were recorded at a holding potential of -70 mV (including -10 mV tip potential referring to the liquid junction potential between the pipette-filling solution and bath) at room temperature. Membrane currents were acquired by Digidata 1322A interface (Axon Instruments) with a PC computer. Currents were recorded with an Axopatch 200B amplifier and data was collected using pClamp9 software (Axon Instruments, U.S.A.)

2.4 Western blotting

The expression levels and molecular weight of the $P2X_1$ receptor proteins were estimated by Western blotting, and both total and plasma surface protein expressions were revealed by the anti-$P2X_1$ antibody. Different pre-treatments were required for total, surface and other protein detections before running on the SDS-PAGE gel. The $P2X_1$ receptor protein was treated in different ways. It was targeted and amplified by primary and secondary antibodies respectively, and the immunostaining was visualised by enhanced chemiluminescent detection (ECL) kit in the end.

(i). Total protein detection

For the total expressed proteins, the oocytes injected previously with 50 ng of cRNA were homogenized in buffer H (100 mM NaCl, 20 mM Tris·Cl, pH 7.4, 1% Triton X-100, 10 µl/ml protease inhibitor cocktail (Sigma P8340)) at a dilution of 20 µl/oocyte. After centrifugation at 16,000 × g (4 °C) for 2 min, a 10 µl aliquot of the supernatant as extracted and mixed with 10µl gel sample buffer (50 mM Tris·Cl, pH 6.8, 10% β-mercaptoethanol, 2% SDS, 10% glycerol).

(ii). Surface protein detection

To detect the proteins expressed on the cell surface, oocytes were incubated in 0.5 mg/ml Sulfo-NHS-LC-Biotin (Pierce) for 30 minutes for biotinylation. After washing five times in ND96, oocytes were homogenized in buffer H (20 µl/oocyte) with

the protease inhibitor cocktail and centrifuged at $16000 \times g$ (4 °C) for 2 min. For isolation of biotinylated proteins, 30 µl of streptavidin agarose beads (Sigma) were added to 400 µl of supernatant and mixed on a rolling shaker at 4°C for 3 h. Beads were washed in homogenisation buffer for three times and 20 µl of gel sample buffer added.

(iii). Cross-linking with DTSSP

Oocytes previously injected with wild-type or mutant $P2X_1$ cRNA were homogenized in phosphate-buffered saline plus 1% Triton X-100 (20 µl per oocyte; 15 oocytes per reaction) and rolled at 4°C for 15 min. After centrifugation (16000 g at 4 °C for 2 min), 20 µl of the supernatant was mixed with an equal volume of 3,3'-dithio-bis(succinimidyl-proprionate) (DTSSP; Pierce) in phosphate-buffered saline plus 1% Triton X-100 to give the appropriate concentration of cross-linking agent. Reactions were incubated at room temperature for 30 min and 2 µl of 1 M Tris·Cl, pH 7.4, was added to quench the reaction. An equal volume (40 µl) of SDS-PAGE sample buffer (minus the reducing agents DTT and β -mercaptoethanol) was added and the samples heated at 70°C for 2 min before separation on a 10% SDS-PAGE gel. Cross-linked $P2X_1$ receptors were visualized by Western blotting and anti-$P2X_1$ antibody staining as described below.

SDS-PAGE staining and visualization

Samples were heated for 5 min at 95 °C, and separated on 8% SDS-PAGE gel. The gel was transferred to nitrocellulose and blocked in TBST (20 mM Tris·Cl, pH 7.6, 145 mM NaCl, 0.05% Tween 20) plus 5% milk powder overnight. The membrane was incubated with anti-$P2X_1$ antibody (1:1000 dilution) (Alamone, Israel) in TBST + 5% milk powder for 1.5 h, washed three times for 5 min in TBST, and incubated with anti-rabbit horseradish peroxidase secondary antibody (1:2000 dilution) (Sigma) for 60 min. After three 5-min washes in TBST, visualization of the protein bands was achieved with an ECL (Plus) kit (Amersham Pharmacia Biotech).

2.5. Data analysis

All data are shown as means ± SEM. For comparisons among more than two groups against the control (e.g. WT and mutant current amplitudes, time-courses, agonist potency, and MTS reagent modifications), any significant differences were determined by one-way ANOVA, followed by Dunnett's test for comparisons using the Graphpad

Prism 5 for Windows (GraphPad Software, San Diego, CA). For studies comparing two groups, the differences of any changes were determined with the appropriate Student's *t* test and considered to be significant when $p<0.05$. *n* corresponds to the number of oocytes tested for electrophysiological data. For potential studies the level of regulation was variable between batches, so data are compared with in the same batch.

Chapter 3. Concatenated P2X$_1$ receptor channels

3.1 Introduction

The subunit assembly of P2X receptors has been suggested to be trimeric. The initial evidence came from chemical cross-linking and BN-PAGE methods (Nicke *et al*, 1998; Kim *et al*, 2001), in which the trimer was estimated via the molecular mass and shown as the preferable form for P2X$_1$ and P2X$_2$ receptors in the native state. Recent studies with atomic force and electron microscopy further illustrated that the trimer is the major form for P2X receptors (Barrera *et al*, 2005; Mio *et al*, 2005; Young *et al*, 2008). For example, the molecular volumes of P2X$_2$ and P2X$_4$ receptors were determined and both of them corresponded to the size of trimers. Nevertheless, the contributions of indivudial subunits to channel responses were still unclear. The roles that individual subunits play in the homotrimeric or heterotrimeric P2X receptor channel remains as a major question.

3.1.1 Using concatenation channels to study subunit interaction

Subunit assembly of heteromeric and homomeric channels has been applied to a wide range of ligand-gated channels. For example, to study the assembly of heteromeric 5-HT$_3$ receptors, 5-HT$_{3A}$ and 5-HT$_{3B}$ subunits were expressed in cells, and the surface expression was estimated by agonist applications and western blotting (Boyd *et al*, 2002). In addition, the chemical cross-linking method was also a useful approach to analyse the properties of single subunits (Barrera *et al*, 2005). DSS (disuccinimidyl suberate) is able to link the neighbouring subunits together and higher oligmers of P2X$_2$ subunits were revealed on the gel subsequently. Subunit co-expression is useful to detect the properties of heteromeric channels, however, when two or more individual subunits are mixed together it is difficult to determine the ratios and positions taken by each subunit in mutated homomeric or heterotrimeric channels. This gives rise to a range of possible subunit combinations that complicate (See figure 3.1) the analysis of the properties of the channels following heteromeric assembly. For example, the P2X$_1$ and P2X$_2$ subunits were confirmed to make up P2X$_{1/2}$ heteromeric channels following co-expression (Torres *et al*, 1999) and the P2X$_{1/2}$ heteromeric channel is expressed in neurons (Calvert *et al*, 2004). However, co-expression does not indicate whether any of the six different expression patterns (P2X$_1$- P2X$_1$-P2X$_2$, P2X$_1$- P2X$_2$- P2X$_1$, P2X$_2$-P2X$_1$- P2X$_1$, P2X$_2$- P2X$_2$- P2X$_1$, P2X$_2$- P2X$_1$- P2X$_2$, P2X$_1$- P2X$_2$- P2X$_2$) (See figure 3.1)

is more preferable *in vivo*. To overcome this difficulty and evaluate the properties and interactions of each subunit to the whole channel in a more reliable way, P2X concatenated channels which arrange the subunits in a fixed order will be used.
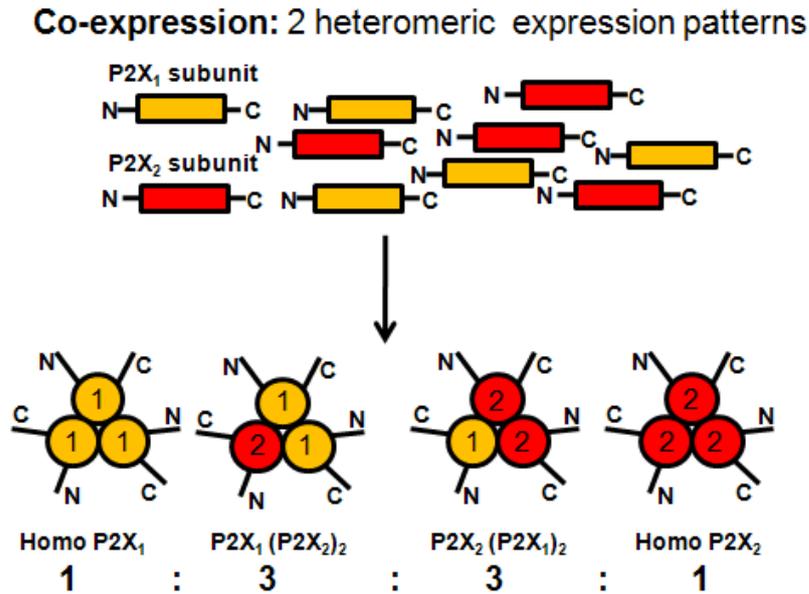
Figure3.1: The six different expression patterns of P2X$_{1/2}$ heteromeric channel.
The trimer is the essential form of P2X receptors. **(A).**The P2X$_1$ and P2X$_2$ subunits were confirmed to make up P2X$_{1/2}$ heteromeric channel by co-expression (Calvert *et al*, 2004). When P2X$_1$ and P2X$_2$ subunits were co-expressed together, the expression ratio of four different expression patterns should be 1:3:3:1 assuming random association. (yellow circle for P2X$_1$ subunit and red for P2X$_2$).

Concatenation refers to the attachment of multiple copies of a cDNA sequence arranged in an end to end order (See figure 3.2). The concatenation approach is a popular strategy to assess the function of specific subunits in a multimeric channel, and its most prominent usage is providing a feasible way to investigate subunit interactions. It can be used to manipulate the channel components at the cDNA level, and the interactions between different subunits at specific positions can be detected. By using concatenation, six different concatenated P2X$_{1/2}$ channel trimers can be generated by linking the sequence of P2X$_1$ or P2X$_2$ subunit in different orders (See figure 3.1). The expressions and properties of these heteromers can be distinguished afterwards by electrophysiological or biochemical methods.

Subunit concatenation
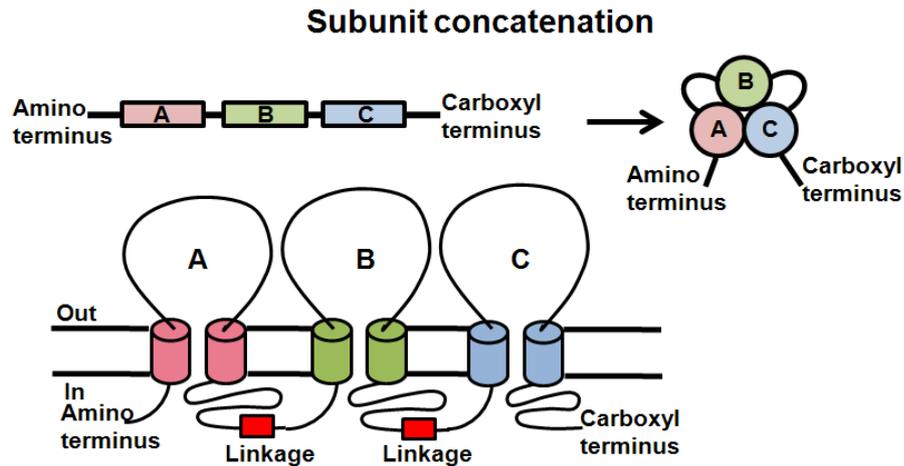
Figure 3.2: Concatenated channel linking the subunits in an end-to-end manner.
Concatenation refers to the attachment of multiple copies of a cDNA sequence arranged in an end to end order. Compared to the co-expression method, concatenated channels are able to link subunits together in a specific order. The composition of single channel can also be determined and fixed by the concatenated channel.

3.1.2 Various applications of concatenated channels

Subunit concatenation has been a popular method and used in the potassium and sodium channels (Isacoff *et al*, 1990; Liman *et al*, 1992; Pessia *et al*, 1996; Firsov *et al*, 1998). The application of concatenated channels in research started from the study of voltage-gated potassium channels heteromultimers (Isacoff *et al*, 1990). Subsequently, the quaternary structures (Liman *et al*, 1992), positional effects of subunits around the channel pore (Pessia *et al*, 1996), functions of specific amino acid residues (Hurst *et al*, 1995) and the interaction between subunits of potassium channels (Preisig-Muller *et al*, 2002) were investigated by producing concatenated constructs.

Liman *et al* tried to examine the subunit stoichiometry by linking together the coding sequences of two, three, four and five Kv1.1 channel subunits, and these constructs lead to channel expression only through the formation of functional tetramers. This indicated that functional Kv1.1 channels tend to be made up of four subunits (Liman *et al*, 1992). Later, the subunit positional effects of Kir4.1/5.1 heteromeric channels were revealed by Pessia (Pessia *et al*, 1996). The order of subunits within the potassium channels was found to contribute different functional properties, heteromeric channels of Kir4.1 and Kir5.1 produced normal currents only when the subunits of Kir4.1 and Kir5.1 were arranged in the order of 4-5-4-5, not 4-4-5-5 (Pessia *et al*, 1996). This finding stressed the importance of the position of the subunits within the ion channel, and gave us a clue

to further explore the properties of the heteromeric channels by using the concatenated approach.

Concatenated channels have also been used to study the effects of a single residue in multimeric ion channels. The effects of proline residues in the S4 transmembrane domains of Kv1.1 were studied by introducing point mutations in concatenated cDNA sequences (Hurst *et al*, 1995). The results suggested the Kv1.1 channels can only be formed with proline substitution in one of the subunits. The channels appeared to be formed as multimerized concatemers with two proline substitutions, in which the pro-containing domains are excluded from the pore formation (Hurst *et al*, 1995).

In addition, the interactions between the intracellular domains of different subunits were probed by the concatenation methods in the Kir 2.2/2.3 heteromeric channel. Kir2.2/2.3 concatenated potassium channels were produced to study the relationship between different phenotypes and Anderen's syndrome (Preisig-Muller *et al*, 2002). The interaction of N-terminus and C-terminus was detected from yeast two-hybrid analysis, and this interaction was presumed to be involved in the assembly of the potassium tetramer channels.

Concatenated constructs were also helpful to find out the recognition site which is necessary for heteromeric but not homomeric channel assembly within the same subfamily (Lee *et al*, 1994). The deletion of 225 amino acids in the amino-terminal of hKv1.4 channels prevented the formation of hybrid channels containing the hKv1.4 and hKv1.5 subunits, but had no effect on the formation of homomeric hKv1.4 channels (Lee *et al*, 1994).

Not only potassium channels, but also many other membrane proteins have been studied by the concatenation strategy, including ligand-gated GABA$_A$ receptors (Baumann *et al*, 2001) and ENaC (Firsov *et al*, 1998). The pentameric arrangements of the GABA$_A$ receptor were confirmed by linking different subunits using linkers of different lengths. The minimal length of the linker was determined to be 10 and 23 amino acid residues for α-β and β-α respectively, and in addition to glutamine, alanine and proline residues were introduced to the linker sequence to prevent early termination of protein synthesis (Baumann *et al*, 2001). Finally, the GABA$_A$ receptor composed of α and β units was

proposed to contain two α and three β units, and the receptor composed of α ,β and γ units was proposed to have the arrangement of βαγβα (Baumann *et al*, 2001). Furthermore, ENaC was found to have a four subunit stoichiometry (using a linker of eight glutamines as the inter-subunit bridge) and the arrangement of the subunits around the channel pore prefers to form a α-β-α-γ configuration (Firsov *et al*, 1998).

Although the majority of the trials produced the concatenated channels as designed, some of them failed. These results either implied that the concatenated constructs had influences to the associations among the subunits, or the subunits formed the ion channels pore from different concatenated constructs (Liman *et al*, 1992; Hurst *et al*, 1995).

3.1.3 Concatenation applications on P2X receptors

P2X receptors have been studied using the concatenated approach (Stoop *et al*, 1999; Nicke *et al*, 2003), and $P2X_2$ concatenated channels were successfully generated. The first concatenated P2X channels were constructed by Stoop using the compatible restriction sites MfeI (CAATTG) and *EcoRI* (GAATTC) in the conjunctional regions of $P2X_2$ subunits (Stoop *et al*, 1999). These two restriction sites can overlap with each other for ligation, and the cohesive ends are not re-cleaveable afterwards. During the series of digestions and ligations, the *EcoRI* restriction site will be lost, and the MfeI site can be used repeatedly to obtain longer concatemers. A linker of 16 amino acids was applied to link the subunits together. There was a unique BsrGI site in the linker sequence. Hence, although the fragment of the linker is quite small and hard to visualize on a gel, its existence could be detected by digestion. The concatenated $P2X_2$ ion channel was found to be functional. It was subsequently studied by the substituted cysteine accessibility method and the responses after the application of ATP are shown in figure 3.3. MTSET ((2-(trimethylammonium) ethyl methanethiosulfonate, Bromide) is a methanethiosulfonate reagent that can bind to accessible cystienes. Previous studies (Rassendren *et al*, 1997; Egan *et al*, 1998) demonstrated complete inhibition by MTSET modification at T336C mutant whether ATP is binding to the receptor or not, and indicated this amino acid lined the ion permeation pathway. To find out whether there is any correlation between the number of MTSET molecule bind to the channel and inhibition levels, concatenated trimeric $P2X_2$ channels bearing the WT and T336C mutated subunits in different composition were produced. As controls, the C-C-C

(consists with 3 cysteine mutated subunits) and T-T-T (consists with 3 WT subunits) trimeric channels as control groups exhibited fully inhibited and non-affected by MTSET. Compared to the C-C-C, the T-T-C, T-C-T, C-T-T trimeric channels (containing one mutated subunit at different positions) and T-C-C, C-T-C, C-C-T trimeric channels (containing two mutated subunit at different positions) shown about 1/3 and 2/3 of the full inhibition respectively. To conclude, introduction of one, two or three point mutations into the trimeric receptor resulted in a progressive increase in sensitivity to inhibition by MTSET, and the effects were not dependent on the subunit position (Stoop *et al*, 1999). The results show that a "per-subunit" channel block causes the blocking effects of MTSET and they suggest that maximally three subunits participate in the channel formation. However, Stoop did not suggest if the properties of the concatenated channels were affected by the linker sequence (Stoop *et al*, 1999).
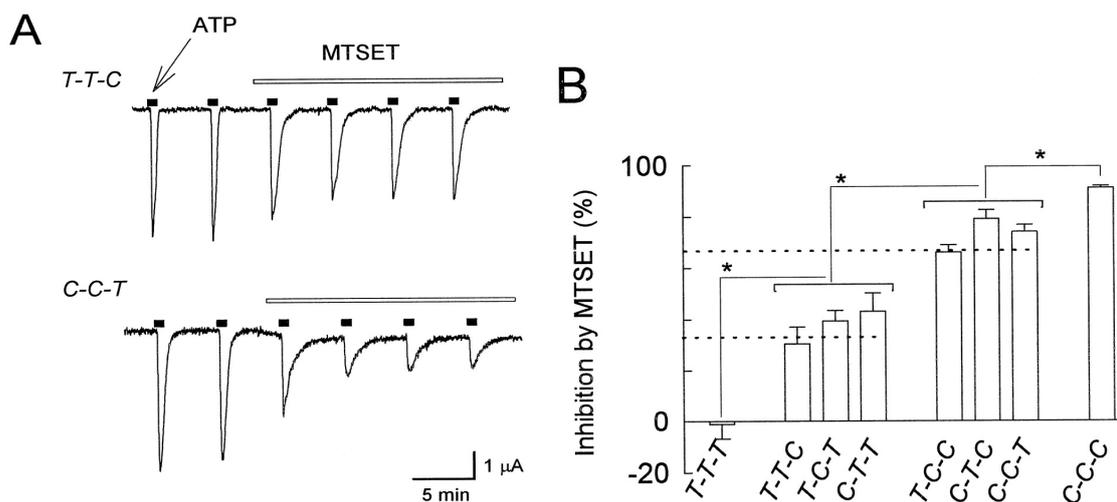
Figure 3.3 Responses of concatenated trimeric P2X$_2$ receptor subunits.
The functional concatenated P2X$_2$ ion channels were produced by using the designed linker of 16 amino acids. MTSET reagents can binds to the free cysteine at the extracellular loop, and inhibit over 90% of the peak response to ATP at T336C mutant of P2X$_2$ receptor. The concatenated trimeric P2X$_2$ receptor containing the cysteine mutated subunit constructed, and the inhibition induced by MTSET were reduced by 1/3 and 2/3 respectively to the complexes with one or two mutated subunit. This effect is independent to the subunit position (Stoop *et al*, 1999).

Recently, the concatenated strategy was used to characterize the P2X$_2$ receptor intersubunit dependence of zinc potentiation (Nagaya *et al*, 2005). Previous studies suggested that histidine contributes to the binding of the allosteric modulator zinc, and two residues His[120] and His[213] at the rat P2X$_2$ receptor have been identified relating to zinc potentiation . Single or double alanine mutations of these histidine residues were introduced at first. Subsequently, the P2X$_2$ monomers were concatenated with modifications at the intracellular ends, and the trimers with (HH-HH-HH, HA-AH-HH,

and HA-AA-AH) or without (AA-AA-HH) at the intersubunit zinc binding site were regenerated. As a result of the application of zinc, no potentiation was observed for the trimer without the intersubunit zinc binding site, and the potentiation levels measured on the three trimers with three, two or single intersubunit binding site decreased with the gradient. The likely explaination is the His^{120} and His^{213} residues that are close to each other across the interface between the subunits form the intersubunit zinc binding site.

Nicke and colleagues tried to modify the N and C terminals of the $P2X_1$ subunit and generated concatenated channels using a similar strategy as applied for $P2X_2$ receptor concatenation (Nicke *et al*, 2002). Instead of MfeI and *EcoRI* restriction sites, another pair of restriction sites *NcoI* (CCATGG) and *BspHI* (TCATGA) with compatible cohesive ends were selected for concatenation. Only one *NcoI* site will be kept to repeatedly introduce the $P2X_1$ subunit cDNA sequences. The linker sequences used to link the adjacent two subunits was a double-stranded oligonucleotide of 45 base pairs encoding $G(Q)_5VMA(H)_6$. Cloning was performed many times to engineer the $P2X_1$ receptor multimeric channels and the junction sequences were then confirmed by sequencing. The strategies Nicke and colleagues used to construct the concatenated $P2X_1$ receptor trimers were quite similar to those used in generating the $P2X_2$ concatenated trimers (Stoop *et al*, 1999). Nevertheless, Nicke showed that concatenated $P2X_1$ receptors were not functional, only a minor amount of concatenated trimer reached the cell membrane (Nicke *et al*, 2003).

To understand the reasons why the $P2X_1$ subtype subunits cannot express concatenated cDNA using the methods above, while $P2X_2$ subunits can, the structural differences should be considered carefully. Compared to the $P2X_2$ subunit, the length of $P2X_1$ receptor carboxy terminus is 44 amino acids which is 74 amino acids less than $P2X_2$ receptor (North, 2002). This indicates that the length of the carboxy terminus may be a significant factor towards the concatenated channel expression. It is possible that the $P2X_1$ subunits require longer linkers to allow the intracellular domains, which play important roles in channel gating, to be folded properly, or the linker of only 15 amino acids is too short to make the intracellular domains of $P2X_1$ subunits flexible.

3.1.4. Aim

Concatenated channels are useful models to investigate the intersubunit regulation of multimeric ion channels. Functional $P2X_2$ concatenated channels have been constructed and used in studying subunit stoichiometry and binding sites. Once a functional concatenated $P2X_1$ trimer ion channel has been produced, there will be certainly more insights about the $P2X_1$ receptor intersubunits interactions. For the homomeric $P2X_1$ concatenated channel, single mutations can be introduced in the sequence, and the roles of individual subunits in receptor regulation can be determined (See figure 3.4). Nicke's group found the $P2X_1$ trimeric concatemer with similar linker as applied to the $P2X_2$ channel tended to break down in the endoplasmic reticulum and failed to express efficiently at the cell membrane (Nicke, 2003). Therefore, I attempted to see if more flexible or longer linkers can allow functional expression of $P2X_1$ concatenation, and these concatenated constructs can be used as a model to further investigate the roles of individual subunit.
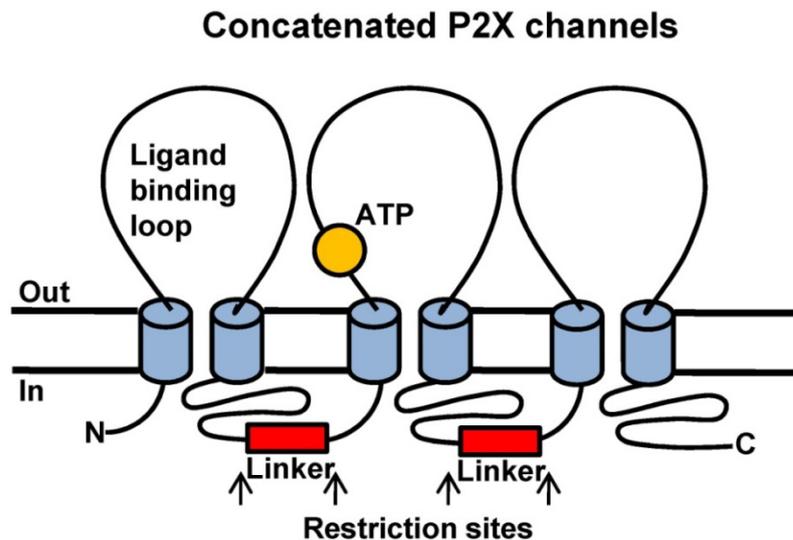
Figure 3.4: The roles of individual subunits in regulating the receptor can be studied by a concatemer approach.
This schematic illustrates the model of concatenated P2X channels. Three subunits contributing to a functional P2X channel were linked by designed linkers (red box). Compatible restriction sites were added to the N and C terminals of P2X subunit to facilitate concatenation. The yellow dot indicates a single mutation at the assumed binding-related residue in one of the subunits. Once the trimeric P2X channel with mutation at different subunits are produced by concatenation, the intersubunit binding sites for agonists and the roles of single amino acid to functional receptor can be investigated.

3.2 Results
3.2.1   P2X$_1$ concatenated channel construction

3.2.1.1 Generation of linker sequences for concatenation

In a concatenated P2X$_1$ trimeric channel, the P2X$_1$ subunits will be joined together by linker sequences between the intracellular domains (See figure 3.4). Since both the length and the sequences of intracellular domains of P2X receptors are involved in channel expression, the linker sequence should be designed with caution. The concatenation approach has been applied to the P2X$_1$ receptor previously, and Nicke reported that their concatenated P2X$_1$ trimeric channels cannot be expressed on the cell membrane (Nicke *et al*, 2003), while the P2X$_2$ concatenated channel can be expressed very well using the same linker sequence. Most of the P2X$_1$ concatenated complex was broken down into monomer or dimer in the ER. By comparing the sequence of the P2X$_1$ and P2X$_2$ receptor, the C-termini of P2X$_1$ receptor subunit is much shorter than the P2X$_2$ subunit. As the intracellular domains of the P2X receptor are essential in regulating channel folding (Boue-Grabot *et al*, 2000; Jiang *et al*,2001; Ennion *et al*, 2002a), and a conserved YXXXK at the C-termini is involved in the protein trafficking (Chaumont *et al*, 2004) a longer length of the intracellular C-terminal may be required for P2X$_1$ concatenated channel expression. A longer linker which further extended the length of P2X$_1$ intracellular regions could provide more possibility to the interactions in these domains and aid the subunit folding of intracellular domains. Therefore, the linker strategy is a key factor to determine the feasibility of the concatenation and a long sequence linker for P2X$_1$ subunit needs to be generated. In this project, a shorter linker sequence with 14 amino acids for gaining a more flexible linkage will be produced at the first stage. A longer linker with 52 amino acids will be synthesised as well, its length is about four times of the shorter one.

The shorter linker containing an amino acid sequence of "HGQ$_4$GQ$_4$GLM" was generated firstly (Linker 2 as described in 3.4 appendix) (See figure 3.5). Glycine and glutamine are the two predominant amino acids that constitute the linker sequence. Both of the two amino acids are non-charged and are expected to have no effect to receptor folding and gating properties. In addition, unlike other amino acids, glycine contains a hydrogen rather than a carbon in its side chain. This property allows the glycine-rich sequence to be more conformationally flexible, and this sequence with two more glycines than used in Nicke's study may show more flexibility.

(A)

C CAT GGA CAA CAG CAA CAA GGA CAA CAG CAA CAG GGA CTC ATG A

NcoI · G · Q · Q · Q · Q · G · Q · Q · Q · Q · G · BspHI

(B)
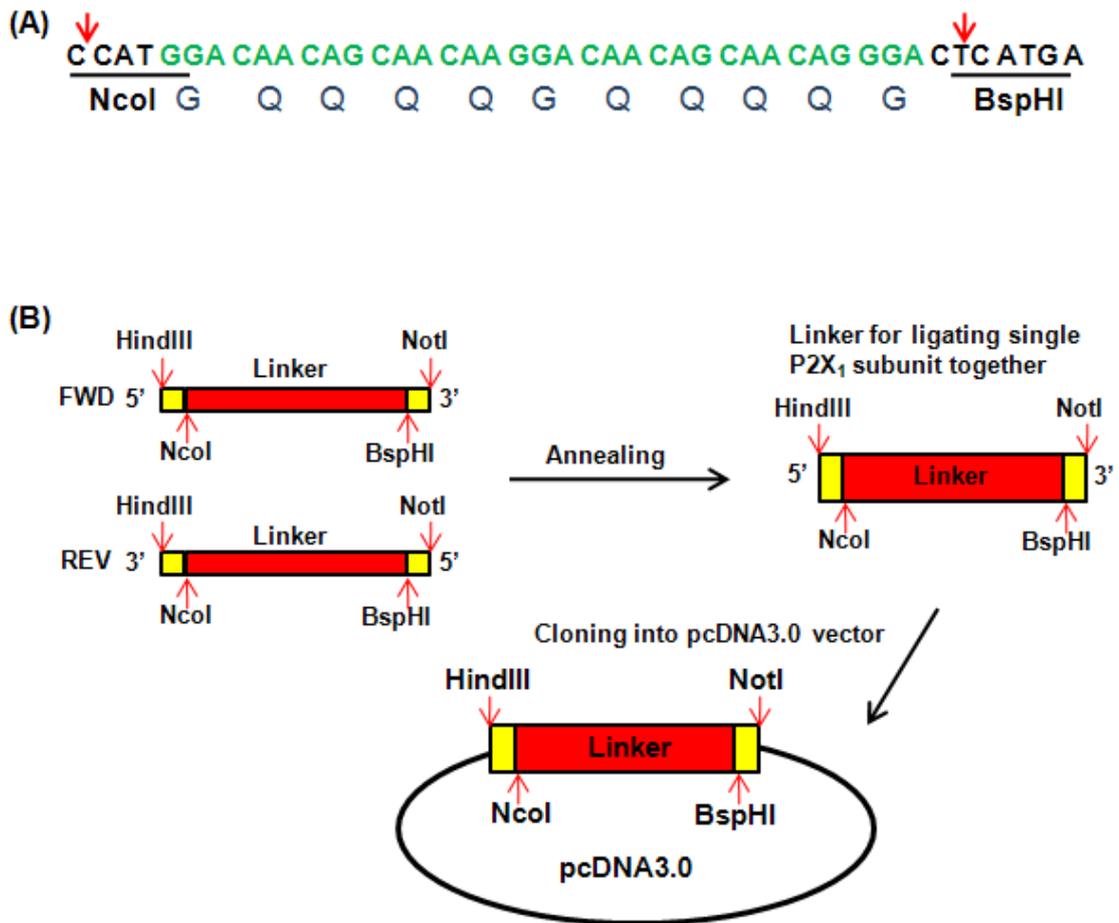
Figure 3.5 The linker was generated by annealing two primers together
(A). Non-charged glycine and glutamine (blue) were used in the designed primer sequences. *NcoI* and *BspHI* restriction sites (bold and underlined) for further insertion in the concatenated constructs were added to the ends. **(B).** To make up a single linker, two complementary primers were annealed together at 50°. The forward (FWD) and reverse (REV) primers encoding the same sequences as indicated in red box, and the *HindIII* and *NotI* restriction sites for cloning in pcDNA3.0 vector were shown as yellow box.

The linkers for the concatenated channel were generated by annealing two complementary primers together. Then these sequences were cloned into the native pcDNA 3.0 vector as the linker vector using the *HindIII* and *NotI* restriction sites at the ends of the linker sequence. The generation of the longer linkers started from this short one. Linker sequences without *NcoI* and *BspHI* sites were produced by annealing two double-stranded oligo-nucleotides, and they can be added in to the linker vector directly using the overlapped restriction sites. Then, the length of the linker can be extended by repeated ligation of Linker1 into the linker vector containing Linker 2 (See figure 3.6). The linker sequences and the complementary primers used for annealing are show in table 2.4 (refer to material and methods chapter).

Due to the existence of compatible *NcoI* and *BspHI* restriction sequences at the ends of Linker 1, one Linker 1 sequence ligated to another Linker 1 sequence in an end to end manner automatically during the annealing period. As a result, the sequence of Linker 1 was extended by duplication and a longer linker of four times the originally designed "HGQ$_4$GQ$_4$GLM" sequences was obtained. With the additional 52 amino acids, the length of P2X$_1$ receptor C-terminal was close to that of the P2X$_2$ receptor and may give a increased flexibility. Therefore, I constructed the concatenated channel by using the four times linker, to find out if it was long enough for efficient channel gating and expression. The sequences of the linkers were verified by sequencing (See figure 3.7).

3.2.1.2 Restriction sites selection

The conjunction regions in the concatenated complexes were modified with restriction sites to facilitate the concatenation, and the compatible *NcoI* and *BspHI* sites (Refer to figure 3.5) were introduced to the ends of the P2X$_1$ subunits and linkers. The sequences of the *NcoI* (C^CATGG) and *BspHI* (T^CATGA) restriction sites share the same sequence "CATG" in the middle, they are therefore compatible to each other. Take the

P2X$_1$ subunit cDNA sequence for example, the *NcoI* site ( ) was placed at the

beginning and the *BspHI* site ( ) was placed at the end. When the *NcoI* site was cut by the corresponding restriction enzyme, another sequence with *NcoI* and *BspHI* at the ends would be able to ligate with the original *NcoI* site. However, the site which is
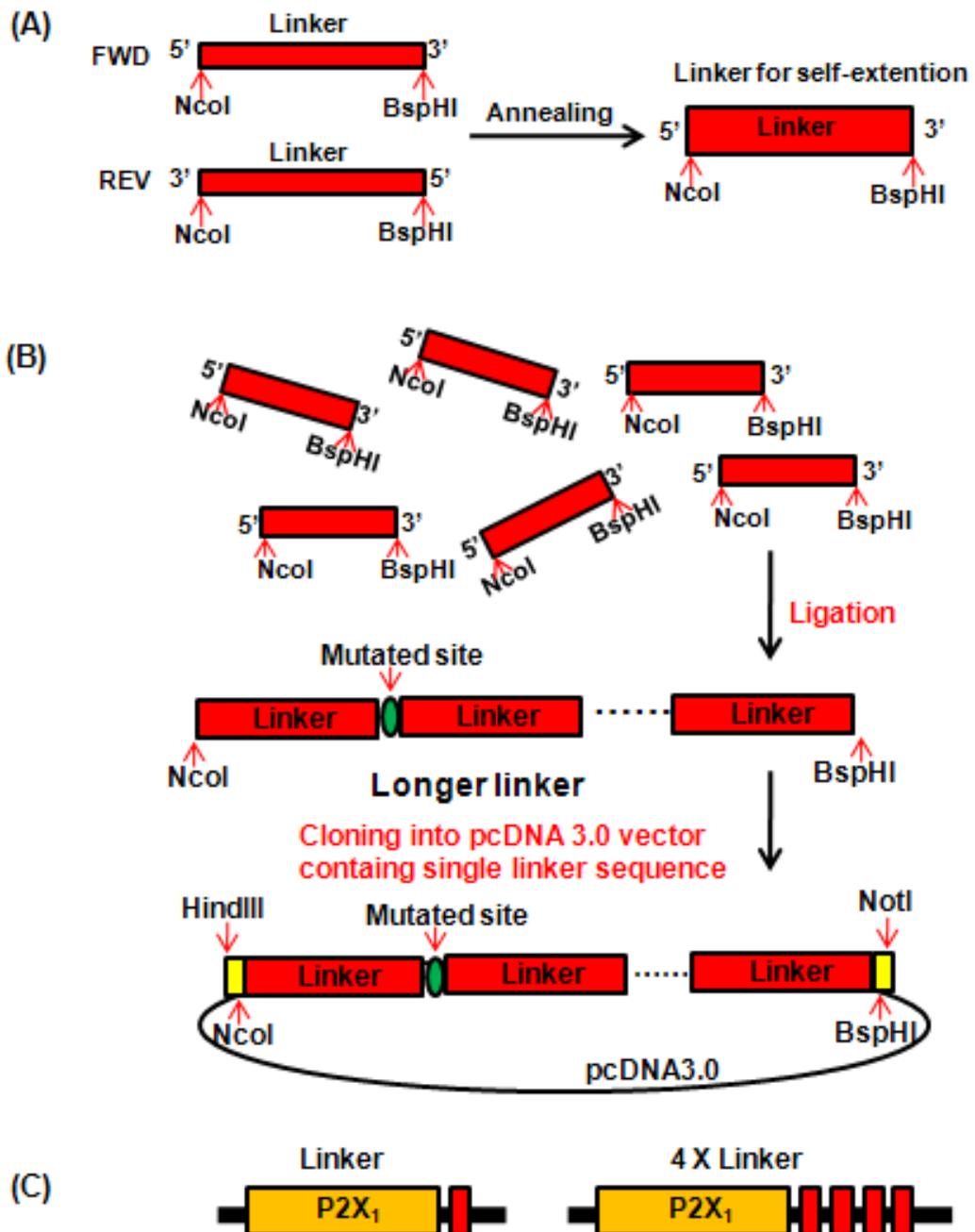
Figure 3.6 The length of linker sequence can be extended by repeating the linker ligation
(A). The linker sequence without the *HindIII* and *NotI* restriction sites at both ends used for extension of linkers before introduction into the plasmid vector. It was generated by annealing two complementary primers as described.**(B).** Due to the existence of compatible *NcoI/BspHI* ends, the linkers will be able to recognize another linker fragment and extend itself by repeating the ligation automatically. The mutated site is shown in green. Once the longer linker was constructed , it was cloned into the pcDNA3.0 vector for further usage.**(C).** Both single linker and 4 times length linker have been produced.
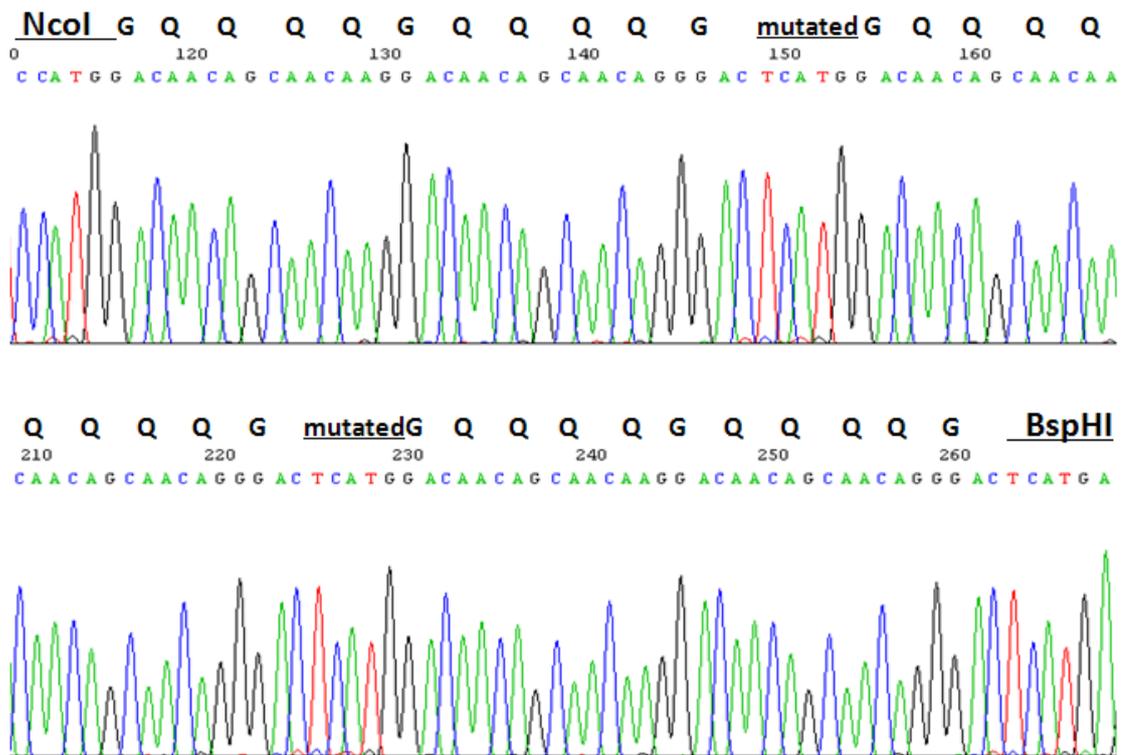
Figure 3.7 Sequencing of the longer linker
Sequencing was analyzed by Chromas 2.3 (Tchnelysium). Four different bases are labeled in different colours (A is green, T is red, C is blue and G is black). The background of the sequencing is clean and the *NcoI* site at the beginning of the linker sequence is at about 120bp and the *BspHI* site as the end of the sequence is about 230bp. *NcoI* and *BspHI* sites are compatible to each other. The linker sequence was extended by its automatic ligations and restriction sites were mutated after the ligations. The restriction sites are highlighted.

made up by *NcoI* and *BspHI* will form a new site of "TCATGG" (), which cannot be recognized by either restriction enzyme, and the only *NcoI* site at the beginning of the entire sequence will be maintained and used after. Thus, new sequences can be introduced to form the concatenated channels by cutting and ligating using these two restriction sites.
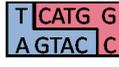
3.2.1.3 P2X$_1$ subunit concatenation

Preparation of the vectors and the P2X receptor sequences

Since the *NcoI* and *BspHI* sites were selected to generate concatenated channels, the endogenous *NcoI* and *BspHI* restriction sites in plasmid pcDNA 3.0 vector were required to be removed first. There are 3 *NcoI* restriction sites and 2 *BspHI* sites present in the pcDNA3.0 vector and the locations were determined from the plasmid map as shown in figure 3.8. Respectively, the locations are 610 (inside of the CMV promoter), 1958 (inside of the SV40 promoter), 2693 (inside of the Neomycin resistance gene) base pairs for *NcoI* and 4332 and 5430 (intergenic regions, not important for expression) base pairs for *BspHI* from the replication origin site of the plasmid, and the sites were all removed by site-directed mutagenesis.

Take the *NcoI* sites for example. During the point mutations, a single thymine (T) was converted to cytosine (C) in the *NcoI* restriction site. Although the nucleic acid sequences were changed, the protein sequence of the Neomycin resistance gene for expression on pcDNA3.0 vector will not be affected by the changing this single base pair. In this example, the codon "CAT" codes for threonine in the previously *NcoI* site, after converting the "T" to be "C" , the new codon "CAC" is still coding threonine. The mutations were confirmed by digestion with *NcoI* restriction enzyme, and runing the products on a gel (See figure 3.8). For the WT pcDNA3.0 vector, there were 3 bands which indicated 3 *NcoI* sites exist in the plasmid. The bands obtained after digestions were fewer as the mutation had removed the original sites. The last PCR product pcDNA 3.0 T613C was no different from the uncut plasmid after *NcoI* digestion. All other endogenous *NcoI* and *BspHI* sites inside of the P2X$_1$ receptor sequences were removed by mutagenesis as well. These mutations were checked by *NcoI* and *BspHI* digestions individually.

(A)

NcoI
610bp

NcoI
1958bp

pcDNA3.0
5428bp

origin

BspHI
5430bp

BspHI
4332bp

NcoI
2693bp

After the removal
of 3 NcoI sites

pcDNA3.0
5428bp

origin

BspHI
5430bp

BspHI
4332bp

(B)

A B C D E

5.4kb
4.1kb
3.3kb   uncut uncut

1.3kb 1.3kb

0.7kb

(C)

Sample	A	B	C	D	E
Primers for mutation	pcDNA3.0	T4445C	T3707C T4445C	T613C T3707C T4445C	Uncut plasmid
Size of band 3	0.7kb				
Size of band 2	1.3kb	1.3kb			
Size of band 1	3.3kb	4.1kb	5.4kb		

Figure 3.8 Three endogenous NcoI sites in the pcDNA 3.0 vector were removed and examined on agarous gel
(A). There are three *NcoI* restriction sites as shown in the pcDNA 3.0 vector. To use the *NcoI* site at the beginning of P2X$_1$ receptor sequence in concatenation, the endogenous *NcoI* sites present in the pcDNA 3.0 plasmid need to be removed first. (B). The *NcoI* sites were removed by site-directed mutagenesis one after the other, and the mutations were checked by digestions and visualized on gel. The sizes of bands after each mutagenesis step were calculated and shown in the table. (C). After the removal of T613, there were no more *NcoI* restriction sites. Thus, the bands shown as uncut pattern of the final stage where the supercoiled, coiled and linear DNA bands were presented.

Construction of "donor" and "acceptor" vectors

To simplify the steps for making the concatenated channels, the donor vector and acceptor vector were generated first. Once the linker with the desired length was obtained, $P2X_1$ receptor sequences without a stop codon can be inserted into the vector containing the linker, making this vector the "donor" vector (Figure 3.9). The fragment with the $P2X_1$ receptor and linker sequences is the basic construct for multiple subunit concatenation. This donor construct can extend the number of subunits put into the final concatenated channel. The other construct is the "acceptor" vector. This vector contains the $P2X_1$ subunit with the stop codon at the end and this subunit is the last subunit in the concatenation construct (See figure 3.9). All of the $P2X_1$ subunits with linker constructs from the "donor" will be ligated into the "acceptor" at the end, and the "acceptor" vector is the final one for the concatenated construct expression.

Human $P2X_1$ receptor sequences with and without a stop codon were obtained by PCR from pcDNA3.0 containing the $P2X_1$ receptor cDNA. The $P2X_1$ sequences with a stop codon were cloned into the pcDNA3.0 to form the acceptor vector, while the $P2X_1$ receptor sequences without a stop codon were ligated into the linker vector making up the donor vector. There are two donor vectors with $P2X_1$ receptor sequence, either with a single linker or four times length linker at the end. These two donor constructs and acceptor constructs were all checked by double digestion with *NcoI*/*NotI* or *EcoRI*/*NotI* respectively (See figure 3.9) followed by sequencing.

Construction of $P2X_1$ concatenated channel

By repeating the usage of the *NcoI* site at the beginning of the $P2X_1$ receptor sequence, individual subunits can be integrated into the "acceptor" vector (see figure 3.10). Following ligations, the concatenated dimer and trimer constructs were produced. The concatenated dimers were generated with single and four times length linker, and these sequence were checked by restriction digestion and sequencing. The concatenated $P2X_1$ receptor trimer construct was generated from the dimer with four times length linker, and it has been confirmed by restriction digestion (See figure 3.11).

3.2.2 Properties of the $P2X_1$ concatenated channels

The expression level and channel properties of the concatenated constructs were studied by electrophysiological recordings. The monomer, dimer and trimer with two lengths of
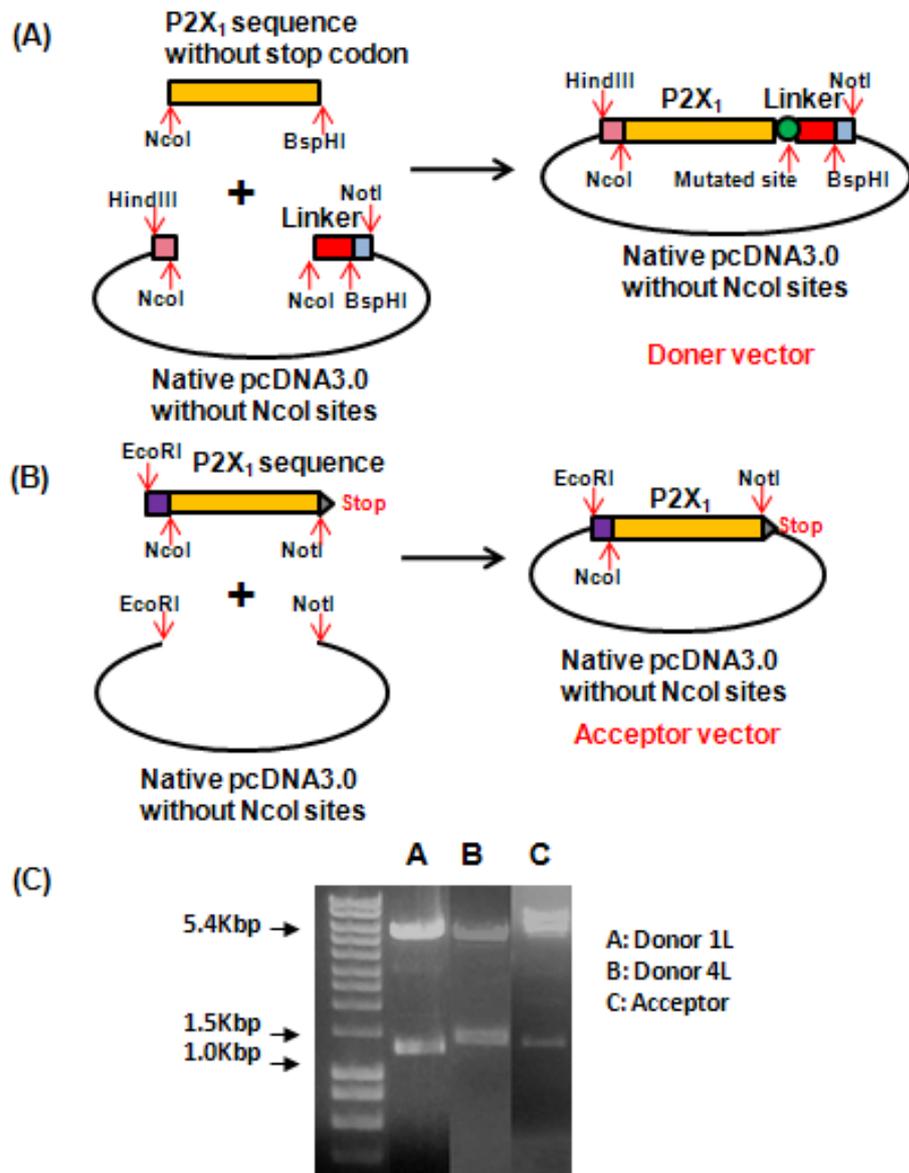
Figure 3.9 Architechture of donor and acceptor vectors
(A). P2X$_1$ receptor sequence without a stop codon amplified from PCR was ligated into the "linker" vector using *NcoI* and *BspHI* sites. Ligation of *NcoI/BspHI* removes the restriction sites for both enzyme, and the pcDNA3.0. containing the P2X$_1$ cDNA sequence without stop codon and linker construct became a "donor" vector. **(B).** The P2X$_1$ receptor sequence with a stop codon was ligated into the native pcDNA3.0 vector without the *NcoI* site using the *EcoRI* and *NotI* restriction sites. The vector containing the P2X$_1$ receptor became an "acceptor" vector for the concatenated channel. **(C).** The "donor" vectors with single and four times length linkers were digested with *NcoI* and *NotI* restriction enzymes and visualized on the gel. The positive bands are between 1000-1500bp and the vector bands are aboout 5400bp. The faint bands in the middle maybe the remaining uncut plasmids. The acceptor vector was double digested by *EcoRI* and *NotI* restriction   enzymes which do not work together very well , and there are multiple bands appeared around 5000-8000bp. The positive band stand for P2X$_1$ receptor sequence with stop codon is between 1000-1500bp.
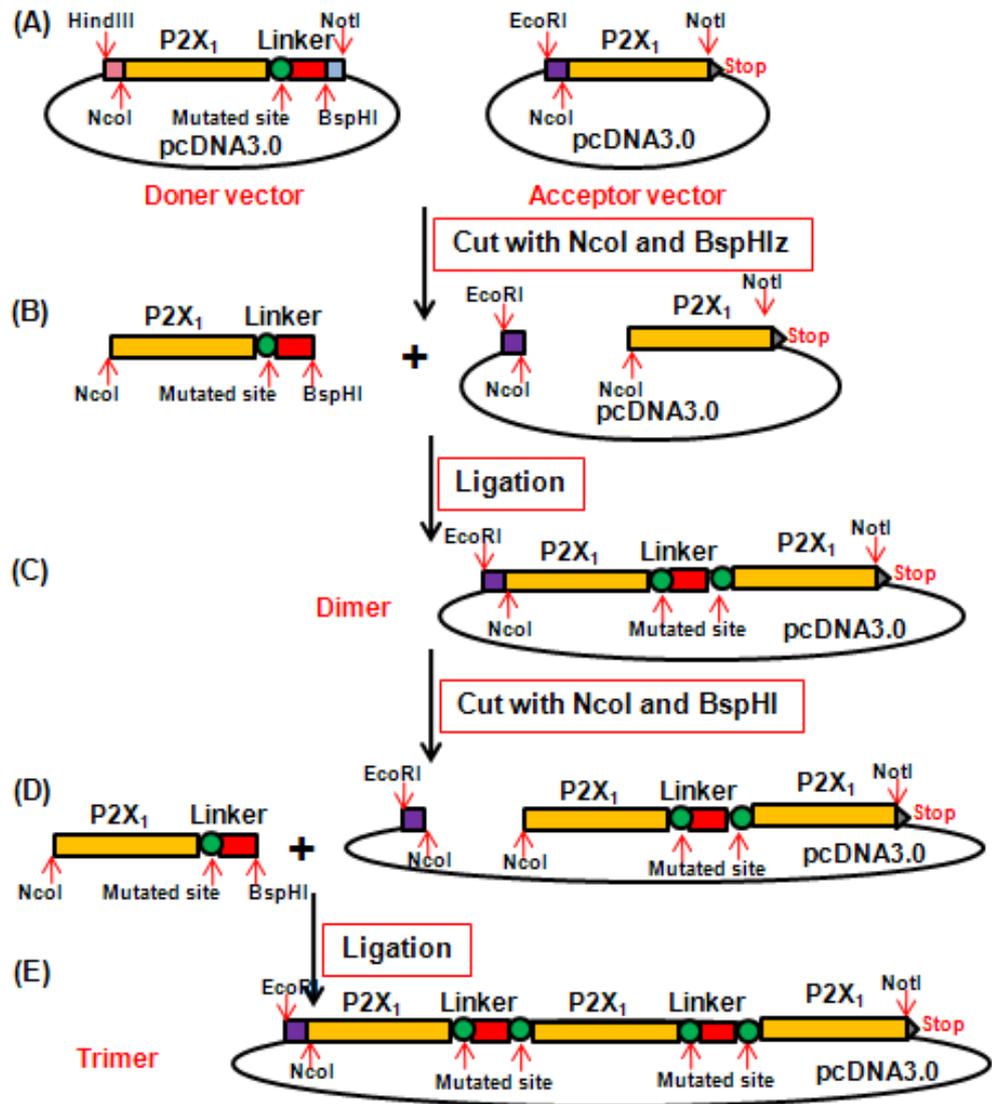
Figure 3.10 Strategies of P2X$_1$ concatenated channel construction
By repeatedly using the compatible *NcoI* and *BspHI* restriction sites, the concatenated channel can be generated in the pcDNA3.0 plasmid. **(A).** The "donor" and "acceptor" vectors were prepared and cut with the *NcoI* and *BspHI* enzyme. **(B).** After digestion, the P2X$_1$ plus linker sequence was obtained from the donor vector, and the acceptor vector was ready for the acceptance of another P2X$_1$ sequence. **(C).** The dimer was constructed by ligating the P2X$_1$ plus linker sequence from the donor vector into the acceptor vector. After ligation, only the *NcoI* site present at the beginning of the concatemer sequence existed and can be used later. **(D).** The dimer construct was cut with *NcoI* enzyme again for trimer concatenation, and **(E)** the concatenated trimer was obtained finally after ligation of the P2X$_1$ plus linker construct into the dimer.
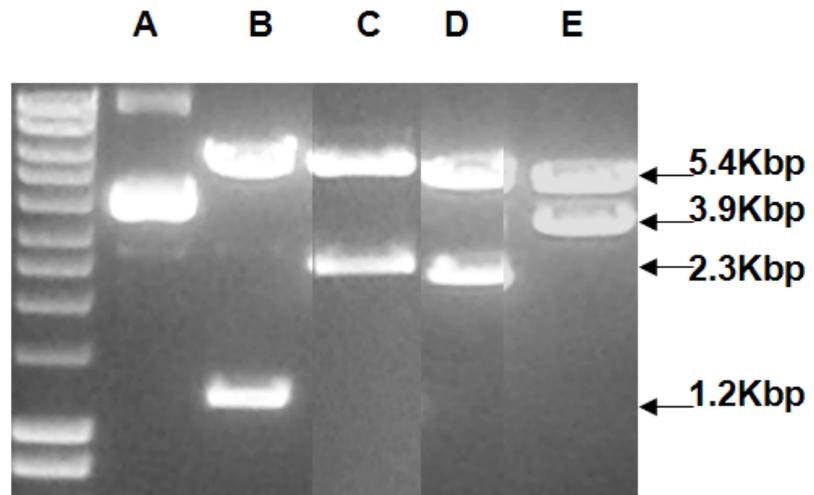
Figure 3.11 The constructs of concatenated P2X₁ subunits were visualized on a gel
The P2X₁ concatenated constructs were digested with *NcoI* and *NotI* restriction enzymes. After digestion , the bands indicated the sizes of the concatemers and   are estimated as 1200 bp, 2300 bp and 3900 bp for monomer, dimer and trimer respectively. Multiple bands indicating the supercoiled , coiled and linear   DNA were observed for uncut plasmid.

by electrophysiological recordings. The monomer, dimer and trimer with two lengths of linker have been produced, and all of the constructs were expressed in *Xenopus* oocytes.

3.2.2.1 Expressions and Properties

In order to maximise $P2X_1$ receptor expression, the optimal amount of mRNA needed for injection was estimated initially. The mRNA of WT $P2X_1$ receptors at 10 ng, 20 ng, 30 ng, 50 ng, 90 ng, 100 ng and 125 ng was injected into oocytes, and the peak amplitudes evoked by 100 μM ATP was studied by electrophysiological recording. Less than 20 ng mRNA of the WT $P2X_1$ receptor gave only small responses less than -2500 nA. When the quantity of injected mRNA was increased from 20 ng to 50 ng, the peak current was increased to the highest level at -9466 ± 499 nA ($n=6$), and further increasing the mRNA quantity did not cause a further rise of the peak current (See figure 3.12). Hence, 50 ng of mRNA was chosen for all constructs. Once the concatemers were produced at the cDNA level, the mRNA of the four constructs were synthesised using the RNA transcription kit as described in methods. The quantity and sizes of the mRNA were estimated by visualization on a RNA gel (See figure 3.12). The sizes of the dimer mRNA is apparently larger than the monomer, and the trimer has bands with the biggest molecule size. The quantities among four constructs are estimated to be similar.

To examine the sizes and amounts of the expressed proteins of the concatenated constructs, all of the samples were run on a western gel at 0.8% with 2.5% β-mercapthethanol. The sulfurous compound β-mercapthethanol is a reducing agent which can break the secondary structure of proteins. It disrupts the covalent bonds between individual subunits, and the non-concatenated $P2X_1$ receptor dimer or trimer will be broken down and revealed as a monomer on the SDS-PGAE gel. $P2X_1$ receptors were labeled by 1:500 dilutions of primary antibodies, both of surface and total proteins expressed in the oocytes for each constructs were tested (See figure 3.12). The size of the $P2X_1$ monomer is about 50 kDa, and the dimer and trimer were predicted to be above 100 kDa and 150 kDa. From the western blotting results, reduced total expression levels were observed on all of the concatenated constructs. The linker sequences added to the end of monomer affected its total and surface expression to a great extent.
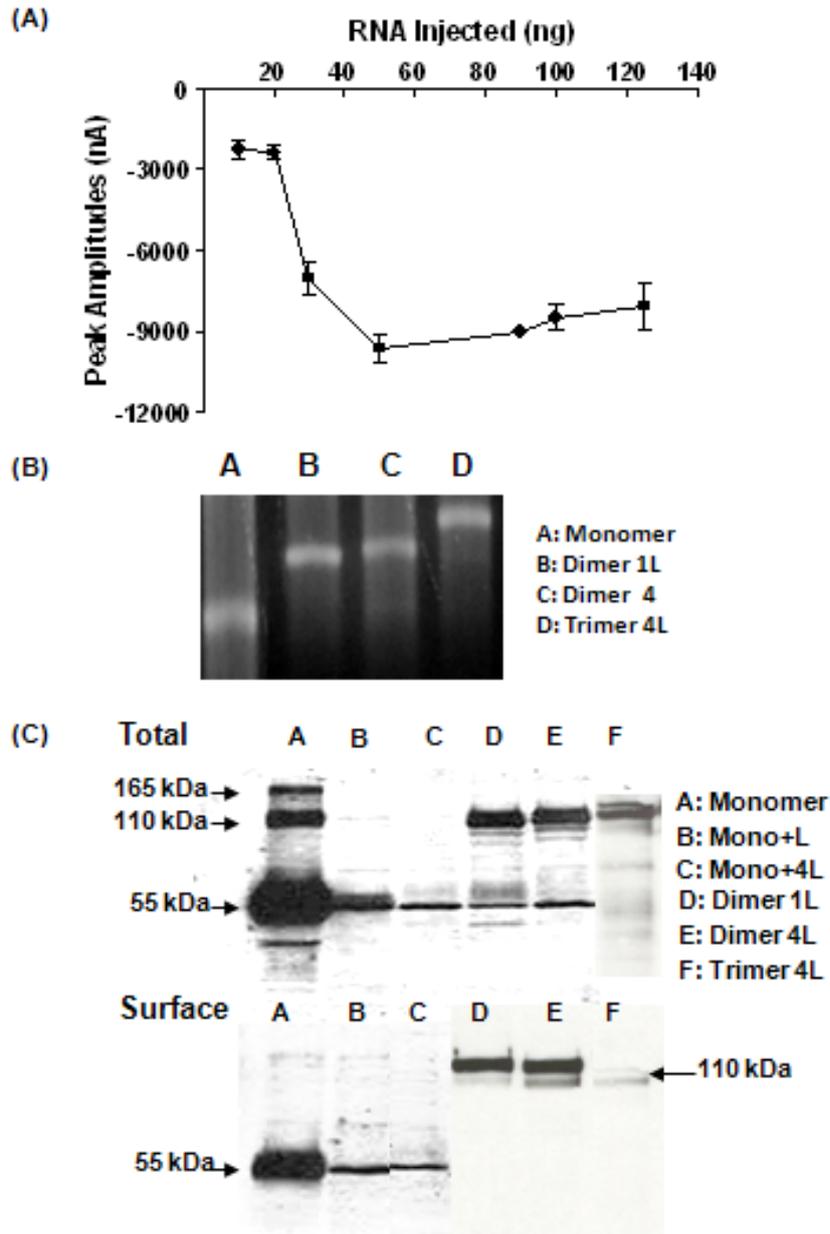
Figure 3.12 Expression of P2X$_1$ concatenated constructs
(A). Plot of mean peak amplitudes against the RNA injection for P2X$_1$ receptor standard. Different concentrations of RNA were injected into oocytes, and the peak amplitudes were studied by electrophysiology. The maximum amplitude of over -9000 nA were evoked by 50 ng RNA injection. **(B).** mRNAs of the P2X$_1$ concatenated constructs were made from cDNAs. 0.5 μl of 1 μg/ μl mRNA of the P2X$_1$ monomer, dimers and trimer constructs were visualized on a RNA gel. **(C).** Total and surface expression levels of P2X$_1$ concatenated constructs were revealed on SDS-PAGE gel, and probed by anti-P2X$_1$ antibody (1:1000 dilution). From the blotting results, monomers, dimers were generated with bands of about 55 and 110 kDa respectively. The trimer was expressed as dimer with quite low expression level.

Double bands at about 55 kDa and 100 kDa respectively were revealed for the dimers. It was shown that most of these constructs were expressed at the 100 kDa level at cell surface, only a low proportion of these constructs was broken down. Although more total and surface protein was detected in the dimers than monomer plus linker constructs, the protein expressed level of dimers are still lower than the $P2X_1$ receptor monomer. The trimer construct did not express as predicted. The expression level of the surface trimer protein is barely detected and most total protein was expressed as dimer for both total and surface proteins and small portion was shown as monomer. Therefore, the small currents evoked to ATP applications may result from the broken down constructs.

ATP as the agonist to $P2X_1$ receptors can evoke the fast desensitizing inward currents. The peak current reflects the amount of the functional P2X receptors at the cell membrane in response to the application of the agonist. To seek the relative expression levels of each construct in the *Xenopus* oocytes, the initial peak current to 100 µM ATP was studied (See figure 3.13). The maximum amplitude of WT $P2X_1$ receptor was -4877 ± 446 nA (*n=9*) which is the highest among all of the constructs in this batch of oocytes. Compared to the WT $P2X_1$ receptor, the expression levels of the monomer plus linker constructs were about 50% lower (*** p<0.001). The initial peak amplitudes of the two linker constructs was -2108 ± 188 nA (*n=19*) for the single linker construct and -2941 ± 248 nA (*n=30*) for the four times linker construct. The dimers exhibited similar peak amplitudes as the monomer plus linker constructs (*** p<0.001). After the application of 100 µM ATP, the mean peak amplitudes for dimers are -2134 ± 224 nA (*n=13*) for the $P2X_1$ dimer with single linker and -2367 ± 353 nA (*n=8*) for the $P2X_1$ dimer with four times linker. The lowest expression level was exhibited by the $P2X_1$ trimer construct, it gave a mean peak current of -247 ± 59 nA *(n=7, *** p<0.001)* which indicated little of the $P2X_1$ trimer channels were expressed in *Xenopus* oocytes. These data are consistent with the western expression results.

Although the receptor expression levels were dramatically reduced by concatenation and addition of the extra linker sequence at the C-terminal, the basic channel activation and gating properties were essentially the same, which can be interpreted from the study of desensitization time-course. Desensitizing represents the decay period of the response elicited during the binding of the agonist, and the decay time can be captured by using the pClamp 9.0 programme. The $P2X_1$ receptors exhibit fast desensitizing current to the
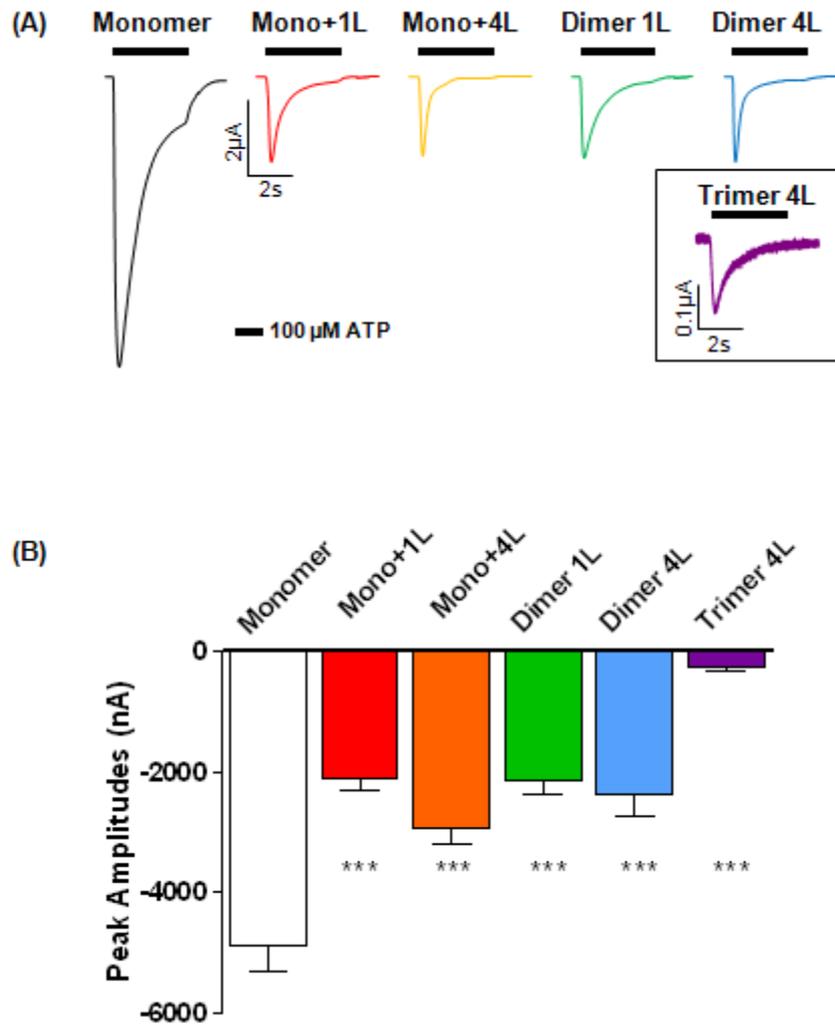
Figure 3.13 Mean peak currents of concatenated P2X$_1$ receptors
(A). Example traces of the peak amplitudes of P2X$_1$ receptor concatenated constructs to ATP (100 µM) application as indicated by black bars. **(B)**. The initial peak amplitudes of WT P2X$_1$ receptor was -4877 ± 466 nA (*n*=9) which is the highest among all of the constructs. The initial peak amplitudes of the other constructs are -2108 ± 188 nA(*n*=19), -2941 ± 248 nA(*n*=30), -2134 ± 224 nA (*n*=13), -2367 ± 353 nA (*n*=8) and -247 ± 59 nA (*n*=7) for the P2X$_1$ plus single linker (red) , four times linker construct (yellow), the dimer with single linker (green) and four times linker construct (blue), and trimer with four times linker (pruple) respectively. *** p<0.001.

application of ATP, and the ATP evoked current decays during the continued application. We have measured the speed of the "desensitization" as the time for the peak current to decay from 100% to 50%, and no statistical differences among all of the constructs were observed (See figure 3.14). The mean decay times are 249 ± 71 ms ($n=21$) for the WT P2X$_1$ receptor, 266 ± 92 ms ($n=17$) for the P2X$_1$ receptor plus single linker and 253 ± 101 ms ($n=12$) for the P2X$_1$ receptor plus four times linker construct, 268 ± 76 ms ($n=20$) for the P2X$_1$ dimer with single linker and 265 ± 65 ms ($n=25$) for the P2X$_1$ dimer with four times length linker respectively.

3.2.2.2 Linker sequences to channel function

The properties of the P2X$_1$ plus linker sequence constructs were further studied by repeating the applications of 100 μM ATP. In response to the application of ATP, the P2X$_1$ receptor produced desensitizing currents and at least 5 minutes wash before subsequent application was required for reproducible responses to be recorded. For the WT P2X$_1$ receptor, a fast desensitizing inward current was observed to the first application of 100 μM ATP (See figure 3.15). ATP was applied after 10 minutes and the second peak current was reduced to about 80% of the initial one. The following applications of ATP at 10 minute intervals showed the responses are reproducible and the peak values were maintained at a stable level. These results suggested the receptors can be readily recovered from the desensitization during the 10 minutes intervals.

The P2X$_1$ plus linker constructs also exhibit the fast inward desensitizing response as the WT group, whereas and these responses were dramatically decreased to about 30% (*** $p<0.001$) of the initial current after 10 minutes wash (See figure 3.15). During the following ATP applications at 10 minute intervals, the peak currents became stable and kept at the similar level of the second response. It is suggested that most of the channels at the cell membrane lost their functions after the first activation of the P2X$_1$ receptor channels with extra length at the C-terminal. However, the basic channel gating properties as revealed by 100-50% decay time were not affected by the linker sequences. In this case, the two sequences were used as the basic constructs for further channel concatenations.
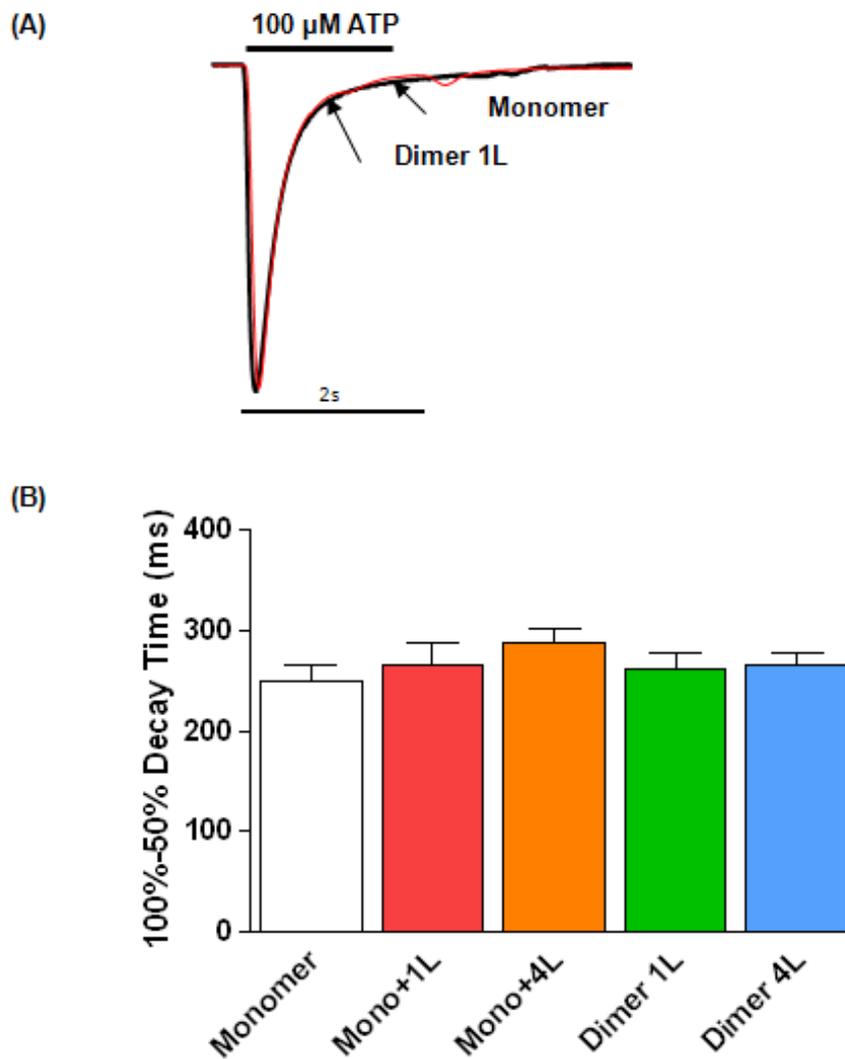
Figure 3.14 The decay time (100%-50%) of concatenated P2X$_1$ receptors
(A). Example traces of the decay time of P2X$_1$ receptor concatenated constructs to ATP(100 µM) application as indicated in bar. (B). The decay time course of the concatenated P2X$_1$ receptor constructs were measured from 100% to 50% of the peak current. The mean decay times have no significant difference among all of the groups. WT P2X$_1$ monomer (white) exhibited a decay time of 249 ±71 ms (n=21), and 266 ±92 ms(n=17) for P2X$_1$ receptor plus single linker (red), 253 ±101 ms(n=12) for P2X$_1$ receptor plus four times linker construct (yellow), 268 ±76 ms(n=20) for the dimer with single linker(green), and 265 ±65 ms(n=25) for dimer with four times linker (blue) respectively.
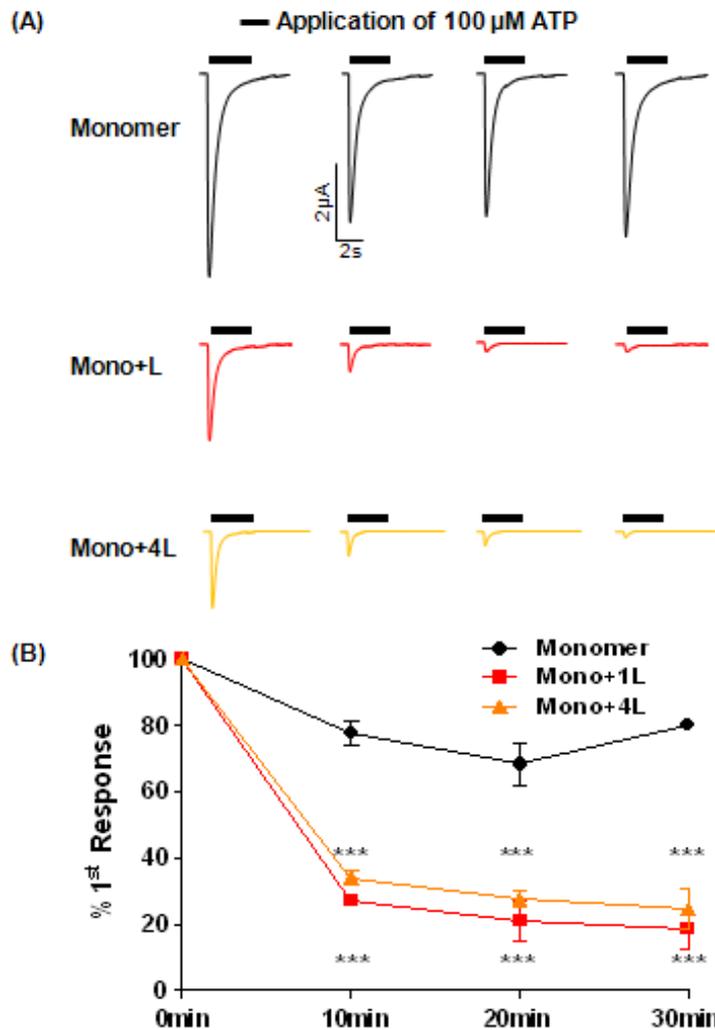
Figure 3.15 Responses of P2X$_1$ receptor plus linker constructs to repeated ATP applications

(A). Example traces of the fast desensitizing inward currents for the P2X$_1$ monomer plus linker constructs (red for single linker construct, yellow for 4 times linker construct). The application of ATP (100 µM) as indicated in bar was repeated every 10 minutes. (B). Mean peak amplitudes to the ATP applications at 10 minutes intervals are summarized, n=3 for monomer and mono+1L groups, n=6 for mono+4L construct . The peak values for both linker constructs reduced to about 20-30% of the first   responses after the second application, and were maintained in subsequent responses. *** p<0.001.

3.2.2.3 Properties of the concatenated channels

The properties of the dimer constructs were studied by repeated applications of 100 μM of ATP. After channel activation, the $P2X_1$ dimer constructs produced the inward fast desensitizing responses as the WT $P2X_1$ receptor (See figure 3.16). However, the peak current of dimers decreased during the 10 minutes intervals and the currents were not recovered to a stable level as was the case with the WT. This suggested the linker sequence used for concatenation affected the channel recovery time from desensitization. Hence, the interval between each application was extended to 15 minutes and relatively maintained peak amplitudes were obtained. When the second application of ATP was applied after 15 minutes, the peak amplitude of the dimer constructs were reduced to about 60% of the first response and the similar recovery levels were obtained for both dimers (Figure 3.16). Apart from the prolonged desensitizing recovery period, the concatenated $P2X_1$ dimers had normal properties.

3.2.2.4 The function of $P2X_1$ trimer receptor

Due to the long and tandem organized trimeric construct sequences, it cannot be verified by full sequencing. Thus, there may be mutations at the subunit junction regions. However, two clones of trimers were tried and both showed to be non-functional with low expression levels.

From previous study, residues at the amino and carboxy terminal regions of $P2X_1$ receptor could interact with each other to regulate the channel function (Vial *et al*, 2006). T18A and K367A, which are insensitive to the ATP application, are both non-functional mutants with normal cell surface expressions. Co-expression of T18A and K367A mutant $P2X_1$ receptors surprisingly produced larger ATP evoked responses than either mutant alone. The recombinant T18A/K367A channels consist of one pair of WT intracellular termini from neighbouring subunits, and enabled the partial rescue of $P2X_1$ receptor function through the normal interactions between subunits. The intracellular residues Thr^{18} and Lys^{367} were implied to be essential in the functional recovery due to the intracellular interactions. To study if the trimeric construct was broken down to non-functional monomer and the function of the monomer can be rescued in the same way, the mRNA of $P2X_1$ receptor trimer was injected into the oocytes at equal quantity with either mutant T18A or K367A.
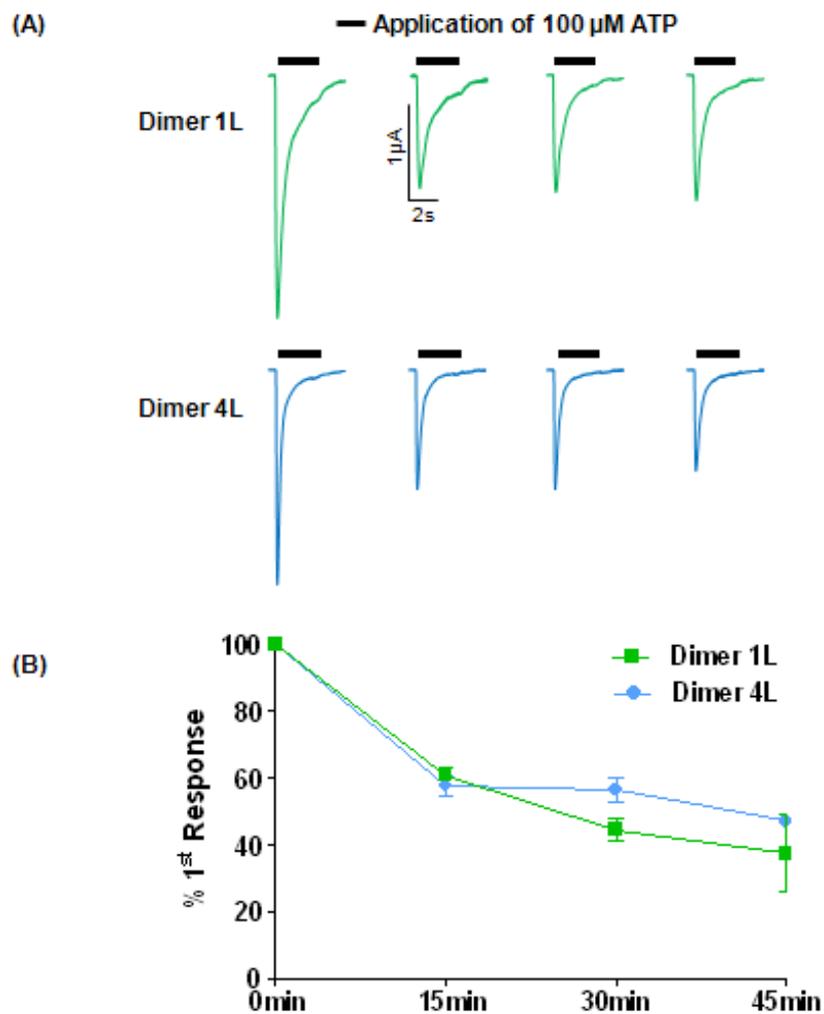
Figure 3.16 Responses of P2X$_1$ receptor dimers with different linkers to repeated ATP applications

(A). Example traces of the fast desensitizing inward currents at P2X$_1$ dimer constructs (green for single linker dimer and blue for four times linker dimer) evoked by ATP(100 µM) every 15 minutes as indicated in bars.**(B).** Mean peak amplitudes to the ATP applications during 15 minutes intervals are summarized, *n*=3 for each. The peak values for both linker constructs reduced to about 40-60% of the first responses after the second application, and were maintained in subsequent responses.

The peak amplitudes evoked by 100 µM ATP at oocytes expressing mutants and mutant with trimer constructs are summarized in figure 3.17. It was found the mutants T18A and K367A exhibit even lower peak values (-25 ± 7 nA, $n=5$ and -31 ± 8 nA, $n=5$ respectively, *** $p<0.001$) than the trimer (-181 ± 52 nA, $n=10$), and the trimer cannot help to recover the peak amplitudes of the mutants (-13 ± 2 nA, $n=6$ for T18A+Trimer and -17 ± 5 nA, $n=9$ for K367A+Trimer respectively, *** $p<0.001$). Futhermore, the peak currents of the mutants or the mutants with trimer were the same. The results indicated the existence of WT intracellular domains were unable to re-establish the channel function of P2X$_1$ trimer, and the ATP sensitivity of trimer cannot be simply rescued by either T18A or K367A mutant. The trimer complex which containing modified intracellular domains lost its function in a more complicated way rather than the misfolding of single residue or fragment.

3.2.2.5 Expression patterns of the concatenated constructs

The functional channels of P2X receptors are proposed to be made up of three subunits, and the patterns of the concatenated dimers in forming the functional channels are interesting to be further studied.   Chemical cross-linking is a useful approach to examine the multimeric forms of the concatemer (Figure 3.18). The oocytes were treated with 150 µM DTSSP as the cross-linking reagent before being run on the SDS-PAGE gel. As a result, most of the P2X$_1$ monomers were revealed to be trimers or higher aggregation forms as expected after cross-linking, and only few of them were shown as dimer with a faint band of 100 kDa (See figure 3.18). Multiple bands indicating monomers (~50 kDa), dimers (~100 kDa) and trimers (~150 kDa) were observed in all of the dimer and trimer groups. Nevertheless, the amounts of trimer revealed in cross-linked concatenated constructs are significantly lower than the monomers, and no bands higher than 150 kDa can be observed in all concatenated constructs.   Since no hexamers or higher aggregation forms were detected for the concatemers, these constructs failed to generate proper trimer channels and the extended linker sequence may affected the subunit aggregation. For concatenated dimer and trimer constructs, the cross-linked bands may come from the dimer and non-concatenated monomer. When the dimers make functional channels, the dimer constructs may be broken down to monomer and contribute to the reduced peak current amplitude.

The non-functional P2X$_1$ receptor mutants T18A and K367A were injected with or without trimer constructs into the oocytes at a ratio of 1:1, and cross-linked with 150 μM DTSSP after expressions. The blotting results suggested that all of the samples can produce trimers, tetramers and even hexamers which were about 250 kDa, but the ones including trimer constructs shown less intensities. This indicated mutations at Thr^{18} and Lys^{367} only interrupted the subunit interactions mechanism but not subunit aggregation, while both of them were impaired on the trimer construct with artificial linker sequence.
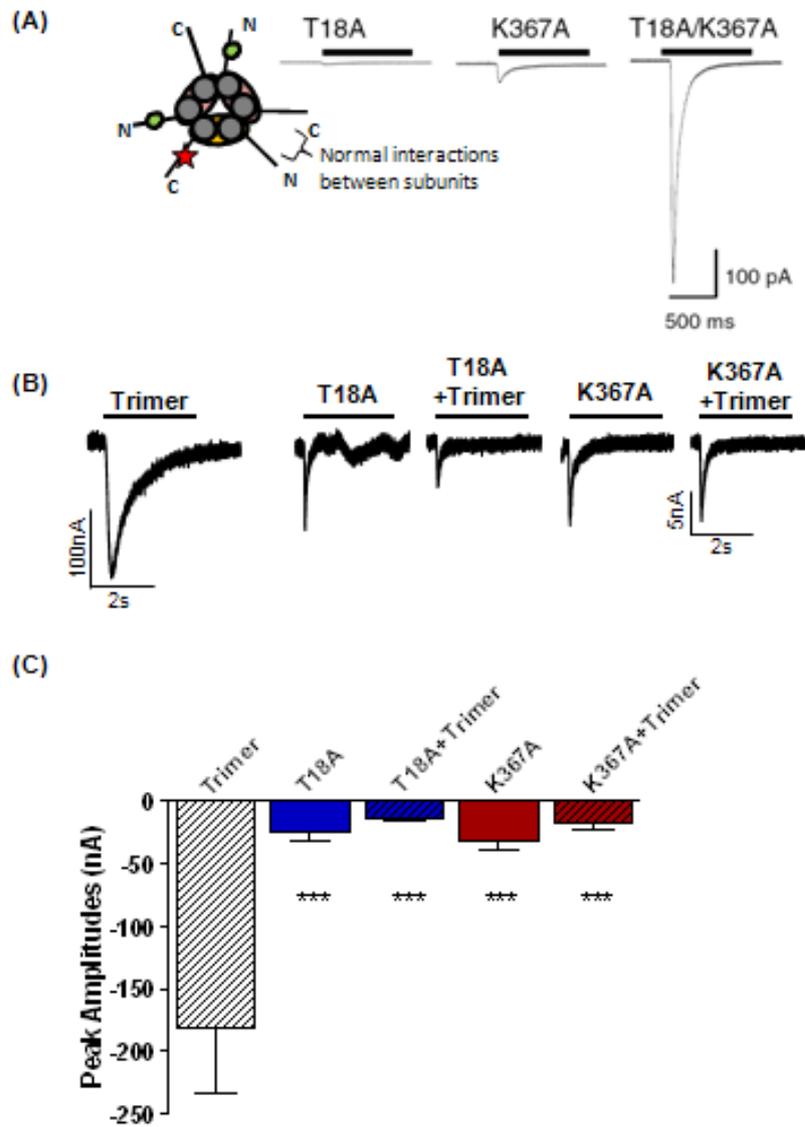
Figure 3.17 The peak amplitudes and traces of P2X$_1$ receptor mutants and concatenated trimer

(A).The interactions between intracellular domains are important for channel properties. A previous study suggested the responses of non-function T18A and K367A mutants can be recovered by co-expression (taken from Vial *et al*, 2006). The possible interactions between the intracellular termini were indicated on the left. B). Example trace of the inward fast desensitizing current evoked by ATP(100 µM) as indicated by bars at P2X$_1$ mutants and concatenated trimer. (C). Summary of peak amplitudes of P2X$_1$ receptor mutants with or without the co-expression of concatenated trimer. The mutants exhibited even lower peak values than the trimer. *** p<0.001 comparing to the trimer construct.
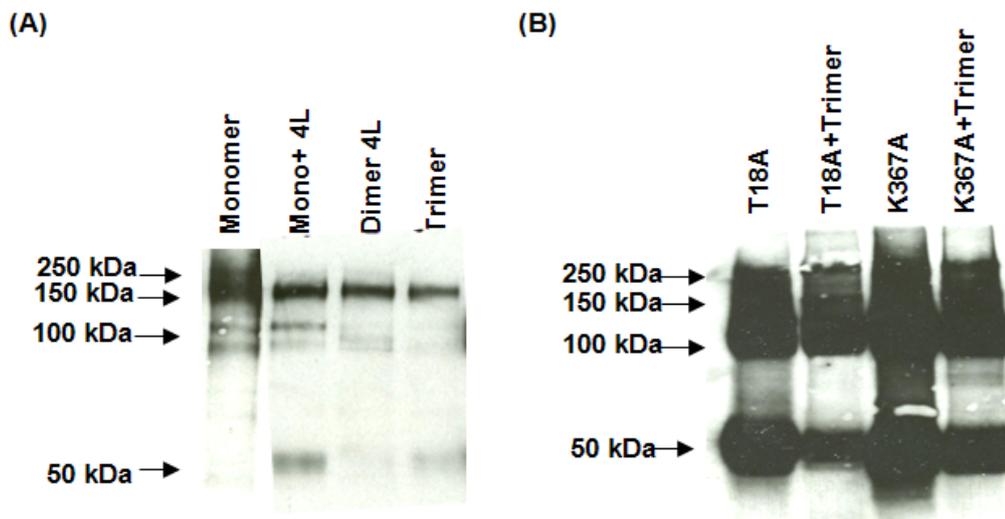
Figure 3.18 Expression pattern of P2X$_1$ concatenated constructs
(A). The oocytes expressing P2X$_1$ receptor monomer, dimers and trimer were treated with 150 µM DTSSP as the cross-linking reagents before running on the SDS-PAGE gel. 1:1000 diluted anti-P2X$_1$ antibody were used in western blotting. All of the constructs were able to cross-link to form trimers, but the higher aggreations can only be observed in the monomer group. Besides, there are still bands of monomers and dimers for the concatenated constructs.(B). Non-functional P2X$_1$ receptor mutants with or without the trimer were injected to the oocytes at 1:1 ratio. The mutants can produce trimer and even hexamer which is about 250 kDa, but the ones including trimer shown less intensities for monomers as well as the multimers.

3.3 Discussion
3.3.1 Concatenated channels are necessary for detecting intersubuits properties

The properties of homomeric and heteromeric channels have been commonly studied by co-expression of mixed subunits followed by chemical cross-linking. They are effective ways to study the assembly patterns of the receptor, especially the intrasubunit properties. However, there is a disadvantage that the arrangement of the subunits contributing to the receptor ligand-gated channel is not fixed and the composition of the expressed channel cannot be determined. Alternatively, the contribution of single subunits to the trimeric channel can be studied by subunit concatenation, which is an efficient approach to making up the P2X channels in a designed pattern.

Up to now, concatenated $P2X_2$ channels have been constructed successfully and widely used in the study of receptor membrane topology, subunit assembly and the intersubunit binding site (Stoop *et al*, 1999; Newbolt *et al*, 1998; Nagaya *et al*, 2005). However, the subunit concatenation of $P2X_1$ receptors failed to produce functional trimers using similar linkers as for the $P2X_2$ receptors (Nicke *et al*, 2003). In this study, I tried to generate the concatenated $P2X_1$ receptor using different length of linkers and two linkers with single or multiple copies of "GQ_4GQ_4G" sequences were used. The $P2X_1$ dimers and trimer were generated by using these linkers and estimated at the RNA level, while this construct cannot express properly at the cell surface. However, this study suggested the importance of the contact between amino and carboxy terminus of the $P2X_1$ receptors.

3.3.2 P2X receptor intracellular domains are important for protein expression at plasma membrane

The expression levels of the concatenated constructs were revealed by western blotting and significant decreases were observed. The $P2X_1$ subunit with a linker of 14 amino acids exhibited a reduction of 60% of the peak amplitude to 100 μM ATP applications, and when the length of linker was increased to 52 amino acids, the reduction was 40% of the control. The longer linker was supposed to provide more flexibility in the intracellular junction domains of the neighbouring subunits, however, the four times length linker did not to make a better functional channel than the single linker constructs.

The P2X$_1$ plus linker construct containing the single subunit made up the P2X$_1$ channels form monomers, and the reduced peak currents and protein expression levels suggested the linker sequence itself affects channel expression. However, the hexahistidyl tag (Nicke *et al*, 1998) and FLAG tag (Barrera *et al*, 2005) have been inserted in to either the N-terminus or C-terminus of the P2X receptors and shown to be well tolerated. The linker used for concatenation shared the similarity of repetitive non-charged amino acids in sequence with these peptide tags. Thus, the amino acids used for the attached sequence at the C-terminus of P2X$_1$ receptor should not be responsible for the expression reduction.The possible explanation for the reduced expression level is the length of the linker might not be long enough to maintain proper folding of the receptor channel. As described previously, the length of the C-terminal of the P2X$_1$ receptor is about 70 amino acids less than the P2X$_2$ subunit which is equivalent to about 210 amino acids long. The P2X$_2$ functional concatenated channel has been produced with limited length of linker, while P2X$_1$ concatenated trimer fails to express at the cell membrane. The length of the linker could be a major determinant factor in the expression of the concatenated constructs. Functional P2X$_1$ EGFP-tagged receptor was generated previously by an insertion of an EGFP sequence of over 200 amino acids at the end of the C-terminus and had no influence to receptor expression and properties (Vial *et al*, 2006). These results indicated it is feasible to add a long linker sequence to the C-terminus of P2X$_1$ receptor. However, the EGFP protein forms a tightly compressed structure after expression which may not interfere with other surrounding proteins, while the expressed linker sequences for P2X$_1$ receptor concatenation lack secondary structure modifications. The unfixed extra artificial end introduced by linker sequence to the P2X$_1$ subunit C-terminus may move and disrupt the normal protein expression by interacting with other intracellular residues.

For the dimers, the amounts of mRNA injected into the oocytes were estimated by RNA gel visualization. After expression, the surface and total expressed proteins were extracted and studied by Western blotting. For the dimer constructs, only few of them were broken down into monomers and suggested the linker strategy worked at this stage. In contrast to the P2X$_1$ channel constructed by monomers, the expression levels at the plasma membrane of the dimer constructed channel were dramatically reduced by about 50%. The decreased surface expression levels were according to the observation at peak

current amplitudes. Furthermore, the total protein expression levels were reduced to a smaller extent.

One interesting phenomenon was noticed that the different length of linkers made no significant difference to the expression of dimers, and the dimers had a better expression than the $P2X_1$ monomer plus linker constructs on the western gel. The peak current amplitudes among all of the monomer and dimer concatenated constructs are similar, while the protein expression levels of monomer constructs revealed from western blotting seem less than the dimer. Therefore some of the dimers could be "silent" receptors at the cell surface. This suggests that the $P2X_1$ subunit expression was affected by the linker sequence, and also the dimers may not form the channel properly due to the formation of channel pore was normally required three subunits. It is likely that the functional channels were formed with a dimer and a monomer from breaking down.

From the above results, the linker sequence on the $P2X_1$ subunits was inferred to be associated with the receptor expression. The linkers make up dimers by connecting the C-terminal of the first subunit to the N-terminal of the second one. Hence, the possible interactions between the two intracellular domains and the interactions between the linker and N-terminal could be considered as one of the factors influenced the protein expression of the concatenated dimer as well.

The surface expression of concatenated trimeric constructs was barely observed, while this construct was well established at the cDNA and RNA level. It may not be able to be synthesised or have been synthesised but broken down afterwards. A band indicating the size of dimer was detected for the total protein expression of $P2X_1$ concatenated trimeric construct by western blotting, and it was hardly detectable on the surface expression gel. In addition to the structural break down, this construct had trouble in protein trafficking. A previous study (Vial *et al*, 2006) suggested both of the mutants, T18A on the PKC site at amino termini, and the mutant K367A at carboxy termini will lead to channel non-function. However, these two mutants can partially rescue each other to some extent in a heterotrimeric channel, the neighbouring WT amino and carboxy termini may work together to help the subunit interactions. The formed trimer lost its function at the cell membrane and can only produce very small currents like the

above mutants, and this reduced response may due to the monomers chopped from the concatenated constructs. Nevertheless, the subunit interactions could not help the channel trafficking of the concatenated trimer. Co-expression of the trimer with either mutant did not result higher peak currents.

From the cross-linking results, the concatenated channels are difficult to produce the high molecular weight aggregated complex. The dimer and trimer failed to generate tetramers or hexamers indicating the intracellular domains of $P2X_1$ receptor may be important for subunit recognition or joining during the formation of the multimeric channels. The reduction of tetramers and hexamers expression from the T18A or K367A mutant with trimer protein further suggested this point.

3.3.3 Channel recovery from desensitizing was interrupted by the concatenation

It is noticeable that there are significant shifts of the channel recovery time from desensitization and levels demonstrated by the concatenated constructs. The recovery time for $P2X_1$ receptor to the application of 100 μM ATP was normally about 5 minutes. The responses of $P2X_1$ plus linker constructs require 10 minutes intervals to be reproducible, and the amplitudes of the currents were maintained at a low level. Only 1/5 of the initial current remained after the first 10 minutes. For the dimer constructs, the recovery period during each agonist application needed to be extended to 15 minutes, and there was no significant different between the two dimers at recovery levels.

Channel gating refers to a complicated procedure including agonist binding, channel activation and agonist unbinding, which can be interpreted by the rise time and decay time of evoked currents and the channel recovery time respectively. Rettinger *et al* suggested that after the activation of the channel, the P2X receptor requires the unbinding of the agonist before the recovery from desensitization (Rettinger *et al*, 2003). The above results indicated either it takes a longer time for the ATP molecules unbinding from the agonist binding site, or the concatenated constructs requires longer time to recover from desensitization because of the extra sequence at the C-terminus. The extended channel recovery time indicated that the dimers require an extra period to wash off the ATP. Therefore the attached linker sequences may cause conformational changes of the intracellular domains and subsequently the agonist binding pocket, and these modifications induced the prolonged ATP unbinding time-course. There was no

obvious difference observed at channel rise and 100-50% decay time among all concatenated constructs, the channel activation and agonist binding mechanisms are likely not to be affected.

It is also possible that the linker sequence had interactions with intracellular sites that contribute to channel gating. The C-terminal of the P2X receptor was considered involved in protein trafficking by the study of the conserved intracellular YXXXK motif (Chaumont *et al*, 2004). The mutations at this region caused great reduction of the receptor expression at cell membrane by rapid internalization. The receptor internalisation period could be alternatively responsible for the running down of current amplitudes, and the course of internalization maybe associated with the potential recovery period of the response. Internalisation is important for the $P2X_1$ receptor, as suggested by the previous study about half amount of receptors can be recycled after the channel activation (Ennion *et al*, 2001). Therefore, the concatenation modifications to the $P2X_1$ receptor may affect the normal recycling progressing which is dependent on the recycling and trafficking period of the receptor back to cell surface. For the $P2X_1$ receptor, this motif is located at about 362 to 365 amino acids which are close to the end of the 399 amino acids sequence. In this study, the additional length of the linker added artificially to the end of the C-terminal was possible interfere with this YXXXK motif or blocked the function of it.

Channel recovery time is also relevant to the channel expression levels. The poorly expressed receptors have difficulties in responding to the agonist's stimulations efficiently. Slower recovery time observed at dimers may suggest low channel expressions as well.

3.3.4 Subunit concatenation
To explain the reason for the reduction in total receptor synthesis, the sequence used in my project need to be considered. The amino acids sequences used in the linkers are single or multiple copies of "GQ_4GQ_4G". The two amino acids used in the linker sequence are non-charged glutamine and glycine, they are expected having no effect to the receptor folding and gating properties. The additional glycine residues were designed to provide more flexibility to this region. This sequence was derived from the idea of using the glutamate-rich sequences for concatenation linkage by Nicke's group

(Nicke *et al*, 2003), and it is essentially similar to the linker3 "GQ$_{13}$G".This group also adopted the compatible *NcoI* and *BspHI* restriction sites for subunit concatenation. The peak amplitudes observed for the concatenated dimeric and trimeric P2X$_1$ receptor channels were found to be 1/3 and 1/4 of the ones made up by monomers. The concatenation patterns were revealed on the SDS-PAGE gel with the reducing reagents, and the amount of concatenated trimers and dimers expressed in total are much less than the control as equivalent to the amounts of peak currents. However, most of the trimer was suggested to be non-functional as only few trimeric constructs remained with the presence of reducing reagent DTT and most of the trimeric constructs were broken down to monomers.

In my study, the concatenated trimer construct was visualised at DNA and RNA levels, whereas it is shown as dimer after the expression in oocytes. Due to the similarity of the strategies used in previous studies, one possible reason for it is the protein synthesis was interrupted by the existence of an accidentally mutated stop codon in the sequence of trimeric channel. There is no specific primers available for the tandem arranged sequences of trimeric P2X$_1$ channel, it was unable to be fully sequenced. However, one more clone of the trimeric construct was tried and showed no increased peak amplitudes and protein expression levels.

Although the expression pattern of the trimer construct is similar to the concatenated dimers, it was non-functional and barely detectable at the cell surface. This was according to the previous observations, and thus apart from the influence to protein synthesis, this linker strategy may affect the protein trafficking pathway. The concatenated channel may be modulated in the endoplasmic reticulum (ER) during the protein trafficking. As proposed in Nicke's study, the channel formation pattern of trimeric P2X$_1$ receptor from concatenated dimers can be either from two dimers (one contribute two subunits as a whole, the other only contribute subunit) or three dimers (one subunit of each), and dimers can only exit ER by combining with monomer byproducts during the modifications in ER (Nicke *et al*, 2003) (See figure 3.19). The other possibility is the concatenated constructs did not form a functional channel properly, and the ATP response came from the trimeric channel made up by the monomer byproducts rather than the dimers.
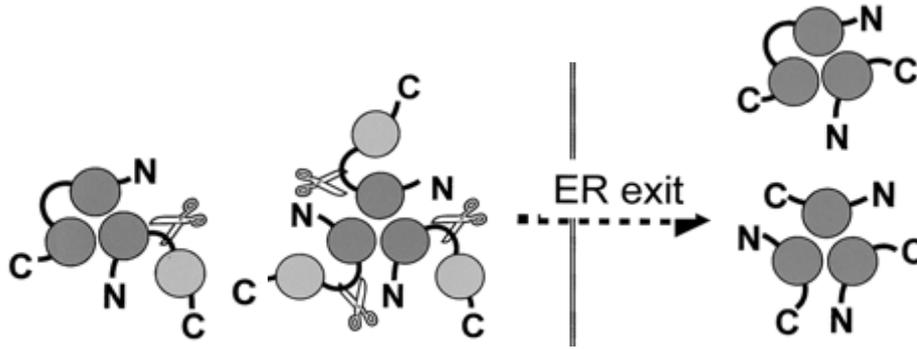
Figure 3.19 P2X$_1$ trimeric receptor formations from concatenated dimer
The concatenated dimer forms trimeric channel either by two dimers with one subunit left out of the channel pore, or by three dimers with one subunit from each dimer. These complex will finally modified in the ER and expressed as a timeric channels on the cell surface (Modified from Nicke *et al*, 2003)

3.3.5 Alternatively methods for intersubunit study
The C-terminal of the P2X$_2$ receptor could be alternatively used to construct the P2X$_1$ concatenated channel. Since the construction of P2X$_2$ concatenated channel had less requirements to the linker designation, part of the C-terminal domain of the P2X$_2$ subunit can be cut and used as a long and flexible linker to add to the end of the P2X$_1$ subunit. However, the P2X$_2$ receptor oriented linker also has the possibility to influence the properties and the expression of the P2X$_1$ concatenated channel. This sequence from C-terminal the P2X$_2$ subunit may interact with the intracellular domains of P2X$_1$ subunits like a P2X$_1$/P2X$_2$ chimera receptor.

In addition to the concatenated channel, Jiang and colleagues studied the subunit arrangement of P2X$_2$/P2X$_3$ heteromeric receptor using a novel method (Jiang *et al*, 2003). Without using the linkers, they engineered cysteines residues which formed intersubunit disulfide bonds between the transmembrane domains (TMs). Nagaya *et al* also introduced double cysteine substitutions to His[120] and His[213] at P2X$_2$ receptor where the subunits can be linked by the formation of disulfide bonds (Nagaya *et al*, 2005). It therefore can be an additional approach for the intersubunit interactions study.

3.3.6   Conclusion
Concatenated P2X channels may provide a useful approach to investigate the intersubunits properties in the ligand-gated ion channels. P2X$_2$ concatenated channel have been widely used to study the channel assembly, positional effects of single

subunits in heteromeric channel and the properties of individual residue in the whole functional channel.

However, there are many requirements to the linker sequences in generating the $P2X_1$ concatenated channel. The results suggested that both the length and the sequences of the linker play important roles in channel gating and expression. The length of the linker might associate with the protein trafficking at the plasma membrane, while the linker sequences is involved in protein synthesis. Besides, the intracellular domains may involve in subunit recognition or joint during the trimeric channel formation.

3.4 Appendix: Concatenated channels generation

3.4.1 Preparation of the pcDNA3.0 Vector

The concatenated P2X channel used *NcoI* (CCATGG) and *BspHI* (TCATGA) sites to link the subunits, these endogenous *NcoI* and *BspHI* sites are contained in the pcDNA3.0 plasmid (See section 2.1.1) therefore needed to be removed. Site-directed mutagenesis reactions were performed on the native pcDNA 3.0 vector to remove the three endogenous *NcoI* and two *BspHI* restriction sites by converting single bases. The *NcoI* restriction sites were located at positions 610, 2540 and 3185 (numbering from the origin replication site) and the *BspHI* sites were located at 4821 and 5830 base pair of the native pcDNA3.0 vector from the origin replication site. The primers used in the reactions were listed in table3.1.

Primers	Sequences of the Primers	Conversion
*NcoI*610FWD	5'-GTCATCGCTATTA **CCACGG** TGATGCGGTTTTGGC-3'	**T→C**
*NcoI*610REV	5'-GCCAAAACCGCATCA **CCGTGG** TAATAGCGATGAC-3'	**A→G**
*NcoI*1958FWD	5'-CCATTCTCCGCC **CCACGG** CTGACTAATTTTTTTT-3'	**T→C**
*NcoI*1958REV	5'-AAAAAAAATTAGTCAG **CCGTGG** GGCGGAGAATGG-3'	**A→G**
*NcoI*2693FWD	5'-GTCGTGAC **CCACGG** CGATGCCTGC-3'	**T→C**
*NcoI*2693REV	5'-GCAGGCATCG **CCGTGG** GTCACGAC-3'	**A→G**
*BspHI*4332FWD	5'-GGGATTTTGG **TGATGA** GATTATCA-3'	**C→G**
*BspHI*4332REV	5'-TGATAATC **TCATCA** CCAAAATCCC -3'	**G→C**
*BspHI*5430FWD	5'-GGTTATTGTC **TGATGA** GCGGATAC-3'	**C→G**
*BspHI*5430REV	5'-GTATCCGC **TCATCA** GACAATAACC-3'	**G→C**

Table3.1. Sequences of the primers used for mutagenesis reactions to remove the endogenous NcoI and BspHI sites on the native pcDNA3.0 vector
Endogenous *NcoI* and *BspHI* sites were removed by converting single bases on the native pcDNA 3.0. Mutated *NcoI* (numbering 610, 1958, 2693 base pair from the origin replication site) or *BspHI* (4332 and 5430 from the origin respectively) sites are in bold, and the mutated base is indicated in red and underlined. The conversions on each site are listed in the table above, and these mutations did not change the amino acids encoded. The removal of sites were confirmed by digestion with correspondence restriction enzyme.

The plasmid DNA (3 μl) was then digested with 10 units of *NcoI* restriction enzyme (New England Biolabs® Inc.) to check if the *NcoI* sites were removed from the pcDNA 3.0 vectors. The digested sample was run on a 1% agarose gel to visualize the bands obtained after the digestion. After the removal of the first *NcoI* site, individual colonies were selected in order to mutate the second *NcoI* site. The same steps as previously described were repeated, until all of the *NcoI* sites were removed from the native

pcDNA3.0 vector. The two *BspHI* sites were removed using the same strategy.

3.4.2 Preparation of the P2X$_1$ cDNA sequences as the inserts

Removal of the NcoI and BspHI restriction sites

Besides the pcDNA3.0 vector, the endogenous *NcoI* and *BspHI* sites inside of the P2X$_1$ receptor cDNA sequences were removed by site-directed mutagenesis. Although single base pairs were changed, the amino acid sequences were not changed by these point mutations. The setting up of the reaction and cycling parameters for the mutagenesis were the same as described previously and the primers for removing these sites were listed in table 3.2. The mutations were checked by digestion with *NcoI* and *BspHI* restriction enzyme (New England Biolabs® Inc.)

Primers	Sequences of the Primers	Conversion
*NcoI*614FWD	5'-CCATCTATGAGTT **CCACGG** GCTGTACGAAGAGAA-3'	**T→C**
*NcoI*614REV	5'-TTCTCTTCGTACAGC **CCGTGG** AACTCATAGATGG-3'	**A→G**
*BspHI*307FWD	5'-GGGACAACTCCTTCGTGG**TGATGA**CCAATTTCATCGTG-3'	**C→G**
*BspHI*307REV	5'-CACGATGAAATTGG **TCATCA** CCACGAAGGAGTTGTCCC-3'	**G→C**
*BspHI*1018FWD	5'-GGATCTTGCTAACAT **TTATGA** ACAAAAACAAGG-3'	**C→T**
BspHI 1018REV	5'-CCTTGTTTTTGT **TCATAA** ATGTTAGCAAGATCC-3'	**G→A**

Table 3.2 Sequences of the primers used for mutagenesis reactions to remove the endogenous NcoI and BspHI sites inside of the P2X$_1$ cDNA sequences.
Endogenous *NcoI* and *BspHI* sites inside of the P2X$_1$ receptor cDNA sequences required to be removed by site-directed mutagenesis. Mutated *NcoI* (numbering 1912 base pair from the origin of P2X$_1$ receptor sequence) or *BspHI* (307 and 1018 from the origin of P2X$_1$ receptor respectively) sites are in bold, and the presumed mutated bases are indicated in red and underlined. The conversions on each site are listed in the table above, and these mutations did not change the encoding amino acids. The sequences were confirmed by digestion with the correspondence restriction enzyme.

Amplification of P2X$_1$ receptor coding sequences

To generate the P2X$_1$ subunits for concatenation, PCR was performed on human P2X$_1$ receptor cDNAs where the *BspHI* restriction site has been removed and only the *NcoI* restriction site present at the start codon of the receptor remained. For both of the P2X cDNA, the sequences with stop codon and without stop codon were amplified and the primers used were listed in table 3.3.

P2X₁ sequence + stop

<center>*EcoRI Start codon*</center>

Forward primer: 5' TTA **GAATT**<u>CC</u>   **ATG**   **G**CA   CGG   CGG   TTC   CAG3'

<center>*NcoI*</center>

<center><u>   **NotI**   </u></center>

Reverse primer: 5'TTT   **GCGGC CGC**   **TCA**   GGA   TGT   CCT   CAT   GTT   C 3'

<center>*Stop   codon*</center>

P2X₁ sequence

<center><u>   *NcoI*   </u></center>

Forward primer:5'AGA**CC**   **ATG**   **G**CA   CGG   CGG   TTC   CAG   GAG   G 3'

<center>*Start codon*</center>

<center><u>   *BspHI*   </u></center>

Reverse primer: 5'TTGT**TC**   **ATG**   **A**GA   TGT   CCT   CAT   GTT   CTC C 3'

Table 3.3 The primer sequences used of amplifying the P2X₁ receptor cDNA
The primer sequences for amplifying the P2X₁ receptor cDNA sequences are listed above. Both of the sequences of the P2X receptor with or without stop were generated by PCR. The restriction sites (*NotI*, *EcoRI*, *NcoI* and *BspHI*) for further cloning are indiated in bold and underlined, and the start and stop codons are shown in bold and red.

3.4.3 Construction for initial vectors

Preparation of the Linker Vector

The "Linker" sequence was required for the formation of P2X receptor concatemers to provide linkage and some flexibility to the contruct. To obtain the linker, two complementary 5' phosphorylated primers were annealed together. The primers for making the two initial linkers were as described in table 3.4. The linker 1 with *NcoI* and *BspHI* restriction sites at the ends was used to extend the length of linker and the linker 2 with *HindIII* and *NotI* restriction sites was used to generate the linker vector and used as the basic construct to further generating the long linkers.

<center>102</center>

Linker 1

Forward primer

5' **CAT GG**A CAA CAG CAA CAA GGA CAA CAG CAA CAG GGA 3'

      H   G   Q   Q   Q Q   G   Q   Q   Q   Q   G

   __*NcoI*__

Reverse primer

5'   **CAT GA**G TCC CTG TTG CTG TTG TCC TTG TTG CTG TTG T**C** 3'

      M   L   G   Q   Q   Q   Q   G   Q   Q   Q   Q   G

  __*BspHI*__   __*NcoI*__

Linker 2

Forward primer

  __*part of*__   __*part of*__

  __*HindII*__   __*NotI*__

5' **AGCTT**C **CAT GG**A CAA CAG CAA CAA GGA CAA CAG CAA CAG GGA C**TC ATG A**GC 3'

          H   G   Q   Q   Q   Q   G   Q   Q   Q   Q   G   L   M

    __*NcoI*__   __*BspHI*__

Reverse primer

  __*part of*__   __*part of*__

  __*HindII*__   __*NotI*__

5' **GGCCGC**T **CAT GA**G TCC CTG TTG CTG TTG TCC TTG TTG CTG TTG T**CC ATG G** A 3'

          M   L   G   Q   Q   Q   Q   G   Q   Q   Q   Q   G   H

    __*BspHI*__   __*NcoI*__

Table 3.4 The linkers were produced by annealing two primers together.
The primer sequences for linkers are listed above. The linker 1 with *NcoI* and *BspHI* restriction sites at the ends was used to extend the length of linker. The linker 2 with *HindIII* and *NotI* restriction sites was used to generate the linker vector and used as the basic construct to generate the long linkers. The restriction sites *HindIII* and *NotI* for cloning in pcDNA 3.0 vector are indicated in red and bold, and the restriction sites *NcoI* and *BspHI* for linker and P2X1 receptor concatenation are in bold and underlined.

Amplification conditions:

Forward primer	100 μM
Reverse primer	100 μM
10X T4 ligase buffer (New England Biolabs® Inc.)	5 u

The annealing reaction was performed in a final volume of 20 μl in a Techne Genius thermocycler. The linker strand mixture was heated to 95 ºC for 2 minutes. Slowly (over a period of 15 minutes), the mixture was cooled to 50 ºC and incubated at that temperature for 5 minutes to allow hybridization of the linker-duplex strands. The linker-duplex was cooled to room temperature and was then ready for further ligation.

Native pcDNA 3.0 (1.5μg) which had 3 *NcoI* restriction sites removed was digested with 20 units of *NotI* and 20 units of *HindIII* restriction enzymes (New England Biolabs® Inc.) for 2 hours at 37 ºC. The digested vector was then run on a 1% agarose gel. The band of linearized pcDNA3.0 plasmid was cut and extracted and dephosphorylated.

The linker 2 sequences were then cloned into the pcDNA3.0 vector by ligation. Each linker was ligated in to the pcDNA3.0 vector and transformed into *E.coli*. Then the transformations were performed. Once the linker vector was obtained, the linker 1 sequence can be further added in to the linker vector by repeating the above ligation. The sequences of the linkers were checked by digesting with 10 units of *MluI* and 10 units of *NcoI* enzymes and sequencing Sp6 primer (PNACL sequencing service, Leicester University).

Construction of the "Donor" Vector

The pcDNA 3.0 containing the linker (1.5μg) was digested with 20 units of *NcoI* restriction enzymes (New England Biolabs® Inc.) for 2 hours at 37 ºC. The digested vector was then run on a 1% agarose gel. The band of linearized pcDNA3.0 plasmid was cut and extracted using the QIAquick Extraction kit (Qiagen®, U.S.A) and eluted in 25 μl H_2O. The vector containing the linker sequence was then dephosphorylated and quantified for ligation. The P2X receptor sequence lacking the stop codon was ligated in to the native pcDNA 3.0 vector containing linker. After transformation, 3μl of plasmid DNA was digested with 10 units of *NcoI* and 10 units of *NotI* enzyme to check if the insert was present in the native pcDNA 3.0 vectors. Then, the sequence of the plasmid DNA construct was also checked by sequencing as described.

Construction of the "Acceptor" Vector

a. Preparation of the Native pcDNA 3.0 Vector for Insertion of P2X Sequence

Native pcDNA 3.0 vector (1.5 μg) which has had the 3 native *NcoI* restriction sites removed was double digested with corresponding restriction enzymes (New England Biolabs® Inc.) for 2 hours at 37 ºC. The digested vector was then run on a 1% agarose gel. The band of linearized pcDNA3.0 plasmid was cut and extracted using the QIAquick Extraction kit (Qiagen®, U.S.A) and eluted in 25 μl H_2O. Dephosphorylation, precipitation and quantification of the native vector were the same as described.

b. Cloning of P2X receptor sequences in pcDNA 3.0 vector

P2X receptor pcDNA was ligated into the native pcDNA3.0 vector previously double digested with the corresponding restriction enzymes.Transformation was performed, and 3 μl of plasmid DNA was digested with 10 units of *NotI* and 10 units of *EcoRI* enzyme to check if the insert was present in the native pcDNA 3.0 vectors. The sequence of the plasmid DNA construct was also checked by sequencing.

3.4.4 Concatenated Channel Construction

Construction of P2X receptor dimer

The acceptor vector with P2X$_1$ receptor cDNA plus stop codon sequence (1.5 μg) was digested with 20 units of *NcoI* restriction enzymes (New England Biolabs® Inc.) for 2 hours at 37 ºC. The digested vector was then run on a 1% agarose gel. The band of linearized acceptor vector was cut and extracted using the QIAquick Extraction kit (Qiagen®, U.S.A) and eluted in 25 μl H$_2$O. Dephosphorylation, precipitation and quantification were the same as described.

The donor sequences with the P2X receptor sequence lacking the stop codon and linker sequences was digested from the donor vector with 10 units of *NcoI* and 10 units of *BspHI* restriction enzymes and purified from a 1% agarose gel. The sequences were quantified and ligated into the linerized acceptor vector with proper quantities to form a dimer. This dimer construct was confirmed by digestion with 10 units of *NcoI* and 10 units of *NotI* enzymes, and later verified by sequencing.

Construction of P2X receptor trimer

To generate the P2X receptor trimer constructs, the donor sequence was ligated to the dimer construct. The acceptor vector with dimer construct (1.5 μg) was digested with 20 units of *NcoI* restriction enzymes (New England Biolabs® Inc.) again and purified from the agarose gel. The same donor fragment with P2X receptor and linker sequences was ligated into the dimer constructs in the acceptor vector with proper quantity. Since the final trimer constructs containing the repeating sequences, the sequencing primers are not able to attach to a unique region. In this case, this construct was check by double digestion with *NcoI* and *NotI* restriction enzymes.

Chapter 4. MTS reagents at P2X$_1$ and P2X$_2$ receptors

4.1 Introduction
4.1.1 MTS reagents are effective tools to investigate the structure and function of ion channels

The substituted cysteine accessibility method (SCAM), or "cysteine scanning", is a popular method to map the structure and properties of ligand-gated receptors. In SCAM, individual cysteine residues are introduced to the protein by site-specific mutagenesis. Cysteine is a non-polar amino acid and can form covalent bonds with the thiol of the methanethiosulfonate (MTS) reagents as shown in the following reaction:
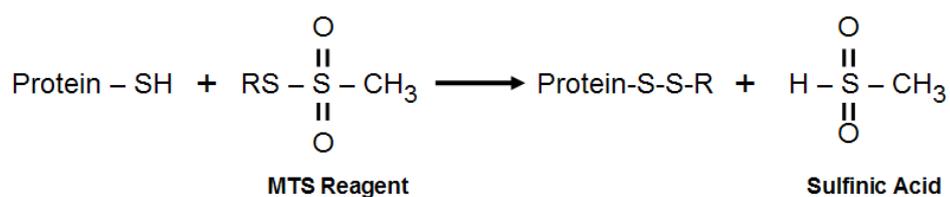
If the new disulfide bond is formed, the protein will carry the group from the MTS reagent and sulfinic acid will be released after the rapid reaction within 5 minutes. The advantage is it can introduce modifications at the side chain of the accessible cysteines. When the MTS reagents which contain the sulfhydryl active groups are applied to the ion channels, the chemical modifications will only happen to the mutated cysteine residue which is accessible in the aqueous environment. A range of MTS compounds could be used to introduce charged head groups with different sizes, and these modifications may bring some changes to the channel properties. The influence caused by the MTS reagents at specific residue then can be analyzed by electrophysiological recording (Akabas *et al*, 1992). For example the applications of MTS reagents alter the properties of some mutants, if the residue is exposed to the outer layer and close to important region for channel regulation. Furthermore, when charged MTS reagents are applied to the protein, a positive or negative charge can be introduced to the position bearing the neutral cysteine. If this modification influenced the ion influx or the desensitization of the receptor, the mutated residue should be necessary for channel regulation and the nature of charge is also important at this position.

SCAM was first used to investigate the structural basis of muscle-type nicotinic acetylcholine (ACh) receptors in 1992 by Akabas (Akabas *et al*, 1992). The residues in the membrane spanning domains of the alpha subunit were substituted to cysteine individually, and followed by application of MTS reagents. The residues Ser[248], Leu[250],

Ser^{252} and Thr^{254} were accessible to the small, positive-charged MTSEA ((2-aminoethyl) methanethiosulfonate) reagent and were suggested to be exposed to the channel lumen. This segment was thus considered to form a beta strand. Two years later, this group further substituted fifteen consecutive residues from the extracellular end of first transmembrane domain (Akabas et al, 1994). Large inhibition of the peak amplitudes were induced by MTSEA at seven mutants, and the assumption is the binding of MTSEA at the corresponding residues blocked ion influx through the pore. Therefore these residues may be lining the channel pore. This result also suggested the first transmembrane domain of ACh receptor alpha subunit is important for the channel gating. A similar strategy, of combining the site-directed mutagenesis and application of MTS reagents, was applied to the GABA$_A$ receptor (Xu et al, 1993). These studies showed the region from $_{\alpha1}$Val^{257} to $_{\alpha1}$Thr^{261} was important the lining the pore and the charge selectivity filter.

Cysteine residues in the extracellular domain of the P2X receptor play an important role in maintaining the relative spatial locations of the amino acid sequence. The tertiary structure of the binding loop has been already proposed to be maintained stably by five disulfide bonds of ten conserved cysteines on P2X$_1$ receptor as described above (Ennion et al, 2002b).Up to now, SCAM has been used to study different aspects of P2X receptor properties by using a range of MTS compounds (Rassendren et al, 1997; Jiang et al, 2001). For P2X receptors, SCAM was first used to study the second transmembrane domain of the P2X$_2$ subunit by Rassendren and his colleagues. Cysteine mutations throughout the putative TM2 were produced and characterized using positively charged MTS reagents of different sizes (Rassendren et al, 1997). Charged MTS reagents, such as MTSET and MTSEA, are frequently used to study the properties of specific residues. After the reaction, if a positive charged MTS reagent was added to the introduced cysteine residue it may result in some influence to the whole channel functions. The ten cysteines in the extracellular loop of the P2X$_1$ receptor are thought to form disulfide bonds naturally and there is no free cysteine in this domain as assessed by MTSEA-biotinylation (Ennion et al, 2002b). One conserved cysteine Cys^{349} in P2X$_{1-6}$ is present in the second transmembrane segment; however, it cannot be accessed by the MTS reagents (Rassendren et al, 1997). The relatively smaller side group of MTSEA allows it across the cell membrane freely in its uncharged form (Holmgren et al, 1996). By contrast, MTSET with a larger diameter can only enter the cell through

the channel pore during channel opening. As a result, the ATP evoked currents were inhibited by both MTS reagents at mutants I318C, N333C and T336C suggesting those corresponding residues are accessible to these chemicals and lie in the outer channel pore (Rassendren *et al*, 1997). In addition, the action of MTS compounds may block ionic permeation. The mutants that can only be accessed by smaller MTS reagents (MTSEA) not the larger ones (MTSET) when the channels were opened by ATP indicated the relevant residues are located inside of the channel gate.

Negatively charged MTSES (Sodium (2-sulfonatoethyl) methanethiosulfonate) can be used to probe the importance of positively charged residues in the ligand binding domain. Since it is not membrane permeable, it usually used to study the residues at extracellular loop of the P2X receptor. Take the $P2X_4$ receptor for example (Roberts *et al*, 2008); positive charges of lysines were removed by the neutral- charged cystienes at residues Lys^{67}, Lys^{69} and Lys^{313}. The treatment of MTSES induced a dramatic reduction by 80-95% of the ATP evoked peak amplitudes. When the positive charges were recovered by binding of MTSEA, the ATP sensitivity at mutants K67C, K69C and K313C was increased. This indicated these residues are important for ATP binding and the positive charges of the lysines are important at these localizations.

MTSM (methyl methanethiolsulfonate) and MTSB (butyl methanethiosulfonate) are small neutral molecules which can permeate the cell membrane freely. They are suitable to detect the inner side of the structure, and may be helpful to plot the topology of the ion channel. These two chemicals were applied in the study of $P2X_2$ receptor transmembrane and intracellular domains (Jiang *et al*, 2001), and the ATP evoked responses of mutants D15C, P19C, V23C, V24C, G30C, Q37C, F44C and V48C can be strongly inhibited. In this study, the MTSM and MTSB were used to test the effects to WT $P2X_2$ receptor and no influence was observed (Jiang *et al*, 2001). They therefore were further used to probe the accessibility of the whole range of residues and the suspected residues will be further studied by positive MTS chemicals with larger sizes (Jiang *et al*, 2001). Some of the popular used MTS reagents were listed in table 4.1.

In addition to the transmembrane domains, the SCAM approach has been used to establish the basis of extracellular ATP binding model of P2X receptor as described in the introduction.

MTS Reagents	Mol Formula	MW	Charge	Structure
MTSM	$C_2H_6O_2S_2$	126.20	no	
MTSB	$C_5H_{12}O_2S_2$	168.28	no	
MTSEA	$C_3H_9NO_2S_2 \cdot HBr$	236.15	+	
MTSES	$C_3H_7NaO_5S_3$	242.27	−	
MTSET	$C_6H_{16}BrNO_2S_2$	278.24	+	
TMA-Cl	$C_9H_{15}ClN_2O_2$	218.68	+	
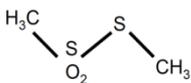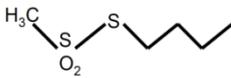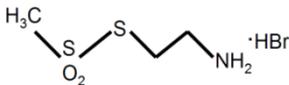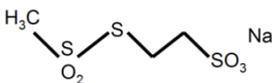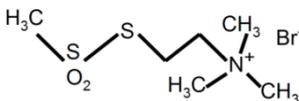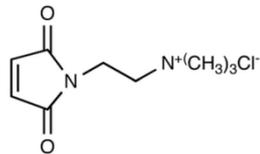
Table 4.1 The properties of commonly used MTS reagents.
Some of the popular used MTS reagents are listed in the table. MTSM is the smallest chemical which can permeate to the cell membrane freely, while MTSET is the largest positive charged chemical in this list can only get inside of the cell when channel is open.

4.1.2 Aim

The effects of MTS reagents on WT $P2X_1$ receptors will be determined in the following studies. However, only MTSEA and MTSES were previously tested on $P2X_1$ receptor. In this chapter, I aim to explore more available MTS compounds. Therefore, the effects of a range of MTS reagents will be investigated at the WT $P2X_1$ receptor and the WT $P2X_2$ receptor as these have been broadly studied with MTS compounds will be used as a reference.

4.2 Results
4.2.1 The application of MTS reagents to WT P2X$_1$ receptor
ATP evoked transient inward current at WT P2X$_1$ receptors as shown in figure 4.1. This response desensitized rapidly during the application of ATP and was recovered within 5 minutes. After the first application, subsequent responses had over 70% of the initial peak current amplitude.

ATP evoked concentration dependent inward currents with an EC$_{50}$ (half maximal effective concentration) of 1 μM at the WT P2X$_1$ receptor (See figure 4.1). To estimate the EC$_{50}$ value of P2X$_1$ receptor, a range of different concentrations of ATP from 0.1 μM to 100 μM was applied. As summarized in figure 4.1, the ATP evoked peak amplitudes increased as the concentration of agonist increased. Furthermore, response evoked at the EC$_{50}$ value of 1 μM for ATP was sensitive to changes (increase or decrease) in peak amplitude current on treatment, thus this concentration will be used for looking at the effects of MTS and other chemical treatments to the P2X$_1$ receptor in the subsequently study. In addition, the time-course of the response (rise time and decay) was also concentration dependent. For instance, when a lower concentration of ATP was applied, slower channel activation and desensitizing observed (Figure 4.1).

Some of the MTS reagents are not soluble in water and DMSO (dimethyl sulfoxide) or ethanol as the organic solvent was required to make up these MTS solutions. DMSO and ethanol at high concentrations can have effects on P2X receptor peak amplitudes. Previous studies suggested ethanol could reversibly inhibit the currents of P2X$_2$ and P2X$_4$ receptors (Davies *et al*, 2002; Xiong *et al*, 2000) and potentiate the ATP induced current of P2X$_3$ receptors (Davies *et al*, 2005). This potentiation was indicated to be allosteric as supported by a 3-fold decrease in ATP EC$_{50}$ and a left shifted ATP concentration-response curve. Therefore the concentrations of DMSO and ethanol used in this study should be carefully controlled.

1μM ATP was applied to the WT P2X$_1$ receptor every 5 minutes as a control group for the DMSO and ethanol vehicles treatment, and reproducible currents were observed for up to 45 minutes (Figure 4.2). Chemicals were perfused in the buffer after the fourth ATP application when the stable responses were obtained. As a control, the peak values from the fifth to the eighth ATP applications were compared to the fourth application,

and there was no significant difference (1.24% ± 4.34, $n=3$) shown. 0.01% of DMSO and 0.005% of ethanol were made up in the ND96 buffer solution. The average effects were revealed as 3.37% ± 1.01 ($n=3$) and 9.21% ± 8.27 ($n=4$) of potentiations to the continued ATP applications respectively (Shown in figure 4.2), and they have no significant difference to the ATP control group. These concentrations will be further used in MTS compound preparation.

1mM MTSEA, MTSET and TMA-Cl (N-[2-(trimethylammonium) ethyl] maleimide chloride) were subsequently made up in ND96, and 0.01% DMSO and 0.005% ethanol made from ND96 were used for MTSM and MTSB dissolving respectively. MTS compounds were prefused to the oocytes in the bath and applied with 1 μM ATP four times every five minutes after the fourth ATP application. The maximum effects of the reagents were compared to the ATP evoked response just before the chemical treatment and summarized in figure 4.3. MTSEA (6.42% ± 1.45, $n=7$) and MTSET (3.97% ± 3.30, $n=3$) had no significant effect on the peak amplitudes of WT $P2X_1$ receptors from the ATP control group. However, the small neutral MTS reagents MTSM (-88.76% ± 1.50, $n=5$) and MTSB (-91.24% ± 5.44, $n=3$) inhibited about 90% of the peak currents (*** $p<0.001$), and the effects cannot be washed off after 10 minutes. These inhibitions may be due to the binding of MTSM and MTSB to WT $P2X_1$ receptors, and these binding caused fundamental changes in the channel properties.   Since these two MTS compounds are the smallest and uncharged ones used, they can readily permeate the plasma membrane and should be more capable to access the residues in narrow regions of the protein. Previous studies used them in cysteine scanning for $P2X_2$ receptors N-terminus and first transmembrane domain, whereas they had no obvious influence to the WT $P2X_2$ receptor current. In order to find out if there is a free cysteine in the WT $P2X_1$ receptors, TMA-Cl as a sensitive and potent free cysteine detector was used. It is slightly smaller than MTSEA and membrane permeable. The 20 minutes perfuse of 1 mM TMA-Cl in bath had no significant influence to the control group (2.76% ± 2.07, $n=3$), and indicated either there is no free cysteines at WT $P2X_1$ receptors or the TMA-Cl was not able to reach the narrow regions for disulfide bond forming.

The inhibitions induced by MTSM were further analyzed by reducing the concentration to 100 μM. As shown in figure 4.4, when the reproducible responses were obtained, the

(A)

(B)
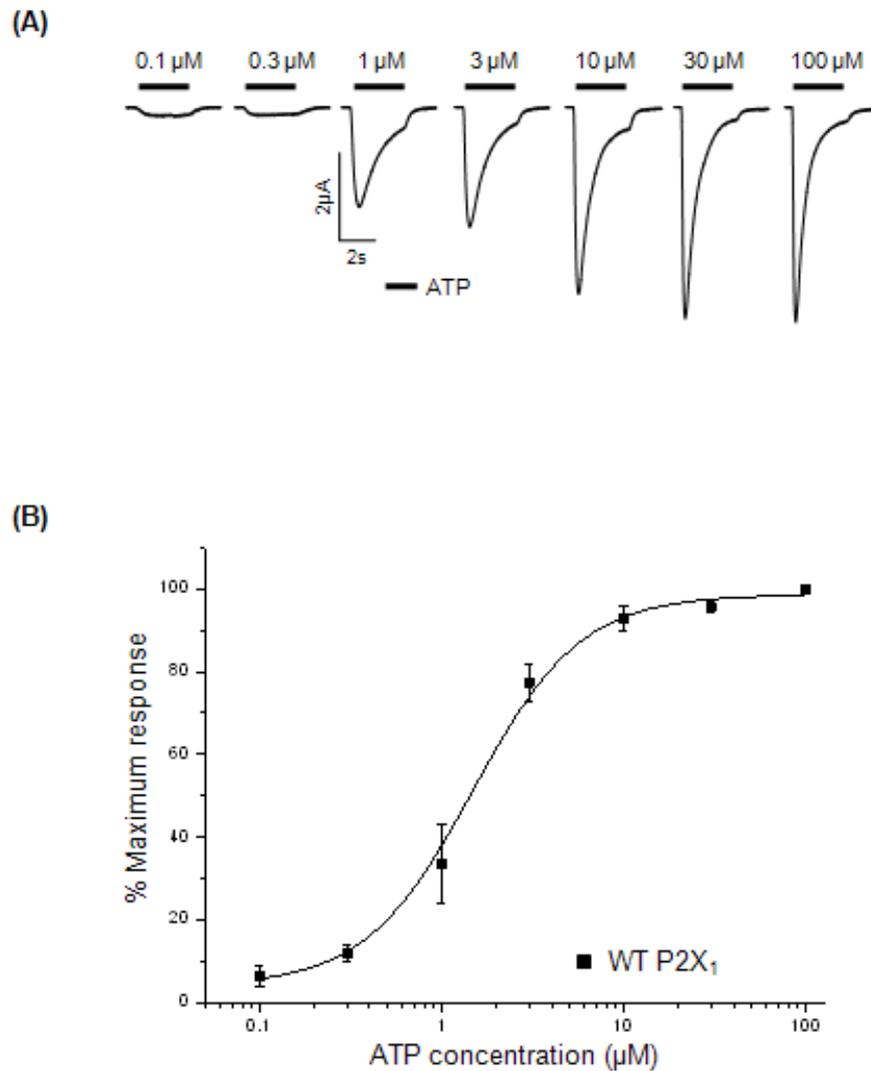
Figure 4.1 Concentration-response curve of the WT P2X$_1$ receptor
(A). The peak amplitude of ATP evoked current is concentration dependent. A range of concentrations of ATP (from 0.1 µM to 100 µM) were applied to the WT P2X$_1$ receptor as indicated by bars. Maximum response was obtained at 100 µM ATP, and the peak currents were reduced with the decreasing of ATP concentration.**(B).** The ATP concentration response curve were plotted by fitting the mean peak values at different concentrations (*n*=3) together. The EC$_{50}$ value estimated for P2X$_1$ receptor is about 1 µM, which will be used in the further study with MTS reagents.
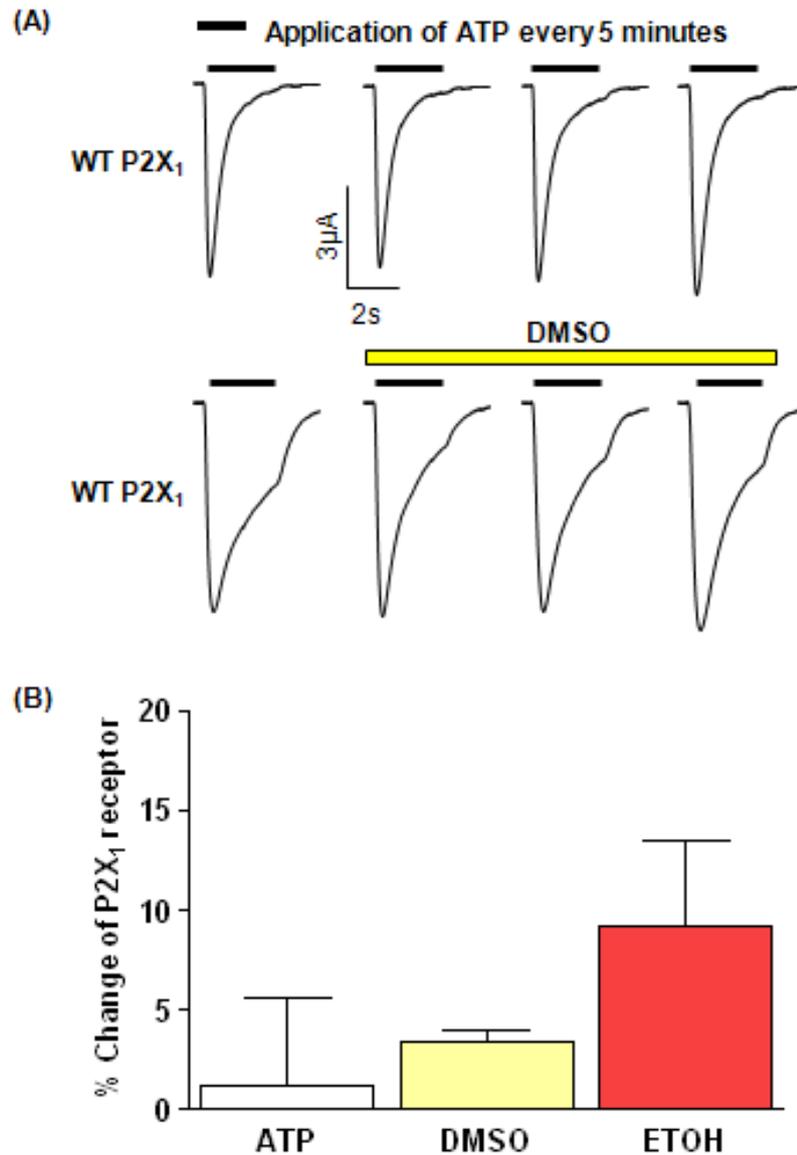
Figure 4.2 Both DMSO and ETOH had no effect on P2X$_1$ receptor currents
(A). ATP (1 µM as the EC$_{50}$ for P2X$_1$ receptor, indicated in bar) was applied on the WT P2X$_1$ receptor, and the fast desensitizing currents were triggered as shown above. Reproducible currents can be evoked at the 5 minutes intervals. The application of DMSO (0.01%) (indicated in yellow bar) had no influence to the WTP2X$_1$ receptor. **(B).** Summary of % effects of DMSO (0.01%) and ETOH (0.005%) on P2X$_1$ receptor peak (*n*=3 for ATP and DMSO, *n*=4 for ETOH).
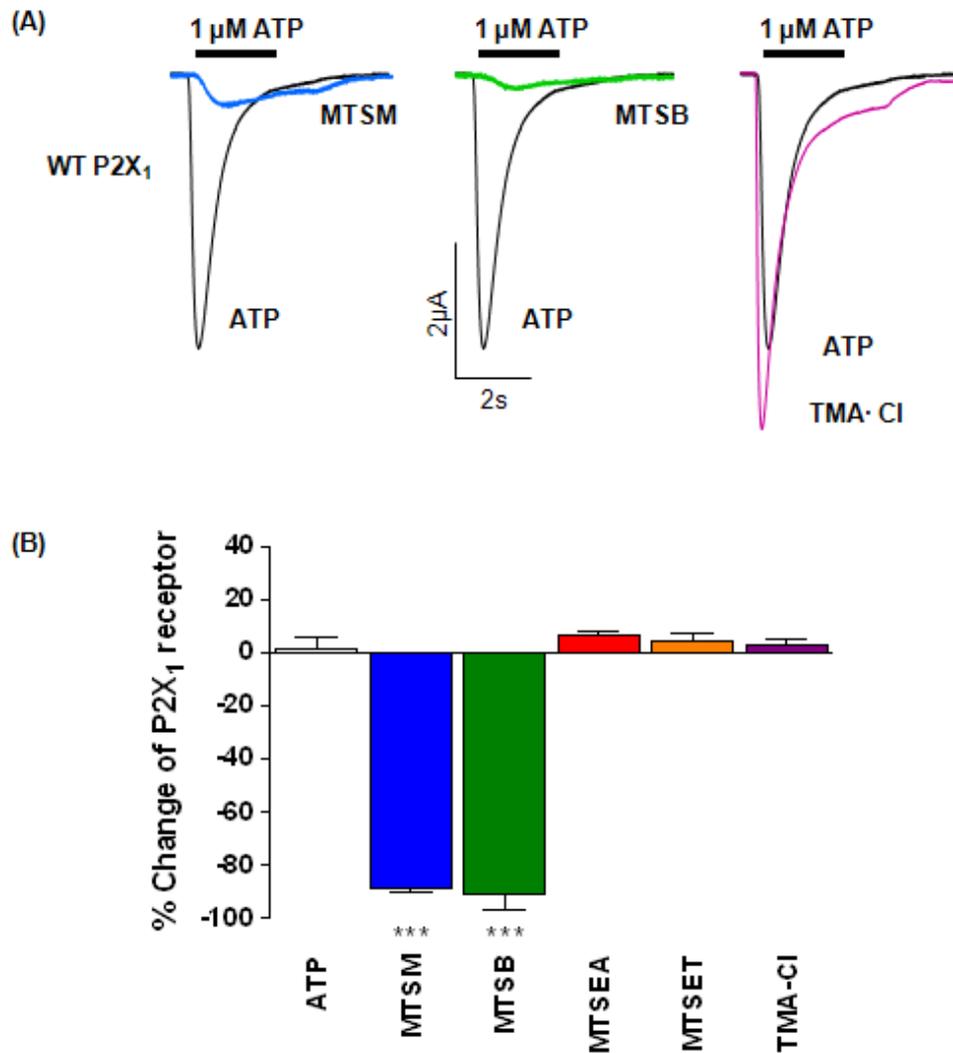
Figure 4.3 Effects of MTS compounds on P2X$_1$ receptor currents
(A). Example traces of the WT P2X$_1$ receptor evoked by ATP (1 μM). The amplitudes of WT P2X$_1$ receptor under the application of 1 μM ATP, can be dramatically inhibited by MTSM (blue) and MTSB (green). While the TMA-Cl (purple) had no effect. **(B).** The summary of % changes of the different reagents on WT P2X$_1$ receptor. 1 mM MTSM (*n*=5) and MTSB (*n*=3) inhibited about 90% of the peak currents, while 1 mM MTSEA (*n*=7), MTSET (*n*=3) and TMA-Cl (*n*=3) had no effect. *** $p<0.001$

100 μM MTSM was perfused to the WT P2X$_1$ receptors during the 5 minutes intervals for ATP applications. The decrease in peak amplitudes seems related to the application period. After 10 minute perfusion of 100 μM MTSM, the inhibition is about 30% of the peak current before the MTSM treatment; while the perfusion time was increased to 20 minutes, 60% inhibition was demonstrated (Figure 4.4). Hence, it was suggested to be a time dependent effect for MTSM. This inhibition is irreversible and the blockage caused by MTSM cannot be removed after 10 minutes wash in ND96 bath. Comparing to the 1 mM MTSM treatment, the 100 μM MTSM is less effective (maximum effect is -59.90% ± 6.39, *n*=4, *** p<0.001) to reduce the ATP evoked response. The irreversible time-dependent inhibition pattern was also observed following 1 mM MTSM treatment. In addition, when the ATP concentration was increased to 100 μM, the maximum inhibition induced by 1 mM MTSM was still 76.09% ± 13.26 (*n*=4, *** p<0.001).

4.2.2 The application of MTS reagents to WT P2X$_2$ receptor

In contrast to the WT P2X$_1$ receptors, ATP evoked slowly desensitizing currents at WT P2X$_2$ receptors. The P2X$_2$ receptors have been widely used in SCAM studies as a good model for receptor expression and giving reproducible current. Previous study suggested a variety of MTS compounds including the MTSM and MTSB had no effects to the P2X$_2$ receptor (Jiang *et al*, 2001), and it therefore was used as a control in the following study to the P2X$_1$ receptors. In order to find out if there is subtype differences in the effects to MTS compounds, the WT P2X$_2$ receptors were given the same treatment as for WT P2X$_1$ receptors.

P2X$_2$ receptors gave reproducible currents in response to ATP application at 12 μM which evokes half of the maximum response, and it was used in the following applications. The effects of 0.01% DMSO and 0.005% ethanol as the solvent for MTS compounds to P2X$_2$ receptors were examined firstly, and the group with only the continued ATP applications was set to be the control. Consequently, the P2X$_2$ receptors were tolerate to these vehicles, and no change can be observed for the DMSO (-2.09% ± 9.08, *n*=3) and ethanol (-0.04% ± 5.04, *n*=3) treatment groups (See figure 4.5). These two chemicals will be subsequently used in the same concentration for dissolving the MTS compounds.

P2X$_2$ receptors displayed relatively non-desensitizing currents triggered by the agonists, and none of the MTS reagents had an effect as shown in figure 4.6.   Compared to the fourth ATP evoked response before the treatment of MTS compounds in bath, MTSEA (15.23% ± 4.87, *n=3*) and MTSET (7.71% ±6.47, *n=3*) had no effect to P2X$_2$ receptor and similar observation was reported in a previous study (Rassendren *et al*, 1997). In contrast, the two small MTS compounds MTSM and MTSB which affected the normal function of P2X$_1$ receptors did not cause any significant inhibition to the WT P2X$_2$ receptors. These results are consistent to what have been shown previously (Jiang *et al*, 2001), and indicated the P2X$_2$ receptor is insensitive to small MTS compounds. 1 mM TMA-Cl was applied to the P2X$_2$ receptor to confirm the absence of free cysteines, and it induced no change (-11.27% ± 6.93, *n=3*) to the control group. These suggested either there is no detectable free cysteine present at WT P2X$_2$ receptors, or the influence caused by these MTS compounds is non-measurable.
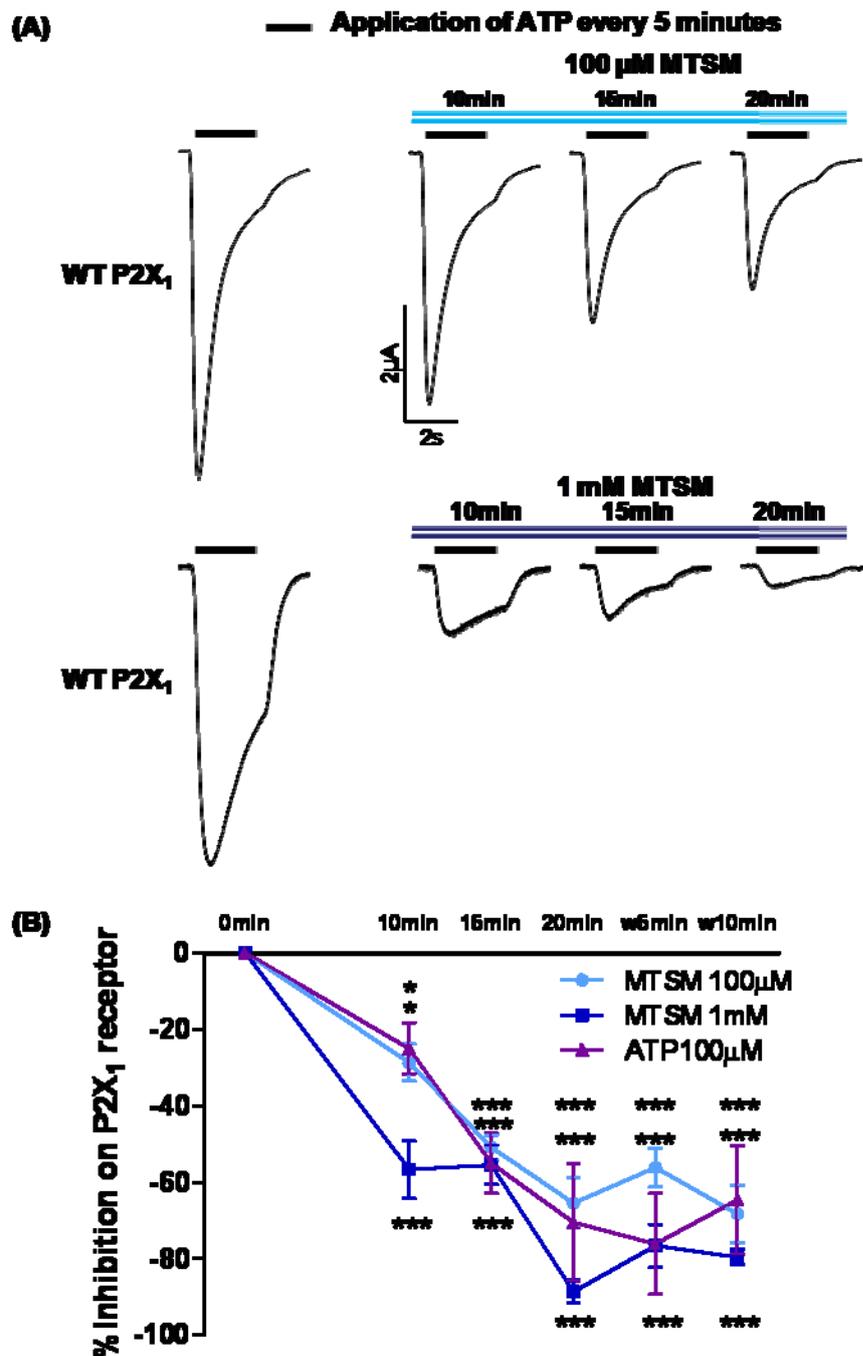
Figure 4.4 The inhibition by MTSM on WT P2X$_1$ receptor is concentration dependent
(A). The traces of the P2X$_1$ receptor response evoked by ATP(1 μM) with the treatment of MTSM (100 μM in light blue or 1 mM in dark blue). The ATP was applied every 5 minutes as indicated by the bar. **(B).** Summary of the peak currents of the WT P2X$_1$ receptor inhibition by 100 μM and 1 mM MTSM. About 90% of the peak current was inhibited by 1 mM MTSM after 20 minutes, while the 100 μM MTSM only inhibited 65%. Besides, the lower concentration has slower speed of the inhibition. When the ATP concentration increased to 100 μM (in purple), similar inhibition still remained for the treatment with 1mM MTSM. These effects can not be wash off after 10 minutes in bath. *** $p<0.001$, *$p<0.05$
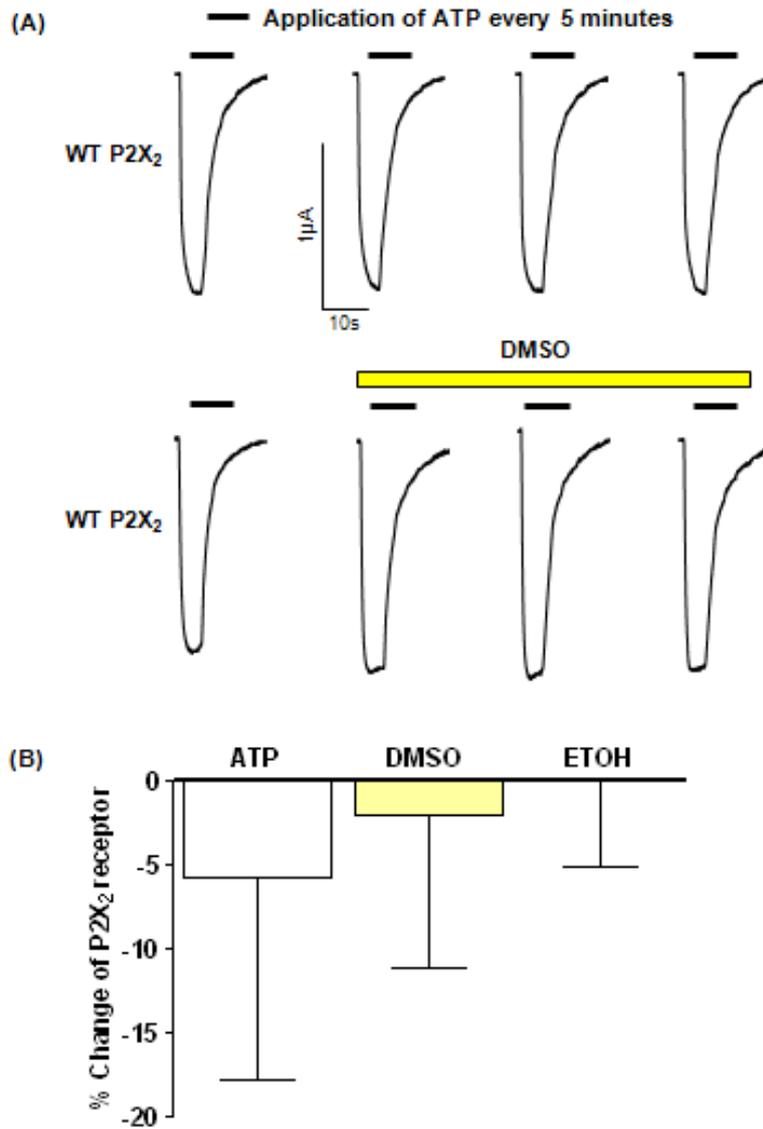
Figure 4.5 Lack of DMSO and ETOH induced effects on P2X$_2$ receptor current
(**A**). ATP (12 μM as the EC$_{50}$ level) was applied on the WT P2X$_2$ receptor as indicated in bar, and the slowly desensitizing currents were evoked as shown above. Reproducible responses were evoked at 5 minutes intervals. The DMSO (0.01%)(shown in yellow bar) had no influence on the WT P2X$_2$ receptors. (**B**). Summary of the % effects of DMSO (0.01%) and ETOH (0.005%) on P2X$_2$ receptor currents. *n*=3 for each.
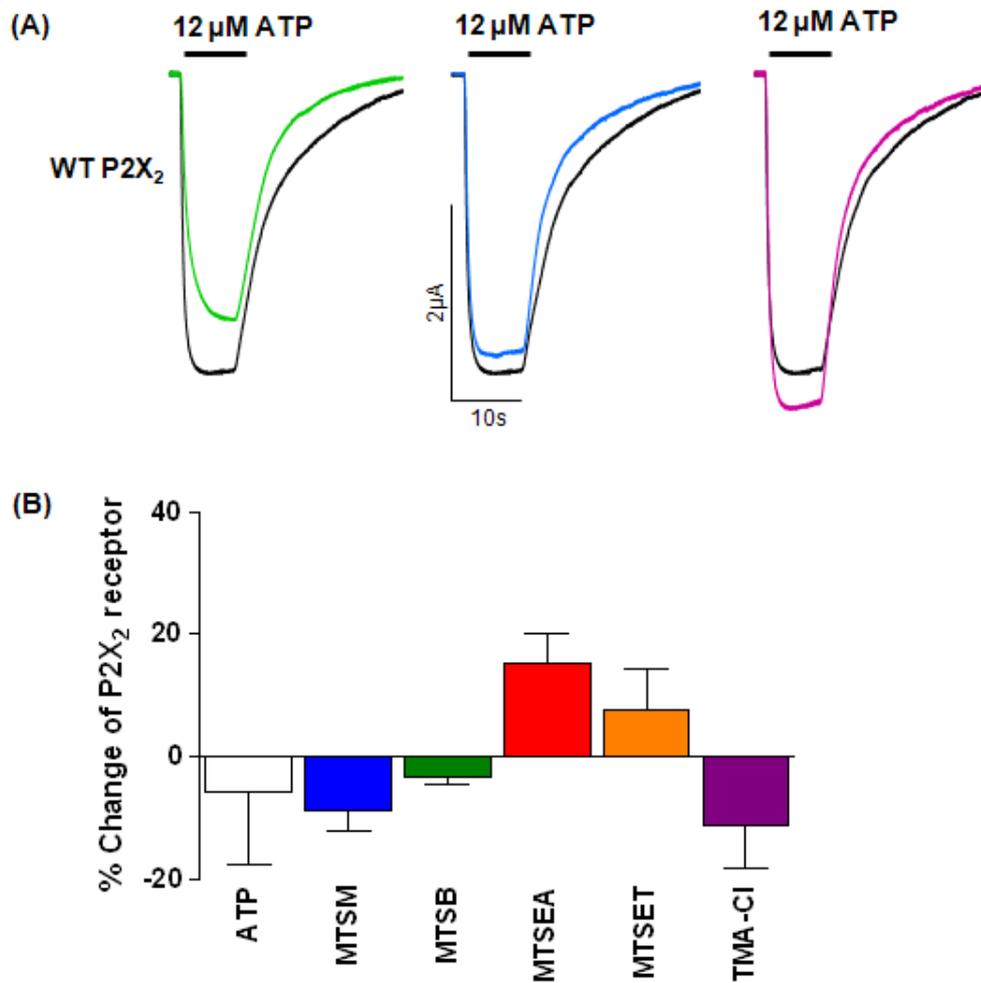
Figure 4.6 MTS reagents have no effect on WT P2X$_2$ receptors

(A). Example traces of the WT P2X$_2$ receptor evoked by ATP (12 µM) as indicated in bars. 1 mM MTSM and MTSB had little effect to the peak currents. **(B).** Summary of effect of the different reagents on WT P2X$_2$ receptor. All of the reagents (*n*=3 for MTSM as in blue, *n*=4 for MTSB as in green, *n*=3 for MTSEA as in red, *n*=3 for MTSET as in orange and *n*=3 for TMA-Cl as in purple) at 1 mM had no significant influence.

4.3 Discussion

The ten conserved cysteine residues in the extracellular loop of the P2X receptors have been suggested to form disulfide bonds this is based on biochemical and electrophysiological studies. MTSEA-biotin was used to label the WT P2X$_1$ receptor but no bands can be seen on the PAGE gel (Ennion *et al*, 2002b). Since the MTS compounds are potent rapid sulfhydryl active reagents, this result indicated there are no detectable free sulfhydyl groups from cysteine existent at WT P2X$_1$ receptor. However it is circumstantial and not definitive. It therefore still remained to be further investigated until the reliable evidence come from the crystal structure study by X-ray crystallography or mass spectrometry analyses.

4.3.1 The MTS compounds selection for P2X$_1$ receptor studies

The overall results show that MTSEA and MTSET are feasible for the following SCAM study at P2X$_1$ receptor with no fundamental effects to its normal response. The continuous application of MTSEA and MTSET had either small or no effect to the peak amplitudes at the WT P2X$_1$ receptor as demonstrated in a number of previous studies (Rassendren *et al*, 1997; Stoop *et al*, 1999; Jiang *et al*, 2001; Spelta *et al*, 2003; Roberts *et al*, 2007; Roberts *et al*, 2008). When the cysteine was introduced at specific residues, the MTS reagents can be used as indicators for its structural or functional changing. Besides, the charged side chains of these two compounds may introduce or restore the positive charges to the mutated residue, and help to estimate the relevant molecule binding or regulation mechanisms. For instance, the MTS effects at P2X$_1$ receptor mutant K309C were dependent on the charge of the MTS reagent (Roberts *et al*, 2007). Positively charged MTSEA induced about 20-fold increase to ATP potency, while its maximum response was abolished by the negatively charged MTSES. Thus the positive charge is essential at the Lys^{309} position, and it may interact with the negatively charged phosphate chain of ATP directly. Consequently, MTSEA that is permeable to the cell membrane is preferable to the following SCAM study in the intracellular domains. The MTSET which only gets through the cell membrane when the channel is open can also be used as a larger positively charged MTS compounds alternatively.

MTSM and MTSB are small MTS compounds with the molecular weight of less than 170. Their small and non-charged nature allows them to be ideal cysteine detector for

the narrow regions of the receptor. Additionally, they are permeable to the cell membrane, which make them suitable for the study of intracellular domains and the TMs of the P2X receptor. Since the MTSM and MTSB are non-charged compounds, they are usually used in the whole-range scanning at first to rule out the accessible residues. Subsequently, the MTSEA will be treated to the "significant residues" to introduce the positive charges and give more structural evidence afterwards. It was a surprising finding that the $P2X_1$ receptor cannot tolerate these small neutral MTS compounds which affected the peak currents of $P2X_1$ receptor fundamentally to about 90% and cannot be used further. However, they showed no effects to $P2X_2$ receptors (Jiang *et al*, 2001 and current study). Cysteine at $P2X_1$ receptors are conserved at $P2X_2$ receptors, so the existence of potential cysteine binding site suggests small structural variations between these two subtypes.

4.3.2 Possible binding regions of the MTS compounds at WT $P2X_1$ receptor

As shown clearly in the results, the MTSM compounds affected the ATP at EC_{50} concentration stimulated response of WT $P2X_1$ receptor to 90%, while the $P2X_2$ receptor was not influenced at all. MTSM also caused up to 80% inhibition to the maximum response of $P2X_1$ receptor evoked by 100 µM ATP indicating there is no shift at ATP potency.

MTSM is the smallest MTS compound with only an additional methyl to the MTS group. It recognizes the cystienyl sulfhydryls selectively and should alter the conformation of cysteine residue to minimum extent. Sulfinic acid as the byproduct of the sulfhydryl reaction contains a methanethiosulfonate, it decomposes to smaller volatile products quickly and does not influence the disulfide bonds formation or the reaction activity.

The fundamental affects caused by MTSM indicated the possibility of the existence of free cysteine in $P2X_1$ receptor. Previous studies used MTSEA-biotin to recognize the conserved cysteine residues at the extracellular loop (Ennion *et al*, 2002b), however, the MTSEA has been shown as no effect to the WT $P2X_1$ receptor and it is much larger than the MTSM in size. TMA-Cl as another rapid sulfhydryl active reagent is effective in detecting the free cysteine for receptors. However, the molecule weight of it (218.7) is less than MTSEA but is still about double of the MTSM in size. Although no effect

was observed for TMA-Cl applications, it may due to the TMA-Cl is not small enough to access the narrow region with free cysteine.

The ten conserved cysteines were suggested to be linked in pairs by using MTSEA-biotinylation. No single free cysteine was revealed by the MTSEA-biotin, whereas the size of MTSEA-biotin is larger than the MTSM and may have limitation to access the narrow part of the tertiary structure. For example, The Cys^{117} and Cys^{165} cannot be pulled down on the SDE-PAGE gel after the MTSEA-biotinylation and suggested these two cysteines may not be accessible to the MTSEA-biotin (Ennion et al, 2002b). It gave rise the possibility of the existence of free cysteine.

Apart from the extracellular cysteines, there is a single cysteine residue Cys^{348} (P2X$_2$ numbering) present at the second transmembrane domain of P2X receptor. This cysteine was considered as a silent residue. Since both MTSEA and MTSET showed no influence to either WT or C348A mutants at the P2X$_2$ receptor, it was proposed to be inaccessible for these MTS compounds (Rassendren et al, 1997). The successful usage of MTSM and MTSB in the cysteine scanning study of first transmembrane domain of P2X$_2$ receptor further suggested this residue is located in the inside layer of the transmembrane domain (Jiang et al, 2001). However, this variation of MTSM and MTSB applications between P2X$_1$ and P2X$_2$ receptor might suggest a slight structure difference between these two subtypes.

One characterizing feature between the P2X$_1$ and P2X$_2$ receptor is their desensitizing patterns. The chimeras of P2X$_1$ and P2X$_2$ receptors were generated by Werner, and the two transmembrane domains played important roles in maintaining the fast desensitizing behaviors for P2X$_1$ receptor (Werner et al, 1996). However, the sequences of the transmembrane domains at these two subtypes are essentially the same. The decisive residues in these regions have not been identified, but they may cause significant difference in structure. In other words, there is obvious functional diversity in the TM2 of P2X receptors, and it might indicate potential structural diversity. Thus, there is an assumption that the residue Cys^{349} is more accessible at P2X$_1$ receptor than P2X$_2$ receptor, and it explained the inhibition caused by MTSM and MTSB at only P2X$_1$ receptor. The Cys^{349} at the TM2 was thus suggested to be associated with the MTSM binding. It is noticeable that the small MTS compounds exhibited striking

inhibitions to the peak amplitudes to ATP application but not the time-course from 100% to 50% of the peak amplitude. This might also imply the modification of these MTS compounds impaired the channel opening mechanism, so that the ions have difficulties to get through the channel and evoke maximum current. Since great inhibition still can be observed with the 100 μM ATP evoked currents, this inhibition could associate with the decreasing in ATP potency.   However, since no effect on time-course of response was observed, this regulation may be via channel gating modulation. Another assumption is the intracellular regulation pathway for $P2X_1$ receptor was blocked by these small MTS compounds. MTSM and MTSB could bind to the accessory proteins for $P2X_1$ channel opening modulation and abolished the ATP evoked responses subsequently.

4.3.3 Strategies for looking at the MTS compounds binding regions

The results of the neutral MTS compound applications to the $P2X_1$ and $P2X_2$ WT receptors were quite interesting.   However, the reasons why the $P2X_1$ WT receptor was not able to tolerate the application of some small neutral MTS reagents remain unknown. Up to now, the number of available small cysteine binding chemicals is limited. It is therefore difficult to solve the question by introducing a range of small site groups and comparing their effects. Nevertheless, the site-directed mutagenesis and chimera synthesis may shed lights to allocate the regions involved in the MTS modifications.

In order to investigate the potential MTS compounds binding site Cys^{349} at the $P2X_1$ receptor second transmembrane segment, it can be mutated into a small neutral alanine residue at the $P2X_1$ receptor. Single or double mutations to the consensus extracellular cysteines could also be generated, and the MTS compounds treatment tested on mutants. If the inhibition is absent, the corresponding cysteine(s) would be responsible for the MTS binding site(s).

Alternatively, $P2X_{1/2}$ chimeras are useful models to study the properties in specific region of the receptor. Different fragments of $P2X_1$ and $P2X_2$ subunits, such as the transmembrane domains, cysteine rich loop, can be swopped to produce $P2X_{1/2}$ chimeras. The properties of the chimeras can be studied by using a range of MTS compounds and compared with the effects on WT receptors.   If any of these chimeras

shown the similar patterns to the MTS compounds as WT $P2X_1$ receptor, the MTSM or MTSB binding domain will be identified.

4.3.4 Conclusion

The effects of MTS compounds to the WT $P2X_1$ and $P2X_2$ receptors were measured in this study. The larger MTS compounds MTSET and MTSEA which did not affect the responses of both WT receptors will be used to probe the function and structure of $P2X_1$ receptor.

The smaller MTS compounds MTSM and MTSB caused striking inhibitions to the WT $P2X_1$ receptor, while the WT $P2X_2$ receptor was unaffected. The conserved cysteines at the $P2X_1$ and $P2X_2$ receptors have been inferred to form disulfide bridges in pairs, and no subtype differences were suggested from previous studies. These compounds specifically recognize the cysteine residue and may bind to the narrow part of the receptor that are hardly accessible by other MTS reagents. However, the evidence for the free cysteine is still deficient, and the mutations on the conserved cysteine residues or the $P2X_{1/2}$ chimeras could be generated to address the problem.

Chapter 5. Cysteine scanning of the P2X$_1$ receptor N-terminus

5.1 Introduction

The extent of the P2X receptor amino terminus was firstly identified by hydrophobicty analysis as described in chapter 1 (refer to 1.5.1.). The sequences of the amino terminus are similar amongst the P2X receptor family (P2X$_{1-7}$), and it is 30 amino acids long for the P2X$_1$ receptor (North, 2002). The P2X receptor amino terminus has been suggested to be located intracellularly through a range of studies, for example signal peptide sequence analysis (Brake *et al*, 1994) and glycoslation studies (Newbolt *et al*, 1998). The properties of the amino terminus were investigated in a range of studies subsequently, and its roles in channel regulation especially the residues important in channel desensitization, gating and protein trafficking will be investigated in this chapter.

5.1.1 The roles P2X receptor N-terminus in time-course regulation

The roles of the amino terminus of P2X receptor in channel desensitization were firstly suggested by generating P2X$_1$ and P2X$_2$ chimeras (Werner *et al*, 1996). The ATP evoked current at P2X$_1$ receptors shows remarkable desensitization during the continued presence of ATP within a few hundred milliseconds, whereas the current of P2X$_2$ receptor can be maintained with little desensitization during the continued ATP presence of over 10s of seconds. The chimera splicing the first 47 amino acids of P2X$_2$ receptor including the amino terminus to the P2X$_1$ receptor sequence gave a non-desensitising receptor. This indicated the N-terminal region and first transmembrane segment may regulate the time-course of responses.

The role of the amino terminal at P2X$_3$ receptor was also studied. P2X$_3$ is known for its fast desensitizing phenotype. However, a truncated P2X$_3$ clone lacking the intracellular N-terminus was generated and shown to be functional but the desensitization was abolished during ATP application. Therefore a correlation between the time-course and N-terminal region at the P2X$_3$ receptor was demonstrated. King's group also injected the calcineurin auto-inhibitory peptide into the oocytes expressing fast desensitizing P2X$_3$ receptor (King *et al*, 1997). Calcineurin is a type of protein phosphatase and known for its roles in the desensitization of cation gated NMDA and 5-HT channels

(Tong *et al*, 1995; Boddeke *et al*, 1993). After the injection of the calcineurin inhibitor, the desensitizing speed was slowed down progressively (King *et al*, 1997). Hence, intracellular phosphorylation may be essential for the desensitizing regulation, and the N-terminal region may be required in the calcineurin-containing protein dephosphorylation signalling.

5.1.2 Consensus PKC site is involved in the channel desensitizing mechanism

There is a conserved protein kinase C (Thr^{18}-X-Lys/Arg^{20}) ($P2X_1$ receptor numbering, see figure 5.1, Boue-Grabot *et al*, 2000) consensus site located at the N-terminus among all known P2X receptor subtypes and it is a putative target for intracellular phosphorylation regulation. This site combines the completely conserved threonine and two residues downstream there is a positively charged residue (either lysine or arginine). The threonine bearing a hydroxyl side chain is a potential phosphorylation residue, while the positively charged residue is necessary for the negatively charged phosphorylation kinase recognition and docking.

YXTXK/R PKC motif   TM1

```
DDB0217630     -------------------MTIDWDSILSYNTIKVV----------
DDB0203089     ------------------MLDWDSILAYNTIKVVRIRDRRLGIL
DDB0187892     ------------------MDWDNIFSYNTAKIVTIKDRRLGGL
DDB0168616     --------------MG-FSFDWDDIFQYSTVKIVRIRDRRLGIL
DDB0219300     -------------MNFRNIDWDSLFSYSTIKIVRIRDKRLGIL
Schistosome    ----------------MVKGIAVLFEYETPKLVQISNIKIGVT
HumanP2X1      -----------MARRFQEELAAFLFEYDTPRMVLVRNKKVGVI
HumanP2X2      MAAAQPKYPAGATARRLARGCWSALWDYETPKVIVVRNRRLGVL
HumanP2X3      ----------------MNCISDFFTYETTKSVVVKSWTIGII
HumanP2X4      -------------MAGCCAALAAFLFEYDTPRIVLIRSRKVGLM
HumanP2X5      -----------MGQAGCKGLCLSLFDYKTEKYVIAKNKKVGLL
HumanP2X6      -----------MGSPGATTGWGLLDYKTEKYVMTRNWRVGAL
HumanP2X7      -------------MPACCSCSDVFQYETNKVTRIQSMNYGTI
```

Figure 5.1 Alignment of intracellular amino terminus sequences in human, *Schistosome* and *Dictyostelium* P2X receptor subtypes
The sequences of P2X receptor amino terminus of P2X receptor members are shown. The consensus protein kinase C site (Tyr^{16}-X-Thr^{18}-X-Lys/Arg^{20}) with a complete conserved tyrosine, threonine and positively charged lysine or arginine resiudes are circled (Taken from Fountain *et al*, 2007).

Several studies have used a mutagenesis based approach to address the importance of the conserved YXTXK/R motif. The first study focused on the PKC site was performed at the $P2X_2$ receptor by Boue-Grabot and his colleagues (Boue-Grabot *et al*, 2000). To remove the consensus PKC site, residue Thr^{18} was substituted by alanine or asparagine at the $P2X_2$ receptor. The WT $P2X_2$ receptor gave a substained response during the application of extracellular ATP, whereas these mutants T18A and T18N exhibited

complete desensitization within 5 seconds. This demonstrated that the threonine residue has a modulatory role in the desensitizing kinetics of $P2X_2$ channels. Threonine substitution at Lys^{20} displayed the same phenotype as the T18A and T18N mutants, and indicated the important role of the T-X-K domain in determining receptor kinetics. To eliminate the effects of potential residues associated with intracellular phosphorylation, for example the intracellular serine, threonine and tyrosine, the carboxy terminus of $P2X_2$ receptor sequence was truncated and the slow desensitization remained as a significant phenotype for the truncated receptors (Boue-Grabot et al, 2000). Additional mutation on the Thr^{18} residue still displayed a quickly desensitizing course as for the full-length T18A mutation. In addition, they concluded the slow desensitization rate of $P2X_2$ receptor was due to the constitutive phosphorylation of the intracellular domains.

Ennion further studied this Thr-Pro-positive combined N-terminus regulatory site at the $P2X_1$ receptor (Ennion et al, 2002a). The alanine substitution at $P2X_1$ Thr^{18} led to a 10-fold faster desensitization rate and a marked reduction in peak current amplitude. The reduction in peak amplitude did not reflect an ATP potency shift as increasing ATP concentration up to 10 mM caused no effect to peak amplitude. In contrast to the T18A, previous study suggested the $P2X_1$ receptor ATP binding domain mutant K68A produced a 90% fold prolongation of the time-course of ATP current. When the T18A was co-expressed with K68A mutant, it resulted in a faster desensitizing response without influence to the peak current amplitudes. It suggested the dominant role of T18A mutant in the heteromeric channel.

Similar findings were demonstrated at the $P2X_3$ receptor by site-specific mutagenesis studies (Paukert et al, 2001; Franklin et al, 2003). The intracellular serine and threonine residues and the lysine residue (corresponding to the Lys^{20} for $P2X_1$ and $P2X_2$ receptor) as the potential PKC regulation sites were mutated to alanine, and the response of mutant T12A (corresponding to the Thr^{18} at $P2X_1$ receptor) was non-measureable. This observation was also suggested to be a result of accelerated rapid desensitization.

There is a distinctive cyclic structure of the side chain of proline residue where a hydrogen bond may form within itself. Since it cannot act as a hydrogen bond donor or acceptor in the peptide chain, it leads to kinks and can play unique roles in the secondary structure of proteins. However, the middle residue Pro^{19} was not involved in

the structural maintenance of this regulation site since the P19A mutant did not show any difference to the P2X$_2$ WT receptor (Boue-Grabot *et al*, 2000).

5.1.3 Other N-terminus residues involved in channel gating

In addition to the PKC regulatory domain, the roles of other residues in the amino terminus in channel gating have been investigated by site-directed mutagenesis. The conserved intracellular tyrosine (Tyr^{16}) (Figure 5.1) is another potential phosphorylated residue that could participate in channel modulation. Although the existence of the conserved Tyr^{16} at the N-terminus is throughout the P2X subtypes, the phosphorylation at tyrosine residue was not detected in both P2X$_1$ (Toth-Zsamboki *et al*, 2002) and P2X$_2$ (Kim *et al*, 2001) receptors. The hydroxyl of the Tyr^{16} was removed by the substitution of another aromatic amino acid phenylalanine. This modification had no effect to the receptor expression, while the peak current amplitudes were dramatically reduced by over 90% at P2X$_1$ receptor (Toth-Zsamboki *et al*, 2002). Thus, this residue may play a structural other than a direct functional role at the intracellular domain.

The intracellular region close to the first transmembrane domain (from Asp^{15} to Gly^{30}) was studied by cysteine substitutions followed by whole-cell recording at P2X$_2$ receptors (Jiang *et al*, 2001). These mutants were initially scanned with the neutral, membrane permeable methanethiosulfonates MTSM and MTSB, and the D15C, P19C, V23C, V24C and G30C mutants were inhibited. This was not reversible after up to 10 minutes washing. This finding indicated these intracellular residues are accessible and contribute to channel properties. The concentration-response curves for ATP of these mutants were plotted to investigate if the reductions at current amplitudes were due to the change of ATP potency, and the MTSM modification only resulted in decreasing the maximum ATP effect without an ATP potency shift. A shift in ATP potency indicates the impairment of channel binding or gating mechanism, whereas a reduction in the maximum response effect suggests an effect on basic ionic permeation. It was concluded the residues Asp^{15}, Pro^{19}, Val^{23} and Val^{24} at P2X$_2$ receptor are involved in ionic permeation. The immediate action of the MTSM at residue V24C and G30C further suggested these residues are able to be accessed with little obstacle. The residue Gly^{30} which is at the end of the first transmembrane domain was considered to be the "gate" of the channel pore.

5.1.4 The end of N-terminus associate with the protein trafficking

Recent studies on the $P2X_6$ receptor revealed roles of an uncharged region at the N-terminus in protein trafficking (Ormond *et al*, 2006). The $P2X_6$ subunit cannot make a homomeric channel and tends to be retained within the endoplasmic reticulum (ER) in the core glyscosylated state. 14 non-conserved amino acids immediately after the first methionine were deleted and this deletion increased the surface expression of $P2X_6$ receptor significantly. The glycosylation was confirmed by the Endo H digestion, and indicated the transportation through the Golgi complex to the cell surface. For these mutations, both negative and positive substitutions at positions 3 and 11 enhanced the protein trafficking pathway. Furthermore, the introduction of positive charge to the Ser^2 promoted the assembly of $P2X_6$ homotrimeric channel by increasing the amount to the trimers, though this mutant was non-functional. The overall results suggested the distal N-terminus of $P2X_6$ receptor exert an inhibitory effect of the inappropriate receptor export through the cell membrane.

5.1.5 Aim

The amino terminus of P2X receptor has been considered as an essential domain for channel regulation, especially for the time-course of responses (Boue-Grabot *et al*.2000; Jiang *et al*.2001; Ennion *et al*. 2002a; Vial *et al*. 2004a), however, the roles of individual residues were still remained for further studied. To understand the structure and the contribution to the channel regulation of individual intracellular residues, cystiene substitution was used. 15 residues from the TM1 at the $P2X_1$ receptor amino terminus were focused in this study, and both the highly conserved PKC site and the region close to the first transmembrane segment are included. These 15 amino acids have a structural link to the transmembrane domain and may have roles in channel gating and time-course regulation. This study will therefore highlight the accessible functional residues and provide the basis to further identify the roles of important residues in the GPCRs (G-protein coupled receptors) regulation pathway.

5.2 Results

5.2.1 Point cysteine substitutions on basic P2X$_1$ receptor properties

Cysteine substitution mutagenesis was used to investigate the contribution of the 15 amino acids before TM1 to channel properties. The cysteine mutants from Y16C to G30C of the P2X$_1$ receptor N-terminus were generated by site-directed mutagenesis and confirmed by sequencing (See figure 5.2). The mRNAs of the mutants were synthesised and injected into the *Xenopus* oocytes, and the expression levels, channel desensitizing times and EC$_{50}$ values and reproducibility of responses were initially studied.

ATP (100 μM, a maximal concentration) evoked a transient inward current that desensitized during the continued presence of ATP at WT P2X$_1$ receptors (6513 ± 179 nA, *n*=14) (See figure 5.3). The majority of mutants (12/15) had no effect on the peak current amplitude, however responses were reduced for Y16C (-1297 ± 93 nA, *n*=7), T18C (-52 ± 4 nA, *n*=5) and R20C (-4153 ± 273 nA, *n*=3) (*** p<0.001) (Figure 5.3). For the mutants with decreased peak amplitudes, ATP concentration was increased up to 10 mM to see if there had been a change in agonist sensitivity (See figure 5.4). However, 10 mM ATP did not induce further significant change to these mutants compared to 100 μM ATP. The peak current of T18C was too small to analyse further in term of its EC$_{50}$ determination or MTS reagent sensitivity. To determine whether the reduced peak current of these mutants resulted from decreased surface expression, I used a sulfo-NHS-LC biotinylation assay to label the P2X$_1$ receptors expressed on the surface of the oocytes, and the total and surface expression levels were revealed on SDS-PAGE gel by western blotting. The bands for the P2X$_1$ receptors were revealed as monomers which are about 55 kDa, and similar amounts of total and surface protein to the WT receptor was shown for all mutants (See figure 5.4). V29C exhibited comparable peak amplitudes to the WT P2X$_1$ receptor that was run as a control. It is interesting that the significantly reduced peak currents of these mutants were not likely to result from the ATP potency shift or the reduction in protein trafficking. The residues Tyr[16], Thr[18] and Arg[20] were then suggested contribute to the channel gating regulation.

For the WT P2X$_1$ receptor, the maximum peak current can be evoked by 100 μM ATP and the mean EC$_{50}$ value is around 1 μM. The ATP EC$_{50}$ levels of the mutants were
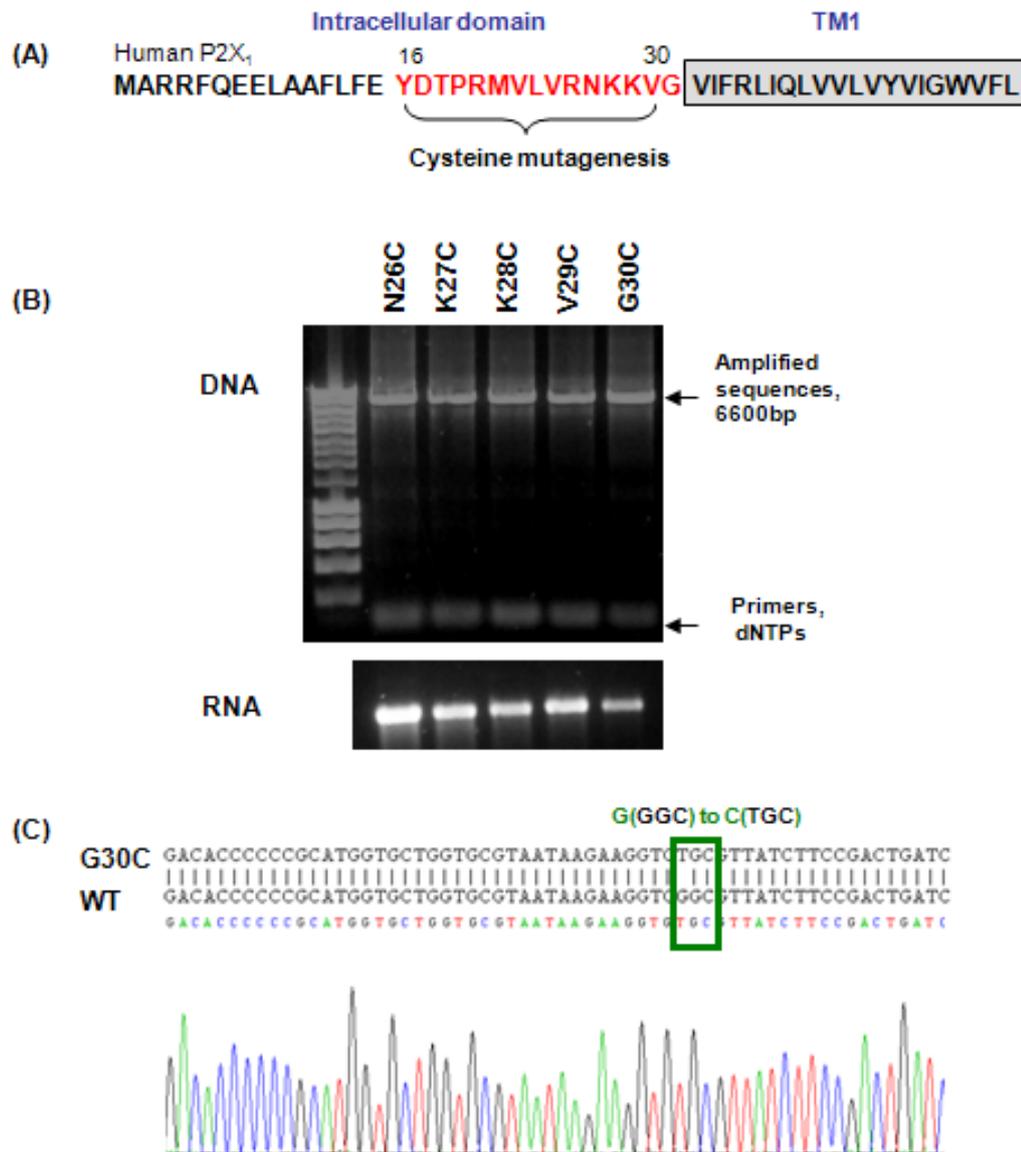
Figure 5.2 15 amino acids on N-termini of P2X₁ receptor were mutated to cysteine
(A). The intracellular residues that were mutated to cysteines are indicated in red, these are just before TM1 (in grey box) . **(B).** Examples of the mutants from N26C to G30C generated site-specific mutagenesis, and the bands obtained from PCR with mutagensis primers were revealed on a gel. mRNAs were made from the cDNAs and injected to *Xenopus lavis* oocytes for expression. The amount of mRNA generated is illustrated on the RNA gel in the lower panel.**(C).** Example sequencing figure of mutant G30C from chromas, the sequence GGC was converted to TGC at the cDNA level to make a convertion from glycine to cysteine. All of the mutants were checked by fully sequencing (C for blue, G for black, T for red, A for green).
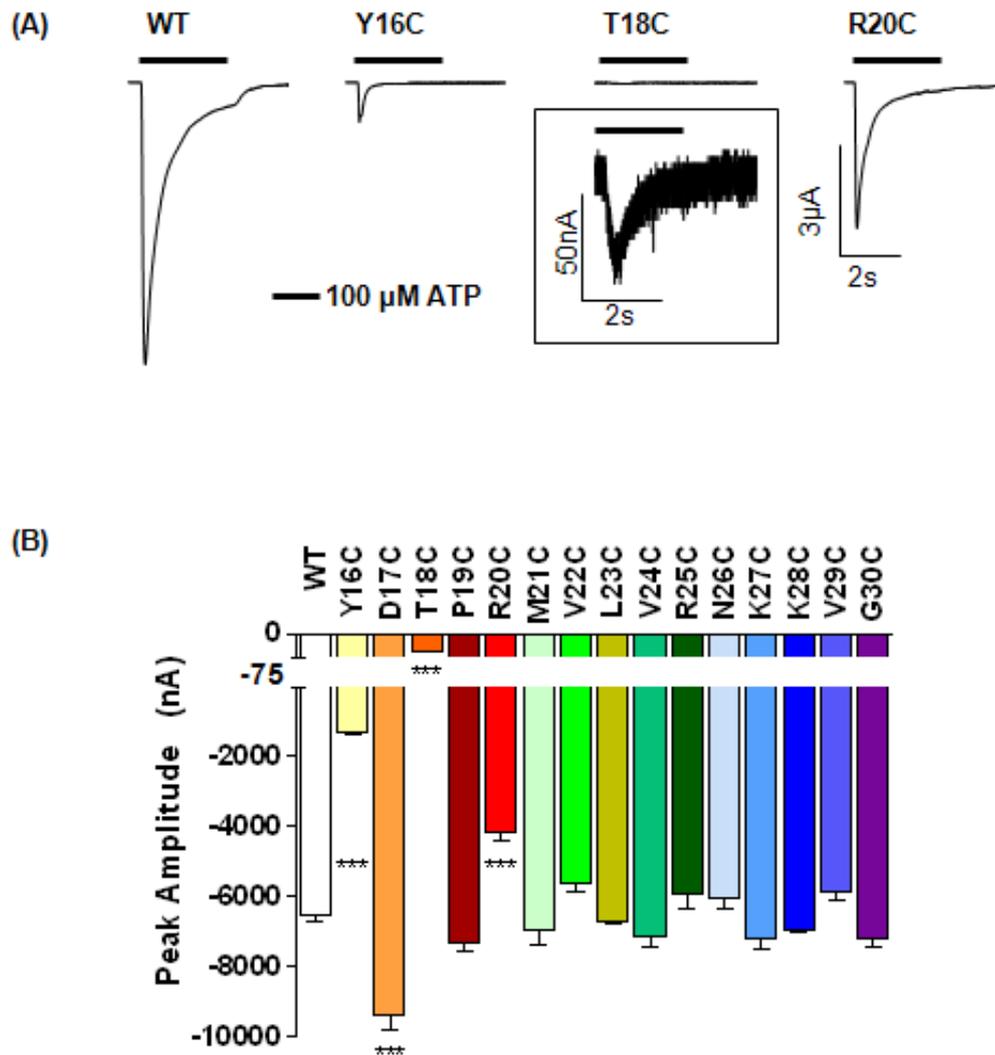
Figure 5.3 The peak current amplitudes of WT P2X$_1$ receptor and cysteine mutants
(A). Traces of initial currents of the P2X$_1$ receptor WT and mutants to ATP(100 μM) (application period as indicated in bar).**(B).** Summary of the peak current amplitudes of the wild type P2X$_1$ receptor and cysteine mutants at the maximal concentration of ATP. The segment between 0 to -75 nA is amplified to show the small current for the T18C mutant. Most of the mutants exhibited a similar peak currents as the WT P2X$_1$ receptor (-6878 ± 86 nA, n=14), except Y16C, T18C and K20C that showed a significantly lower peak currents, n=3-14 for mutants. *** p<0.001.
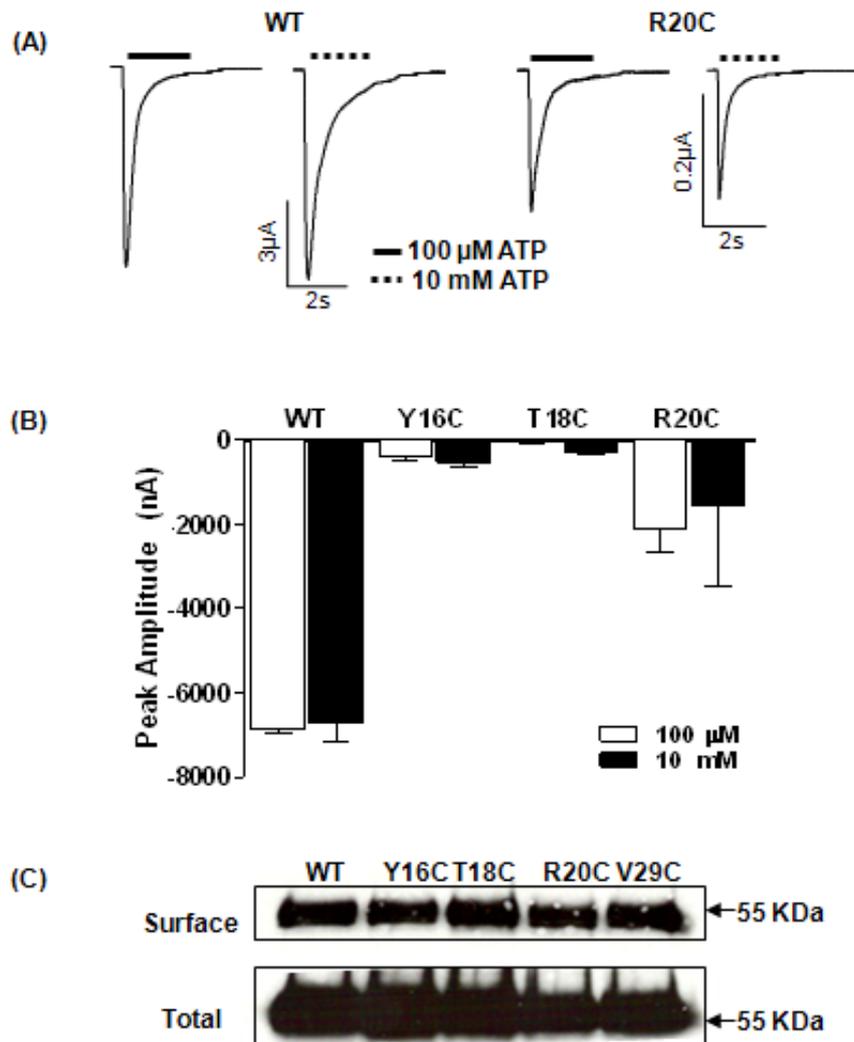
Figure 5.4 Normal levels of expression for mutants with decreased maximal ATP responses
(A). Traces of the peak currents of P2X$_1$ WT and R20C in response to 100 µM (black line) or 10 mM (dashed line) (ATP application period showed in bar). **(B).** Summary of peak currents evoked by 100 µM and 10 mM ATP at WT and mutant P2X$_1$ receptors. **(C).** The expression levels of the mutants with lower peak amplitudes were studied by western blotting, and V29C with normal current expression level as a control. All of the mutants did not show any difference to the wild type P2X$_1$ receptor in total and surface protein expression.

estimated by comparing the relative amplitude of responses evoked by 1 μM and 100 μM of ATP. There were no major changes in ATP sensitivity at the mutant receptors compared to WT (60.06 ± 4.90 %, $n=4$), since 1 μM ATP evoked between 30-70% of the maximum current amplitudes for each of them (See figure 5.5, *** p<0.001, *p<0.05). Y16C exhibited the smallest percentage peak amplitude to 1 μM ATP to its maximum response. When full range of concentrations were used, the potency was slightly shifted to about 6 μM. Therefore, the cysteine substitutions to the intracellular N-terminus of P2X$_1$ receptor did not affect the ATP potency fundamentally.

The time-course of response for WT receptor was measured by the decay time from 100 to 50% peak current amplitudes are summarized in figure 5.6, and 7/15 of the mutants showed similar values as WT receptor (258 ± 7 ms, $n=15$) including all of the mutants with lower peak current expression. Some variations were observed for the mutants with modifications around in the conserved PKC motif (Thr^{18}Pro^{19}Arg^{20}). The cysteine mutation on residue Thr^{18} had a significantly faster desensitization (** p<0.01), which was similar to the previous studies on T18A (faster) and T18V (93 ± 35 ms) of P2X$_1$ receptor (Ennion et al, 2002a and Vial et al, 2004a). Whereas, the cysteine substitutions on the residues next to T18C strikingly prolonged the decay times. The D17C had the greatest decrease in desensitization, decays to a 50% time-course of 1501 ± 12 ms ($n=17$), and the mutant P19C showed a 50% decay time of 1218 ± 20 ms ($n=6$). However, no significant difference in desensitizing pattern was found for R20C. The fastest desensitization was observed for the mutant V22C (87 ± 6 ms, $n=10$) which was 3 times faster than wild type. A moderately slower desensitizing pattern can also be observed in mutants M21C, L23C and K28C (respectively 409 ± 13 ms, $n=7$; 528 ± 20 ms, $n=10$ and 666 ± 21 ms, $n=9$, *** p<0.001, *p<0.05). The overall results of the desensitizing time indicated a few residues on the amino terminus, including Asp^{17}, Thr^{18}, Pro^{19} and Val^{22}, may be involved in the channel time-course of response regulation.

One disadvantage of the oocyte is the time-course of solution exchanges, and the ATP which is released from the U-tube cannot access to the whole oocyte simultaneously. For this reason we can only estimate the time-course using this method. To minimize the effects of agonist access time, I have determined the time-course by patch clamp recording from HEK cells expressing the P2X$_1$ receptor mutants. The DNAs of the

mutants with significant changes in time-course to the WT tested in oocytes were transfected into the HEK293 cell and responses to 100 μM ATP was detected. Currents evoked at T18C mutants were barely detectable and their time-course could not be analyzed. The time-courses observed for other mutants had a similar pattern as seen in the study with oocytes (See figure 5.7). Faster desensitization was observed at WT receptor and all mutants in HEK cell than oocytes. Interestingly, the differences between either D17C or V22C to wild type receptor were increased to about 7 folds and 10 folds respectively comparing to that obtained in oocytes (see figure 5.7C, ***$p<0.001$). The P19C and K28C showed moderately slower desensitization (*$p<0.05$), by contrast, the L23C showed a doubled time-course in oocytes study found to be no difference to the WT in HEK cell.

5.2.2 Effects of MTS compounds to the N-terminus cysteine mutants.

SCAM (substituted cysteine accessibility method) has been a popular method in the investigation of the structure and properties of specific regions of ligand-gated ion channels. It allows modifications at targeted residues. A range of MTS (methanethiosulfonate) compounds (including MTSM, MTSB, MTSEA and MTSET) have been used to study the intracellular regions of the $P2X_2$ receptor (Jiang *et al*, 2001). Previous study (See chapter 3) indicated only MTSEA and MTSET are applicable to access the $P2X_1$ receptor intracellular domain without influence to the WT receptor. Both MTSEA and MTSET are positively charged MTS reagents. MTSEA is relatively small and can cross the cell membrane freely in its uncharged form, while MTSET with a larger diameter can only enter the cell through the channel pore during the channel opening. In this study, I have tested whether positively charged MTSEA and MTSET have an effect on ATP evoked currents at WT and mutant $P2X_1$ receptors.

ATP evoked responses at WT and mutants P2X receptors decay between the initial and 2nd ATP applications but then were maintained essentially when ATP was applied at 5 minute intervals. Approximate EC_{50} concentration of ATP (1 μM) was used in MTS studies as this would be the most sensitive concentration to any changes.

MTSEA (1 mM) and MTSET (1 mM) gave 10-25% potentiation to the WT $P2X_1$ receptor (24.52 ± 4.28% *n*=5 for MTSEA and 13.41 ± 8.93%, *n*=3 for MTSET,
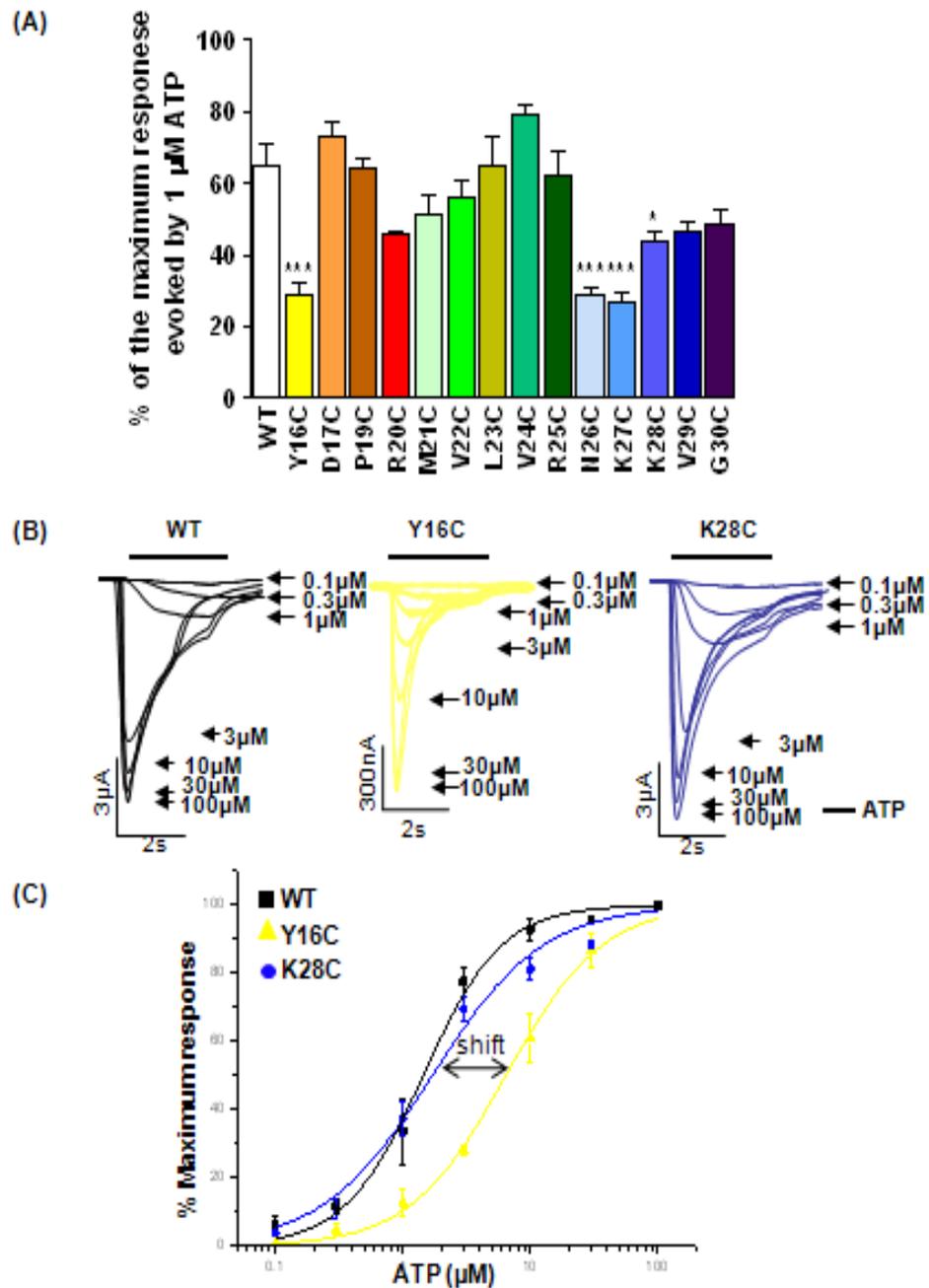
Figure 5.5 The cysteine mutation did not alter the EC$_{50}$ value of mutant P2X$_1$ receptors
(A). Summary of the % amplitudes evoked by ATP (1 μM) to the maximum response (100 μM). All of the mutants exhibit current between 30-70% of the maximum amplitudes under 1μM of ATP. **(B).** Example traces of the WT and mutant Y16C (Yellow) and K28C (Blue) during the application of different concentrations of ATP, the peak amplitudes of P2X$_1$ receptor was dependent on the ATP concentration applied.**(C).** The example of concentration-response curve of the wild type and mutant P2X$_1$ receptor. There was a small shift at EC50 observed for mutant Y16C (*n*=4) compared to the WT (*n*=3). ***p<0.001,*p<0.05.
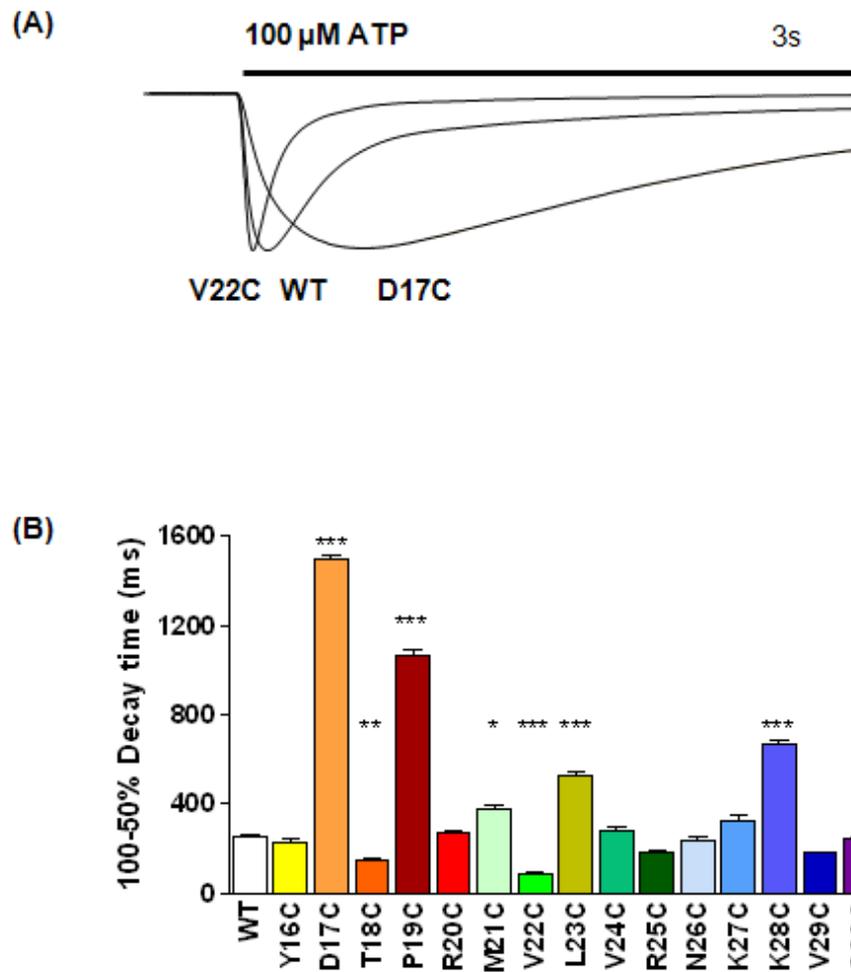
Figure 5.6 The time course of N-termini cysteine mutant currents measured in oocytes
(A). The traces of the wild type and mutant P2X$_1$ receptor currents in response to the application of ATP (100 μM) application period as indicated by bar. The mutant D17C (Orange, 1501 ± 12 ms, n=17) showed a slower desensitizing current, while the V22C (Green, 87 ± 6 ms, n=10) showed a faster desensitizing current comparing to the WT(258 ± 7 ms, n=15). **(B).** The peak current decay time from 100%-50% of the peak currents of WT P2X$_1$ receptor and all cysteine mutants were summarized. *** $p<0.001$, ** $p<0.01$, *$p<0.05$.
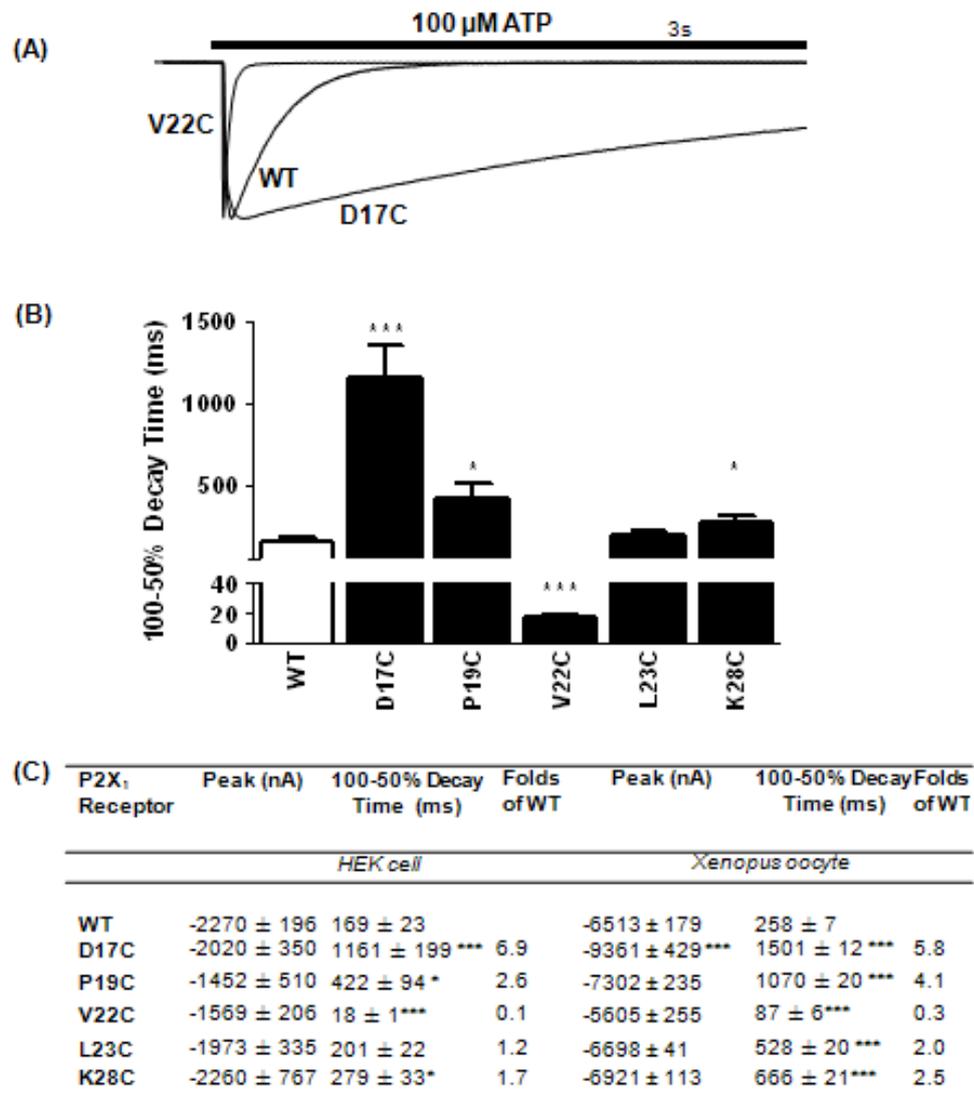
Figure 5.7 The time course of peak currents decay time obtained from patch clamping recording on HEK293 cells

WT and mutants of P2X$_1$ receptors were transiently expressed in HEK293 cells and the time course of desensitization was studied by patch clamp recording. **(A).** Example traces of the P2X$_1$ WT receptor(100µM ATP, application period indicated in bar). D17C and V22C mutants exhibit similar trend to the currents recorded in oocytes. **(B).** The decay time from 100%-50% of the peak currents of WT P2X$_1$ receptor and the mutants show significant difference to the WT except for L23C. **(C).** Comparison of the changes on the 100-50% peak current decay time between HEK cells and oocytes are showed in table.***$p<0.001$, *$p<0.05$.

*p<0.05) (Figure 5.8) as reported in previous studies (Rassendren *et al*, 1997; Roberts *et al*, 2007). Since free cystiene at the P2X receptor could not be detected by MTSEA or larger chemicals (Clyne *et al*, 2002a; Ennion *et al*, 2002b), the potentiation is most likely to be a nonspecific effect.

MTSEA

At 6 mutants, there was no significant change from WT P2X$_1$ receptor to MTSEA (1 mM) treatment for 20 mintues in bath, including the D17C, R20C, V22C, L23C, R25C and K28C. MTSEA treatment resulted in larger potentiation for the mutants compared to the changes in WT, M21C (102.45 ± 6.84%, *n*=3), V24C (82.60 ± 3.90%, *n*=6), N26C (74.29 ± 3.31%, *n*=4), K27C (98.63 ± 8.96%, *n*=7) and V29C (63.56 ± 11.40%, *n*=5) (***p<0.001, **p<0.01, *p<0.05). However for the mutants M21C, N26C, K27C and V29C this potentiation was reversed back to control values following 5 minutes washout of MTSEA suggesting that this effect does not result from the irreversible covalent modification of the introduced cysteine. By contrast for V24C the potentiation was sustained following 5 minutes of washout of the MTSEA. On the other hand, the mutants Y16C, P19C and G30C were inhibited by MTSEA treatment (***p<0.001, **p<0.01), and these effects were not reversed following 5 minutes washout of MTSEA (Figure 5.9). This inhibition showed more time dependence than the effects of MTSEA at WT or other mutants with at least 10 minutes application of MTSEA required before inhibitory effects were seen. The lack of reversal indicates that this results from covalent modification of the introduced cysteine by MTSEA. A large inhibition was observed for the mutant G30C (-45.4 ± 4.9%, *n*=5). Moderate inhibitions were observed for mutants Y16C (-19.1 ± 3.4%, *n*=4) and P19C (-29.9 ± 10.6%, *n*=4), the corresponding residues which are associated with the PKC motif and may also be involved in channel regulation. This level of MTSEA inhibition at 20 minutes was the same whether mutants were exposed to ATP or not indicating that the channel does not need to be activated for the introduced cysteines to be modified by MTSEA. These results are similar to those reported for P2X$_2$ receptors (Jiang *et al*. 2001), especially for the residues Val[24] and Gly[30]. This observation confirmed that the changes to the channel properties of V24C and G30C were indeed induced by the binding of MTSEA.

The largest potentiations were observed at mutants M21C and K27C of about doubling to the current amplitudes. This massive potentiation may indicate an ATP potency shift
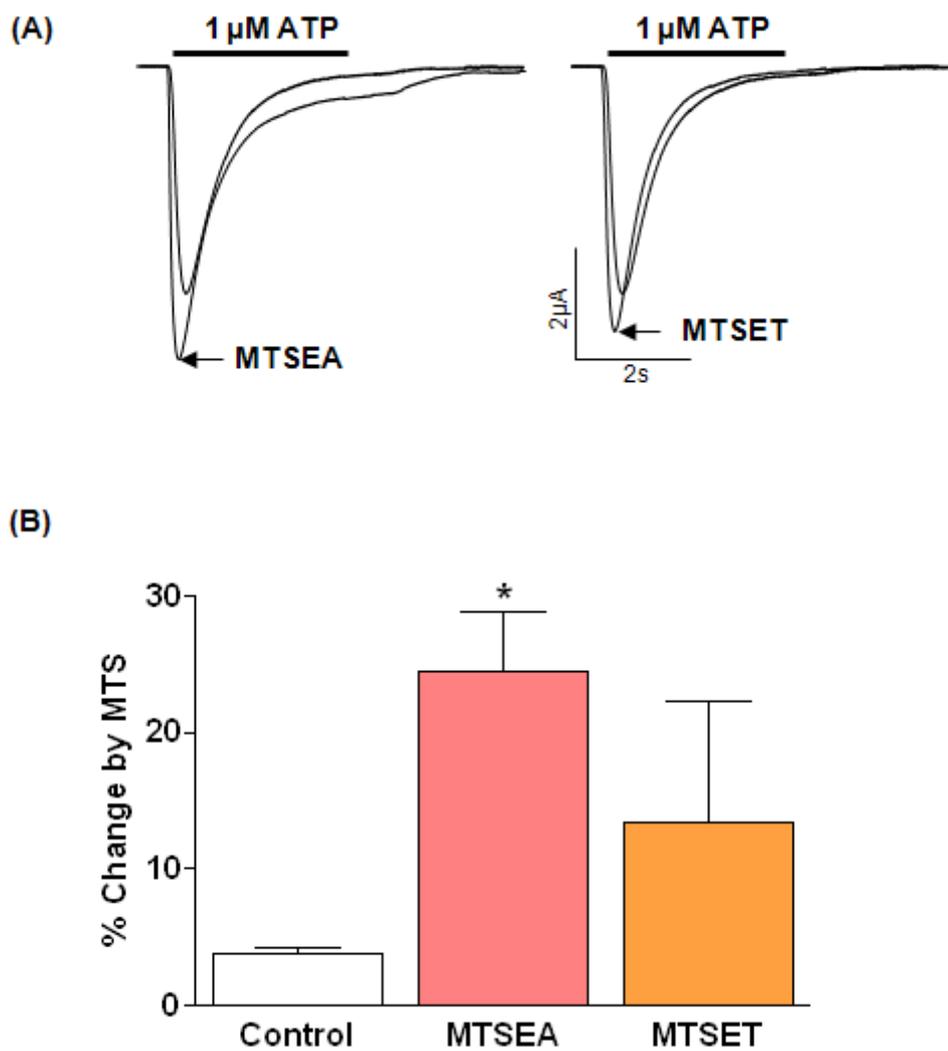
Figure 5.8 Effect of MTSEA and MTSET on WT P2X$_1$ receptor
(A). Traces of the WT P2X$_1$ receptor evoked by MTS(1 mM) reagents with ATP(1µM, application indicated in bars). **(B).** Summary of percent changes of the different reagents on wild type P2X$_1$ receptor. MTSEA (pink, 24.52 ± 4.28 %, *n*=5) and MTSET(orange,13.41 ± 15.47 %,*n*=3) induced potentiations to the WT P2X$_1$ receptor to small scale as reported previously. *p<0.05.
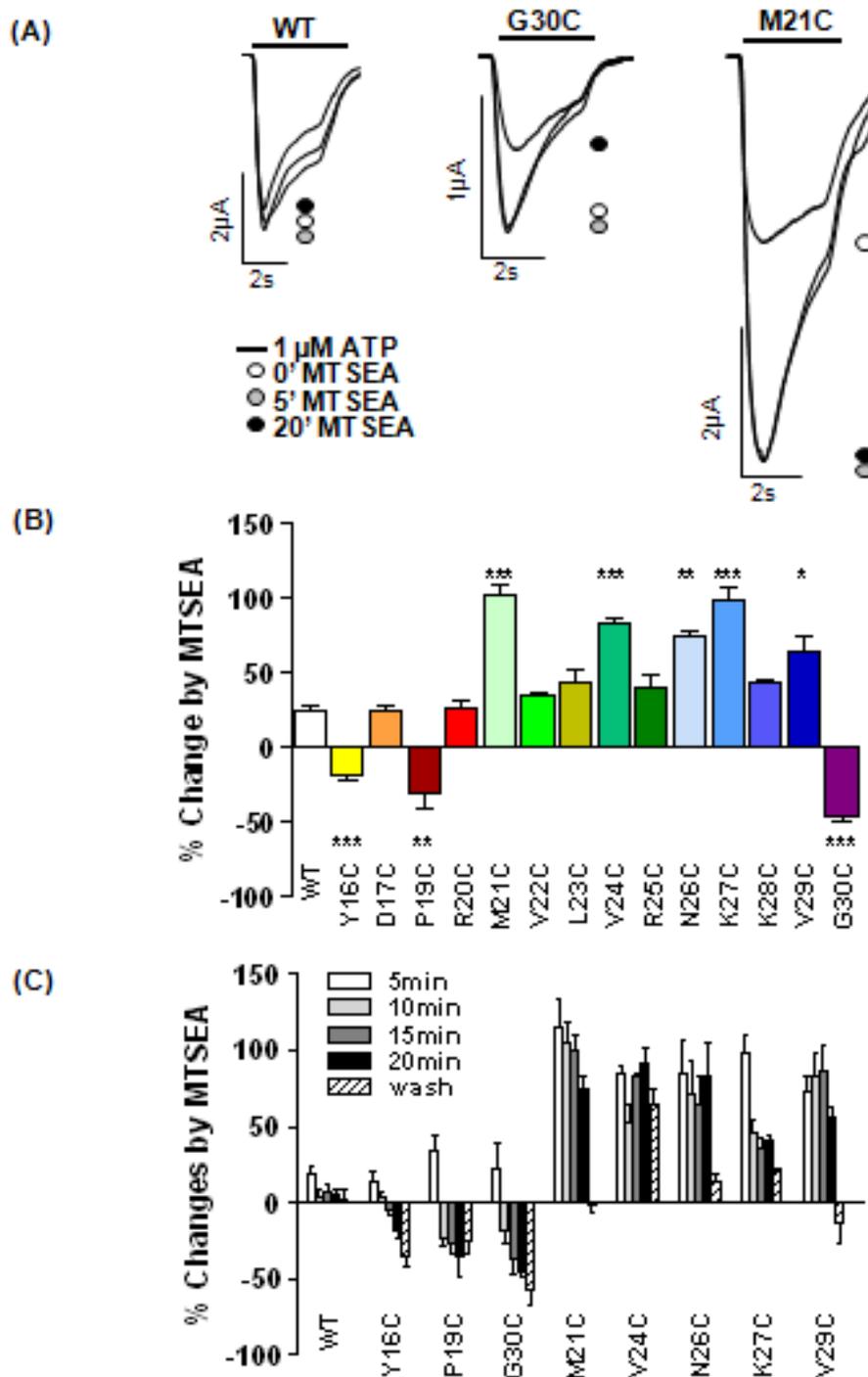
Figure 5.9 The effects of MTSEA on N-terminal cysteine mutants
(A). Representative traces of ATP (1 µM, application period indicated by bar) evoked currents from single oocytes of WT and mutant G30C (purple) and M21C (green) of $P2X_1$ receptors before (open circle) and after the application of 1mM MTSEA (5 minutes application grey circle 20 minutes black circle). The inhibition of G30C (-45.42 ± 4.86%, n=5) by MTSEA was time dependent; in contrast the potentiation of ATP currents at M21C (102.45 ± 6.84%, n=3) was recorded within 5 minutes of MTSEA application. **(B).** Summary of the maximum percentage changes of the wild type and cysteine mutants by MTSEA. **(C).** Summary of time-dependent effects of MTSEA on WT and cysteine mutant $P2X_1$ receptors. ***$p<0.001$, **$p<0.01$, *$p<0.05$.

induced by the MTSEA binding. Hence ATP at 100 μM (full potency concentration) was used to activate the M21C and K27C as shown in figure 5.10. The effects of 1mM MTSEA at 100 μM ATP evoked response to these mutants (34.61 ± 7.92% for M21C, $n=5$; 36.07 ± 7.42% for K27C $n=4$) are similar to the WT (29.20 ± 0.70%, $n=3$). Hence, the MTSEA modifications at residue Met[21] and Lys[27] led to an ATP potency shift.

In addition to the peak amplitudes, 1mM MTSEA had an effect on the time-course of some mutants (See figure 5.11). For P19C and V29C responses evoked by ATP were almost twice as fast as under control conditions (time for 100 to 50% decay of the current to an EC_{50} concentration of ATP of 46.7 ± 2.4% and 45.7 ± 2.9% of control respectively , $n=12,18$, ***p<0.001). The MTSEA induced speeding of time-course at P19C may suggest the decreased peak amplitudes was due to the change in channel opening mechnisms.

MTSET

MTSET is larger and not permeable to the cell membrane. In this situation, only 8 residues which were either close to the first transmembrane domain or exhibited inhibition to MTSEA were studied. The maximum effects of MTSET are summarized in figure 5.12. Most of these mutants showed small potentiations to MTSET as the WT receptor during the 20 minutes applications, and only V24C (93.61 ± 10.33%, $n=3$) and V29C (125.52 ± 22.20%, $n=4$) exhibited great potentiations. The V24C showed significantly large potentiation to both of these MTS reagents, and the residue Val[24] was suggested to be located at the outside of the intracellular topology structure.

However, some of the mutants that were affected by MTSEA were not influenced by the MTSET. It indicated the difficulties of MTSET in accessing the intracellular terminus. The accessibility of MTSET was analysed by comparing the potentiation levels during the 20 minutes continued application, while the maximum effects can be obtained since the first application (See figure 5.13) for V24C and V29C. Moreover, the potentiation was sustained following the 5 minutes washout of the MTSEA , which is accord with the finding with MTSEA treatment.

The variations of desensitizing time were found in the two residues that most close to the channel pore (See figure 5.14). The time course for desensitizing at V29C (-36.53 ±

4.43%, $n=13$) and G30C (-43.20 ± 2.95%, $n=9$) (***p<0.001) were significantly reduced. This may due to the MTSEA requiring channel opening for accessing the intracellular residues, and MTSEA binding to these residues blocked the ion influx pathway.
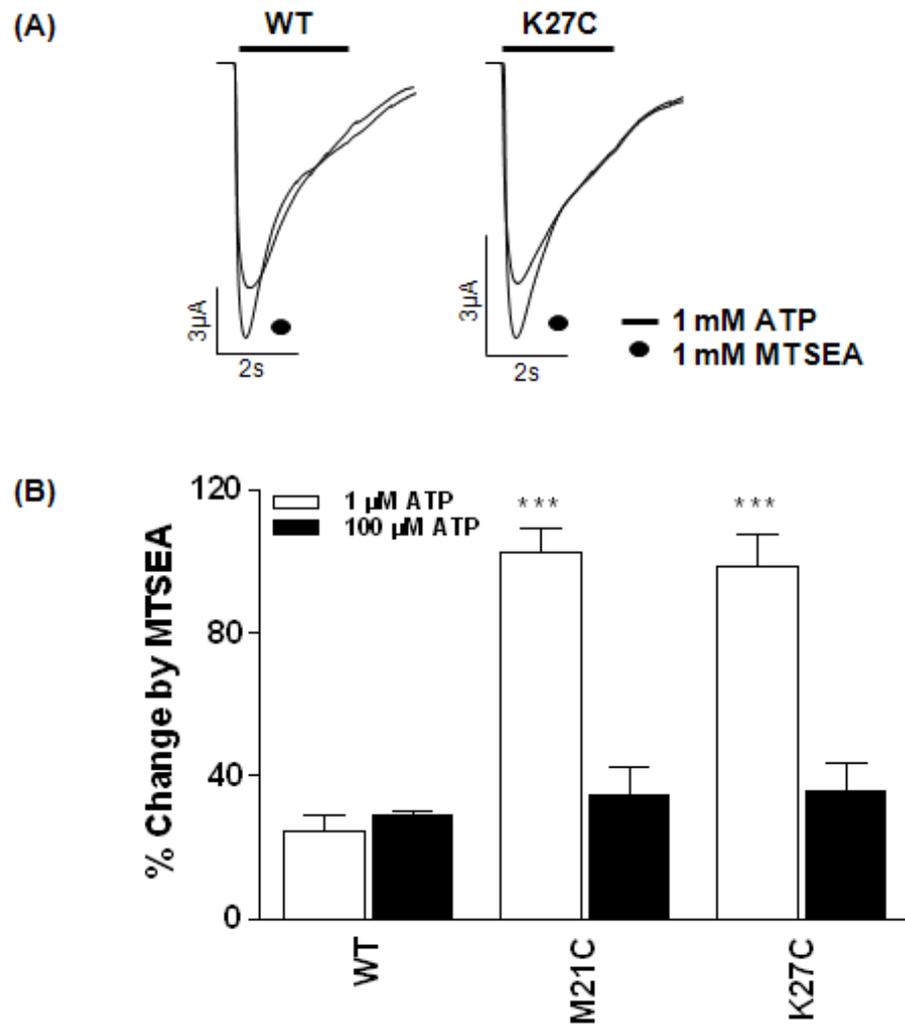
Figure 5.10 Potentiation effects of MTSEA cause obvious ATP potency shift
(A). Representative traces of the maximum effects induced by 100 µM ATP at WT and mutant K27C P2X$_1$ receptors before of after 1 mM MTSEA treatment (black circle). ATP application period is indicated in bar. **(B).** Summary of the maximum percentage potentiation of the WT and M21C and K27C by MTSEA(1 mM) to ATP(1 µM or 100 µM). The MTSEA failed to induce any significant potentiations at M21C (102.45 ± 6384%, *n*=3) and K27C (98.63 ± 8.96%, *n*=7) when the ATP concentration was 100 µM, and indicates no change to the ATP potency. ***p<0.001.
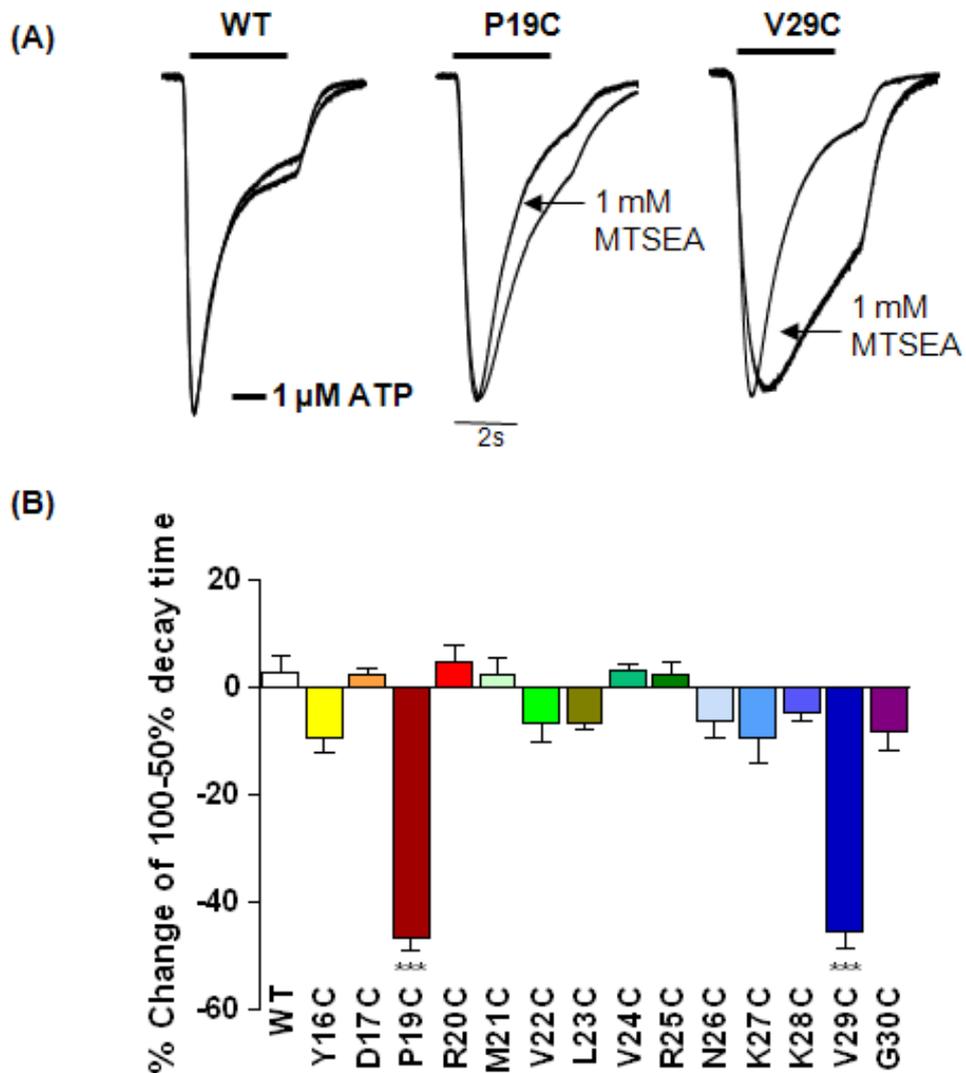
Figure 5.11   Effects of MTSEA on the 100-50% decay time of the N-termini cysteine mutants

(A). Example traces of the 100-50% decay time of the WT and P19C and V29C P2X$_1$ receptor with or without the MTSEA(1 mM) application (indicated with arrow). The decay time for mutant P19C (-46.65±2.37%, *n*=12) and V29C(-45.70±2.91%, *n*=18) was much more rapid with 1mM MTSEA, although interestingly P19C was inhibited by and V29C potentiated by MTSEA.**(B).** Summary of the percentage change of the decay time for WT and cysteine mutants of P2X$_1$ receptor. The decay time was compared by paired recordings.***p<0.001.
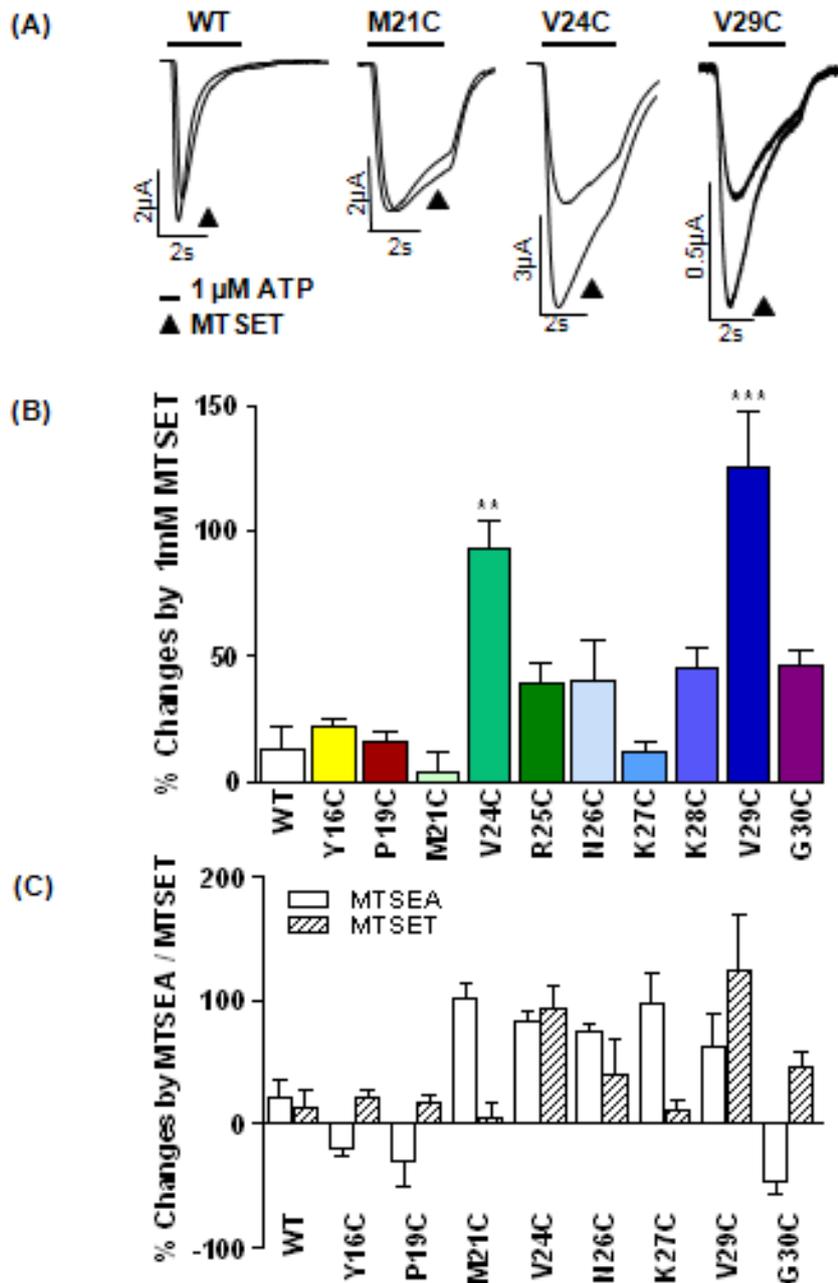
Figure 5.12 Effects of MTSET on N-terminal cysteine mutants
(A). Representative traces of ATP (1 µM, application period indicated by bar) evoked currents from single oocytes of WT (13.41 ± 8.93%, n=3) and mutant M21C (4.48 ± 7.69%,n=3), V24C (light green 93.61 ± 10.33%, n=4) and V29C (125.52 ± 22.19%, n=4) P2X$_1$ receptors before and after the application of 1mM MTSET (black triangle). **(B).** Summary of the maximum percentage changes of the WT and cysteine mutants by MTSET. **(C).** Summary of maximum effects of MTSET comparing to MTSEA on WT and cysteine mutant P2X$_1$ receptors. The Valine residues at 24 and 29 seem to be accessible by both MTS compounds.***p<0.001,**p<0.01.
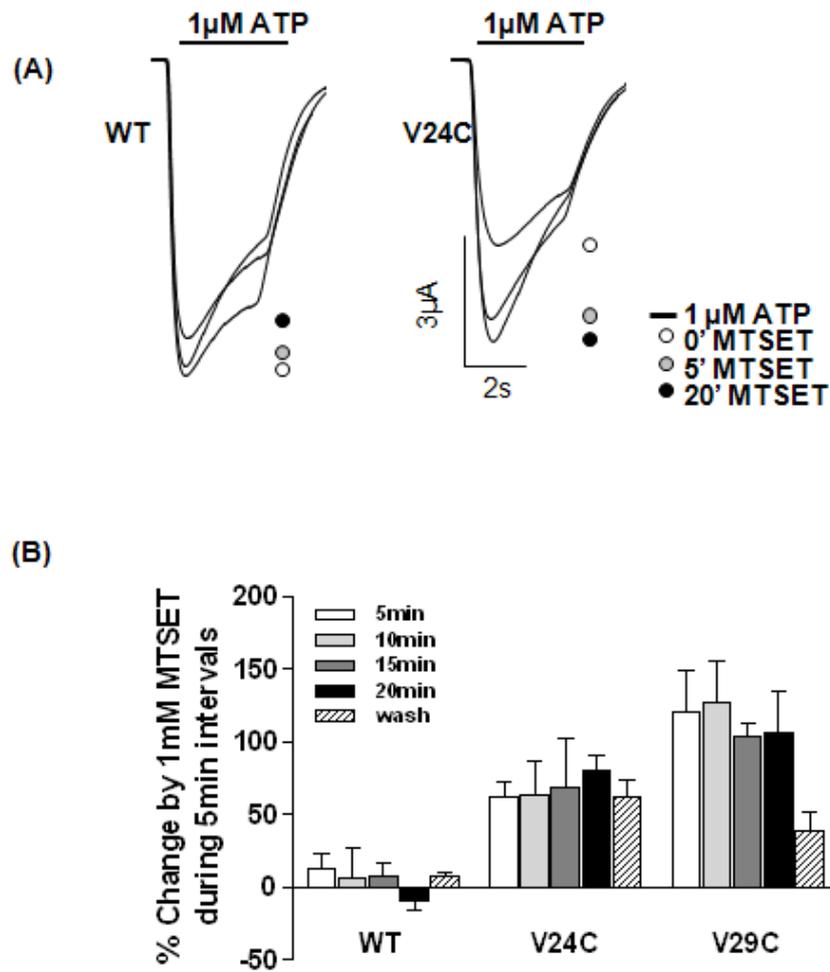
Figure 5.13 The Effects of MTSET on N-terminal cysteine mutants
(A). Representative traces of ATP (1 μM, application period as indicated in bar) evoked currents of WT and mutant V24C of P2X$_1$ receptors before (open circle) and after the application of MTSET (1 mM) (5 minutes application grey circle 20 minutes black circle). The potentiation of V24C by MTSET was time independent. **(B).**Summary of time-independent effects of MTSET on WT P2X$_1$ receptors and V24C and V29C.
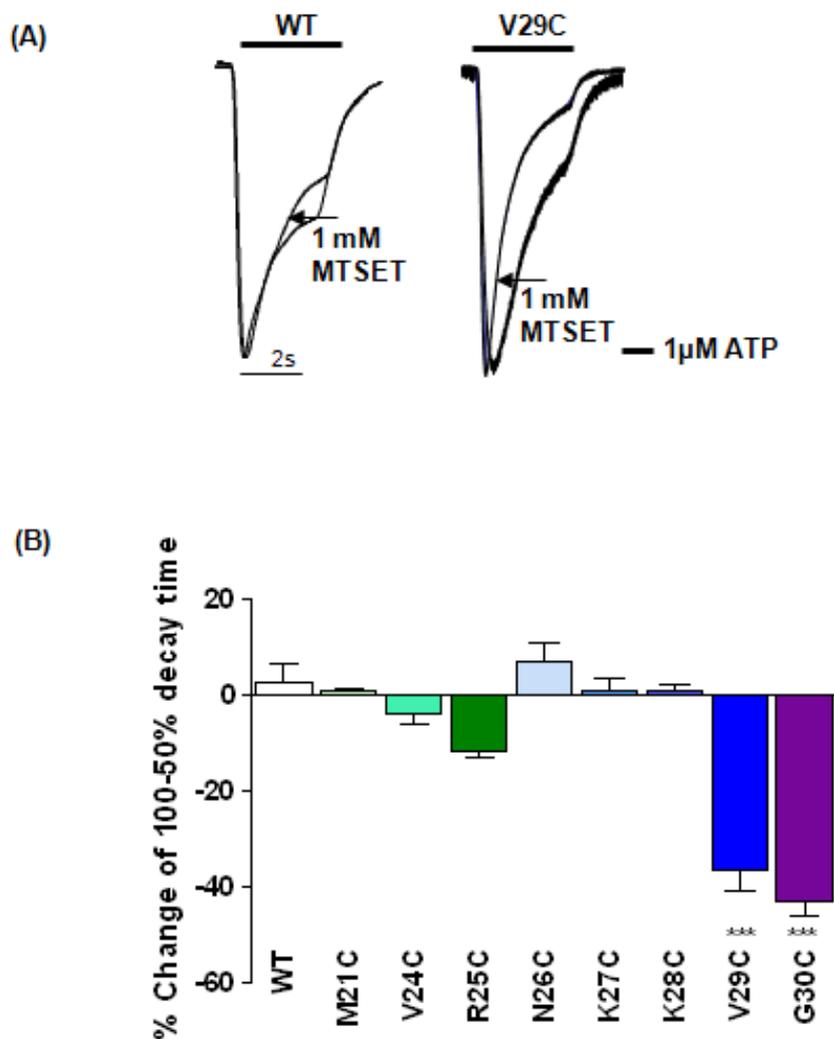
Figure 5.14 Effects of MTSET on the 100-50% decay time of N-termini cysteine mutants
(A). Representative traces of WT and V29C P2X$_1$ receptors evoked by ATP (1 µM, application period as indicated in bar) before and after the application of MTSET(1 mM). Comparing to the response without the MTSET treatment, the V29C showed a faster desensitization. **(B).** Summary of the percentage effects of MTSET to the 100-50% decay time of the WT and cysteine. The mutations at residues Val[29] (-36.53 ± 4.43%, *n*=13) and Gly[30] (-43.20 ± 2.95%, *n*=9) that are close to the channel pore exhibited 40% faster decay time to the MTSET application.***p<0.001.

5.3 Discussion

The amino terminus of P2X receptors play important roles in channel regulation, and its contributions to the $P2X_1$ receptor function have been investigated using chimera construction and mutagenesis approaches in a range of previous studies. Some of the observations on the cysteine substitutions and MTS modifications to the amino termini residues have been published in *Journal of Neurochemistry* (Wen *et al*, 2009). In this cysteine substitution study, 15 residues close to the TM1 were mutated and the majority (8/15) of them had some effect either on the time-course or the current amplitude. It indicated that this region before the TM1 plays a significant role in the regulation of channel gating. Firstly, the PKC motif is important for maintaining the normal function of the channel and maybe involved in the channel opening mechanism. Secondly, residues Val^{29} and Gly^{30} which are close to the channel pore also contribute to the channel gating properties. Lastly, the cysteine substitution or the MTS compounds modifications at the three intracellular valines, Val^{22}, Val^{24} and Val^{29} respectively, affected the channel properties significantly. The underlying explanations will be described in the following discussion.

5.3.1 Important roles of residues around the PKC motif

The consensus PKC site and the tyrosine which is two residues before it (YXTXK/R, see figure 5.1) is conserved in all mammalian and *Dictyostelium* P2X receptors (Boue-Grabot *et al*, 2000; Fountain *et al*, 2007). Peak amplitudes and time-course of the response are two important features for functional evaluation of receptors.   The current data show that the YXTXK/R motif plays a determining role in the basic properties of $P2X_1$ receptors. The disruptions at this domain either affected the peak current amplitudes or the time-course of responses.

The cysteine substitution at Thr^{18} decreased the peak current amplitudes and speeded the time-course of responses significantly. Whereas, there was no reduction observed at the total and surface receptor expression levels. Similar effects were demonstrated in the previous studies at $P2X_1$, $P2X_2$ and $P2X_3$ receptors as the Thr^{18} residue was mutated to cysteine, alanine and asparagines respectively (Boue-Grabot *et al*, 2000; Paukert *et al*, 2001; Ennion *et al*, 2002a; Vial *et al*, 2006). With the thiol group, the threonine residue is assumed as a phosphorylation regulatory site. Mutation at this position could result in a fundamental change to the conformation of the intracellular N-terminus and disturbed

proper regulation pathway. Since this mutation did not apparently influence protein trafficking and agonist sensitivity, the loss in receptor function may be associated with a reluctance of the channel to open. Thr^{18} is thus vital for maintaining the channel opening kinetics to the peak amplitudes and time-course of $P2X_1$ receptor currents. In addition, the cysteine mutation at Val^{22} also displayed an accelerated desensitizing pattern, while the mean peak current amplitudes were not changed. This valine close to the PKC site is also likely to be important for channel gating. In fact, the V22C exhibited a faster desensitizing pattern than T18C and yet had normal peak current amplitude. It showed that speeding of the time-course does not account for a reduction at amplitude at T18C.

In addition to the Thr^{18}, the cysteine mutation at Tyr^{16} also greatly reduced the peak current amplitudes at $P2X_1$ receptor to about 80% with no effect on ATP potency and surface expression. This result is similar to the finding on $P2X_2$ receptors (Jiang *et al*, 2001) where no response was detected for this mutant. Tyr^{16} as a putative phosphorylation target for tyrosine kinase has been previously studied in $P2X_1$ and $P2X_2$ receptors, no direct phosphorylation was detected by the tyrosine-phosphorylation specific antibodies (Toth-Zsamboki *et al*, 2002) and suggested phosphorylation at Tyr^{16} may not be essential. Arg^{20} is considered associated with the binding of the regulatory factors and the R20C mutation exhibited similar features as the Y16C. These two residues can be involved in the channel property regulation incorporate with the Thr^{18}.

D17C and V22C demonstrated striking desensitizing phenotypes, and it is surprising that modifications in the region close to the PKC motif can give speeding and slowing of the response in contrast to WT $P2X_1$ receptor. The D17C led to a more than 6 fold prolonged time-course of ATP responses, while the time-course of V22C is three times faster than the WT receptor. They are two good examples that showed the small changes in the PKC neighboring region can have large effects. The time-course of receptor response reflects the channel gating properties, and the shorter time-course indicates the less capability to maintain the channel opening status during the agonist binding. No ATP potency shift was observed in these two mutations, hence, these residues may be crucial factors in balancing the normal channel gating regulation.

5.3.2 Effects of MTSEA to the N-terminus residues

Membrane permeant MTSEA evoked irreversible inhibition to the current amplitudes at mutant Y16C, P19C and G30C. Two of these mutations are around the PKC motif, and the corresponding residues Tyr[16], Pro[19] were suggested to be involved in channel gating. The mutation at proline 19 by contrast did not affect the peak amplitudes and time-course of $P2X_1$ receptor. However, the currents at the $P2X_1$ P19C mutant receptor were reduced following the application of the cystiene reactive MTSEA, which is consistent with the results for $P2X_2$ receptor at the equivalent mutation (Jiang *et al*, 2001). This effect did not result from the ATP potency reduction in $P2X_2$ receptors and suggested this residue may contribute to ionic conductance rather than ATP affinity. Gly[30] is next to the TM1 and was considered to be in the inner vestibule of the channel pore in the study on $P2X_2$ receptors (Jiang *et al*, 2001).

The inhibitions at these mutants Y16C, P19C and G30C are time dependent, and took about 15 to 20 minutes to reach the maximum effects. This phenomenon suggested the MTSEA compound has difficulties to access these residues or requires longer time to cross the cell membrane. Another reason for these time-courses may due to the conformation changes after channel activation and consequently these residues became unavailable.

On the other hand, significant potentiations to MTSEA were shown by the mutants M21C, V24C, N26C, K27C and V29C. The corresponding residues (Met[21], Val[24], Asn[26], Lys[27] and Val[29]) should be easy accessible to the MTSEA compound at the intracellular domain. The existence of the methionine, leucine and lysine with high-helix-forming propensities and the access patterns in this region may also suggested an alpha-helix arrangement, and this can be further confirmed using protein structure prediction server (PSIPRED).

Unlike the inhibition pattern, the potentiation extents were not dependent on the MTSEA application period. Maximum potentiation can always be observed after the first 5 minutes perfusion of MTSEA. These indicate that the conformation change caused by MTSEA took place immediately. Nevertheless, the potentiation effects were abolished greatly when the MTSEA compound was washed off in bath after the 5 minutes for most of the mutants except V24C. Thus, most of them may not form a

stable bond with the MTSEA, or these potentiation were merely due to the MTSEA effects to the environment round the residues, or they are just simple allosteric effects. The mutants M21C and K27C have been tested at EC_{50} ATP concentration and doubling current amplitudes to the MTSEA treatments were revealed. To further investigate these massive potentiations, the MTSEA treatment was given and the responses to the maximum ATP potency were recorded. As a result, when maximal ATP was applied, only about 20% potentiations can be triggered for these two mutants and this was no difference to the WT receptor. It suggested a shift of ATP potency with the MTSEA modifications at residues Met^{21} and Lys^{27}. The shift on ATP potency is a parameter for the ATP binding capability, and MTSEA may show a role in allosteric effects to these residues.

The fixed binding of MTSEA at Val^{24} was displayed and it was suggested to be an easy-accessed residue as well as a vital residue for maintaining the intracellular conformation to channel ion permeation.

5.3.3 Effects of MTSET to the N-terminus residues

MTSET was less effective (2/8 significant changes) in mediating responses at these mutants in compared to MTSEA (8/15 significant changes). In contrast to the MTSEA effects, the MTSET treatment did not cause any inhibitions to the cysteine mutants, which may because of the limitation of accessibility (See figure 5.15). The size of these MTS compounds were estimated to be about 10 Å in length for both of them, and the maximum diameter is about ~4.8 Å (CH3-SO2-S-CH2-CH2- moiety) for MTSEA and 5.8 Å [$N_1(CH_3)_3$ head group] for MTSET (Kuner *et al*, 1996). The potentiations observed for mutants M21C, N26C and K27C with the application of 1mM MTSEA were no longer observed with 1mM MTSET, since it is not membrane permeable and requires the channel opening to access the intracellular domains.

Despite this, two residues Val^{24} and Val^{29} are still able to exert massive potentiations to 1mM MTSET. Similar to MTSEA, the potentiation effects of MTSET was time independent, and the effect on V24C were able to remain after 5 minute wash in bath. However, the MTSET effects on V29C were washed off in bath after 5 minutes. It may be an allosteric effect resulted by this intracellular mutation. Single residue to channel gating properties via allosteric effect was suggested by study at $P2X_2$ receptor. WT

P2X$_2$ receptor is insensitive to α,β-meATP, whereas a recent published study suggested single mutation in the TM2 by converting the Thr^{339} residue to serine conferred the α,β-meATP sensitivity to it (Cao *et al*, 2007). This indicated the role of mutant T339S in destabilizing the extracellular agonist binding site. It thus can be assumed that the Val^{29} next to the channel pore may contribute to the channel gating through a similar mechanism.
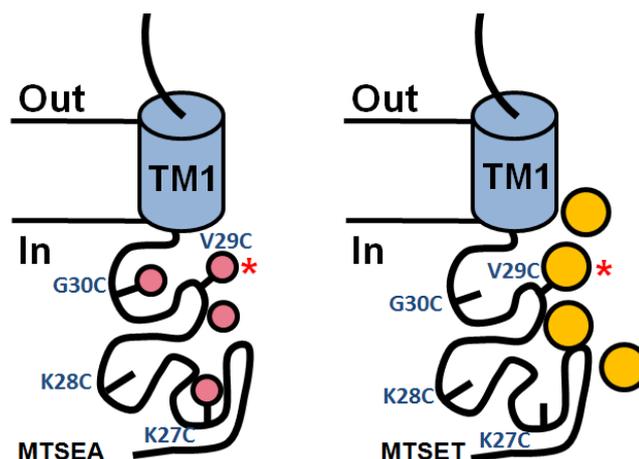
Figure 5.15 Schematic diagram of MTSEA and MTSET accessibility to intracellular domain
The MTSEA (pink) and MTSET (yellow) compounds were showed in smaller and larger balls and the linkage with intracellular residues were indicated as black lines. MTSEA compound (left panel) with smaller size has stronger capability to accessing the residues, whereas the MTSET (right panel) has difficulties to reach the narrow corner of the receptor secondary structure. For instance the residue labeled with asterisk (Val^{29}) is the only one that can only be accessed by both MTSEA and MTSET.

5.3.4 Residues close to the TM1 and PKC motif are important for channel gating

The percentage change of time-courses from 100% to 50% of the peak amplitude decay time were compared in pairs for each mutant. The residues next to the TM1 were suspected to be associated with channel gating, and the speeding of time-course was observed in a few situations. V29C is sensitive to the MTS application; the amplitudes were potentiated and showed a fast decay following either MTSEA or MTSET treatment. The adjacent mutant G30C showed 40% faster desensitizing speed after the MTSET application. The residue Gly^{30} is located at the inner channel pore and the binding of MTSET to G30C may limit the passage of cations. This implied an important role for the channel gating residues Val^{29} and Gly^{30} in the P2X$_1$ receptor. Furthermore, P19C also evoked about 50% shorter decay time following MTSEA application which might contribute to the reduction in current amplitude. Therefore, the regions close to the TM1 may be in charge of the channel gating mechanism.

5.3.5 Conclusion

In summary this study has highlighted two amino terminal regions that are involved in regulation of ionic permeation. The individual residues of the consensus YXTXR/K protein kinase C motif were studied and cysteine mutations in this region caused either reduced current amplitudes or changes in time-course. The residues Thr[18] and Arg[20] as the core compartment of the PKC site might interact with the nearby Tyr[16], Asp[17] and Val[22] in ion conduction regulation. The results from MTS compound treatment further suggested an alpha-helix structure in the region next to the transmembrane domain. Val[29] and Gly[30] were strongly suggested to be a part of the inner channel pore and therefore essential for the channel gating.

The roles of the intracellular valines were also found to be important. There are three valines (Val[22], Val[24] and Val[29]) in the N-terminus of P2X$_1$ receptor and all of them seem to be involved in channel conduction. Val[24] and Val[29] are accessible to both of the MTS compounds, and the Val[29] which is next to the TM1 is especially sensitive to the MTS modification with speeding of the time-course. In addition, the cysteine substitution at Val[22] around the PKC motif exhibited an up to 10 fold faster decay. As a neutral amino acid, cysteine substitution should not interrupt the structure significantly. The valines were then considered as the vulnerable points in regulation at the amino terminus.

The above findings raise the possibility of interactions between these two regions to regulate the channel properties, and the function residues in these regions were further studied in chapter 7.

5.4 Appendix: Site-directed mutagenesis on the N-terminus

15 amino acids (from Tyr^{16} to Gly^{30}) on the N-terminus of the human $P2X_1$ receptor contained in the pcDNA 3.0 vector were converted to cysteine individually. The point mutations were introduced using the QuickChange Mutagenesis Kit (Stratagene, La Jolla, CA), and setting up of the reactions and cycling parameters for the mutagenesis were the same as described previously. Primers for the 15 amino acids were listed in table 5.1

The sequences of the cysteine mutants were checked by sequencing (PNACL sequencing service, Leicester University), and primers (pcDNA 3.0_5', seqA. seqB, seqC, seqE, seqF, seqG and pcDNA 3.0_3') for whole length sequencing were designed as listed in table 5.2. To analyze the result of my sequencing reactions, the programme Chromas 2.3(Technelysium) was used.

Primers	Sequences of the Primers	Conversion
Y16C FWD	5'- C TTC CTC TTC GAG TGT GAC ACC CCC -3'	Y→C
Y16C REV	5'- GGG GGT GTC ACA CTC GAA GAG GAA G -3'	Y→C
D17C FWD	5'- CTC TTC GAG TAT TGC ACC CCC CGC AT -3'	D→C
D17C REV	5'- AT GCG GGG GGT GCA ATA CTC GAA GAG -3'	D→C
T18C FWD	5'- TTC GAG TAT GAC TGC CCC CGC ATG GT -3'	T→C
T18C REV	5'- AC CAT GCG GGG GCA GTC ATA CTC GAA -3'	T→C
P19C FWD	5'- AG TAT GAC ACC TGC CGC ATG GTG CT -3'	P→C
P19C REV	5'- AG CAC CAT GCG GCA GGT GTC ATA CT -3'	P→C
R20C FWD	5'- GAC ACC CCC TGC ATG GTG CTG GTG -3'	R→C
R20C REV	5'- CAC CAG CAC CAT GCA GGG GGT GTC AT-3'	R→C
M21C FWD	5'- AC ACC CCC CGC TGT GTG CTG GTG CGT AA -3'	M→C
M21C REV	5'- AC ACC CCC CGC TGT GTG CTG GTG CGT AA -3'	M→C
V22C FWD	5'- C CCC CGC ATG TGC CTG GTG CGT AAT AA-3'	V→C
V22C REV	5'- TT ATT ACG CAC CAG GCA CAT GCG GGG G-3'	V→C
L23C FWD	5'- CC CGC ATG GTG TGT GTG CGT AAT AA-3'	L→C
L23C REV	5'- TT ATT ACG CAC ACA CAC CAT GCG GG-3'	L→C
V24C FWD	5'- GC ATG GTG CTG TGC CGT AAT AAG AG -3'	V→C
V24C REV	5'- CT CTT ATT ACG GCA CAG CAC CAT GC -3'	V→C
R25C FWD	5'- G GTG CTG GTG TGT AAT AAG AAG G-3'	R→C
R25C REV	5'- C CTT CTT ATT ACA CAC CAG CAC C-3'	R→C
N26C FWD	5'- TG CTG GTG CGT TGT AAG AAG GTG GG-3'	N→C
N26C REV	5'- CC CAC CTT CTT ACA ACG CAC CAG CA-3'	N→C
K27C FWD	5'- TG GTG CGT AAT TGT AAG GTG GGC GT-3'	K→C
K27C REV	5'- AC GCC CAC CTT ACA ATT ACG CAC CA-3'	K→C
K28C FWD	5'- GTG CGT AAT AAG TGT GTG GGC GTT A -3'	K→C
K28C REV	5'- T AAC GCC CAC ACA CTT ATT ACG CAC -3'	K→C
V29C FWD	5'- CGT AAT AAG AAG TGC GGC GTT ATC -3'	V→C
V29C REV	5'- GAT AAC GCC GCA CTT CTT ATT ACG -3'	V→C
G30C FWD	5'- T AAG AAG GTG TGC GTT ATC TTC CG -3'	G→C
G30C REV	5'- CG GAA GAT AAC GCA CAC CTT CTT A -3'	G→C

Table 5.1 Sequences of the primers used for cysteine mutagenesis reactions on the N-terminus of P2X$_1$ receptor

Site-directed mutagenesis reactions were performed on the human P2X$_1$ receptor to convert the single residues from Lys[16] to Gly[30] to be cysteine individually. Primers for the mutagenesis reactions are listed. The mutated base pairs are indicated in red and underlined, and the conversions of amino acids are shown in the table.

Primers	Orientation	Sequences of the Primers	Location
pcDNA3.0_5'	FWD	5'- CATTGACGCAAATGGGCGGTAGG -3'	pcDNA3.0
Seq A	FWD	5'- GATGTGGCTGACTACGTCTTCC -3'	P2X$_1$ sequence
Seq B	FWD	5'- CATCAGCTTTCCACGCTTCAAGG-3'	P2X$_1$ sequence
Seq C	FWD	5'- CAGGTTTGCCAGGCACTTTGTGG -3'	P2X$_1$ sequence
Seq E	REV	5'- GCATCAGGATGTCCTCATGTTCTCC-3'	P2X$_1$ sequence
Seq F	REV	5'- CCATGGAACTCATAGATGGGTCTGC -3'	P2X$_1$ sequence
Seq G	REV	5'- GCACCAGCCAAAGATCTCACACG -3'	P2X$_1$ sequence
pcDNA3.0_3'	REV	5'- GATCAGCGAGCTCTAGCATTTAGG -3'	pcDNA3.0

Table 5.2 Primers for the whole length sequencing of human P2X$_1$ receptor.
The 8 primers for fully sequencing of human P2X$_1$ receptor in the pcDNA 3.0 vector were designed as shown above. pcDNA3.0_5', Seq A, Seq B and Seq C sequences are forward primers, and Seq E, SeqF, SeqG and pcDNA3.0_3' are reverse primers.

Chapter 6. Cysteine scanning of
the P2X$_1$ receptor C-terminus

6.1 Introduction

6.1.1 Roles of P2X receptor C-terminus in time-course regulation

The carboxy terminus of the P2X$_1$ receptor was also considered to be important in channel regulation in several studies. Werner (Werner *et al*, 1996) initially suggested the interactions between the amino and carboxy termini were essential for maintaining the rapid desensitizing pattern at P2X$_1$ and P2X$_3$ receptors. Swap of the 34 amino acids within the C-terminal domain of P2X$_2$ receptor conferred slow desensitization to the P2X$_1$ receptor. However, in order to obtain the fast desensitizing response, both of the intracellular domains are required. At P2X$_7$ receptors, the large C-terminus domain accounts for its non-desensitizing pattern during repetitive agonist stimulation (Surprenant *et al*, 1996). As the BzATP applications were repeated in low concentration of divalent cations, the desensitizing time-course of P2X$_7$ receptor current slowed down gradually. Since this phenomenon had never been observed in other P2X subtypes, the unique long C-terminal sequence was suspected to be involved. As predicted, once the C-terminus of P2X$_7$ receptor was truncated from amino acid 418, the desensitizing kinetic of response was not observed with repeated applications. A P2X$_2$ receptor splice variant (P2X$_{2b}$) bearing a 68 amino acids deletion in the C-terminus was reported (Brandle *et al*, 1997) and showed an over 4 fold faster time-course for desensitizing in contrast to the P2X$_2$ receptor. A proline-rich region with a protential binding motif missing from the P2X$_{2b}$ receptor may contribute to the observed difference in channel desensitization. To further explore the specific region in this fragment that accounts for the P2X$_2$ channel desensitizing, a series of deletions were generated, and the segment from Arg^{371} to Ile^{391} was suggested to be important for sustained calcium influx (Koshimizu *et al*, 1998). Subsequently, triple alanine replacements were made at this segment, and the alanine substitutions from Arg^{371} to Pro^{376} showed significant increase in the desensitization rate. These results were further confirmed by single residue deletion. It is noticeable that the residues Pro^{373} and Lys^{374} are conserved among four members of the slow desensitizing P2X receptors [2,5,6 and 7]. The charged residues in this segment were substituted to alanine individually and suggested to be an influencing factor for the P2X$_2$ receptor desensitization rate. Interestingly, for the fast desensitizing P2X [1,2b,3] receptors, negatively charged residues

instead of the positively charged residues are present in the corresponding segment. As a result, either elimination of negatively charged residues by neutral glutamine or introduced positively charged residues into this sequence at $P2X_4$ receptors decreased the time-course of channel desensitization. Fountain *et al* further identified two residues at the C-terminus of human $P2X_4$ receptors that contribute to desensitization and showed important role of the charge at these positions (Fountain *et al*, 2006). The alanine and cysteine mutants at Lys^{373} speed desensitization kinetics and the WT phenotype can be restored by the binding of positively charged MTS compound at K373C mutant. The Tyr^{374} was replaced with alanine, aspartic acid and lysine respectively and great reductions in peak amplitude and current time-course were also observed. Only the aromatic amino acid phenylalanine substitution at tyrosine 374 showed similar currents and desensitization pattern as the WT receptor, this indicated the desensitization properties of $P2X_4$ receptor require an aromatic moiety at the this position.

6.1.2 The conserved protein trafficking motif at P2X receptor C-terminal

The carboxy terminus of P2X receptors has been shown to have essential roles in protein trafficking to the cell membrane. The sequences of the C-terminal of P2X receptors were aligned and a tyrosine and a lysine separated by three amino acids close to the TM2 were found to be conserved (Chaumont *et al*, 2004). This YXXXK motif presents in almost all of the known P2X receptors including the *Dictyostelium* P2X receptors. To study the property of this conserved site, alanine substitutions were introduced at $P2X_2$, $P2X_3$, $P2X_4$, $P2X_5$ and $P2X_6$ receptors respectively, and the surface expression was determined by a chemiluminescence assay. As a result, disruption at either the conserved tyrosine or lysine led to large decreases of surface expression compared to the WT receptor. However, the total protein amounts were not altered in all cases, which indicated the roles of this motif in maintaining the P2X receptor surface trafficking. The underlying mechanism was further investigated at the $P2X_2$ receptor. WT $P2X_2$ receptor showed little internalization and primarily localized at the plasma membrane that were visualized using Cy3-conjugated and FITC-conjugated secondary antibodies before and after permeabilization respectively (Bobanovic *et al*, 2002). However, a significant internalization during a period of 30 minutes was observed at the mutated $P2X_2$ receptors Y362A and K366A (Chaumont *et al*, 2004). To confirm the role of the YXXXK motif in P2X receptor stability, the WT or mutated C-terminal tails

were fused to the CD4 intracellular domain, and the surface expressions of the CD4 and CD4-P2X chimera were subsequently measured by cheiluminescence assay. The surface expression of the CD4-P2X chimera was found to be significantly higher than the WT CD4, whereas this increased surface expression can not be observed at the chimera where the YXXXK was disrupted (Chaumont *et al*, 2004). Therefore, the YXXXK motif likely enhanced the receptor stabilization, and this regulation can be mediated by interacting with cytoskeletal proteins.

TM2   YXXXK **trafficking motif**
```
LAIRFLPQ------------------RKSYSSLKFQTT 357 DDB0217630
LAIRFLPQ------------------RKSYSSLKFQTT 343 DDB0203089
LAIRFLPE------------------RKTYSSHKFQIT 344 DDB0187892
LAIRLLPQ------------------RKSYSSLKFQVT 351 DDB0168616
IATRIMPQ------------------RSRYQELKFQDS 352 DDB0219300
IALNLLRS------------------RDIYQRAKFETI 376 Schistosome
LLLHILPK------------------RHYYKQKKFKYA 371 HumanP2X1
ILLTFMNK------------------NKVYSHKKFDKV 381 HumanP2X2
ILLNFLKG------------------ADQYKAKKFEEV 361 HumanP2X3
IVLYCMKK------------------RLYYREKKYKYV 375 HumanP2X4
VLIYLIKK------------------REFYRDKKYEEV 373 HumanP2X5
LLLYVDRE------------------AHFYWRTKYEEA 367 HumanP2X6
LIDTYSSNCCRSHIYPWCKCCQPCVVNEYYYRKKCESI 391 HumanP2X7
```

Figure 6.1 Partial aligment of the carboxyl terminal sequences in human, *Schistosome* and *Dictyostelium* P2X receptor subtypes
Sequences of P2X receptor carboxy terminus close to the transmembrane segment of P2X receptor members are shown. The second transmembrane domain is indicated by the bar, and the conserved protein trafficking motif comprised of tyrosine and lysine is indicated in bold. The YXXXK sequence is the only conserved motif in the C-terminal region of P2X receptors (Taken from Fountain *et al*, 2007).

The equivalent Lys[367] residue includes in the YXXXK motif was subsequently studied at P2X$_1$ receptors by alanine substitution (Vial *et al*, 2006). As a result, over 99% of the ATP-evoked peak current amplitude and a much more rapid desensitization pattern was found at the K367A mutant. The surface and total expression levels of this mutant was tested by biotin labeling, however, there was no significant difference observed compared to the expression of WT P2X$_1$ receptors. Hence, there maybe subtype differences for roles of this residue, and it may be involved in channel gating regulation rather than a protein trafficking mechanism.

In addition to the conserved YXXXK protein trafficking motif, an important motif at the C-terminus of P2X$_4$ receptors in determining receptor internalization was demonstrated (Royle *et al*, 2002). WT P2X$_4$ receptor showed rapid constitutive internalization and re-insertion into the cell membrane following channel activation. Three amino acids Tyr[378], Gly[381] and Leu[382] completely conserved in the mammalian P2X$_4$ receptor C-terminal made up an atypical tyrosine regulate site of YXXGL.

Nevertheless, mutations at the YXXGL motif at the C-terminus reduced channel internalization and increased surface expression of P2X$_4$ receptor.

A previous study at the P2X$_7$ receptor suggested roles of a polymorphism Ile^{568} to Asn in protein trafficking (Wiley *et al*, 2003). In addition, a lipid-interaction motif at the P2X$_7$ receptor carboxy terminus has been revealed and two basic residues Arg^{578} and Lys^{579} within this motif were proposed to be important for lipopolysaccharide binding. When these two residues were mutated to glutamic acid, despite normal levels of total protein expression, these two mutants failed to demonstrate surface immunoreactivity (Denlinger *et al*, 2003).

6.1.3 The contribution of the C-terminal to channel dilation

Previous studies demonstrated the channel dilation phenomenon for P2X$_7$ and P2X$_2$ receptors, and the carboxy terminus of the P2X receptors was shown to be essential in this modulation pathway. The C-terminus of the P2X$_7$ receptor is much longer than other subtypes and it was suggested to be required for a unique cytolytic action activated by ATP induced cell swelling. Once the C-terminal of P2X$_7$ was truncated, the P2X$_7$ receptor was still able to function as a ligand-gated cation channel whereas the cytolytic action was absent (Surprenant *et al*, 1996). Furthermore, during repetitive applications of ATP, the channel is able to gradually take up large cations such as NMDG$^+$ and organic dyes such as YO-PRO-1. In this case, this cytolysis procedure was further suggested to be via a progressive dilation and the C-terminal region contributed to this ion-conducting regulation fundamentally.

Eickhorst's group used reversal potential measurements to estimate the pore diameter during state transition (Eickhorst *et al*, 2002) at P2X$_2$ receptors. Although both mouse P2X$_2$ (mP2X$_2$) receptor and rat P2X$_2$ (rP2X$_2$) receptor have a pore diameter of 11 Å, the rP2X$_2$ receptor pore diameter increased at least 3 Å after the selective state transition. Comparing the sequence of C-terminus of the mP2X$_2$ and rP2X$_2$ receptors, rP2X$_2$ receptor contain a shorter C terminal tail which is 14 amino acids different from the mP2X$_2$ receptor. To identify the specific residues responsible for this channel pore dilation, a series of chimeras were generated and two residues at locations 432 and 444 respectively were determined to be essential in this regulation (Eickhorst *et al*, 2002).

When these two residues were inserted into the rP2X$_2$ receptor C-terminal tail, they were shown to be sufficient to remove the pore dilation.

6.1.4 Aim

The P2X receptor carboxy terminal has been considered to be an important region for a range of channel regulations, for example the time-course of desensitization, protein trafficking to the plasma membrane, and channel pore dilation.   However, the structure and roles of the residues next to the channel pore and the ones around the YXXXK motif are still not clear. Due to the great variation of the C-terminal sequence among the P2X receptor family, 16 amino acids from the TM2 at the carboxy terminus of the P2X$_1$ receptor were focused on in this study. The TM2 intracellular flanking region, conserved protein trafficking motif and three conserved tyrosine residues are all incorporated in these 16 residues. Site-directed cysteine mutagenesis and MTSEA were used to characterize the properties and accessibility of these residues.

6.2 Results
6.2.1Point cysteine substitutions on basic P2X$_1$ receptor properties

Cysteine substitution mutagenesis was used to study the contribution of the 16 amino acids after the second transmembrane segment to channel properties. The cysteine mutants from H355C to Y370C of the P2X$_1$ receptor C-terminus were generated by site-directed mutagenesis and the sequenced (See figure 6.2). The mRNAs of the mutants were synthesised and injected into the *Xenopus* oocytes to look at the expression levels, channel time-course of desensitization and EC$_{50}$ values and reproducibility of responses.

A transient inward current was evoked during the continued presence of ATP (100 μM, a maximal concentration) at WT P2X$_1$ receptors (-6442 ± 211 nA, *n*=15) (See figure 6.3). 6 out of the 16 mutants showed no effect on the peak amplitude. Unlike the amino terminus, the majority of mutants exhibited reduced peak current amplitudes by ~30-80% (-3647 ± 298 nA, *n*=12 for H355C; -2333 ± 220 nA, *n*=18 for K359C; -2453 ± 250 nA, *n*=16 for R360C; -4307 ± 429 nA, *n*=14 for H361C; -2876 ± 454 nA, *n*=8 for Y362C; -1496 ± 259 nA, *n*=9 for K367C and -2498 ± 224 nA, *n*=8 for F368C. *p<0.05, ***p<0.001), and the smallest current was obtained at Y363C (-48 ± 11 nA, *n*=12) (See figure 6.3). Y363C where the ATP evoked amplitude was too small to be further analyzed in term of EC$_{50}$ determination or MTS reagent sensitivity. For the mutants with decreased peak amplitudes, the ATP concentration was increased up to 10 mM. However, increased 10mM ATP did not induce further increase the current amplitudes compared to 100 μM ATP for most of the mutants except at K359C, where the peak amplitude was increased from -2333 ± 220 nA (*n*=18) to -3865 ± 1041 nA (*n*=4) (Figure 6.4, *p<0.05) and indicated an ATP sensitivity shift due to this cysteine substitution. To investigate whether the reduced current of the mutants resulted from decreased surface expression or the channel ion permeability, the sulfo-NHS-LC biltinylation assay was used to label the P2X$_1$ receptors expressed on the surface of oocytes. Total and surface expression levels were visualized on SDS-PAGE gel by western blotting. The bands for the P2X$_1$ receptors were revealed as monomers of ~55 kDa. Comparable surface and total staining were showed by most of the mutants. It is noticeable that the reduction (>50%) at the plasma surface expression were only observed at Y362C and K367C (Figure 6.4), and these residues were indicated to be
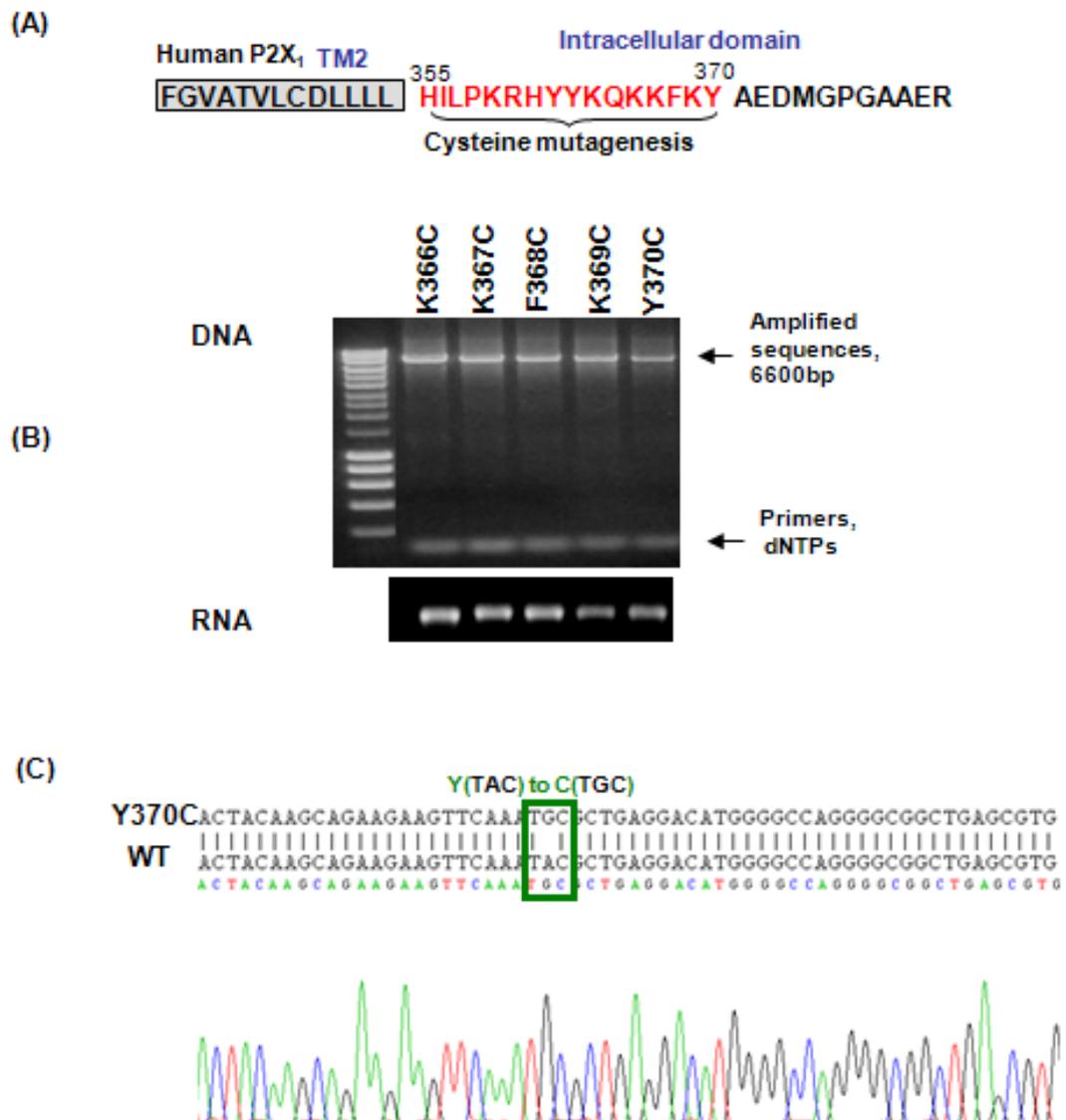
Figure 6.2 16 amino acids on the C-terminus of the P2X₁ receptor were mutated to cysteine

(A). Intracellular residues that were mutated to cysteines are indicated in red, these are just after TM2 (in grey box). **(B).**Example of the mutants from K366C to Y370C generated site-specific mutagenesis, and the bands obtained after mutated from PCR with the mutagenesis primers were revealed on gel. mRNAs were made from the cDNAs and injected to *Xenopus lavis* oocytes for expression. The amount of mRNA generated is illustrated on the RNA gel in the lower panel. **(C)**. Example sequencing figure of mutant Y370C from Chromas, the sequence TAC was converted to TGC at the cDNA level to make a conversion from tyrosine to cysteine. All of the mutants were checked by full sequencing (C for blue, G for black, T for red and A for green).
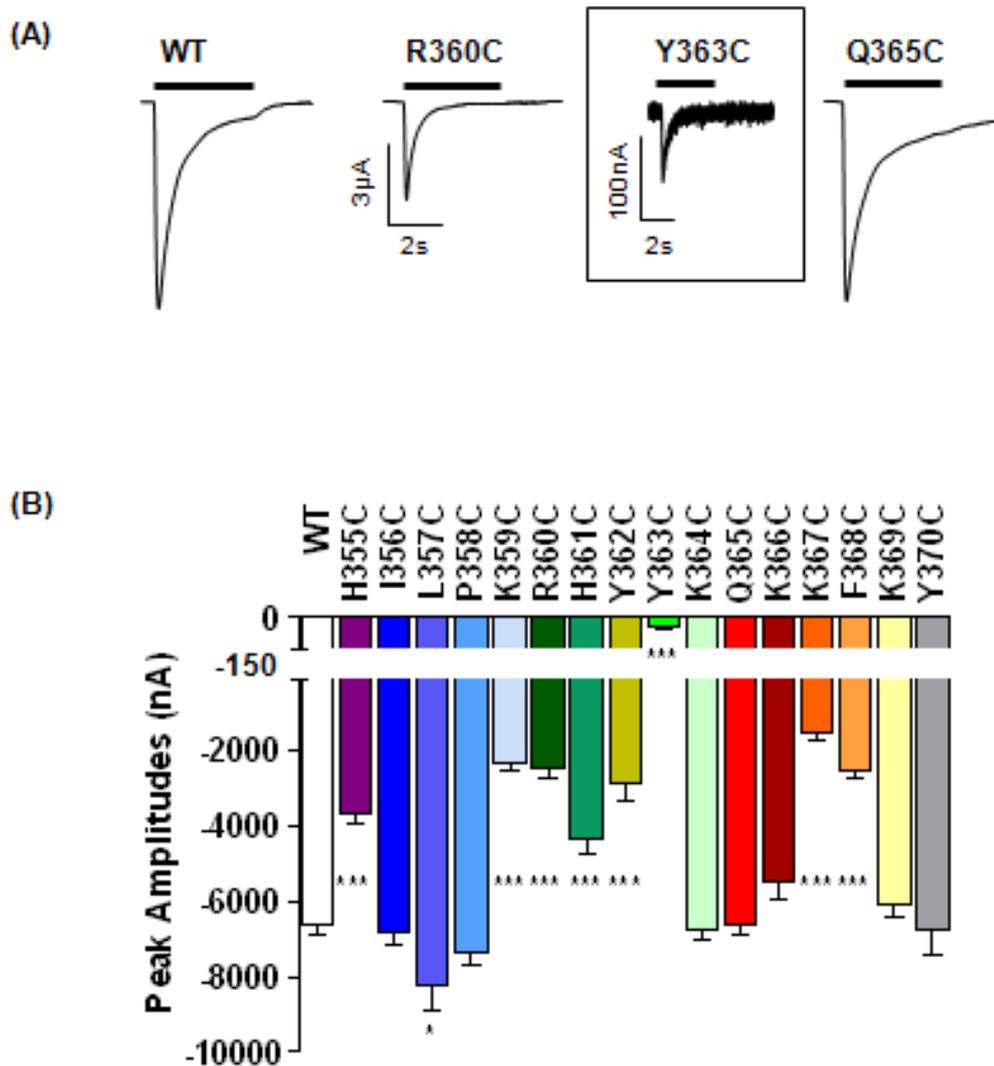
Figure 6.3 The peak current amplitudes of WT P2X$_1$ receptor and cysteine mutants
(A). Traces of initial currents of the P2X$_1$ receptor WT and mutants to ATP (100 μM, application period as indicated in bar). **(B).** Summary of the peak current amplitudes of the wild type P2X$_1$ receptor and cysteine mutants at the maximal concentration of ATP. The segment between 0 to -150 nA is amplified to show the small current for Y363C mutant. Only 6 out of 16 of the mutants exhibit a similar peak currents as the WT P2X$_1$ receptor (-6878 ± 86 nA, n=14)., and reduced peak amplitudes were observed for most of them, n=4-18. *p<0.05,***p<0.001.
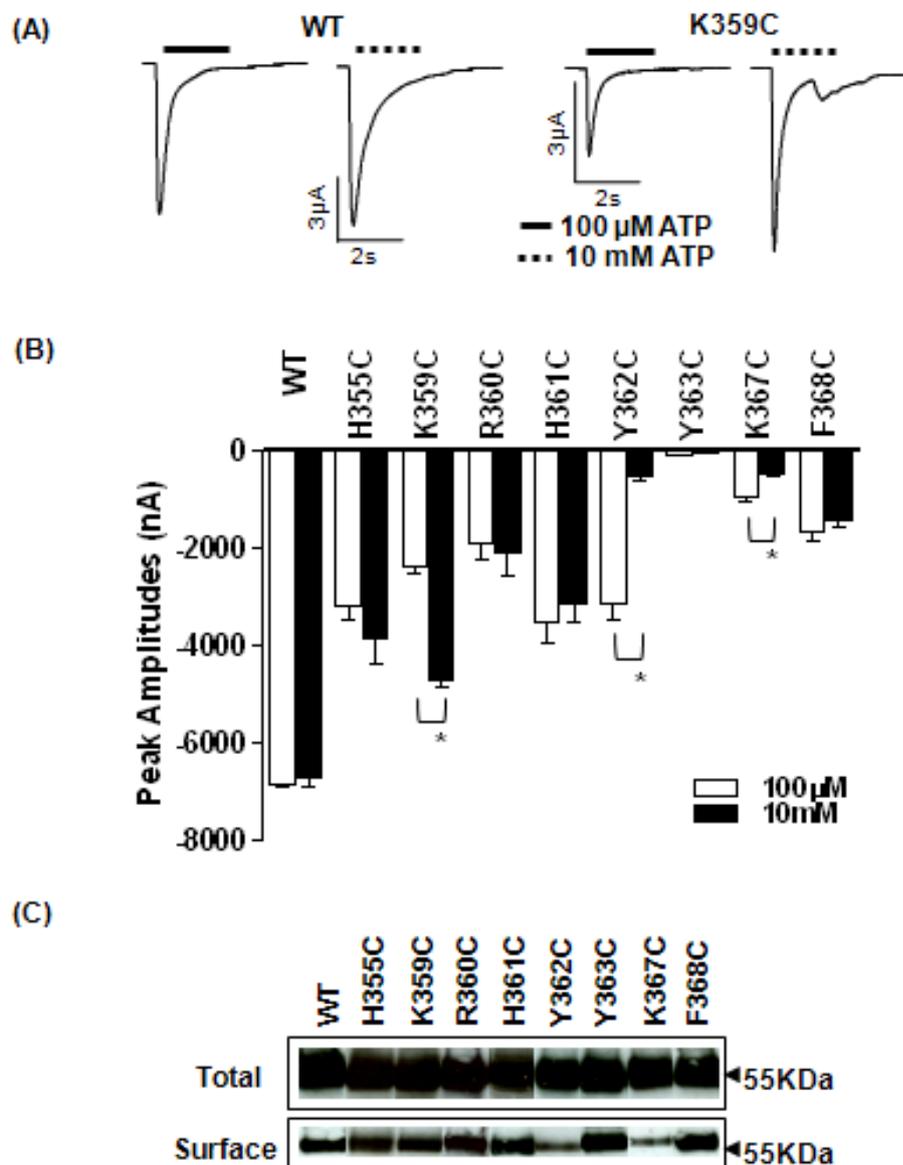
Figure 6.4 Normal levels of expression for mutants with decreased maximal ATP responses

(A). Traces of initial currents of the P2X$_1$ WT and in response to 100 μM ATP (application showed in black bar) or 10 mM (dashed bar). **(B).** Summary of peak currents evoked by 100 μM and 10 mM ATP at WT and mutant P2X receptors, *n*=4-8. *p<0.05. **(C).** The expression levels of the mutants with lower peak amplitudes were studied by western blotting, and most of the mutants did not show any difference to the WT P2X$_1$ receptor in total and surface protein expression, except Y363C and K367C that involved in the YXXXK protein trafficking motif.

important for protein trafficking mechanisms. Lys^{367} is the conserved lysine residue in the protein trafficking motif, previous study disrupted this residue in other P2X subtypes and a similar protein expression pattern (23-58% for $P2X_{3-6}$ mutants) was observed (Chaumont *et al*, 2004). However, Y363C showed the smallest peak current amplitudes but had no effect on the protein expression and suggests this tyrosine residue may be involved in channel gating rather than protein trafficking. It may indicate an $Y^{362}XXXXK^{367}$ trafficking motif for $P2X_1$ receptor.

For oocytes expressing the WT $P2X_1$ receptor, 100 μM ATP application evoked reproducible currents which maintained about 50-70% of the initial amplitudes as shown in figure 6.5. Although a moderate peak amplitude can be triggered by maximum concentration of ATP for the first application at K367C, the currents run down dramatically and cannot be reproduced during the 5 minutes interval (Figure 6.5, *p<0.05). This residue was therefore considered important for internalization regulation for $P2X_1$ receptors.

Maximum peak current amplitude can be evoked by 100 μM ATP at the WT $P2X_1$ receptor as stated before, and the mean EC_{50} value is estimated to be about 1 μM. The ATP potencies for mutants were studied by comparing the relative amplitude of responses evoked by 1 μM and 100 μM ATP. Most of the cysteine mutants showed 20-80% of the maximum current to the application of 1 μM ATP (See figure 6.6). Decreased peak amplitudes to 1 μM ATP were found for 7 out of 16 mutants (***p<0.001), especially for those that showed reduced peak amplitudes to 100 μM ATP. Take P358C for example, its amplitude evoked by 1 μM is only 28.3 ± 3.4% (*n=4*) of the maximal response. When the full range of ATP concentrations were applied to the P358C mutant, the ATP potency only showed a slight shift from 1 μM to 2 μM for EC_{50} (See figure 6.6). Hence, the cysteine substitutions to the C-terminal of $P2X_1$ receptor did not alter the ATP potency fundamentally.

The time-course for WT $P2X_1$ receptor desensitization was measured by the decay time from 100% to 50% peak current amplitudes as shown in figure 6.7. The majority of the mutants had similar time-course as the WT receptor (257 ± 7 ms, *n=15*) including most of the mutants with lower peak amplitudes. The most obvious variations can be
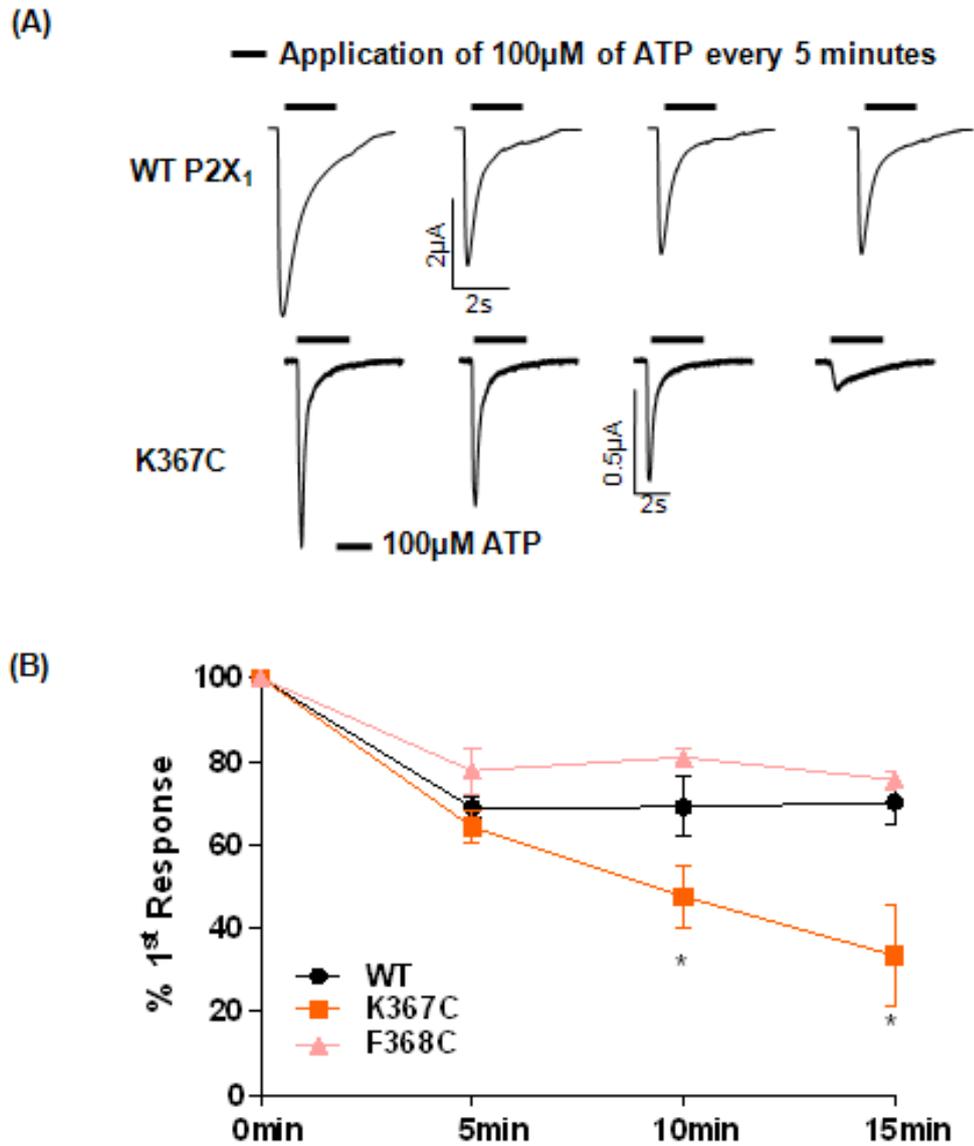
Figure 6.5 Significant rundown of responses at K367C
(A). Representative traces of the WT and P2X$_1$ K367C during ATP (100 μM ATP, application period indicated by bar) application every 5 minutes. **(B).** The first current amplitudes were set to be 100% and compared with the following amplitudes as summarized above. After the second application, WT receptors and F368C (pink) are able to evoke reproducible currents of 60-70% to the first amplitudes. However, the peak currents of K367C (orange) were decreasing gradually during the 5 minutes interval, *n*=3-5. *p<0.05.
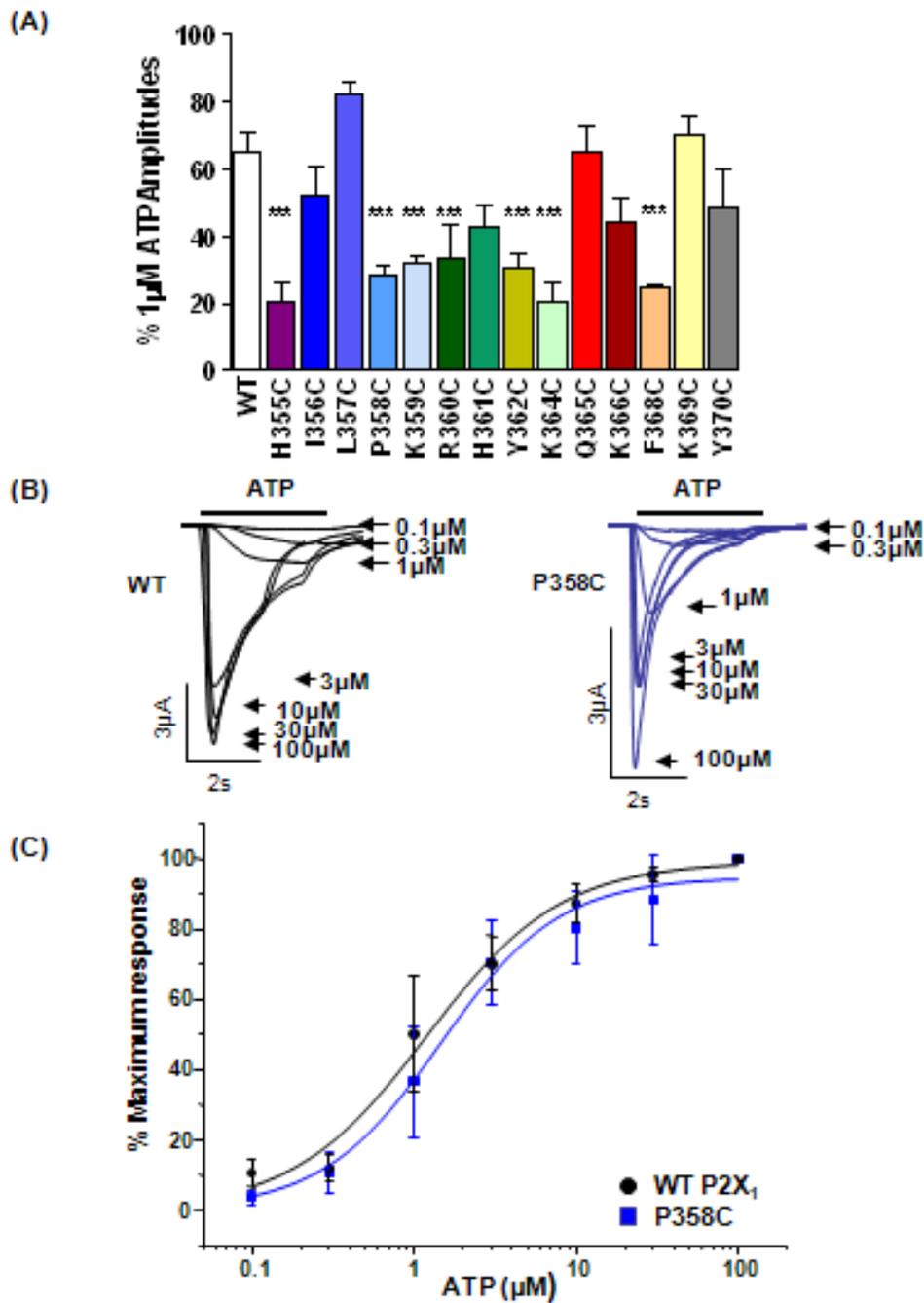
Figure 6.6 Cysteine mutation did not alter the EC_{50} value of mutant $P2X_1$ receptors
(A). Summary of the % amplitudes evoked by ATP (1μM) to the maximum response (100 μM). All of the mutants exhibit current between 20-80% of the maximum amplitudes under 1 μM of ATP, *n*=3-7.***p<0.001. **(B).** Example traces of the WT and mutant P358C (blue) during the application of different concentration of ATP, the peak amplitudes of $P2X_1$ receptor is dependent on the ATP concentration applied. **(C).** Example of concentration-response curve of the WT and mutant $P2X_1$ receptor. Although the significant lower amplitudes levels evoked at P358C to1 μM ATP, there was no obvious shift at EC_{50} observed, *n*=3.
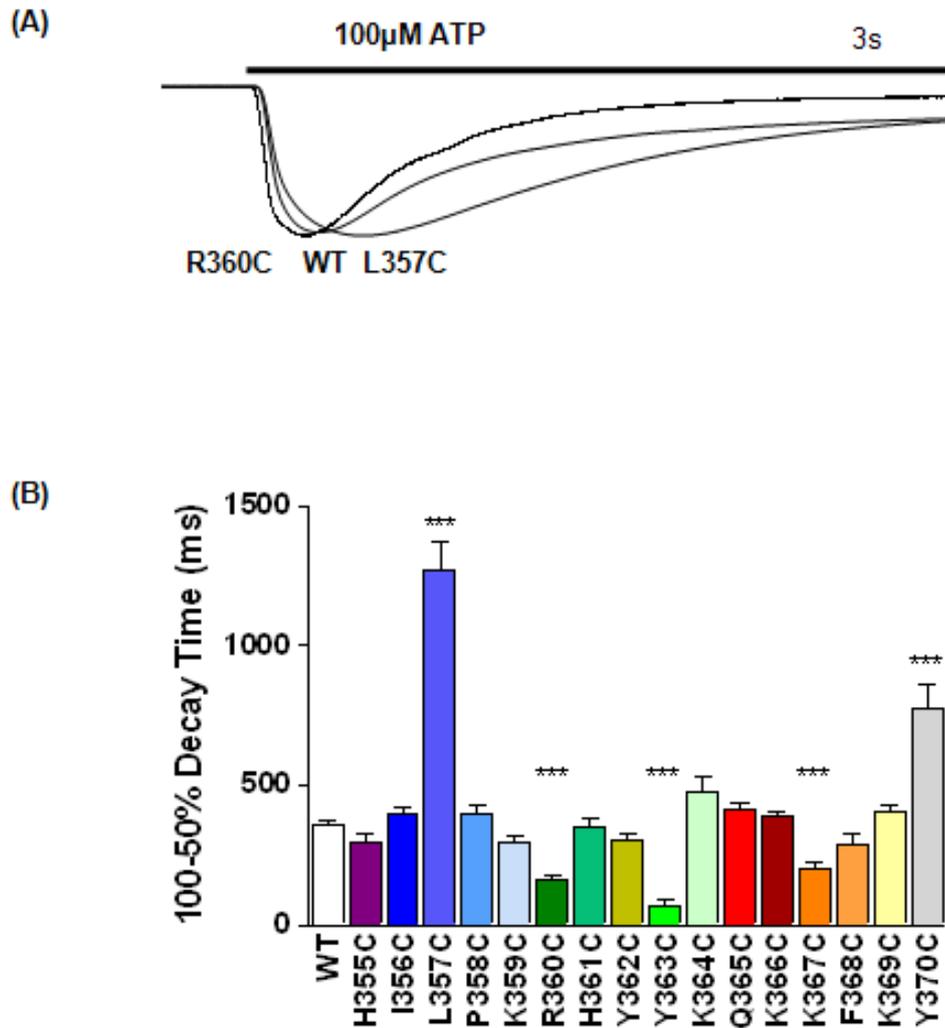
Figure 6.7 The time course of C-termini cysteine mutant currents measured in oocytes
(A). Representative traces of the WT and mutant P2X$_1$ receptor in response to the application of ATP (100 μM, application period indicated by bar). The mutant L357C (1267 ± 108 ms, n=24) showed a slower desensitizing current, while the R360C (165 ± 15 ms, n=17)showed a faster desensitizing current compared to the WT(258 ± 7 ms, n=15). (B). The peak current decay time from 100% to 50% of WT P2X$_1$ receptor and all cysteine mutants were summarized, n=6-31. ***p<0.001.

observed for L357C where the time-course was prolonged by almost 5 fold (1267 ± 108 ms, $n=25$, ***p<0.001) compared to WT receptor in oocytes. In addition, faster desensitizing was observed for R360C (165 ± 15ms, $n=17$), Y363C (71 ± 20 ms, $n=6$) and K367C (199 ± 25 ms, $n=26$) (Figure 6.7, ***p<0.001). The fastest time-course was measured at Y363C which is about 5 fold faster than the WT receptor in oocytes whereas its peak amplitude was reduced by over 90%.

Due to the slower solution exchange period for the oocytes during recording, the time-courses of channel desensitization for mutants were estimated by patch clamp recording from HEK cell expressing the P2X$_1$ receptor mutants. cDNAs of the mutants showed significant changes to the WT receptor time-course measured in oocytes were transfected into HEK293 cell and currents to the application of 100 μM ATP were studied. Currents evoked at Y363C mutant was barely detectable and were not tested in the HEK cell expression. Although similar prolonged or speeding of time-courses were observed for the mutants L357C and R360C, and K367C (See figure 6.8, ***p<0.001, **p<0.01), the time-courses measured in HEK cells for WT and these mutants are much faster than for oocytes. For example, the L357C showed only 1.7 folds slower desensitizing period in HEK cells comparing to the 5 folds slower in oocytes expression system; while the K367C exhibited 10 fold faster desensitization time-courses in HEK cell comparing to 1.3 fold in oocytes. Y370C showed significant slower time-course for desensitization when expressed in oocytes, however, it had no difference to the WT in HEK cells.

6.2.2 Effects of MTSEA on the C-terminus cysteine mutants

SCAM was used to study the accessibility of the cysteine substituted carboxy termini residues, and the residues having important properties in this region were analyzed. MTSEA as a relatively small MTS compound shows permeability to the plasma membrane, and was suggested to be feasible in the previous study at the amino termini of P2X$_1$ receptor (See chapter 5). MTSEA (1 mM) was perfused and applied with ATP (1 μM) for 4 times, the maximum effects on the 14 (except Y363C and Y367C) P2X$_1$ receptor carboxy terminus mutants are summarized in figure 6.9. Only four cysteine substitutions exhibited similar response to MTSEA treatment as wild type. Significant potentiation effects were shown by eight mutants close to the TM2, including the H355C ($122.00 \pm 12.33\%$, $n=5$), I356C ($63.46 \pm 7.41\%$, $n=3$), L357C ($82.46 \pm 6.04\%$,

(A)

100µM ATP   3s

R360C WT

L357C

(B)

(C)

P2X$_1$ Receptor	Peak (nA)	100-50% Decay Time (ms)	Fold of WT	Peak (nA)	100-50% Decay Time (ms)	Fold of WT
		HEK cell			*Xenopus oocyte*	
WT	-2270±196	169±23		-6513±179	258±7	
L357C	-2725±717	288±34**	1.7	-8826±640*	1267±108***	4.9
R360C	-949±217***	11±1***	0.1	-2454±250***	165±15***	0.6
K367C	-1249±616	10±1***	0.1	-1496±259	199±25***	0.8
Y370C	-2649±674	137±36	0.8	-6752±670	774±90***	3.0
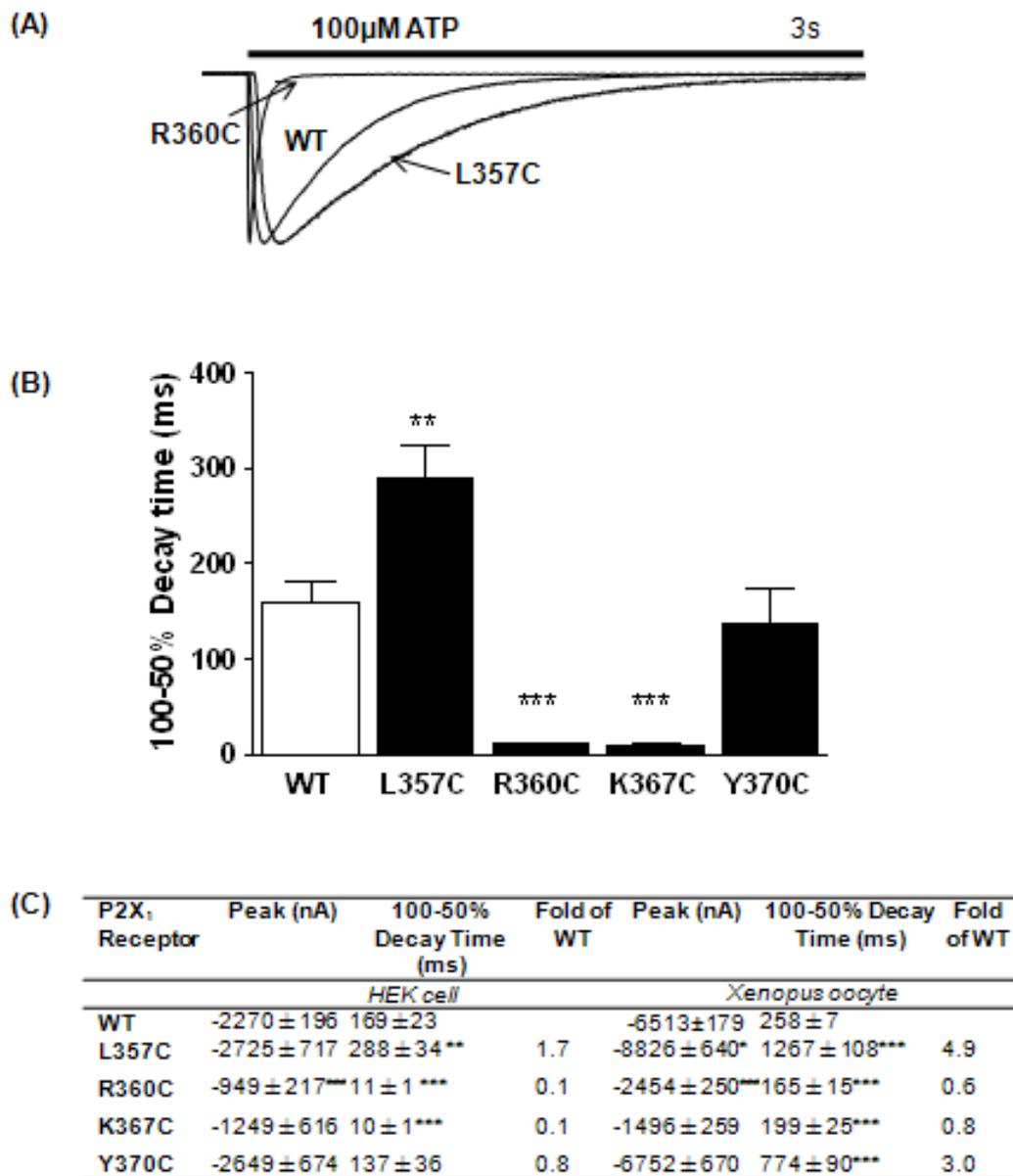
Figure 6.8 The time course of peak current decay time obtained from patch clamp recording on HEK293 cell.
WT and mutants of P2X$_1$ receptors were transiently expressed in HEK293 cells and the time course of desensitization was studied by patch clamp recording. **(A).** Example traces of the P2X$_1$ WT receptor (100 µM ATP, application period indicated by bar), and peak currents were normalized. L357C and R360C mutants exhibit a similar trend to the currents recorded in oocytes. **(B).** The decay time from 100%-50% of the peak currents of WT P2X$_1$ receptor and the mutans show significant difference to the WT except for Y370C, n=5-15. **(C).** Comparison of the changes on the 100-50% peak current decay time between HEK cells and oocytes are shown in the table. ***$p < 0.001$, **$p < 0.01$.
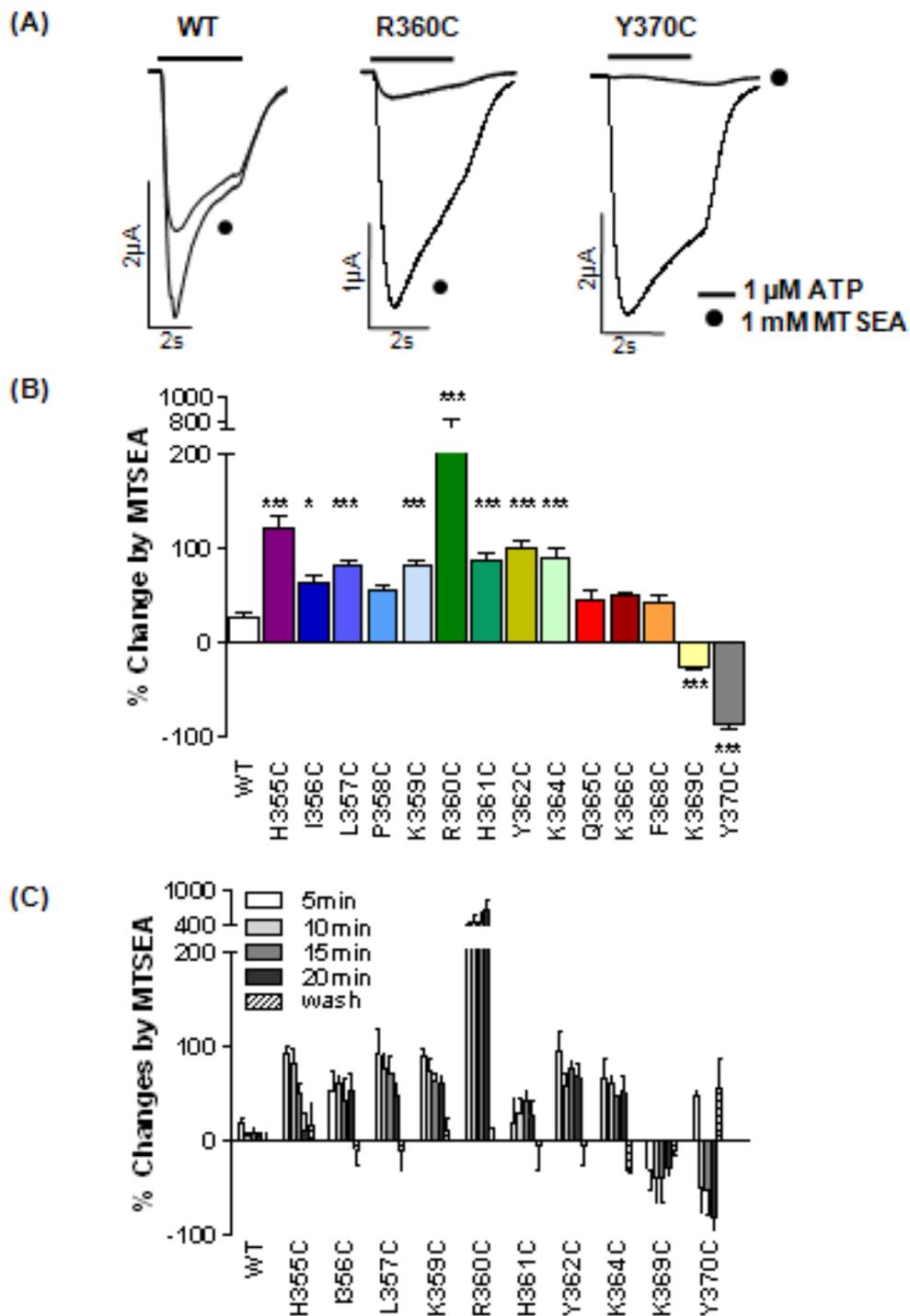
Figure 6.9 The effects of MTSEA on N-terminal cysteine mutants
(A). Representative traces of ATP (1 µM, application period indicated by bar) evoked current from single oocytes of WT and mutant R360C (757.93±71.84%,*n*=4) and Y370C(-85.67±6.81%,*n*=4) of P2X$_1$ receptors before and after MTSEA application (maximum effect black circle). **(B).** Summary of the maximum percentage changes of the WT and cysteine mutants by MTSEA, *n*=3-6. *p<0.05. ***p<0.001. **(C).** Summary of time-dependent effects of MTSEA on WT and cysteine mutant P2X$_1$ receptor.

n=3), K359C (81.35 ± 6.85%, n=4), R360C (757.92 ± 71.84%, n=4), H361C (88.46 ± 7.15%, n=4), Y362C (100.93 ± 6.75%, n=4) and K364C (91.54 ± 8.98%, n=4) (See figure 6.9, *p<0.05. ***p<0.001). The striking potentiation observed at R360C is over 7 fold. By contrast, the mutants K369C (-24.34 ± 2.98%, n=3) and Y370C (-85.67 ± 6.81%, n=4) after the YXXXK protein trafficking motif were inhibited by the MTSEA treatment. However, none of these potentiations remained following 5 minutes washout of MTSEA and are suggested not to result from the irreversible covalent modification of the introduced cysteine. Furthermore, both the potentiation and inhibitory effects at the carboxy terminal mutants took place after the first 5 minutes application and showed no time dependence as seen for the amino terminal mutants.

The MTSEA induced massive reversible potentiation at R360C was further characterized. The MTSEA compound in use contains bromide. To study whether this potentiation was due to the MTSEA or possibly the bromide, NaBr (1 mM) was given to the R360C mutant in the same condition as previous MTSEA treatment. NaBr showed a 99.43 ± 13.15% (n=4, ***p<0.001) potentiation at R360C suggesting the bromine doubled the ATP evoked response at this mutant on its own (Figure 6.10). However, the MTSEA may still contribute to the majority of the potentiated current.

The MTSEA induced effects was also suggested to be concentration dependent, as the working MTSEA were reduced to 100 μM potentiation was reduced to 118.08 ± 42.34% (n=3, ***p<0.001) (Figure 6.11). To investigate the effect of MTSEA to the maximum response induced by ATP, ATP at maximal concentration (100 μM) was applied to the R360C as in figure 6.11. As a result, the MTSEA mediated potentiation was reduced to 206.42 ± 21.76% (n=3) to the 100 μM ATP evoked response suggesting the ATP potency was affected by adding the positively charged MTSEA to this residue. Alternatively, MTSEA (1 mM) was pre-treated to the oocytes expressing R360C mutant for 1 hour before recording to allow an adequate accessing and remove the effect of bath changing during recording. A significant potentiation of 77.51±21.97% (n=6) (Figure 6.11A) to 1μM ATP evoked response was still remained.

In addition to the peak amplitudes, MTSEA had no significant effects to the time-course of all of the C-terminal cysteine mutants (Figure 6.12).
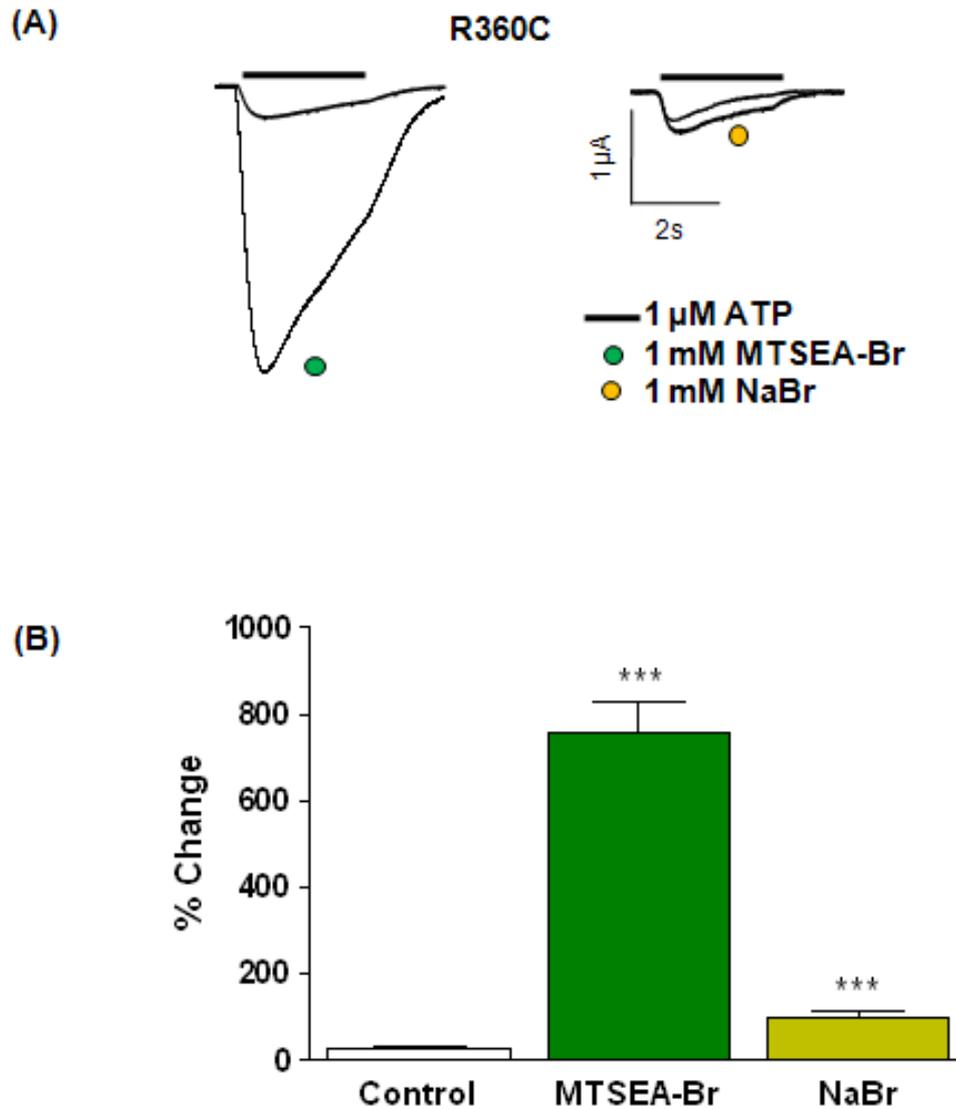
Figure 6.10 The effects of MTSEA on R360C
(A). Sample traces of ATP (1 µM, application period indicated by bar) evoked current from mutant R360C of $P2X_1$ receptors before and after the MTSEA-Br (757.93±71.84%,n=4,green dot) or NaBr (99.43±13.14%, n=4, yellow dot) application (maximum effect black circle). **(B).** Summary of the maximum percentage changes of the WT (control by MTSEA-Br) and R360C mutants by MTSEA-Br and NaBr, n=4-6. ***p<0.001.
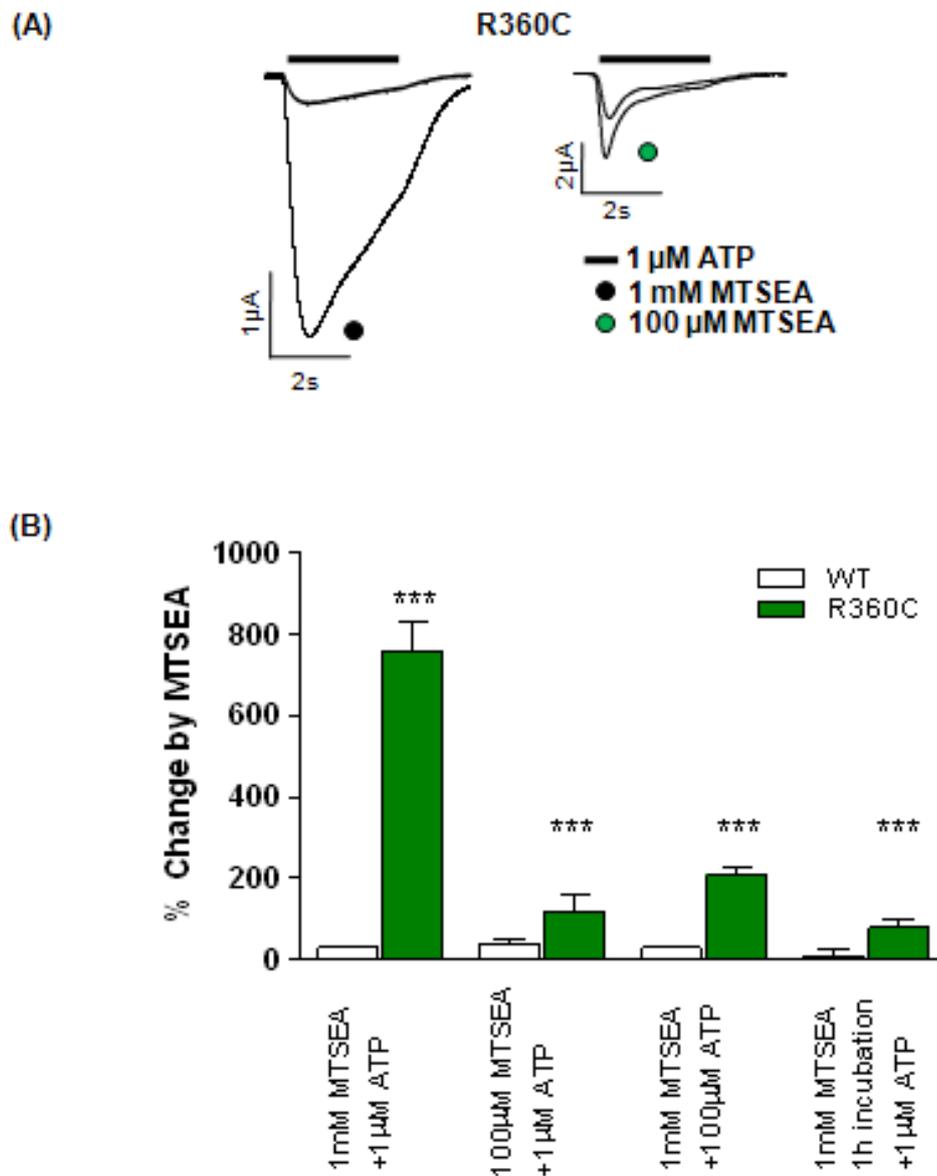
Figure 6.11 MTSEA induced ATP potency shift at R360C
(A).Representative of the ATP (1 µM) evoked currents before and after the stimulation of MTSEA at 1 mM (black dot) and 100µM (green dot) respectively. (B). Summary of MTSEA effects to R360C when different concentrations of ATP and MTSEA were applied, *n*=3-6. ***p<0.001.
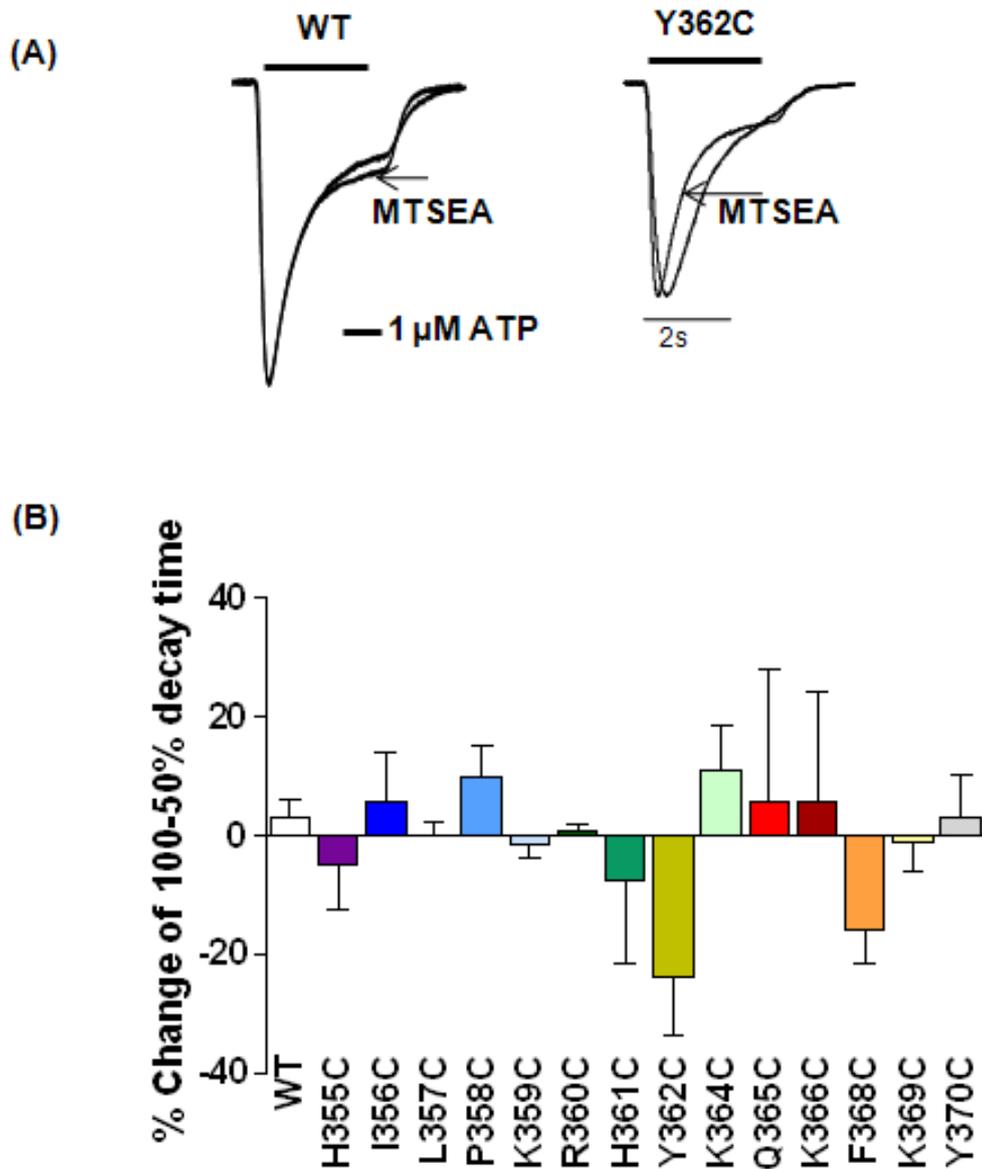
Figure 6.12 Effects of MTSEA on the 100-50% decay time of the C-termini cysteine mutants
(A). Example traces of the 100-50% decay time of the Y362C and WT P2X$_1$ receptor with or without MTSEA(1 mM) application (indicated with arrow). The decay time for mutant Y362C (-23.76±9.79%, n=6) showed no significant difference between before and after the MTSEA treatment.(B). Summary of the percentage change of the decay time for WT and cysteine mutants of P2X$_1$ receptor. The decay time was compared by paired recordings, n=4-11.

6.3 Discussion

The carboxy terminal of P2X receptors is involved in channel gating, and protein trafficking. It was also considered to be important for P2X receptor intracellular signaling. 16 residues close to the second transmembrane segment at the C-terminal of P2X$_1$ receptors were substituted to cysteines individually in this study, and subsequently characterized using MTSEA. The residues at the carboxy terminal showed different patterns to those at amino terminal of P2X$_1$ receptor. Half of the C-terminal cysteine mutants (8/16), especially the ones close to the TM2, exhibited reduced peak current amplitudes, and following biotinlytion demonstrated these decreases were not due to the reductions at surface expressions for most of them (6/8). In addition, most of these mutants with smaller peak amplitude had no effect on ATP sensitivity, and further suggested these residues may be involved in channel gating. By contrast, the MTSEA had no sustained effect at any of these mutants. The conserved Lys^{367} and tyrosines within this domain also exhibited essential roles in channel expression and gating that will be discussed.

6.3.1 Important roles of residues around the YXXXK trafficking motif

Although the sequences of the C-terminal regions are quite variable among the P2X receptor family, the alignment of the subtypes close to the end of the second transmembrane domain showed a tyrosine and a lysine that are separated by three other amino acids which defined a conserved YXXXK motif. This motif is not only found in mammalian P2X subtypes, but also *Dictyostelium* P2X receptors (Chaumont *et al*, 2004). This YX$_3$K motif also exists in a range of G protein-coupled receptors. For example, it was found in the proximal region of the third intracellular loop of α$_2$-adrenergic receptors and plays trafficking and signal stabilizing roles via protein-protein interaction (Chaumont *et al*, 2004). In addition, this sequence is present in other membrane proteins, including the sodium channel SCN8 and the chloride channel CLC3-5 (Chaumont *et al*, 2004). Current data show the YXXXK motif at P2X$_1$ is essential for receptor expression and gating regulation. Cysteine substitutions at the conserved tyrosine and lysine caused reduced peak current amplitude, run down of current amplitude, decreased surface receptor expression, and speeding of time-course of responses.

The cysteine substitution at Lys^{367} led to significantly reduced peak current amplitudes and speeded time-course of response. This seems due to the decreased protein surface expression level, not the total protein synthesis. Since the current amplitude cannot be reproduced during the 5 minute agonist application intervals, disruption at this residue may affect the receptor stability at the cell membrane. Similar results were reported previously for $P2X_2$, $P2X_3$, $P2X_4$, $P2X_5$ and $P2X_6$ receptors where the lysine was substituted with alanine, and a significant internalization was shown for the $P2X_2$ receptor K366A mutant suggesting its importance for channel polarization at the cell surface (Chaumont *et al*, 2004). The positive charged lysine residue can be responsible for the binding of phosphate or other regulatory factors, and mutations at this residue may interrupt possible intracellular interactions. However, the previous alanine substitution at the Lys^{367} at $P2X_1$ showed dramatically reduced peak current amplitude and had no effect on surface receptor expression level compared to the wild type (Vial *et al*, 2006). This region could contribute to an important intracellular structure, and the alanine mutation could alter the local conformation and influence the function of the residues for channel gating. Together with the accelerated desensitization pattern observed at K367C, this residue may be involved in the channel responses via both gating maintenance and surface expression.

In addition to the conserved lysine, Tyr^{363} is important for P2X receptor expression. The ATP evoked response was almost abolished at the Y363C mutant, whereas the surface expression revealed by biotinylation remained the same as the wild type receptor. This is consistent with the previous study at the Y363F and Y363A mutants at $P2X_1$ (Toth-Zsamboki *et al*, 2002) and $P2X_2$ receptor (Chaumont *et al*, 2004). The Y363C also showed a faster desensitizing response and suggested its fundamental role in channel gating. Previous studies demonstrated the reduced protein expression levels at alanine mutations to equivalent residues at $P2X_3$, $P2X_4$ and $P2X_5$ subunits (Chaumont *et al*, 2004). Thus the tyrosine residue could also contribute to both gating and receptor expression. Alternatively, the substitution variation may result from the affected local environment via cysteine substitution.

Reduced surface but not the total expression was also observed at the cysteine substitution at Tyr^{362} adjacent to the conserved Tyr^{363}. Similar to the previous study (Toth-Zsamboki *et al*, 2002), mutation at this residue led to a significant reduced

response. This residue was thus considered important for channel expression. The two neighboring tyrosines may contribute to this proposed protein trafficking motif together with the separated lysine for P2X$_1$ receptor. Chaumont *et al* suggested the regulation at the YXXXK motif could be via a direct interaction. These tyrosines could be potential regulation sites for tyrosine kinase, however, no detectable tyrosine phosphorylation were observed (Toth-Zsamboki *et al*, 2002). Therefore these two residues were suggested to be structural and the underlying regulatory mechanism still remained to be investigated.

Residues around this YXXXK region, such as the Lys^{359}, Arg^{360}, His^{361}, Tyr^{362} and Phe^{368}, exhibited reduced peak amplitudes where the total and surface protein expression levels were unaffected. These decreased responses may be due to the conformational change caused by mutations round the YXXXK motif, and the P2X$_1$ channels tend to open reluctantly following these modifications. In addition to the structural roles, for the Lys^{359}, Arg^{360}, His^{361} that locate close to the TM2 domain, they may have roles in channel gating properties. However, the "X" residues Glu^{365} and Lys^{366} inside of the YXXXK motif showed no effect to the cysteine substitutions, and were indicated to be non-essential. K364C displayed a slight shift in ATP potency and suggested a possible role in channel gating of Lys^{364}.

6.3.2 Other residues contribute to channel gating and expression

Modifications to the residues close to the second transmembrane segment showed significant changes to the P2X$_1$ receptor basic properties as well. Most of the residues in this region from His^{355} to His^{361} exhibited reduced peak amplitudes (4/7) and no reduction in protein expression could be detected. These results indicated a sensitive structure for the C-terminal region close to TM2. Minor disruptions within this segment may cause subsequent channel conformation changes subject to the alteration in residue local environment. This region could contribute to a compact organized structure, and regulate the channel gating by interacting with the TM2 or the amino terminus where close to the TM1.

Almost 1/3 of the 100 μM ATP evoked response was removed at the H355C mutant, and an ATP potency shift (20% of the maximum response to 1 μM ATP) was observed. His^{355} posited just next to the channel pore, and cysteine substitution at this residue may

cause structure shift and subsequently ion influx blockage. H355A was previously studied and showed a reduction in peak current amplitude (Vial *et al*, 2006). The alanine replacement at this residue also exhibited increased channel rectification and removal of voltage dependence of the time-course of receptor desensitization. Thus the histidine located next to the TM2 therefore may be essential for the ion permeation and channel desentisation properties.

A prolonged time-course of response was demonstrated at L357C of almost 5 fold slower as measured in oocytes. By contrast, the R360C that only is separated from the Leu^{357} by two amino acids exhibited a faster desensitization period of 2 fold than wild type. A similar pattern was also reported in the amino terminus study (See chapter 5), where the residues Asp^{17} and Val^{22} showed significantly prolonged and speeded desensitization phenotypes to cysteine substitutions that are located close to each other. These Leu^{357} and Arg^{360} residues may also contribute to a region for basic channel opening maintaining.

Phenylalanine substitution at Tyr^{370} produced a non-functional channel at P2X$_1$ receptors as reported previously (Toth-Zsamboki *et al*, 2002). However, the current data demonstrated the cysteine substitution at this residue exhibited similar ATP evoked current amplitude and agonist sensitivity level to WT P2X$_1$ receptor. The effects of the Tyr^{370} mutant are subject to substitutions and indicated this residue may not be essential. A slower decay time of response was also observed at Y370C in the study at oocytes, whereas this prolonged time-course was showed to be no different to WT receptor when expressed in HEK293 cells.

6.3.3 Effects of MTSEA on the C-terminus

Membrane permeant MTSEA evoked potentiation at eight and inhibitions to two out of the sixteen mutants; however, none of these were irreversible. This suggested the MTSEA did not bind covalently to these residues, and the effects could be due to the local environment changing. Reversible effects of MTS compounds were also observed for P2X$_4$ receptors following 5-10 minutes washout (Roberts *et al*, 2008). The P2X$_4$ receptor showed an agonist induced trafficking pattern (Bobanovic *et al*, 2002), and the washout potentiation was suggested to be a result of either irreversibly modifying or un-modified receptor were being trafficked to the cell surface during the washout period

(Roberts *et al*, 2008). Furthermore, no changes were induced by MTSEA for the time-course of responses for all mutants. Almost all of the residues close to the TM2 showed significant potentiation effects to the MTSEA application. This suggested a structure that is sensitive to modification at this region, and any small change in this region lead to increasing channel current. Residues that showed inhibitory effects to MTSEA modification are located after the YXXXK motif. The positively charged Lys[369] and potential tyrosine regulatory site Tyr[370] may comprise a modification site. In contrast to the N-terminal mutants (Y16C, V29C, G30C) these effects can be washed out after 5 minutes in the bath, the roles of these residues are still not clear.

6.3.4 Roles of Arg[360] in channel regulation

Arg[360] was found to be especially sensitive to MTSEA modifications, and showed over 7 fold potentiation. However, this effect was reversed immediately after 5 minutes washout in the bath. It was therefore suggested to be a transient effect caused by the environment changing which associate with the MTSEA compound. The MTSEA may alternatively bind to other intracellular site, e.g. accessory regulatory proteins. The regulatory sites for accessory protein may be uncovered due to the cysteine replacement at Arg[360], and thus the regulatory protein combine MTSEA to act on the P2X$_1$ receptor to potentiation. The striking potentiation was further suggested to be relevant to the concentration of MTSEA in use. An interesting finding is cysteine substitution at this residue caused a rightward shift of ATP potency, however, the ATP sensitivity can be recovered due to the MTSEA induced effect. Removal of the positive charge at this arginine residue caused a reduced peak amplitude and sharp channel decay period. However, the MTSEA replaces the positive charge and can recover the ATP induced current amplitude suggesting positive charge at this position is essential for channel gating. The extracelluar arginines at P2X receptors play roles in ligand binding due to its positive charge (Ennion *et al*, 2000). The intracellular arginine residue at the amino terminus also partly comprises in a potential PKC modification site for phosphate recognition (Boue-Grabot *et al*, 2000). Therefore, this residue may also have role in intracellular regulatory factor binding, or contribute to a sensor for the intracellular environment to channel properties.

6.3.5 Conclusion

It was the first time that 16 individual residues after the TM2 region were studied by cystine substitution and combined MTSEA characterization and some findings were summarized as follows. This study suggested the C-terminal contributes to a sensitive delicate structure for regulation as little change in the regions close to the transmembrane domain may lead to significant changes to channel properties. The proposed protein trafficking motif was studied, and the conserved Tyr^{363} and Lys^{367} contribute to both surface protein expression and channel gating properties. In addition, the Tyr^{362} may contribute to this protein trafficking regulation together combined with the Tyr^{363} at $P2X_1$ receptor. Furthermore, the intracellular Arg^{360} could be a regulatory region for intracellular signaling.

In general the C-terminal of $P2X_1$ receptor comprises a relatively tight intracellular structure, and play important roles in the maintaining of basic properties. This study provides a basis for the roles of C-terminal residues in $P2X_1$ receptor regulation in the following study.

6.4 Appendix: Site-directed mutagenesis on the C-terminus

16 amino acids (from His[355] to Lys[370]) on the C-terminus of the human $P2X_1$ receptor contained in the pcDNA 3.0 vector were converted to cysteine individually. The point mutations were introduced using the QuickChange Mutagenesis Kit (Stratagene, La Jolla, CA), and setting up of the reactions and cycling parameters for the mutagenesis were the same as described previously. Primers for the 16 amino acids were listed in table 6.1

The sequences of the cysteine mutants were checked by sequencing (PNACL sequencing service, Leicester University), and primers for whole length sequencing were designed as listed in table 5.2.

Primers	Sequences of the Primers	Conversion
H355C FWD	5'- T GAC CTG CTG CTG CTT TGC ATC CTG CCT AAG AGG -3'	H→C
H355C REV	5'- CCT CTT AGG CAG GAT GCA AAG CAG CAG CAG GTC A -3'	H→C
I356C FWD	5'- C CTG CTG CTG CTT CAC TGC CTG CCT AAG AGG CA -3'	I→C
I356C REV	5'- TG CCT CTT AGG CAG GCA GTG AAG CAG CAG CAG G -3'	I→C
L357C FWD	5'- C CTG CTG CTG CTT CAC ATCTGT CCT AAG AGG CAC TA -3'	L→C
L357C REV	5'- TA GTG CCT CTT AGG ACA GAT GTG AAG CAG CAG CAG G -3'	L→C
P358C FWD	5'- C CTG CTG CTG CTT CAC ATC CTG TGT AAG AGG CA -3'	P→C
P358C REV	5'- TG CCT CTT ACA CAG GAT GTG AAG CAG CAG CAG G-3'	P→C
K359C FWD	5'- G CTG CTG CTT CAC ATC CTG CCT TGC AGG CAC TAC TAC -3'	K→C
K359C REV	5'- GTA GTA GTG CCT GCA AGG CAG GAT GTG AAG CAG CAG C-3'	K→C
R360C FWD	5'- G CTT CAC ATC CTG CCT AAG TGC CAC TAC TAC AAG CAG -3'	R→C
R360C REV	5'- CTG CTT GTA GTA GTG GCA CTT AGG CAG GAT GTG AAG C -3'	R→C
H361C FWD	5'- G CTT CAC ATC CTG CCT AAG AGG TGC TAC TAC AAG CAG-3'	H→C
H361C REV	5'- CTG CTT GTA GTA GCA CCT CTT AGG CAG GAT GTG AAG C-3'	H→C
Y362C FWD	5'- C CTG CCT AAG AGG CAC TGC TAC AAG CAG AAG -3'	Y→C
Y362C REV	5'- CTT CTG CTT GTA GCA GTG CCT CTT AGG CAG G-3'	Y→C
Y363C FWD	5'- G CCT AAG AGG CAC TAC TGC AAG CAG AAG AAG TTC -3'	Y→C
Y363C REV	5'- GAA CTT CTT CTG CTT GCA GTA GTG CCT CTT AGG C -3'	Y→C
K364C FWD	5'- C CTG CCT AAG AGG CACT AC TAC TGC CAG AAG AAG TTC -3'	K→C
K364C REV	5'- GAA CTT CTT CTG GCA GTA GTA GTG CCT CTT AGG CAG G -3'	K→C
Q365C FWD	5'- AG AGG CAC TAC TAC AAG TGC AAG AAG TTC AAA TAC GCT G -3'	Q→C
Q365C REV	5'- C AGC GTA TTT GAA CTT CTT GCA CTT GTA GTA GTG CCT CT-3'	Q→C
K366C FWD	5'- C TAC AAG CAGTGC AAG TTC AAA TAC GCT GAG GAC ATG G-3'	K→C
K366C REV	5'- C CAT GTC CTC AGC GTA TTT GAA CTT GCA CTG CTT GTA G-3'	K→C
K367C FWD	5'- C TAC AAG CAG AAG TGC TTC AAA TAC GCT GAG GAC ATG G-3'	K→C
K367C REV	5'- C CAT GTC CTC AGC GTA TTT GAA GCA CTT CTG CTT GTA G -3'	K→C
F368C FWD	5'- AAG CAG AAG AAG TGC AAA TAC GCT GAG GAC ATG G-3'	F→C
F368C REV	5'- C CAT GTC CTC AGC GTA TTT GCA CTT CTT CTG CTT-3'	F→C
K369C FWD	5'- C TAC AAG CAG AAG AAG TTC TGT TAC GCT GAG GAC ATG GGG CC-3'	K→C
K369C REV	5'- GG CCC CAT GTC CTC AGC GTA ACA GAA CTT CTT CTG CTT GTA G-3'	K→C
Y370C FWD	5'- AG AAG AAG TTC AAA TGC GCT GAG GAC ATG GGG CC-3'	Y→C
Y370C REV	5'- GG CCC CAT GTC CTC AGC GCA TTT GAA CTT CTT CT-3'	Y→C

Table6.1 Sequences of the primers used for cysteine mutagenesis reactions on the C-terminus of P2X$_1$ receptor.

Site-directed mutagenesis reactions were performed on the human P2X$_1$ receptor to convert the single residues from His[355] to Lys[370] to be cysteine individually. Primers for the mutagenesis reactions are listed. The mutated base pairs are indicated in red and underlined, and the conversions of amino acids are shown in the table.

Chapter 7. The roles of the intracellular termini in P2X$_1$ receptor regulation

7.1 Introduction
7.1.1 Regulation roles of intracellular domains

P2X receptors are involved in diverse physiological roles including the neuronal control of smooth muscle contraction, platelet thrombi formation, pain sensation, and immune responses (Vial *et al*, 2002a; Mulryan *et al*, 2000; Calvert *et al*, 2004; Souslova *et al*, 2000; Solle *et al*, 2001). The contribution of intracellular signaling to P2X receptors regulation has been described (Chow *et al*, 1998; Boue-Grabot *et al*, 2000; Paukert *et al*, 2001). Among all of the possible intracellular modulations, protein phosphorylation is believed to be significant in a wide range of cellular processes. Protein kinases are targeted specifically to the serine/threonine (for example, protein kinase A and protein kinase C) or tyrosine residues (protein tyrosine kinases, PTK).

There are a few potential regions of the P2X receptor that contribute to the intracellular regulation mechanism. On the amino terminus, there is a highly conserved PKC motif (Thr-Xaa-[Arg/Lys]). Disruption of this PKC motif in the P2X gene led to faster desensitization and reduced amplitude of the response to ATP (Ennion *et al*, 2002a; Boue-Grabot *et al*, 2000). Specific monoclonal antibodies against the phosphothreonine-proline motif were used to determine phosphorylation at the P2X$_1$ receptor PKC site (Liu *et al*, 2003). Immunoblotting results indicated the presence of phosphorylation at WT subunit but not the mutant with disrupted PKC site. Hence, the phosphorylation at the threonine of PKC consensus sequence was suggested to be constitutive.

A study at P2X$_3$ receptors also showed the importance of the threonine in the consensus PKC site (Paukert *et al*, 2001). All of the threonines and serines at the amino terminus of the P2X$_3$ receptor were disrupted individually, and only T12A (corresponding to Thr^{18} for P2X$_1$ receptor) showed abolished peak current. However, the T12E mutant mimicking the constitutive phosphorylation also gave non-measurable currents suggesting that not just the presence of negative charge at this position is important. The neuropeptides substance P and bradykinin can potentiate the peak amplitudes of the

P2X$_{2/3}$ channel, and this effect can be mimicked by phorbol ester which acts via the PKC pathway. Therefore the completely conserved threonine was suggested to be the best candidate for the phosphorylation regulation at P2X$_3$ receptor by inflammatory mediators.

At the carboxy terminus of P2X receptors, there are conserved 3 threonines and 3 tyrosines that may also contribute to regulation by phosphorylation (Vial *et al*, 2004a). The carboxy terminus of the P2X$_2$ receptor was suggested to be regulated by PKA (Chow *et al*, 1998). When the PKA activators 8-Br-cAMP and purified PKA catalytic subunit were internally perfused to the HEK293 cells expressing the WT P2X$_2$ receptor, reduced ATP peak amplitudes were observed. However, cysteine substitution at the carboxy terminus Ser[431] showed unaffected currents to PKA activator treatments. Hence, the phosphyorylation at residue Ser[431] should be required for the basal signaling regulation of P2X$_2$ receptor.

The P2X receptor carboxy terminus was previously demonstrated to have important roles in interactions with other receptors. For example the P2X$_2$ receptor and GABA receptors are co-localized in central synapses, and inhibitory effects can be observed after their co-activation (Boue-Grabot *et al*, 2004). It is interesting that the P2X$_2$ receptor current can be inhibited by the α,β-subunits or α,β,γ-subunits containing GABA$_A$ receptors, whereas the responses of γ-subunit containing GABA$_A$ receptor cannot be inhibited by the P2X$_2$ receptor. To identify the roles of the intracellular domains in this modulation, minigenes encoding the intracellular terminus fragment of P2X$_2$ receptor were generated and co-expressed with the WT receptors. The over-expressed C-terminus minigene as an interfering factor blocked the cross-talk between P2X$_2$ receptors and GABA$_A$ receptors, and the inhibitory effect of the GABA$_A$ receptors on P2X$_2$ receptors was removed. Therefore, the P2X$_2$ receptors C-terminal should contribute to this GABA$_A$ receptors induced inhibitory modulation pathway. In addition, the function of the P2X$_3$ receptors can also be regulated by GABA$_A$ receptors, and a C-terminal motif was identified (Toulme *et al*, 2007). When the P2X$_3$ receptor and the GABA$_A$ receptor were co-activated, the evoked inward current was significantly smaller than the predicted current corresponding to the sum of the individual currents. The responsible region for this regulation was first identified by generating a range of truncated P2X$_3$ receptors at different C-terminal positions. When the truncations took

place before the Thr^{388} the inhibitory effect from the GABA$_A$ receptor was absent, and indicated the distal part of the P2X$_3$ receptor C-terminal plays a predominant role in the functional interaction with the GABA$_A$ receptors. The specific residue(s) involved in this interaction was further investigated by introducing alanine substitutions from Lys^{385} to Gly^{391}. As a result the substitutions at Glu^{386}, Ser^{387} and Thr^{388} gave rise to a significant reduction of the GABA induced inhibitory effects to the peak current amplitudes of P2X$_3$ receptor. Hence, the QST$^{368-388}$ was proposed to be an important C-terminal motif for the cross-inhibition regulation via GABA receptors. The carboxy terminal of P2X$_2$ receptors was also suggested to be responsible for the inhibitory cross-talk with the 5-HT$_3$ receptor (Boue-Grabot *et al*, 2003). The coactivation of P2X$_2$ and 5-HT$_3$ receptor led to inward currents of only 47-73% of the predicted sum in neurons, *Xenopus* oocytes and HEK293 cell heterologous systems. However, this inhibitory cross-talk between these two receptors was disrupted when the intracellular C-terminal was truncated from the P2X$_2$ receptor. Over-expression of the P2X$_2$ receptor C-terminus minigene can also remove this 5-HT$_3$ induced inhibition. Thus the P2X receptors carboxy terminus was considered to be a potential regulatory or docking region for intracellular signaling.

7.1.2 Phosphorylation Pathway of GPCRs

P2X receptors are subject to regulation by G-protein coupled receptors (GPCRs) which are usually naturally co-expressed with P2X receptors in a range of tissues (Vial *et al*, 2004a; Ralevic *et al*, 1998; Kunapuli *et al*, 2003). For example, P2X$_1$ receptor are co-expressed with ADP-sensitive P2Y$_1$ receptor in the human platelets (Kunapuli *et al*, 2003) and with ATP/UTP-sensitive P2X$_2$ receptor in arterial smooth muscle (Ralevic *et al*, 1998). It raises the possibility that the P2X$_1$ receptor function can be regulated by GPCRs Gαq subunit related intracellular PLC (phospholipase C) signal transmission pathway (See figure 7.1). When Gq protein coupled receptors were co-expressed with P2X$_1$ receptors on *Xenopus* oocytes, the GqPCRs could be activated by its agonist, and the GTP-alpha subunit of G-protein will activate the membrane-bound enzyme phospholipase C (PLC) which breaks down inositol phospholipid phosphatidylinositol 4,5-bisphosphate (PI(4,5)P$_2$) into diacylglycerol (DAG) (Elliott, 2005). DAG activates a range of protein kinases which may subsequently bring about phosphorylation and regulate the nearby P2X$_1$ receptors. The first evidence for a regulatory role of GPCRs came from the study of vascular P2X$_1$ receptors in rabbit ear arteries (La *et al*, 1993),

where the fast P2X-like responses were potentiated following the stimulation of endothelin-1 receptor. As suggested by a previous study, the calcium currents triggered by α,β-meATP and ADP together for co-stimulating the $P2X_1$ and $P2Y_1$ receptors on human platelets are faster and greater than the sum of those evoked by either agonist alone (Kunapuli *et al*, 2003). When the $P2X_1$ receptor was co-expressed with the Gαq-mediated mGluR1α, $P2Y_1$ and $P2Y_2$ receptors, activation of GPCRs potentiated $P2X_1$ currents by 250% (Vial *et al*, 2004a). Over 90% of the potentiation effect was abolished by the PLC inhibitor U-73122. Ase's study of the vascoactive mediator 5-HT_{2A} (5-hyroxytryptamine) receptor exhibited similar potentiation effects to the $P2X_1$ receptor, which can also be blocked by the PLC inhibitor in arteries. Therefore, the DAG pathway was suggested to be important for the GqPCRs signaling to $P2X_1$ receptor.
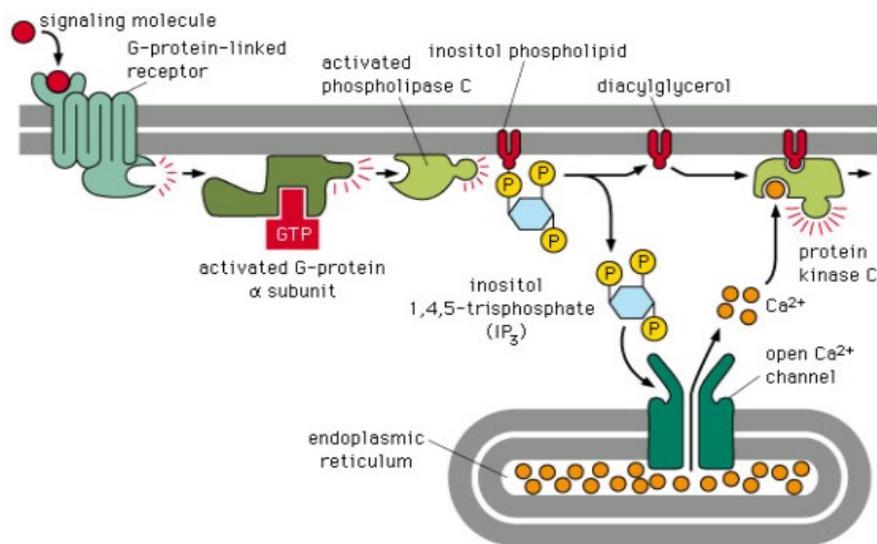
Figure 7.1 Schematic of the GPCRs signaling pathway.
Following the activation of GPCRs, the plasma membrane bound phospholipase C is stimulated via G-protein. The $PI(4,5)P_2$ present at the inner half of the plasma membrane lipid bilayer is hydrolyzed and split into IP3 and diacylglycerol after the activation of phospholipase C. IP3 diffuses through the cytosol and releases calcium from the endoplasmic reticulm; while the diacylglycerol remains in the cell membrane and helps to activate the protein kinase C.(Taken from Elliott *et al*, 2005)

The protein kinase C family can be characterized into three major types (conventional, novel and atypical) that depend on their calcium and DAG requirement for activation. A previous study (Vial *et al*, 2004a) demonstrated that GPCRs and phorbol ester-mediated potentiation was unaffected with the BAPTA/AM (bis (*o*-aminophenoxy) ethane-*N, N, N′, N′*-tetra-acetic acid tetrakis-(acetoxymethyl ester)) and Ro-32043. BAPTA/AM is a potent intracellular calcium chelator with over a hundred times greater affinity for

calcium than magnesium and the Ro-32043 is a PKC inhibitor specific for the conventional PKCs which require calcium for activation. These results suggested that phorbol ester and GPCRs regulate the $P2X_1$ receptor through the calcium-insensitive PKC isoforms, and the novel PKCs that require DAG but not calcium for activation are possibly involved.

Intracellular regulation was further suggested to be independent of phosphorylation at the consensus PKC site, as potentiation was still seen when the conserved threonine residue was mutated (Vial *et al*, 2004a). To study whether any direct phosphorylation to the intracellular domain is involved in the $P2X_1$ receptor modulation, the WT $P2X_1$ receptors were expressed in HEK cells (Vial *et al*, 2004a). $[P^{32}]$ orthophosphate was used to radiolabel phosphorylated $P2X_1$ receptors, however, PMA treatment had no detectable effect to the $P2X_1$ receptor basal phosphorylation level. This implicated that $P2X_1$ regulation is more likely regulated by a phosphorylation of interacting proteins which interact with the intracellular terminus of the receptor.

Vial further suggested that $P2X_1$ receptors were not regulated by direct channel phosphorylation (Vial *et al*, 2004a). In order to investigate the regulation mechanism of the intracellular domains, phorbol ester PMA (phorbol-12-myristate-13-acetate) and kinase inhibitors were applied to oocytes expressing the $P2X_1$ receptor. PMA stimulates kinase and mimics the DAG pathway. After the 5 minutes application of PMA, the response of $P2X_1$ receptor was doubled (See figure 7.2), which showed that the activity of the $P2X_1$ receptor was increased by the regulation DAG pathway. However, when the oocytes were pre-treated with the broad-spectrum kinase inhibitor staurosporine, the potentiation evoked by PMA was abolished (See figure 7.2).   These results indicated that following the activation of Gαq, $P2X_1$ receptors can be regulated by the staurosporine-sensitive pathway. The specific protein kinases that are responsible for this regulation are still remained to be further identified.
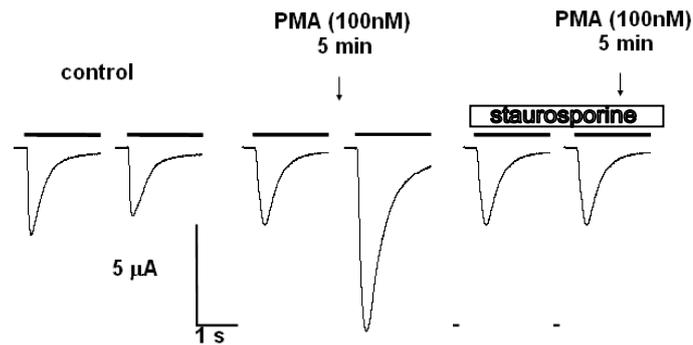
Figure 7.2 P2X₁ potentiation involves activation of kinase.
The left hand panel shows the control. PMA treatment of oocytes expressing $P2X_1$ receptor alone potentiated a $P2X_1$ response to ATP. PMA works as a secondary messenger in the PLC pathway. The potentiation was abolished in the presence of the broad-spectrum protein kinase inhibitor staurosporine (taken from Vial *et al*, 2004a).

Although serine/threonine phosphorylation was considered to be common in ion channel modulation, protein tyrosine phosphorylation can also be involved. For instance, the consensus tyrosine site Tyr^{132} at the amino terminus of the delayed rectifier type potassium channel is essential for maximal channel suppression (Huang *et al*, 1993). The channel suppression level correlates to the extent of tyrosine phosphorylation under muscarinic stimulation as revealed by immunoprecipitation. To study the roles of tyrosine phosphorylation in $P2X_1$ receptor regulation, insulin as an activator was applied to the oocytes expressing $P2X_1$ receptors (Vial *et al*, 2004a). As a result, the ATP-evoked amplitudes were potentiated significantly, and the PTKs were suggested to be involved in $P2X_1$ receptor regulation. However, this regulation was considered to contribute to the basal regulation, since the tyrosine kinase inhibitor genistein reduced the peak response to ATP but had no effect to the potentiation from the co-expressed GPCRs. The roles of the intracellular tyrosines (Tyr^{16}, Tyr^{362}, Tyr^{363} and Tyr^{370}) at $P2X_1$ receptor were further investigated by site-directed mutagenesis (Toth-Zsamboki *et al*, 2002). Despite proper plasma membrane expression, the phenylalanine substitutions at these residues caused either significant reduction to peak amplitude currents or non-functional channels. However, the intracellular tyrosine phosphorylation was undetectable using the anti-phosphotyrosine antibody, and the roles of these tyrosines at $P2X_1$ receptor were suggested to be structural.

7.1.3 Aim

A range of intracellular regulation mechanisms of P2X receptors have been investigated as described, and the DAG pathway has been suggested to be important. To further explore the PKC regulation pathway and indentify the roles of individual intracellular residues or specific regions in control of the $P2X_1$ receptor, the roles of novel PKC isoforms that act on the $P2X_1$ receptor will be identified. Secondly, the minigene strategy will be used to study the contribution of the amino and carboxy terminus of $P2X_1$ receptor in the phorbol ester and GPCRs related regulations. The individual residues at the amino and carboxy temini were mutated to non-charged cysteines respectively by site-directed mutatgenesis and further studied with the PMA treatment and mGluR1α receptor co-expression. Some of these observations on the regulation of phorbol ester and mGluR1α receptors to the amino terminus of $P2X_1$ receptor have been published (Wen *et al*, 2009).

7.2 Results
7.2.1 Regulation mechanisms of PMA and GPCR to P2X$_1$ receptor

To obtain the maximum PMA effect, the optimal concentration required for this study was estimated firstly. The WT P2X$_1$ receptor was treated to 10 nM, 30 nM and 100 nM PMA respectively for 10 minutes before recording. The effects of PMA were concentration dependent, it had no effect at 10 nM, but potentiated the response to 55.45 ± 14.94% ($n=4$) at 30 nM and gave the maximum potentiation at 100 nM where the amplitude doubled (Figure 7.3, *p<0.05). Thus this concentration was used for the following studies.

For oocytes co-expressing P2X$_1$ and mGluR1α receptors ATP (100 μM, a maximal concentration) evoked transient inward currents that desensitized during the application of ATP. P2X$_1$ receptor currents were potentiated by 103.1 ± 11.8% ($n=19$) following 10 minutes pre-treatment with PMA (100 nM) (See figure 7.4). The protein kinases that contribute to the regulation of P2X$_1$ receptor by PMA and GPCRs were characterized using a series of PKC kinase inhibitors (See figure 7.4, ***p<0.001). None of these inhibitors had an effect on peak P2X$_1$ receptor current amplitude (-6420 ± 709 nA, $n=19$ for control; -6458 ± 773 nA, $n=11$ for Calphostin C; -6709 ± 1399 nA, $n=19$ for K252a; -8728 ± 1508 nA, $n=13$ for GÖ6983; -8499 ± 1015 nA, $n=8$ for GÖ6976) or time-course (changes to control was compared in percentage, -5 ± 28 %, $n=4$ for Calphostin C; 7 ± 14 %, $n=4$ for K252a; 44 ± 18 %, $n=4$ for GÖ6983 and 4 ± 24 %, $n=5$ for GÖ6976). Calphostin C (1 μM) acts by competing with the diacylglycerol and phorbol ester binding site of protein kinase C isoforms and reduced potentiation by PMA stimulation to 15.5 ± 13.9% ($n=11$). Potentiation was also reduced by the kinase inhibitor K252a (100 nM) (32.6 ± 10.0%, $n=19$). GÖ6983 is a kinase inhibitor at novel PKCs δ,ε,η,θ, but is ineffective at the novel isoform PKCμ (also called protein kinase D, PKD)(Martiny-Baron *et al*, 1993). Potentiation was reduced to -6.9 ± 12.4 % ($n=13$) by GÖ6983 (200nM) for PMA. GÖ6983 (200 nM) is an effective inhibitor of the novel calcium insensitive protein kinase C isoform PKCμ but is ineffective at the other calcium insensitive novel PKC isoforms (Gschwendt *et al*, 1996) and reduced PMA mediated poetntiation to -3.2 ± 11.4 %($n=8$).

A previous study at the TRPV1 channel suggested the protein kinase C induced phosphorylation can potentiate responses by increasing channel permeability (Chung *et*

al, 2008). To test whether the potentiation in current at the $P2X_1$ receptor following PMA treatment resulted from an increase in permeability, the channel permeability to ions were examined by reversal potential measurement. The cation permeabilities of the $P2X_1$ receptors were tested using a range of cation-containing bath including sodium, demithylamine, Tris and NMDG. Under control conditions when sodium was the only external cation, $P2X_1$ receptor currents reversed at -4.3 ± 1.1 mV ($n=3$) (Figure 7.5). As the size of the cations increased, the reversal potentials decreased to -10.2 ± 0.9 mV ($n=5$) for demithylamine, -47.67 ± 2.6 mV ($n=4$) for Tris to -95.4 ± 17.1 mV ($n=3$) for NMDG (See figure 7.5). This is consistent with previous studies, Evans *et al*, 1996). Since sodium is able to cross the $P2X_1$ channel freely, the demithlamine with a slightly reduced permeability was used to examine any PMA effect on channel pore dilation. Following 10 minutes PMA treatment, the reversal potential for dimethylamine was unaffected (-11.1 ± 1.9 mV, $n=8$) (See figure 7.5) and demonstrated the potentiation of $P2X_1$ receptor currents does not result from an increase in channel permeability.

The activation of mGluR1α receptors by 100 µM glutamate for 5 minutes evoked a transient inward calcium activated chloride current and potentiated the subsequent responses of WT $P2X_1$ receptors to ATP (100 µM) by 61.0 ± 3.9 % ($n=13$) (See figure 7.6). Co-expression with the mGluR1α receptors had no effect on the peak amplitudes and the time-course for the ATP-evoked $P2X_1$ receptor current. This is consistent with the previous studies on the $P2X_1$ receptor (Vial *et al*, 2004a). Significant inhibitory effects on the GPCRs regulated potentiation were observed with the treatment of PKC inhibitors (Calphostin C 1 µM 13.5 ± 2.8%, $n=5$; K252a 100 nM 20.3 ± 5.9%, $n=5$; GÖ6983 200 nM -2.8 ± 3.9%, $n=7$; GÖ6976 200 nM 27.6 ± 0.9%, $n=3$) (Figure 7.6, ***$p<0.001$), and the GÖ6983 showed maximum effect to the PMA mediated potentiation. These findings suggest the novel protein kinase C isoforms mediate $P2X_1$ receptor regulation by both PMA and GPCRs.

7.2.2 Use of minigenes to investigate the roles of the intracellular domains in channel regulation

To determine whether the intracellular domains play an essential role in the phorbol ester and GPCRs regulation pathway of $P2X_1$ receptor, minigenes encoding the sequence of either amino terminus or carboxy teriminus were generated by amplifying the corresponding sequences from WT $P2X_1$ receptors (Figure 7.7). Both of the intracellular domain minigene sequences are less than 200bp, and stop and start codons
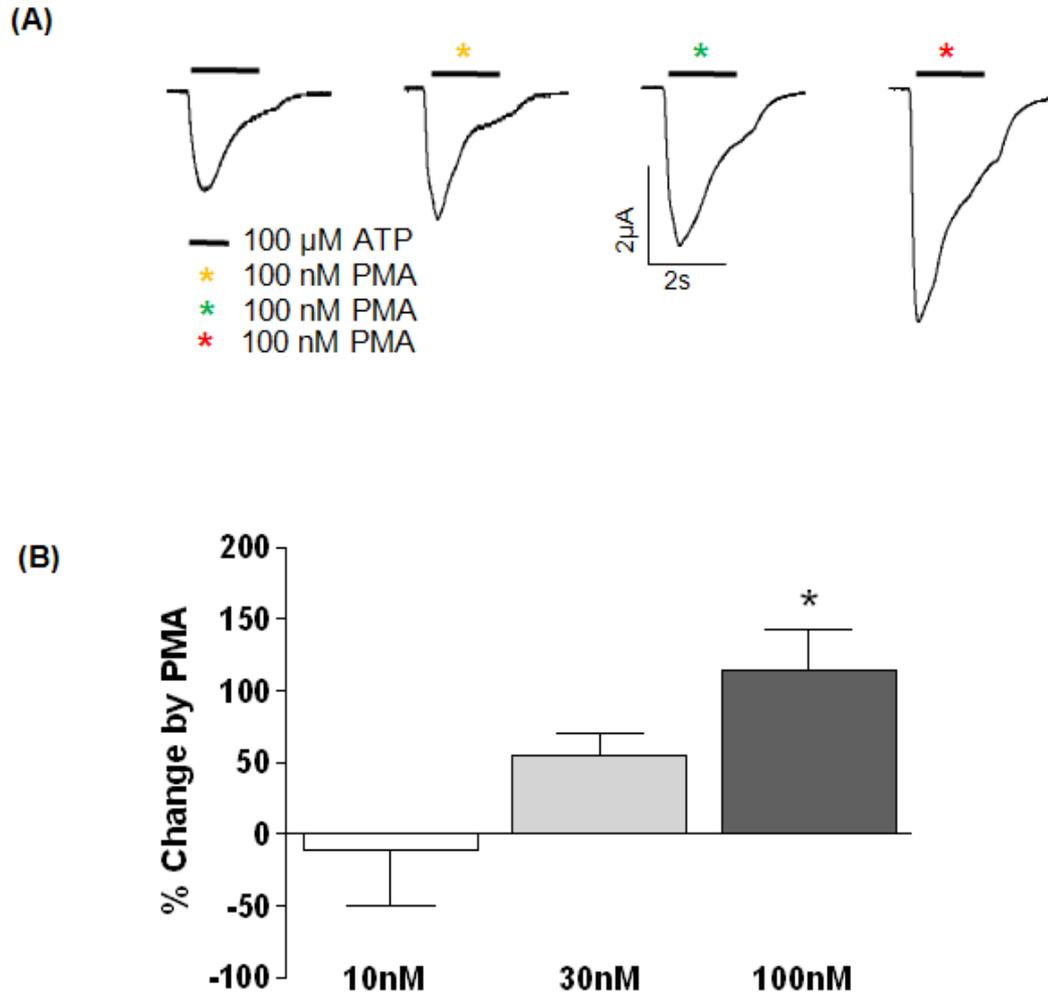
Figure7.3 Concentration dependent effects of PMA on P2X$_1$ receptor currents
(A). Representative traces of currents evoked by ATP(100 µM)   at   WT P2X$_1$ receptor under control conditions and following treatment with PMA (10 nM in yellow, 30 nM in green and 100 nM in red). **(B).** Summary of the effects of PMA potentiation, *n*=4-5.*p<0.05.
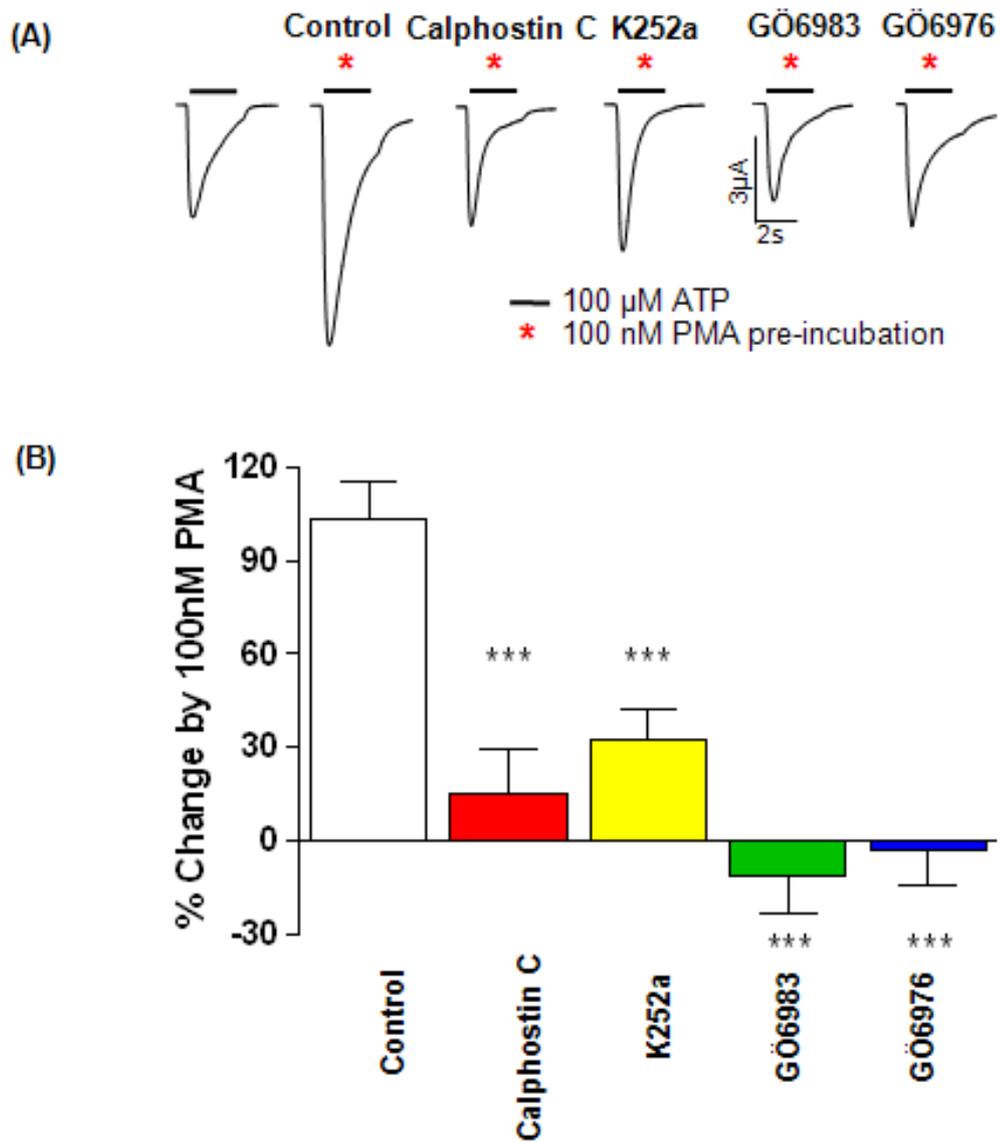
Figure7.4 Potentiation of P2X$_1$ receptor currents by PMA stimulation is sensitive to inhibitors of novel isoforms of protein kinase C

(A). Representative traces of currents evoked by ATP(100 µM) under control conditions (left) and following treatment with PMA (100 nM) following incubation with the PKC inhibitors (1 hr pre-incubation before 10 minutes of PMA, indicated by red asterisk) Calphostin C (1 µM), K252a (100 nM), GÖ6983 (200 nM) or GÖ6976 (200 nM). **(B).** Summary of the effects of the inhibitors on PMA potentiation, n=5-19.***p<0.001.

(A)

Ions	Reversal potential (mv)
Sodium	-4.28±1.07 (3)
Demithylamine	-10.15±0.86 (5)
Tris	-47.67±2.59 (4)
NMDG	-95.38±17.10 (3)

(B)

— 100 µM ATP
* 100 nM PMA pre-incubation

(C)
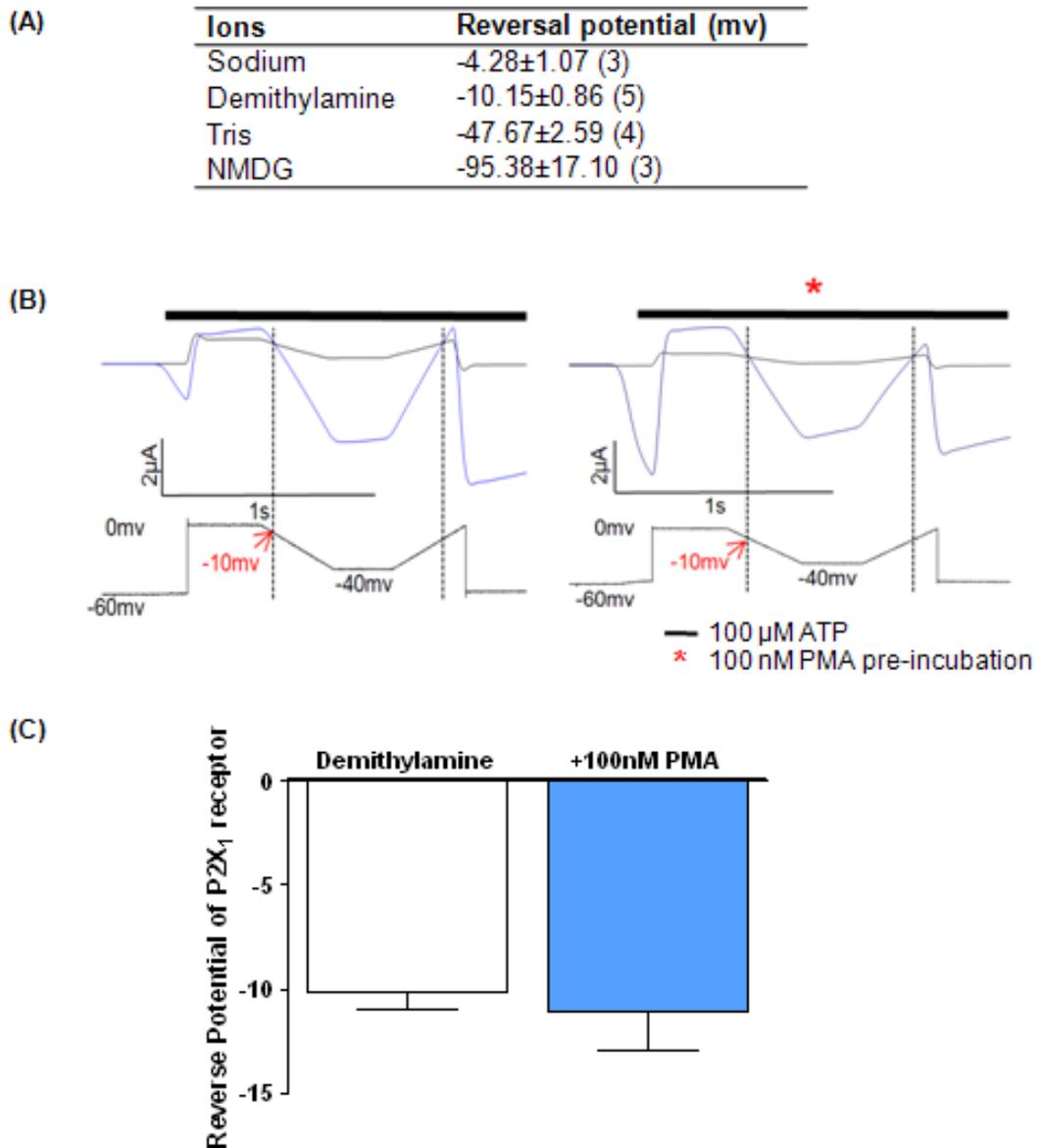
Figure7.5 Reversal potential measurement suggests that PMA did not potentiate the P2X$_1$ receptor via channel pore dilation

(**A**).Summary of the estimated reversal potentials for sodium, dimethylamine, Tris and NMDG at WT P2X$_1$ receptor, *n*=4-5. (**B**).Sample traces of the effects of PMA on dimethylamine permeability. Two ramps increase or decreased the holding potential from 0 to 40 mv around the predicated reversal potential (10-20 mV) for demithlamine. Application of ATP (100 µM) evoked P2X$_1$ receptor current meet the control condition at about 10mV (red) in demithylamine. PMA (100 nM pre-incubation for 10 minutes, indicated in red asterisk) treated P2X$_1$ receptor showed similar reversal potential level. (**C**). Summary of the effects, of PMA treatment to reversal potential of demithylamine at P2X$_1$ receptor, *n*=5-8.
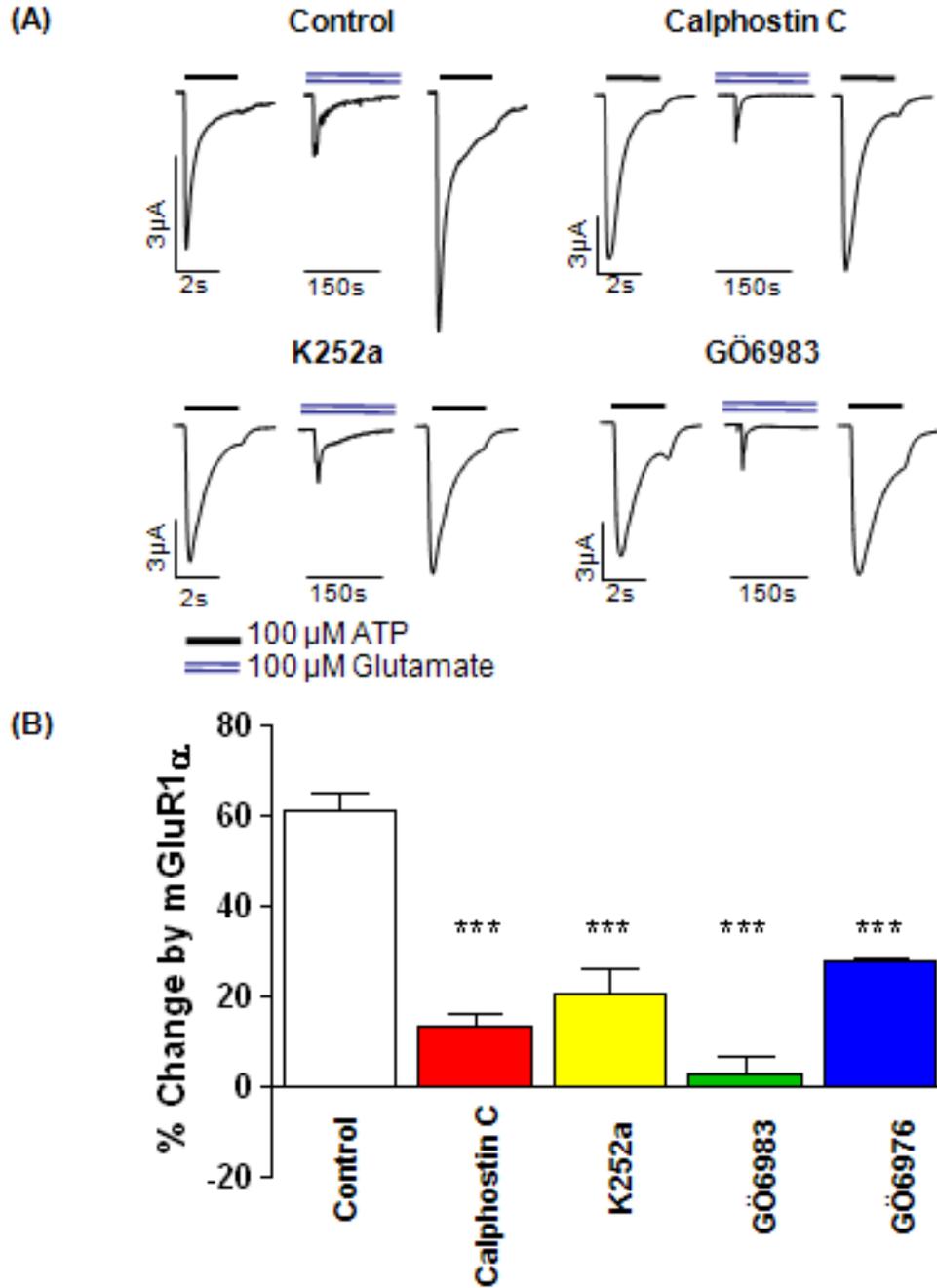
Figure 7.6 Potentiation of P2X₁ receptor currents by mGluR1α receptor stimulation is sensitive to inhibitors of novel isoforms of protein kinase C

(A). Representative traces of the effects of PKC inhibitors on mGluR1α mediated potentiation of P2X₁ receptor currents. Application of glutamate (100 µM, indicated by blue bar) evoked a transient inward calcium activated chloride current and potentiated the subsequent ATP current. Potentiation was reduced following pre-treatment of the oocytes with the PKC inhibitors Calphostin C (1 µM), K252a (100 nM), GÖ6983 (200 nM) or GÖ6976 (200 nM). **(B).** Summary of the effects, of the inhibitors on glutamate potentiation, *n*=3-13. ***p<0.001.

(A)

NH₂ minigene
```
1                              30
MARRFQEELAAFLFEYDTPRMVLVRNKKVG·
```

COOH minigene
```
353                                                    399
*LLHILPKRHYYKQKKFKYAEDMGPGAAERDLAATSSTLGLQENMRTS·
```

(B)

(C)

Stop codon   Start codon
3'TGC   CAT 5'
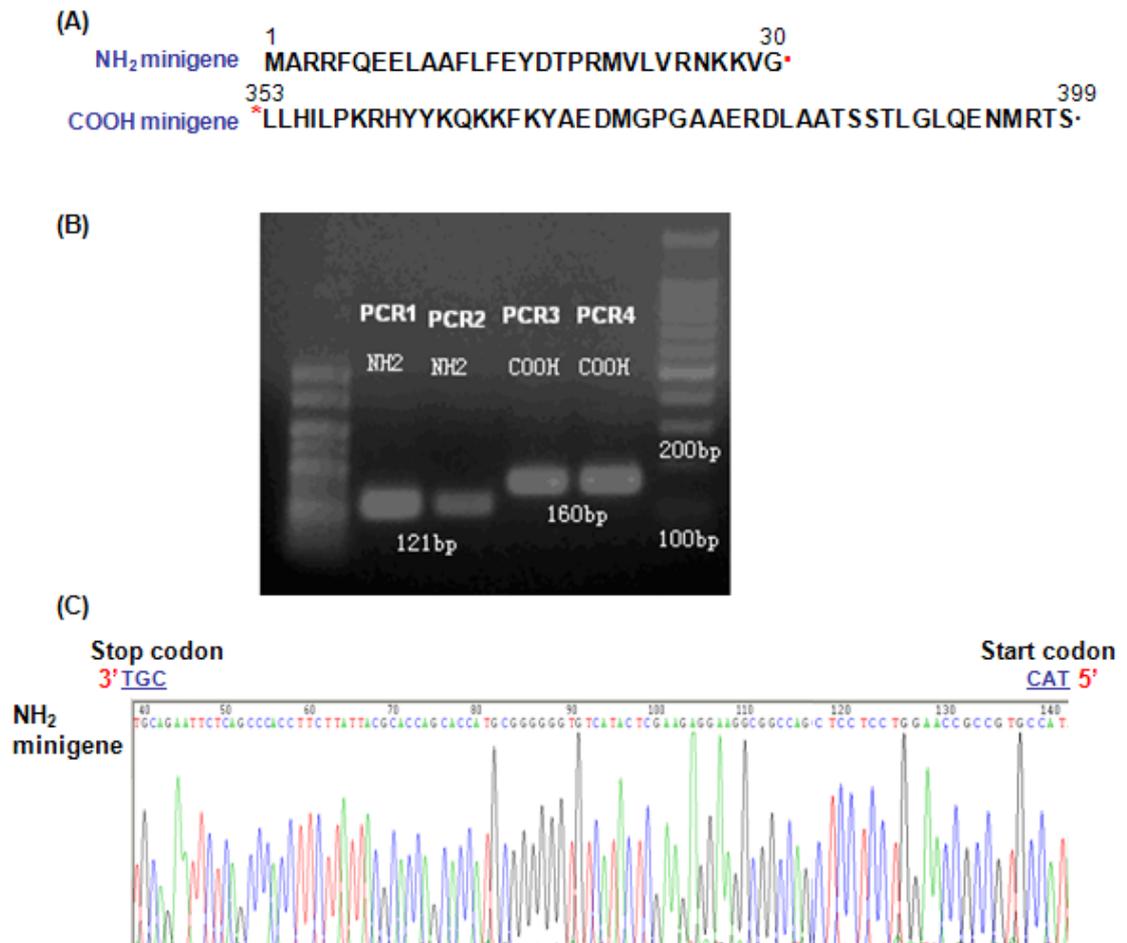
NH₂ minigene

Figure7.7 N-terminal and C-terminal minigenes were generated by PCR
(A). The NH₂ and COOH minigenes encoding the sequence of P2X₁ receptor amino and carboxy termini. Stop (red dot) and start (red asterisk) codons were added to the ends respectively. **(B).** The sequences of minigenes were generated by PCR and the sizes of them were visualized on a DNA gel. **(C).** Example sequencing figure of amino terminus minigene from Chromas and no mutation was found in the NH₂ minigene sequence. Four different bases were labeled in different colours (A is green, T is red, C is blue and G is black).Since the sequencing was preformed with reverse primer, the start codon and stop codon was shown as CAT and TCA respectively.

were added to the end or the beginning of amino and carboxy terminus minigenes respectively. The sequences of the minigenes were verified by sequencing (Figure 7.7). These minigenes were used as interfering factors and over-expressed with the WT P2X$_1$ receptor to look at the modulation roles of the intracellular domains. For example, if the phorbol ester or the GPCRs mediated effects at the WT P2X$_1$ receptor can be reduced by any minigene sequence, the interactions between the corresponding intracellular terminus and the accessory protein should be blocked. In this case, the corresponding intracellular terminus would be suggested to contribute to this receptor modulation. (See figure 7.8).
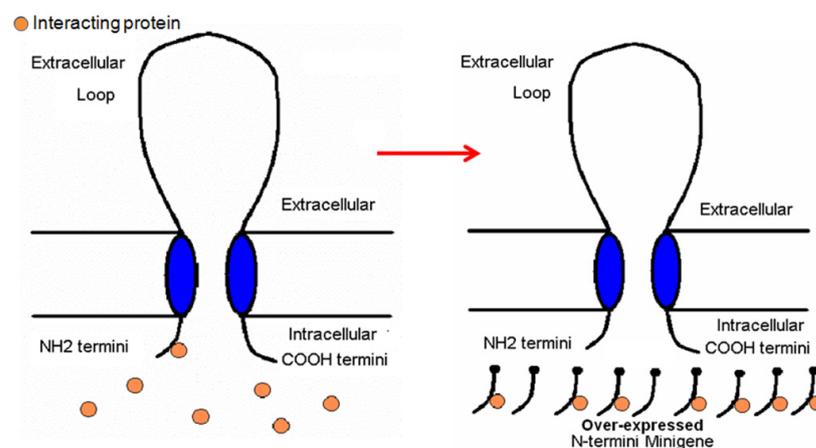
Figure 7.8 The schematic of adding N-terminus to the cell with wild type P2X$_1$.
The N-terminus or C-terminus minigene will be co-expressed with the whole length P2X$_1$receptors to the *Xenopus* oocytes. The quantity of minigene should be much more than the receptors. We predict that the minigenes will reduce the normal signal transduction of the wild type P2X channel.

The full length WT P2X$_1$ receptor was co-expressed with mGluR1α receptors and either P2X$_1$ receptor intracellular minigenes at a ratio of 1:2:7, and the minigene effects were tested by electrophysiological recording after expression in *Xenopus* oocytes. Both of the P2X$_1$ receptor minigenes expression showed no effects on the P2X$_1$ receptor currents (peak current amplitudes to 100 µM ATP of -6875 ± 298 nA, *n=6* for control, -6302 ± 304 nA, *n=7* for amino terminus minigene and -6959 ± 626 nA, *n=7* for carboxy terminus minigene co-expression), or the amplitude of glutamate evoked chloride currents (to 100 µM glutamate of -4996 ± 807 nA, *n=6* for control, -4155 ± 1233 nA, *n=7* for amino terminus minigene and -5511 ± 1178 nA, *n=7* for carboxy terminus minigene co-expression) demonstrating that the minigene does not regulate P2X$_1$ or mGluR1α receptor expression or activation. However co-expression of intracellular terminal minigenes reduced potentiation by PMA from 128.5 ± 12.6%, *n=6*

to 25.8 ± 2.6 %, *n=7* (for amino terminus minigene) and -24.9 ± 7.1 %, *n=6* (for carboxy terminal minigene) respectively (See figure 7.9, ***p<0.001). The over-expressed intracellular minigenes reduced the mGluR1α induced potentiation from 52.5 ± 3.1 % (*n=6*) to 28.3 ± 3.3 % (*n=7*, for amino terminus minigene) and 30.1 ± 2.2% (*n=7*, for carboxy terminus minigene) which is consistent to the observation for PMA effects (See figure 7.10, ***p<0.001). The above results suggest that intracellular termini are important in regulation and that the minigene may work by sequestering regulatory factors associated with the receptor. Compared to the amino terminus, the carboxy terminus of P2X$_1$ receptor may be more involved in the PMA regulation mechanism.

7.2.3 The roles of N-terminus to P2X$_1$ receptor regulation

To identify the intracellular residues involved in the PMA and GPCRs regulation pathway, the effects of PMA treatment and mGluR1α receptor were tested on mutants with cysteine substitutions at the amino and carboxy terminus respectively. The effects of the cysteine replacement have been characterized in chapter 5.

The potentiation ratio by 100nM PMA to WT P2X$_1$ receptor varies at different expression levels. To estimate the potentiation ratio induced by PMA treatment, the peak current amplitudes were required to be standardized. The peak amplitudes evoked by ATP were determined by the RNA injected, and the maximum peak current can be obtained when 50ng was injected per oocyte. There is no significant difference between two different batches oocytes (-10494 ± 1016 nA, *n=4* and -9466 ± 1221 nA, *n=6*) (See figure 7.11). The potentiation ratio for WT and the amino terminus mutants were summarized in figure 7.11B, and a trend of higher peak amplitudes exhibiting lower potentiation ratio was observed (See figure 7.11). Consequently, to gain the optimum potentiation effect, the peak current amplitudes of the P2X$_1$ receptor mutants without PMA treatment were to be no more than -7000 nA.

The effects of PMA to amino terminus mutants were summarized in figure 7.12. WT P2X$_1$ receptors were potentiated by 116.5 ± 14.5% (*n=11*) following 10 minutes application of PMA. A similar level of potentiation was seen for the mutants P19C, V22C, L23C, V24C, V25C, N26C and K28C. For M21C, potentiation was reduced to
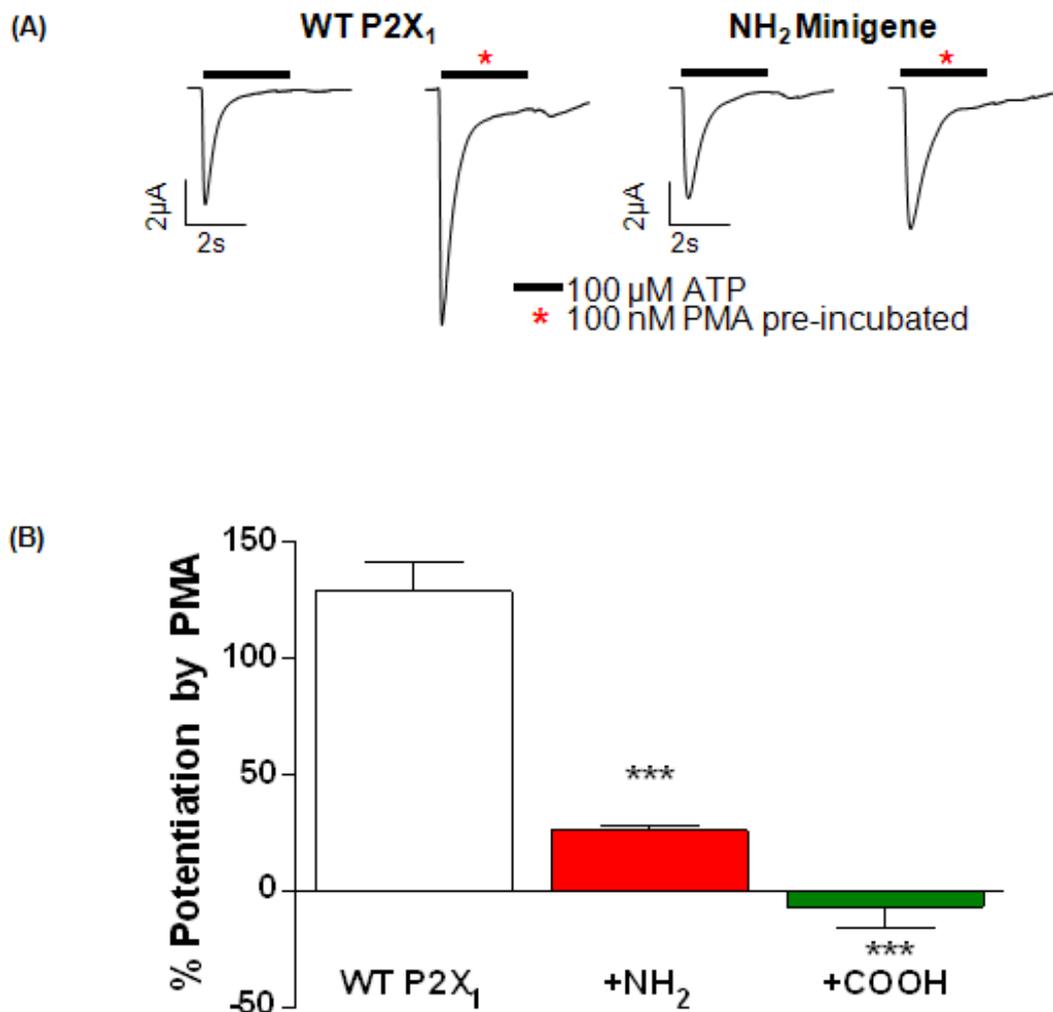
Figure7.9 The P2X$_1$ receptor intracellular minigenes block the potentiating effects of PMA stimulation on P2X$_1$ receptor currents

Minigenes encoding the N-terminal or C-terminal sequences of the P2X$_1$ receptor were co-expressed with wild type P2X$_1$ and mGluR1α receptors in the *Xenopus* oocytes. **(A)**.Representative currents evoked by a maximal concentration of ATP (100 μM, indicated by bar) at control oocytes (WT P2X$_1$) and those following 10 minutes incubation with PMA (100 nM, indicated by red asterisk). The effects of co-expression of the amino terminal minigene (NH$_2$ minigene) on the effects of PMA are shown on the right upper panel. **(B).** Summary of the effects of co-expression with amino (+NH$_2$, in red) and carboxy terminal minigenes (+COOH, in green) on the effect of PMA , *n*=6-7. ***p<0.001.
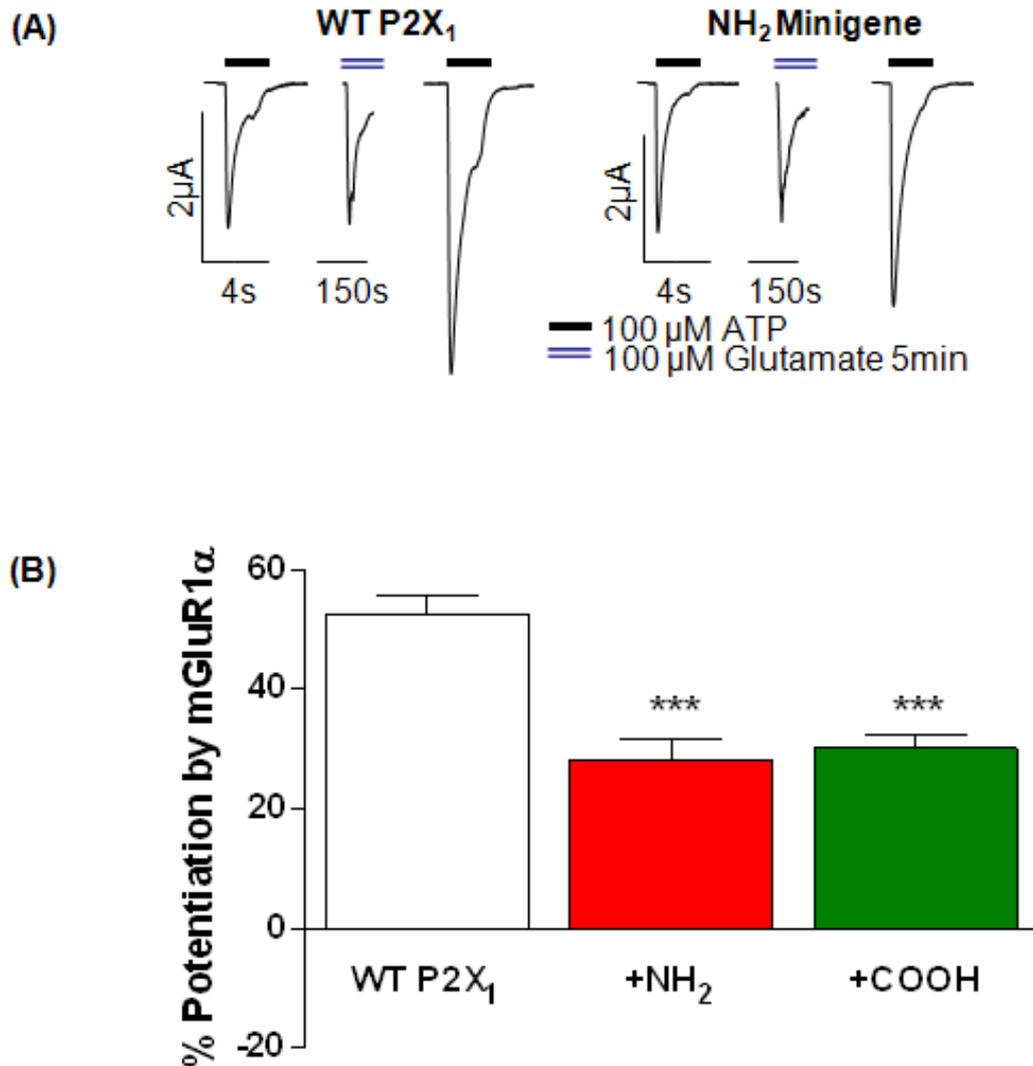
Figure7.10 The P2X₁ receptor intracellular minigenes block the potentiating effects of mGluR1α stimulation on P2X₁ receptor currents

Minigenes encoding the N-terminal or C-terminal sequences of the $P2X_1$ receptor were co-expressed with wild type $P2X_1$ and mGluR1α receptors in the *Xenopus* oocytes. **(A)**. Responses to a maximal concentration of ATP (100 µM, indicated by bar) are shown before and after the application of glutamate (100 µM). Glutamate evoked an inward calcium activated chloride current and potentiated subsequent ATP evoked responses. This potentiation was reduced by co-expression of the $P2X_1$ receptor N-terminal minigene. **(B).** Summary of the effects of co-expression with amino (+NH_2, in red) and carboxy terminal minigenes (+COOH, in green) on the effect of mGluR1α receptor, n=6-7. ***$p < 0.001$.
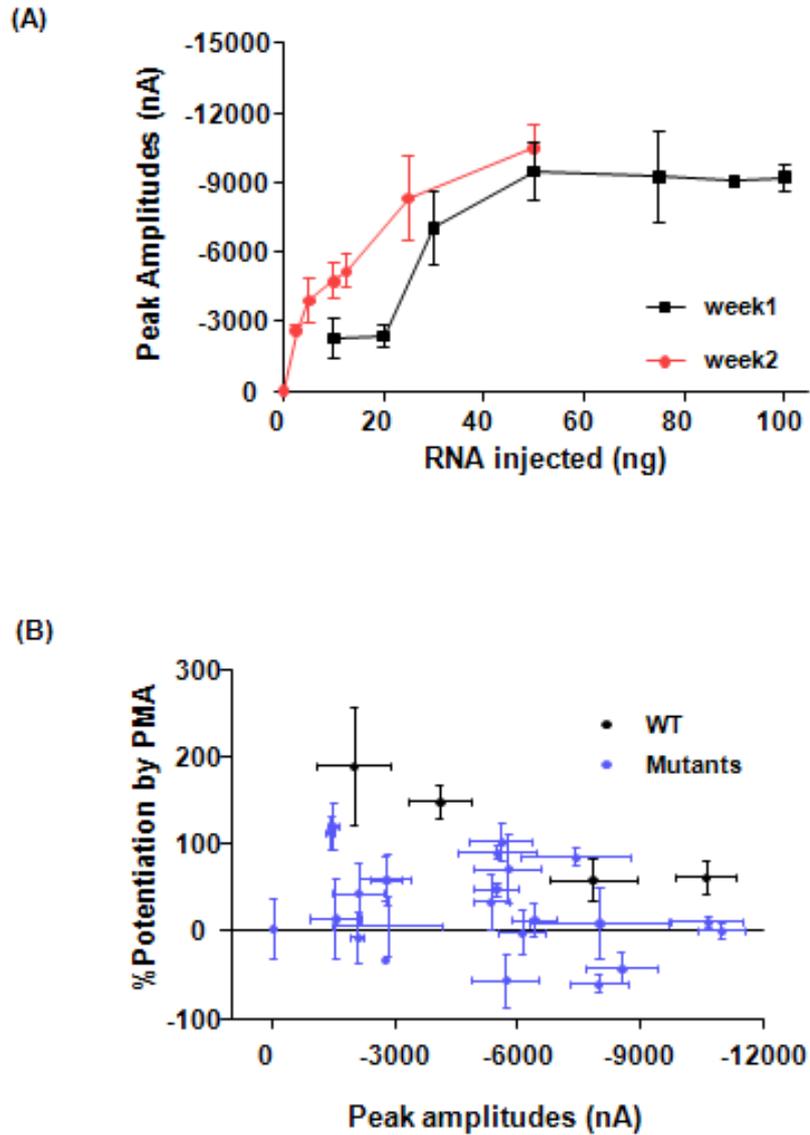
Figure 7.11 The potentiation ratio by 100nM PMA depends on P2X$_1$ receptor expression levels

(A). Plot of the mean peak current amplitudes evoked by ATP (100 µM) at WT P2X$_1$ receptor against the cRNA (from 5 ng to 100 ng) injected in the *Xenopus* oocytes. The biggest amplitude was evoked by the injection of 50ng RNA, and no significant variation may observed for two different weeks, *n*=4-7. **(B).** Plot of the potentiation ratio by 100nM PMA against the peak amplitudes of wild type and all cysteine mutants. It is clear that when the peak amplitude higher -7000 nA, the potentiation ratios for WT and most of the mutants were dominant, *n*=5-11.
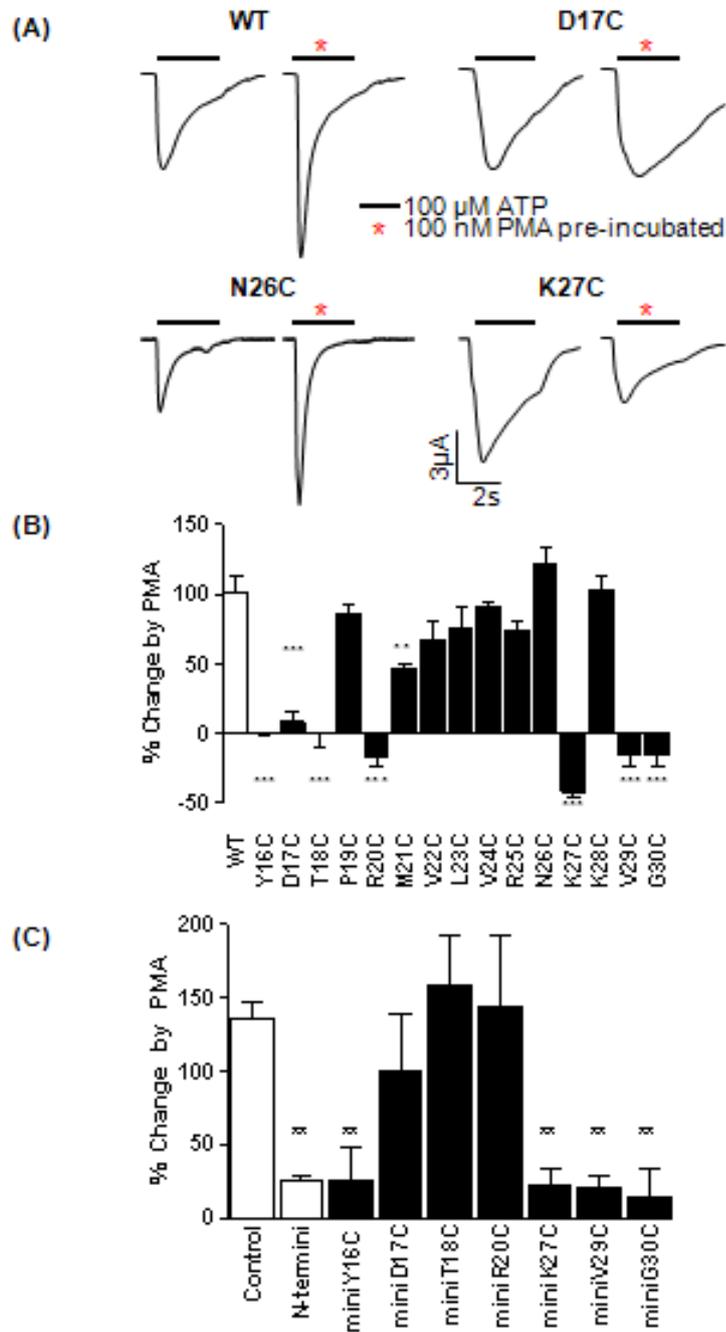
Figure7.12 PMA potentiation can be abolished by cysteine substitution of amino terminal residues

(**A**). Sample traces of ATP evoked currents (100 μM application indicated by bar) from oocytes under control conditions and following PMA (100nM, indicated in red asterisk) treatment WT as well as the mutants D17C, N26C and K27C. (**B**). Summary of the percentage changes of peak amplitudes by PMA treatment for N-termini cysteine mutants. Cysteine mutants around the conserve PKC consensus site and next to the first transmembrane segment were no longer potentiated by PMA, *n*=4-19. (**C**). Effects of mutations of the minigene on PMA potentiation, *n*=4-8 .***p<0.001, **p<0.01.

about 50%. No potentiation was seen for the mutants Y16C, D17C, T18C, R20C, V29C and G30C (Figure 7.12, ***p<0.001, **p<0.01), and the responses were inhibited for mutant K27C. These results suggest a cluster of residues comprising the conserved YXTXK/R motif and those close to the first transmembrane segment of the P2X$_1$ receptor are involved in PMA regulation.

The PMA effects of the amino terminus mutants at different peak current amplitude level were estimated and compared with the WT receptor. The mutants having potent PMA induced potentiation exhibited similar correlations between peak amplitudes and potentiation ratios as WT receptor (See figure 7.13). However, the mutants that were not affected by PMA showed no correlation to the initial peak amplitudes. For instance, the mutants D17C, T18C, R20C, K27C, V29C and G30C had little potentiation even when the peak amplitudes were quite small (Figure 7.13), and suggested the abolished PMA effects at these mutants are reliable.

Cysteine mutants that reduced PMA potentiation could be important for mediating the interaction with a regulatory factor or important in conformational changes induced by the regulatory factor. To address these roles, individual cystiene substitutions that reduced PMA potentiation were introduced into the N-terminal minigene. It was predicted that mutation of residues in the minigene important for interaction with regulatory factors would remove the inhibitory effect of the minigene. Minigenes expressing the mutants D17C, T18C and R20C no longer inhibited the PMA induced potentiation (Figure 7.12) consistent with a role of these residues in mediating interactions with regulatory factors. It is unlikely that these effects result from the disruption of the protein kinase C consensus in the miniegene as PMA is still effective at potentiating P2X$_1$ receptors where the consensus for phosphorylation has been mutated (Vial *et al*, 2004a). In contrast Y16C, K27C, V29C and G30C mutant minigenes caused inhibitions by PMA rather than potentiations and suggested that these residues may be important in conformational changes on the P2X$_1$ receptor associated with PMA potentiation.

The potentiation ratio induced by mGluR1α receptor also showed a trend in correlation to the level of P2X$_1$ receptor amplitude (ATP 100 μM), however, the differences are not

significant. For the mutants where PMA no longer had an effect or reduced the response, I tested to see whether mGluR1α receptor dependent regulation was also attenuated. ATP (100 μM) was applied repeatedly at 5 minute intervals to obtain reproducible responses. Glutamate potentiated WT $P2X_1$ receptor currents by 67.8 ± 4.8 % (*n*=8). For most (4/6) of the mutants that showed no potentiation with PMA treatment the effects of mGluR1α receptor stimulation were also reduced significantly (See figure 7.14. ***p<0.001 for PMA effects; +++p<0.001 for glutamate effects.). However, the mGluR1α receptor regulation was not affected by the mutations D17C and V29C where the application of glutamate gave potent potentiations of 114.5 ± 4.7 % (*n*=4) and 66.2 ± 6.9 % (*n*=5) respectively. These results indicate that PMA and mGluR1α stimulation have some differences in their regulatory mechanisms.

The consensus PKC motif (TXR/K) is conserved on the N-terminus of P2X receptors. When this consensus was disrupted (R20A) comparable potentiation by GPCRs to the WT $P2X_1$ receptor was observed (Vial *et al*, 2004a). As the R20C mutant exhibited a dramatic reduction to the effect of mGluR1α receptor stimulation, the effect of different substitutions at residue Arg^{20} was further studied. In all cases (R20C, R20A and R20I), the effects of PMA were abolished (Figure 7.15, ***p<0.001). However, following the co-expression with the mGluR1α receptor, similar levels of potentiation as for WT receptors were seen for R20A and R20I mutants following application of glutamate (100 μM) (See figure 7.16, ***p<0.001).These results further highlight differences between PMA and mGluR1α mediated regulation. A dependence of the nature of the amino acid substituted was also showed at position Thr^{18}. The mutant T18C blocked the PMA (-0.2 ± 10.5 %, *n*=4) regulation of the $P2X_1$ receptor, while the T18A mutation had no effect on PMA potentiation (194 ± 18.8 %, *n*=7).

7.2.4 The roles of C-terminus to $P2X_1$ receptor regulation

The roles of carboxy terminal residues to WT $P2X_1$ receptors regulation was characterized by PMA (100 nM) treatment. Compared to the WT receptor (116.5 ± 14.5%, *n*=11), similar potentiation levels were showed by most mutants (9/16) including I365C, L357C, K359C, R360C, H361C, Y362C, K364C, Q365C and K366C following 10 minutes PMA pre-incubation before recording. In contrast, no potentiation was seen for the mutants P358C, Y363C and K369C, and the responses were inhibited for mutants H355C, K367C, F368C, and Y370C (See figure 7.17, ***p<0.001). Similar
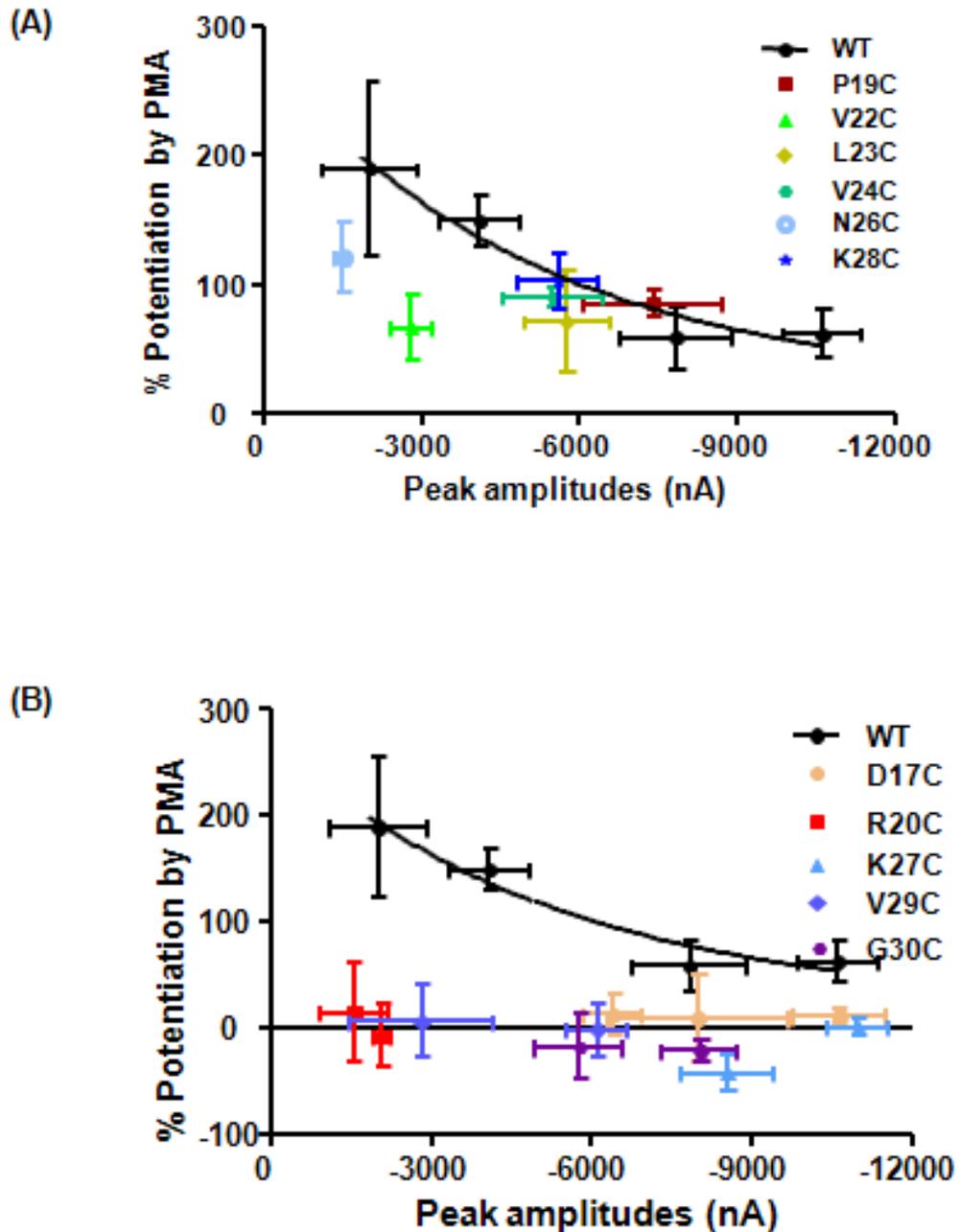
Figure 7.13 Not all of the mutant exhibited correlations between its peak amplitudes and potentiation ratio evoked by 100 nM PMA
(A). For wild type receptor, the higher peak amplitudes, the lower potentiation ratio by 100 nM PMA can be observed. And mutants P19C, V22C, L23C, V24C, N26C and K28C seem to follow the trend of WT P2X$_1$ receptor. **(B).** However, the mutants D17C, R20C, K27C, V29C and G30C did not exhibit a similar correlations between the peak amplitudes to potentiation ratios by PMA. Although the peak amplitudes was varied, almost no potentiation can be observed for all these mutants *n*=5-11.
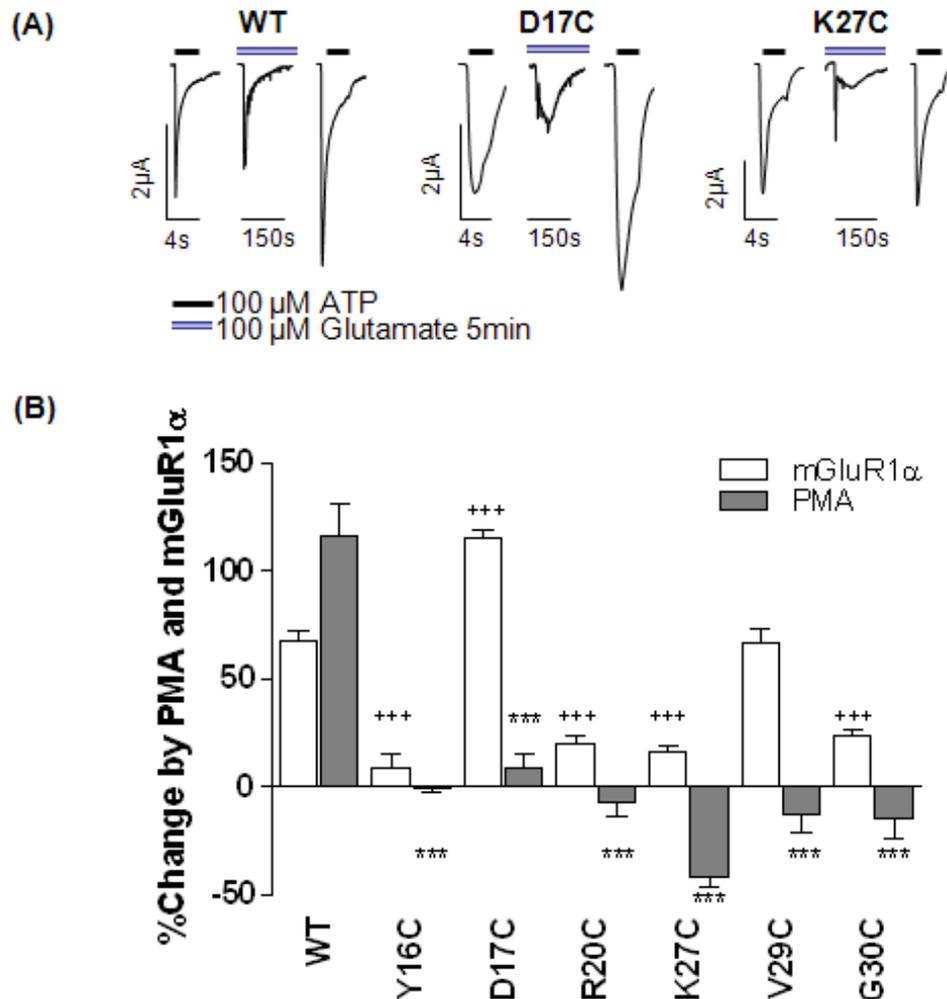
Figure7.14 The effects of mGluR1α receptor activation on P2X$_1$ receptor mutants
(A). Sample traces for a given oocyte co-expressing either WT P2X$_1$, D17C or K27C mutant P2X$_1$ receptor with mGluR1α receptors. Responses to a maximal concentration of ATP (100 μM, indicated by bar) are shown before and after the application of glutamate (blue bar). Glutamate (100 μM) evoked an inward calcium activated chloride current and potentiated subsequent ATP evoked responses for WT and D17C mutants but not for the K27C mutant P2X$_1$ receptor. (B). The effects of mGluR1α receptor (100 μM glutamate) and PMA (100 nM) on WT and the cysteine mutants are shown. For most of the mutants unable to exhibit the PMA potentiation was seen following the activation of mGluR1α receptor. However, the mGluR1α receptor stimulated potentiation was still robust for the D17C and V29C mutants, n=4-9 .***p<0.001 for PMA effects; +++p<0.001 for glutamate effects.
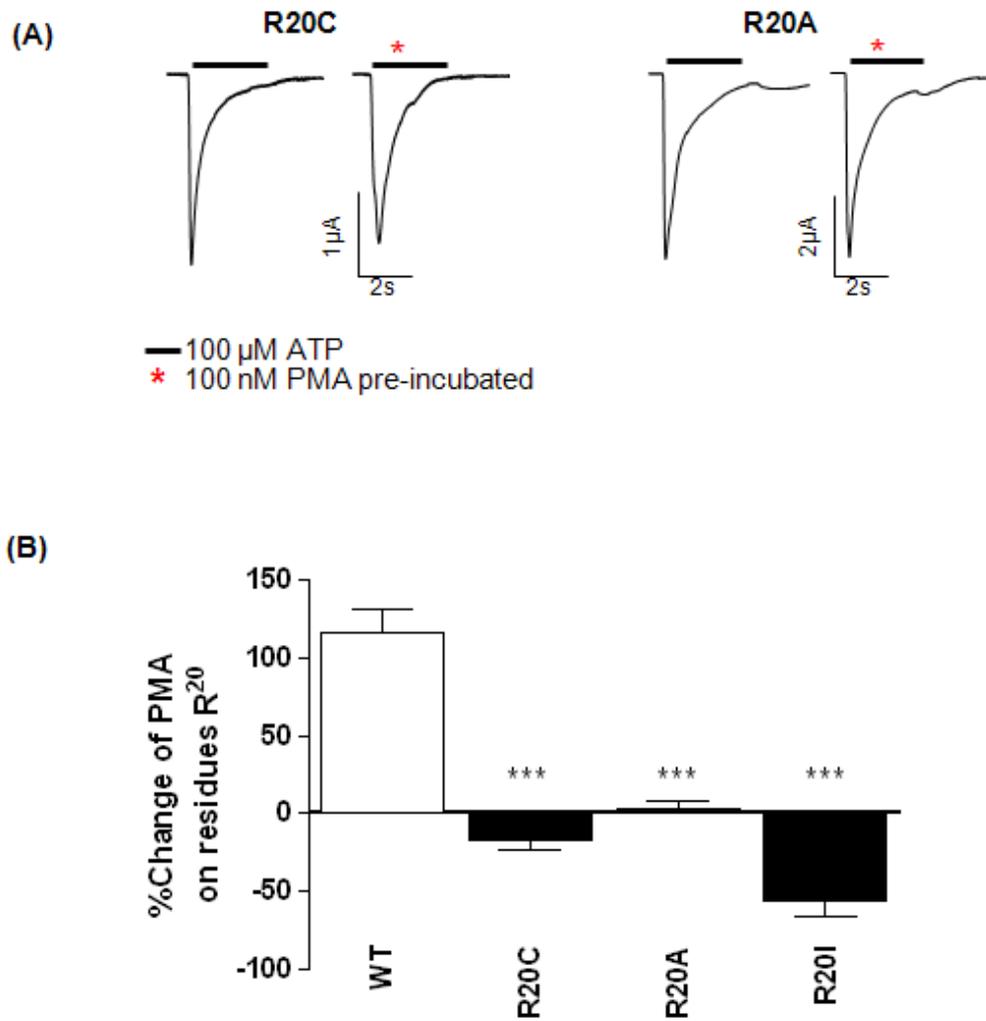
Figure7.15 The effects of PMA to Arg^{20} substitutions
(A). Example traces of R20C and R20A mutants in response to PMA (100 nM, indicated by red asterisk) .Peak amplitudes from control and PMA treated oocytes are shown. **(B).** Summary of effects of amino acid substitution at position Arg^{20} at the P2X$_1$ receptor by cysteine, alanine or isoleucine on potentiation by PMA, *n*=4-11. ***$p<0.001$.
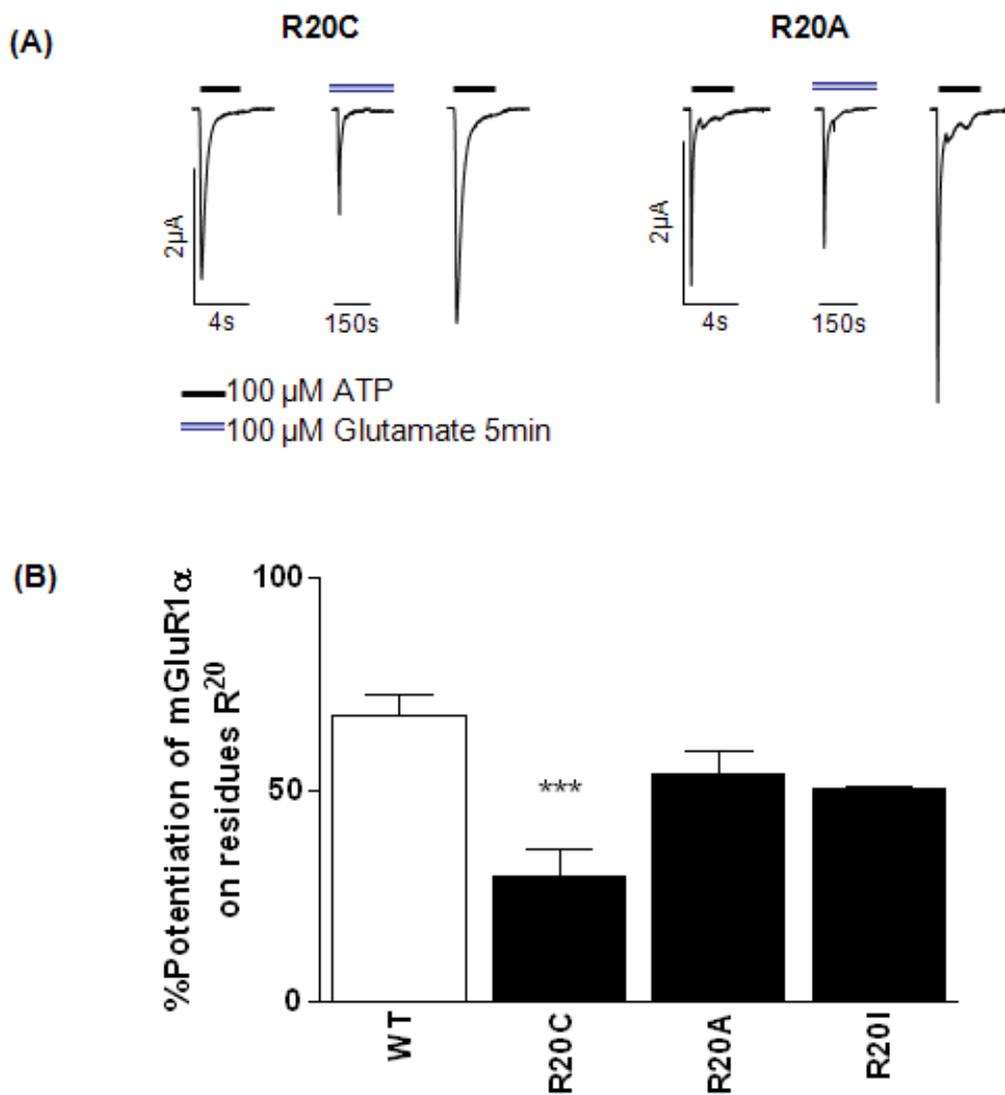
Figure7.16 The effects of mGluR1α to Arg[20] substitutions
(A). Example traces of R20C and R20A mutants in response to mGluR1α receptor (glutamate100 μM, indicated by blue bar). ATP evoked currents before and after mGluR1α receptor activation from either R20C (left) or R20A (right) are shown.**(B).** Summary of effects of amino acid substitution at position Arg[20] at the P2X$_1$ receptor by cysteine, alanine or isoleucine on potentiation by glutamate, *n*=4-6. ***p<0.001.

.

to the amino terminus, these results suggest the residues close to the second transmembrane segment and the ones around the YXXXK protein trafficking motif are involved in the P2X$_1$ receptor PMA regulation.

The cysteine mutants that showed inhibition of the PMA effect were introduced to the C-terminal minigene. Only the minigenes bearing the mutants K367C and Y370C removed the inihibitory effects and suggested to have interaction with the regulatory factors (Figure 7.17). In contrast, the H355C, P358C, Y363C, F368C and K369C minigenes still inhibited the PMA potentiation and the corresponding residues at P2X$_1$ receptor carboxy terminus may contribute to the conformation changes during the binding of regulatory factors.

The mutants that showed no potentiation by PMA were co-expressed with the mGluR1α receptor, and the mGluR1α mediated effects to the P2X$_1$ receptor current were compared with the WT receptor (67.8 ± 4.8 %, $n=8$). ATP (100 µM) was applied repeatedly at 5 minute intervals to obtain reproducible responses. Mutants Y363C and K367C were unable to produce reproducible current to the repeated application of ATP, and only 5 mutants showed no potentiation with PMA were tested. The inhibitory effects were showed by all of these 5 mutants which are consistent with the PMA effects (See figure 7.18. ***$p<0.001$ for PMA effects; +++$p<0.001$ for glutamate effects.). However, the Y370C mutants exhibited reduction at the P2X$_1$ receptor peak amplitudes to the PMA treatment, showed only moderate inhibitory effects by mGluR1α receptor. The residue Tyr^{370} may be more sensitive to the PMA regulation pathway than the GPCRs.
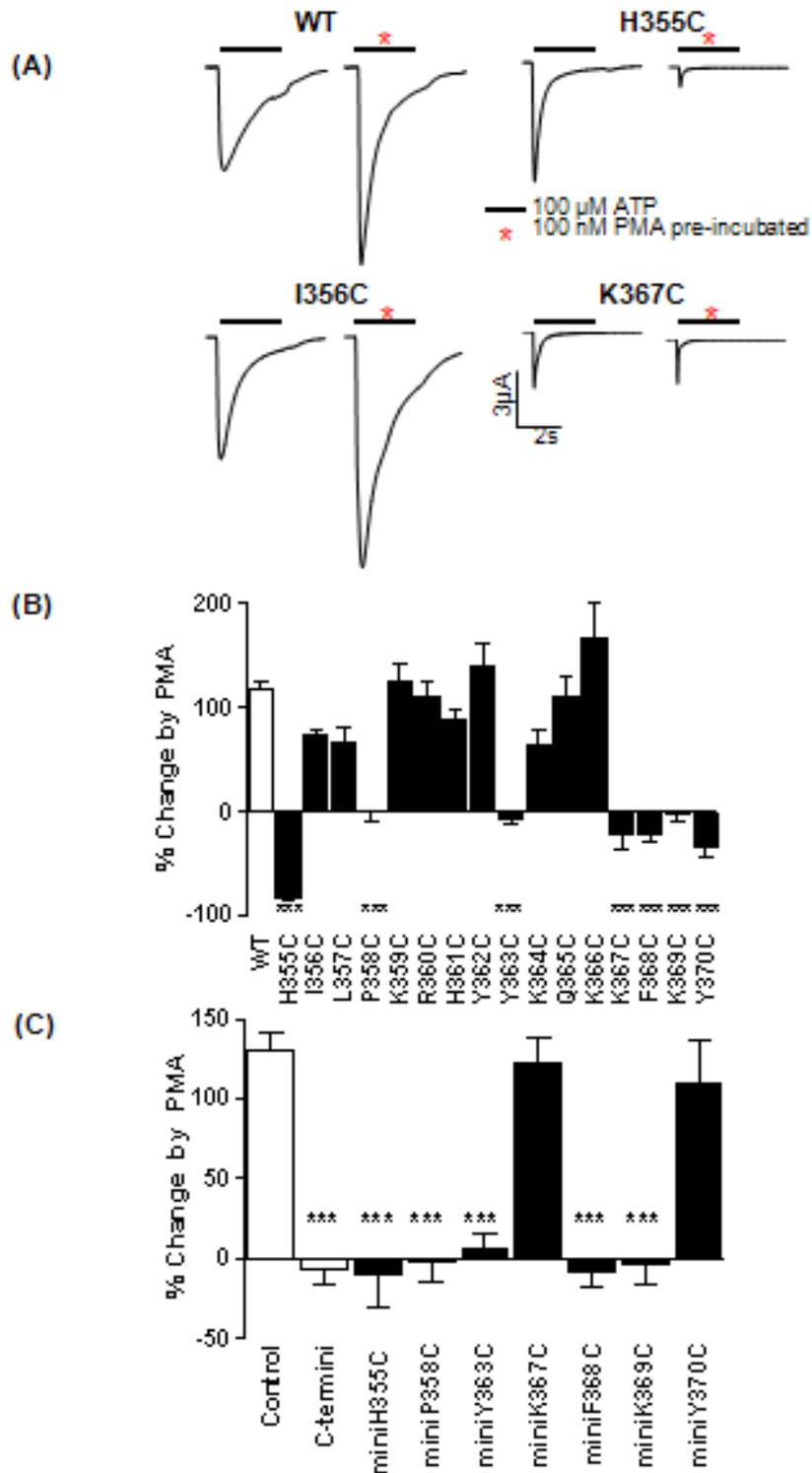
Figure7.17 PMA potentiation can be abolished by cysteine substitution of carboxyl terminal residues

(A). Sample traces of ATP evoked currents (100 μM application indicated by bar) from oocytes under control conditions and following PMA (100 nM, indicated in red asterisk) treatment for WT as well as the mutants H355C, I356C and K367C. **(B).** Summary of the percentage changes of peak amplitudes by PMA treatment for C-termini cysteine mutants. Cysteine mutants around the conserve YXXXK motif and next to the second transmembrane segment were no longer potentiated by PMA, *n*=4-18 . **(C).** Effects of mutations of the minigene on PMA potentiation, *n*=5-15. ***p<0.001.
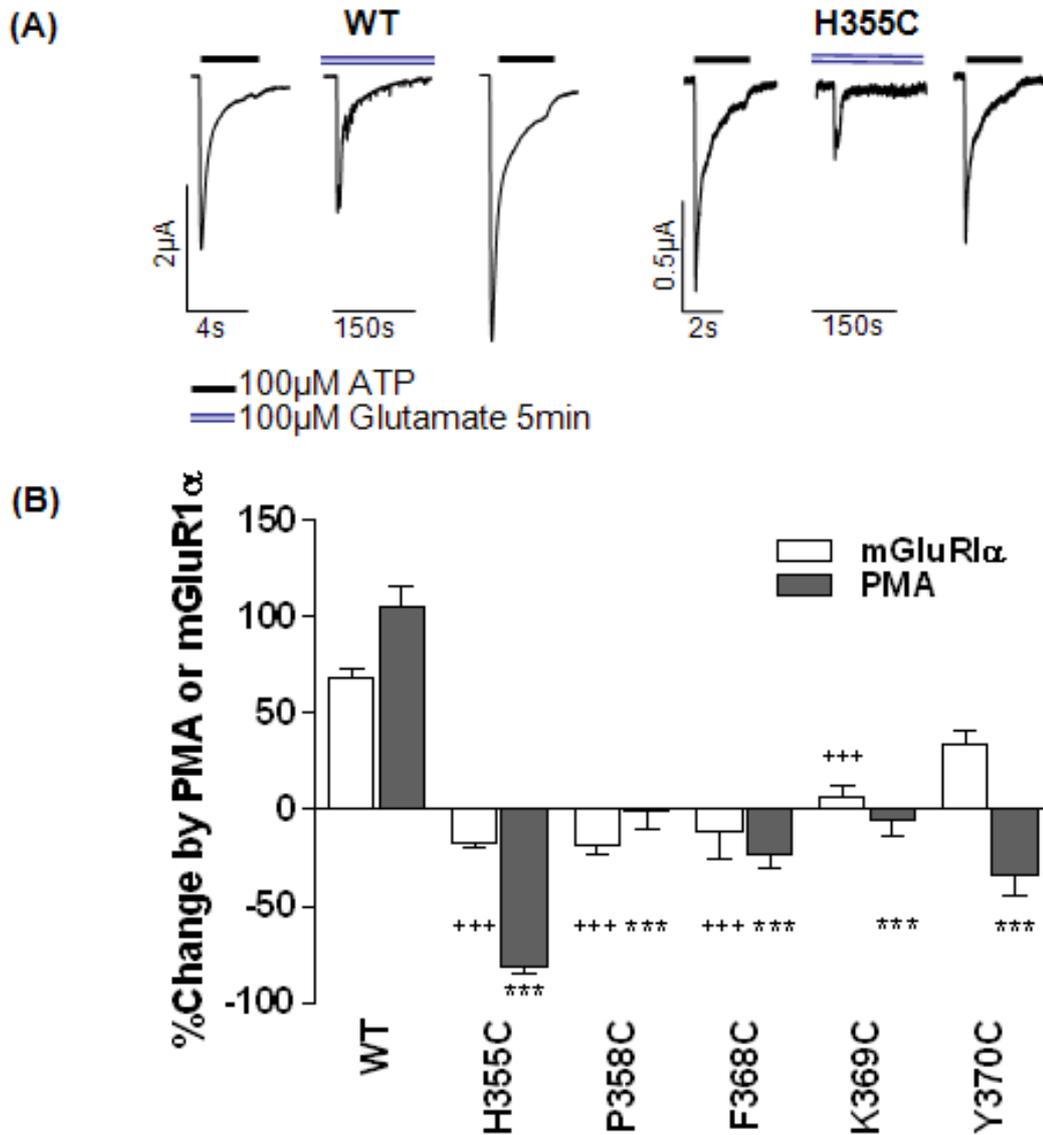
Figure7.18 The effects of mGluR1α receptor activation on P2X₁ receptor C-terminal mutants

(A). Sample traces for a given oocyte co-expressing either WT P2X₁ or H355C mutant P2X₁ receptor with mGluR1α receptors. Responses to a maximal concentration of ATP (100 µM, indicated by bar) are shown before and after the application of glutamate (blue bar). Glutamate (100 µM) evoked an inward calcium activated chloride current and potentiated subsequent ATP evoked responses for WT but not for the H355C mutant of P2X₁ receptor. (B). The effects of mGluR1α receptor (100 µM glutamate) and PMA (100 nM) on WT and the cysteine mutants are shown. For most of the mutants unable to exhibit the PMA potentiation was seen following the activation of mGluR1α receptor. However, the mGluR1α receptor stimulated potentiation was still robust for the Y370C mutants, n=3-8 .***p<0.001 for PMA effects; +++p<0.001 for glutamate effects.

7.3 Discussion
7.3.1 Novel PKC isoforms are involved in the regulation of P2X$_1$ receptor

P2X$_1$ receptor mediated responses can be potentiated by phorbol ester and Gα_q coupled GPCR stimulation and this may allow for regulation of P2X receptor signaling (Vial *et al*. 2004a). In this study we have investigated the molecular basis of this regulation and have shown that it results from activation of novel PKC isoform(s). The over 80% reduction by calphostin C of P2X$_1$ receptor potentiation by PMA or mGluR1α stimulation supports the role of protein kinase C in receptor regulation. A previous study showed that potentiation was not dependent on a rise in intracellular calcium (Vial *et al*. 2004a) and this suggests it is novel calcium insensitive PKC isoforms, and not the classical calcium sensitive PKC isoforms, that are involved. Amongst the novel PKC isoforms GÖ6976 is selective for PKCμ (PKD). The abolition of potentiation by PMA and about 60% reduction in mGluR1α mediated modulation by GÖ6976 suggests a role of PKCμ (PKD) in the regulation of P2X$_1$ receptors, as has been suggested previously for 5-HT regulation (Ase *et al*, 2005). The reduction in potentiation by GÖ6983, that is effective at the concentration used at novel PKC isoforms with the exception of PKCμ (IC$_{50}$ 100 times higher than that used in the current study), suggests that one or more of the isoforms PKC $\delta,\varepsilon,\eta,\theta$ are also involved. This raises the question where these novel PKC isoforms act? Vial *et al* previously showed that mGluR1α potentiation was still observed when the proposed "phosphorylatable" threonine was mutated or the consensus PKC sequence was disrupted by R20 mutation (Vial *et al*. 2004a) and that this ruled out a role of phosphorylation of the P2X$_1$ receptor at the consensus PKC site as a mechanism of action. This conclusion was also supported as no change could be detected in P2X$_1$ receptor phosphorylation on PMA stimulation and studies on the P2X$_3$ receptor also failed to detect receptor phosphorylation associated with PKC regulation (Franklin *et al*. 2007). Interacting proteins that regulate the function of P2X$_7$ and P2X$_2$ receptors have been described (Adinolfi *et al*. 2003; Masin *et al*. 2006) and therefore the modulation of the P2X$_1$ receptor is suggested to occur through the phosphorylation by a novel PKC of a regulatory protein that interacts with the P2X$_1$ receptor.

The underlying mechanisms of PMA to P2X$_1$ receptor potentiation are still unclear. The permeability of P2X$_7$ and P2X$_2$ channels were able to change during continuous agonist application (Khakh *et al*, 1999; Virginio *et al*, 1999). TRPV1 channel (transient receptor potential cation channel, subfamily V, member 1) shows similar permeability change on

the prolonged agonist application. Protein kinase C-dependent phosphorylation at Ser^{800} in the TRPV1 channel C-terminus increases its permeability to the large cation NMDG to 3.5 fold, and this increase can be blocked by application of PKC inhibitor bisindolemalimide (Chung *et al*, 2008). However, the reversal potential measurement showed no increase at the cation permeability to PMA effect suggesting the PMA cannot act on $P2X_1$ receptor via channel pore dilation.

PMA was suggested to modulate the $5-HT_{3A}$ receptor through destabilizing the cytoskeleton and increase the protein trafficking (Sun *et al*, 2003). PMA as a PKC activator can significantly increase the surface expression level of $5-HT_{3A}$ receptor without affecting the total amount of expressed protein. However, phalloidin which stabilizes actin polymerization, significantly inhibited PMA mediated potentiation to $5-HT_{3A}$ responses, while latrunculin-A destabilizes actin cytoskeleton showed enhanced effects. The effects of PMA to the $P2X_1$ receptor expression levels can also be studied by comparing the protein staining after cell surface biotinylation in the future.

Although PMA and mGluR1α receptors activate the $P2X_1$ receptor through the PKC sensitive pathway, these agents regulate the $P2X_1$ receptor in slightly different ways. For instance, the amino terminus mutants D17C and V29C resulted in abolition of PMA's actions with no effect on mGluR1α potentiation.

Substitution dependence on residues compromising the conserved PKC site was also observed in this study, as the mGluR1α mediated potentiation can only be abolished by cysteine substitution not other amino acid substitutions at Arg^{20}. Hence the local amino acid environment not the ability to be phosphorylated regulates channel function in this region.

7.3.2 Minigene as interfering factors are effective in $P2X_1$ receptor functional domain identification

Minigenes have been widely used as interfering factors to identify the specific regions that contribute to regulation. Del Gatto *et al* transfected minigenes encoding a mutant sequence into cells and confirmed a special exon sequence TAGG inhibited splicing (Del Gatto *et al*, 1996). The *PatS* gene signaling motif was identified by generating a range of the minigenes encoding the *PatS* sequences with different numbers of amino

acids (Wu *et al*, 2004). The minigenes of PatS-5 (RGSGR) other than the PatS-4 (GSGR) showed inhibitory effects to heterocyst formation, and indicated the RGSGR sequence comprises a regulatory motif for inhibiting heterocyst differentiation (Wu *et al*. 2004). This strategy has also used to study the intracellular functional domains on P2X receptors (Boue-Grabot *et al*. 2004). As described, the intracellular minigenes of $P2X_2$ receptors have been generated to identify their roles in the cross-talk with $GABA_A$ and $5-HT_{3A}$ receptors.

In this study, the over-expression of a minigene encoding the amino and carboxy termini of the $P2X_1$ receptor reduced PMA and mGluR1α receptor potentiation of $P2X_1$ receptor currents and demonstrated that both intracellular termini play important roles in receptor regulation possibly through providing a docking site for a regulatory protein and therefore over-expression of the minigene led to sequestering of this regulatory protein. The minigene, like the range of PKC inhibitors used, had no effect on the $P2X_1$ receptor currents under resting conditions suggesting that the receptor is not basally regulated, and that PMA and GPCR stimulation provide an auxiliary mechanism to modify channel properties. The greater reduction on the PMA effect compared to GPCR stimulation by the carboxy terminal minigene suggests that the C terminus may play a more significant role in the regulation of the $P2X_1$ receptor by PMA.

Cysteine mutants that reduced PMA potentiation could be important for mediating the interaction with a regulatory factor or important in conformational changes induced by the regulatory factor. To address these roles, the individual cysteine mutants that reduced PMA potentiation can be introduced into the amino and carboxy terminal minigenes respectively. Minigenes had inhibitory effects to the PMA mediated potentiation at $P2X_1$ receptor. The prediction is that mutations of residues in the minigenes important for interaction with regulatory factors would remove the inhibitory/sequestering effect of the minigene. Otherwise, the mutations show similar inhibitory effects as the WT minigenes co-expression with the $P2X_1$ receptor suggest the roles of corresponding residues in channel conformational changes due to the binding of the regulatory protein.

7.3.3 The intracellular regions that are involved in the P2X$_1$ receptor regulation

Amino terminus

The results clearly show the conserved YXTXK/R motif plays a role in determining the basic properties of P2X$_1$ receptors and their regulation by PMA and following GRCR stimulation. Single mutation at almost all residues (4/5) around this motif showed effect on PMA regulation, and the conserved Tyr^{16} and Arg^{20} also exhibited essential roles in the GPCRs related modulation. The Thr^{18} residue is phosphorylated for the P2X$_1$ receptor and the mutation R20T removes this phosphorylation (Liu *et al*, 2003). However it is unlikely that the regulatory effects result from changes in the phosphorylation status at Thr^{18} as P2X$_1$ responses are still potentiated by GPCRs for the T18V mutant (Vial *et al*, 2004a).

The region around the beginning of the first transmembrane segment has also been shown to be involved in regulation of P2X$_1$ receptor mediated responses. K27C and G30C mutants showed decreases in both PMA and mGluR1α effects and V29C mutation resulted in abolition of PMA's actions with no effect on mGluR1α potentiation. In addition, currents evoked at G30C receptors were irreversibly reduced significantly by MTS compounds treatments, and the Gly^{30} was suggested to be involved in the ionic permeation pathway (see chapter 5 and Jiang *et al*, 2001). This glycine residue is conserved throughout the mammalian and *Dictyostelium* families (Fountain *et al*. 2007). However, it is interesting that mutation to cysteine had no effect on the current amplitude or time-course of P2X$_1$ (See chapter 5) or P2X$_2$ (Jiang *et al*. 2001) receptors. This shows that the flexibility associated with the glycine residue is not essential for normal channel function. However it could be possible that following PMA or mGluR1α receptor stimulation that the flexibility associated with this residue is required to mediate the potentiation of the current possibly by changing the single channel properties of the receptor.

Introduction of the cysteine mutants into the minigene further identified substitution that abolished the inhibitory effect of the minigene (D17C, T18C and R20C) and those that had no effect on the inhibitory actions of the minigene (Y16C, K27C, V29C and G30C) at the amino terminus. The abolition of the inhibitory effect of the minigene when Asp^{17}, Thr^{18} or Arg^{20} were mutated demonstrates that these residues are likely to play an important role in the sequestering action of the minigene in competing with the P2X$_1$

receptor for the regulatory factor and identified for the first time residues that are involved in direct association with the regulatory factor. The results with the minigene also show that residues Tyr^{16}, Lys^{27}. Val^{29} and Gly^{30} are not important in the interaction directly with the regulatory factor but mediate the changes in the $P2X_1$ receptor that lead to potentiation of the response. One possibility is that these residues could contribute to the gating of the $P2X_1$ receptor regulation of channel conductance. The cooperations of these two regions in channel regulation were further discussed in chapter 8 (Figure 8.2).

In addition, one would expect a similar phenotype from mutation of either the Thr^{18} or Arg^{20} as both of these would remove the consensus PKC site yet R20C has only a small effect on peak currents and no effect on time-course whereas T18C reduced by >95% current amplitudes and speeded desensitisation. Thus it remains to be determined the mechanism by which PMA and GPCRs regulate the $P2X_1$ receptor. Previous studies have shown the regulation is sensitive to the kinase inhibitor staurosporine (Vial *et al*, 2004a) and the lack of detection of a change in the phosphorylation status of the $P2X_1$ receptor following PMA treatment suggested that regulation may be by phosphorylation of an auxillary protein. The present results suggest that if this is the case such an interacting protein may have a similar effect at all P2X receptors due to the conservation of the YXTXK/R motif.

Carboxyl terminus

For the C-terminal region, conserved Tyr^{363} and Lys^{367} in the YXXXK motif showed important roles in the PMA mediated $P2X_1$ receptor regulation. Cysteine substitutions at these two positions showed dramatically reduced peak currents and reproducible currents to continued ATP applications cannot be obtained. A reduction of surface expression was also observed at K367C as reported in chapter 6 and suggested the contribution of this residue in protein trafficking, which is consistent to the results for other P2X receptors (Chaumont *et al*, 2004). Therefore, the conserved tyrosine and lysine that make this motif had essential roles for $P2X_1$ receptor basic properties and also the regulation pathway. In addition, the regions after the YXXXK motif from Lys^{367} to Tyr^{370} were demonstrated to be fundamental in the PMA and GPCR modulation. It is an interesting observation that the cysteine substitutions at these consecutive four residues led to abolished or even inhibitory effects to the PMA and

mGluR1α induced current potentiations. In this region Try[370] could be a potential tyrosine kinase recognition site, whereas the positively charged Lys[367] and Lys[369] may attract the negatively charged phosphates and provide a docking site for the regulatory protein. However there is no detectable phosphorylation shown for the intracellular tyrosines (Toth-Zsamboki *et al*, 2002) and the regulatory mechanism remained to be discovered. The Y370C showed 40% inhibition to the peak current after the PMA treatment and had no inhibitory effect to the mGluR1α mediated potentiation, and this residue thus maybe exclusive to the PMA regulation pathway.

The His[355] exhibited a striking inhibitory effect to the PMA regulation, and similar inhibition was observed for mGluR1α co-expression. This residue at the gate of channel pore was suggested to be important for the channel gating mechanism and Gly[30], may contribute to the conformational change of the $P2X_1$ channel during the modulation. Together with the Pro[358] and the regions around the YXXXK motif in the intracellular C-terminus of $P2X_1$ receptor may compose in a delicate 3D structure and interact each other in channel modulation.

The residues involved in the direct interaction with regulatory factor at the C-terminial were further studied by coexpressing the minigene mutants. The abolished inhibitory effects were demonstrated at the minigenes bearing K367C and Y370C mutants, whereas the H355C, P358C, Y363C, F368C and K369C showed no effects to the inhibitory action of the minigene. The Lys[367] and Tyr[370] were proposed to have direct roles in accessory protein mediated regulation, and others are contribute to the channel conduction regulation or conformation change indirectly. See chapter 8 for details of the interactions between these regions to channel signalling.

7.3.4 Conclusion

In summary this study has identified both intracellular termini contribute to $P2X_1$ receptor regulation using the minigenes strategy, and intracellular terminal regions that are involved in regulation by PMA and ionic permeation were further determined. For example the YXTXR/K motif at the amino terminus and the regions around the YXXXK motif at the carboxy terminus are the potential docking site for the accessory regulatory protein. Whereas the residues close to the channel pore are also involved in this regulation via conformation change during the binding of the accessory protein.

This raises the possibility that there may be some interaction between these potential regulatory motif and the residues responsible for channel gating to regulate channel properties. Structural models of the intracellular regions however will be required for fuller interpretation of these results.

7.4 Appendix: Minigenes construction

The amino terminal (Met^1-Gly^{30}) and carboxy terminal (Leu^{353}-Stop^{400}) sequences of the human P2X$_1$ receptor were amplified from the pcDNA 3.0 vector containing the human P2X$_1$ receptor cDNA by Polymerase Chain Reaction (PCR) (Techne Genius thermocycler, BioTAQ ^{TM} DNA polymerase, Bioline, U.K.) and two restriction sites *EcoRI* and *HindIII* sequences were introduced to the ends of the minigenes from the PCR primers. Then the minigene sequence was introduced to the plasmid pcDNA3.0 with these two restriction sites by ligation at 14 ºC overnight (T4 DNA ligase, New England Biolabs$^®$ Inc.). In addition, start and stop codons were added to the ends of the minigene sequence for its translation and expression (See table 7.1).

Point mutations were introduced to the minigene sequences and coverted individual residues into cysteines (Stratagene, Amsterdam, Netherlands) using the primers as described in chapter 5 and 6. However, the primers for mutations close to the ends of minigenes were re-designed as in table 7.2. These sequences were confirmed by DNA sequencing (PNACL sequencing service, Leicester University) using pcDNA 3.0_5' or pcDNA 3.0_3' primers (See figure 5.2).

Primers used to amplify the minigene NH₂ terminus (121bp)

	HindIII	*start codon*	
Forward primer :	5' ACC **AAGCTT**	**ATG**	GCACGGCGGTTCCAG G 3'

5'ATG	GCA	CGG	CGG	TTC	CAG	G
M	A	R	R	F	Q	
3'TAC	CGT	GCC	GCC	AAG	GTC	C

AG GAG CTG GCC GCC TTC CTC TTC GAG TAT GAC ACC CCC CGC ATG GTG CTG
E   L   A   A   F   L   F   E   Y   D   T   P   R   M   V   L
TC CTC GAC CGG CGG AAG GAG AAGCTC ATA CTG TGG GGG GCG TAC CAC GAC

GTG CGT	AAT	AAG	AAG	GTG	GGC 3'
V R	N	K	K	V	G
CAC GCA	TTA	TTC	TTC	CAC	CCG 5'

Reverse primer :	3'CGCA TTA TTC TTC CAC CCG	**ACT**	**CTTAAG** CAC 5'
		s*top codon*	*EcoRI*

Primers used to amplify the minigene COOH terminus (160bp)

	HindIII	*start codon*	
Forward primer :	5' ACC **AAGCTT**	**ATG**	CAC ATC CTG CCT AAG AGG 3'

5'CTG	CTT	CAC	ATC	CTG	CCT	AAG	AGG	CAC
L	L	H	I	L	P	K	R	H
3'GAC	GAA	GTG	TAG	GAC	GGA	TTC	TCC	GTG

TAC TAC AAG CAG AAG AAG TTC AAA TAC GCT GAG GAC ATG GGG CCA GGG GCG GCT GAG CGT GAC CTC GCA GCT
Y   Y   K   Q   K   K   F   K   Y   A   E   D   M   G   P   G   A   A   E   R   D   L   A   A
ATG ATG TTC GTC TTC   TTC AAG TTT ATG CGA CTC CTG   TAC CCC GGT CCC CGC CGA CTC GCA CTG GAG CGT CGA

ACC AGC TCC ACC CTG GGC CTG CAG GAG	AAC	ATG	AGG	ACA	TCC	TGA 3'
T S S T L G L Q E	N	M	R	T	S	. *
TGG TCG AGG TGG GAC CCG GAC GTC CTC	TTG	TAC	TCC	TGT	AGG	ACT 5'

Reverse primer :	3' C CTC TTG TAC TCC TGT AGG	**ACT**	**CTTAAG**	CCT 5'
		stop codon	*EcoRI*	

Table 7.1 Sequences of primers to amplify the minigene of NH₂ terminus and COOH terminus
The sequences of primers used to amplify minigene NH₂ terminus and COOH terminus are shown above. There are start and stop codon (bold) and Hind III or *EcoRI* restriction sites (bold and underlined) on either side of the designed primer sequences. Minigene sequences are highlighted in yellow. The amino acid sequence for amino terminus is "MARRFQEELAAFLFEYDTPRMVLVRNKKVG", and the sequence of carboxy terminus is "LLHILPKRHYYKQKKFKYAEDMGPGAAERDLAATSSTLGLQENMRTS·" respectively.

Primers	Sequences of the Primers	Conversion
Mini K27C FWD	5'- C ATG GTG CTG GTG CGT AAT <u>TGT</u> AAG GTG GGC TGA GAA TTC -3'	**K→C**
Mini K27C REV	5'- GAA TTC TCA GCC CAC CTT <u>ACA</u> ATT ACG CAC CAG CAC CAT G -3'	**K→C**
Mini V29C FWD	5'- G GTG CGT AAT AAG AAG <u>TGC</u> GGC TGA GAA TTC TGC AG -3'	**V→C**
Mini V29C REV	5'- CT GCA GAA TTC TCA GCC <u>GCA</u> CTT CTT ATT ACG CAC C -3'	**V→C**
Mini G30C FWD	5'- CGT AAT AAG AAG GTG <u>T</u>GC TGA GAA TTC TGC AG -3'	**G→C**
Mini G30C REV	5'- CT GCA GAA TTC TCA GC<u>A</u> CAC CTT CTT ATT ACG -3'	**G→C**
Mini H355C FWD	5'- G AGA CCC AAG CTT ATG <u>TG</u>C ATC CTG CCT AAG AG -3'	**H→C**
Mini H355C REV	5'- CT CTT AGG CAG GAT G<u>CA</u> CAT AAG CTT GGG TCT C -3'	**H→C**
Mini P358C FWD	5'- C AAG CTT ATG CAC ATC CTG <u>TG</u>T AAG AGG CAC TAC TGC AAG -3'	**P→C**
Mini P358C REV	5'- CTT GCA GTA GTG CCT CTT A<u>CA</u> CAG GAT GTG CAT AAG CTT G -3'	**P→C**

Table 7.2 Sequences of the primers used for cysteine mutagenesis reactions on minigenes sequences.
Site-directed mutagenesis reactions were performed on the amino and carboxy terminal minigene constructs, the primers for mutations close to the ends of the minigene sequences were re-designed. The mutated base pairs are indicated in red and underlined, and the conversions of amino acids are shown in the table.

Chapter 8. General Discussion

The aim of this thesis was to investigate the contribution of $P2X_1$ receptor intracellular amino and carboxy termini to channel function. A range of approaches, including subunit concatenation, electrophysiological cysteine scanning and biochemical methods have been used to characterizing the roles of intracellular domains for $P2X_1$ receptor modulation.

Predicted secondary structure for intracellular domains

Site-directed cysteine substitution has been used to study the intracellular residues and the residues important for channel properties were determined (Table 8.1). In addition, this study also provided information for the intracellular secondary structures by testing the amino acid accessibility using MTS compounds. For the amino terminus, cysteine substitutions at Val^{29}, Lys^{27}, Asn^{26} and Val^{24} exhibited significant potentiations to MTSEA. These residues may locate at positions sensitive to the MTSEA modifications and suggest a beta-sheet arrangement pattern in this segment. This observation was confirmed by protein structure prediction (PSIPRED, McGuffin *et al*, 2000) (Figure 8.1) which predicts the secondary structure based on the profile of individual amino acids. PMA treatments indicated the interactions between the regions next to the TM2 and residues after the YXXXK trafficking motif at the carboxy terminal (Table 8.2), these residues therefore could be easily accessible by regulatory factors and suggested to be beta-sheet structure by PSIPRED as well.

Figure 8.1 Sequences alignment of the intracellular domains of $P2X_1$ receptor
Secondary structure predictions (PSIPRED, McGuffin *et al*, 2000) for the $P2X_1$ receptor amino and carboxy termini are shown above, and the residues focused in these thesis were indicated in red circles. Cylinders correspond to alpha-helix and arrows to beta-strands. Conf indicates the confidence of prediction, Pred for predicted secondary structure and Aa for target sequence.

MTSEA	TC	N-terminal	No	C-terminal	TC	MTSEA
Inhibition	NE	Gly^{30}	1	His^{355}	NE	Accessible
Accessible	NE	Val^{29}	2	Ile^{356}	NE	Accessible
NE	Slower	Lys^{28}	3	Leu^{357}	Slower	Accessible
Accessible	NE	Lys^{27}	4	Pro^{358}	NE	NE
Accessible	NE	Asn^{26}	5	Lys^{359}	NE	Accessible
NE	NE	Arg^{25}	6	Arg^{360}	Faster	Accessible
Accessible	NE	Val^{24}	7	His^{361}	NE	Accessible
NE	Slower	Leu^{23}	8	*Tyr^{362}	NE	Accessible
NE	Faster	Val^{22}	9	Tyr^{363}	Faster	NE
Accessible	NE	Met^{21}	10	Lys^{364}	NE	Accessible
NE	Slower	Arg^{20}	11	Gln^{365}	NE	NE
Inhibition	Faster	Pro^{19}	12	Lys^{366}	NE	NE
NE	Slower	Thr^{18}	13	*Lys^{367}	Faster	NE
NE	NE	Asp^{17}	14	Phe^{368}	NE	NE
Inhibition	NE	Tyr^{16}	15	Lys^{369}	NE	Accessible
			16	Tyr^{370}	Slower	Accessible

Table 8.1 Roles of P2X$_1$ receptor intracellular residues to channel properties
The roles of human P2X$_1$ receptor amino and carboxy terminus to channel properties were studied by cysteine substitutions, and the surface expression (red asterisk for residues involved in protein trafficking), time-course of channel desensitizing (TC) and effects of MTSEA at individual residues are summarized as above. The conserved regulatory motifs (TXTXK/R and YXXXK) are showed in shade and conserved tyrosines are labelled in blue. Significant changes are shown in colors (light/dark blue for slower /faster desensitizing, light/dark green for MTSEA accessible residues and residues showed inhibition effects respectively. (NE: no effect).

mGluR1α	PMA	N-terminal	No	C-terminal	PMA	mGluR1α
sensitive	sensitive	Gly^{30}	1	His^{355}	sensitive	sensitive
insensitive	sensitive	Val^{29}	2	Ile^{356}	insensitive	_
_	insensitive	Lys^{28}	3	Leu^{357}	insensitive	_
sensitive	sensitive	Lys^{27}	4	Pro^{358}	sensitive	sensitive
_	insensitive	Asn^{26}	5	Lys^{359}	insensitive	_
_	insensitive	Arg^{25}	6	Arg^{360}	insensitive	_
_	insensitive	Val^{24}	7	His^{361}	insensitive	_
_	insensitive	Leu^{23}	8	Tyr^{362}	insensitive	_
_	insensitive	Val^{22}	9	Tyr^{363}	sensitive	sensitive
_	insensitive	Met^{21}	10	Lys^{364}	insensitive	_
sensitive	*sensitive	Arg^{20}	11	Gln^{365}	insensitive	_
	insensitive	Pro^{19}	12	Lys^{366}	insensitive	_
sensitive	*sensitive	Thr^{18}	13	Lys^{367}	*sensitive	sensitive
insensitive	*sensitive	Asp^{17}	14	Phe^{368}	sensitive	sensitive
sensitive	sensitive	Tyr^{16}	15	Lys^{369}	sensitive	sensitive
			16	Tyr^{370}	*sensitive*	insensitive

Table 8.2 Roles of P2X$_1$ receptor intracellular residues to phorbol ester and GPCRs regulation
Roles of human P2X$_1$ receptor amino and carboxy terminus to phorbol ester PMA and GPCRs regulation are summarized. The conserved regulatory motifs (TXTXK/R and YXXXK) are shown in shade and conserved tyrosines are labelled in blue. Residues showed sensitivity to PMA mediated effects are shown in pink, the ones that involved in the direct binding with possible regulatory factor are indicated with red asterisk, the ones that showed sensitivity to mGluR1α mediated effects are in green, non-tested residues are indicated in dash.

Substitution dependency

Cysteine replacement was used in the current study; however, substitution variations subject to the converted amino acids were demonstrated. For example the K367A had no difference to surface protein expression level in a previous study (Vial *et al*, 2006), whereas the K367C exerted remarkable reduction in the peak current in this study. The substitution dependence was also demonstrated for channel regulatory mechanisms. The PMA mediated potentiation can triple the $P2X_1$ receptor current at T18A mutant, however it was abolished at T18C. These differences raise the importance of interpretations of the mutagenesis results, and the local amino acid environment is also a contributing factor.

Identification of $P2X_1$ receptor intracellular regulation pathway

The P2X receptor regulation mechanism remains unclear. The properties of the $P2X_1$ receptor are subject to regulation by GPCRs, and similar effects can be mimicked by phorbol ester PMA which stimulates the PKC pathway. This study suggested the novel protein kinase C isoforms may be involved in the regulation of $P2X_1$ receptor. The intracellular tyrosines were also of interest to be further investigated. Although the tyrosine phosphorylation was undetectable, conserved Tyr^{16}, Tyr^{363} and Tyr^{370} were shown to be involved in the phorbol ester and $G\alpha$ coupled GPCRs mediated potentiation and the Tyr^{370} further exhibited a direct binding role for the regulatory protein. In addition, cAMP-dependent protein kinase (PKA) and cyclin-dependent protein kinase 5 (CDK5) also exhibited roles in current potentiation for P2X receptors in PC12 cells (Sato *et al*, 2006). These results increase the complexity for P2X receptors regulation pathway determination. Since the intracellular regulation was suggested be an indirect modification via certain accessory protein (Vial *et al*, 2004a), this accessory protein thus should be involved in diverse regulation mechanisms.

The possibility of the existence of interacting proteins for regulation has been hinted in studies at $P2X_7$ and $P2X_2$ receptors. HSP90 account for about 1-2% of the total cytosolic proteins. It previously demonstrated roles in protein aggregation prevention and refolding (Csermely *et al*, 1998), and showed to be involved in serine, threonine (Lees-Miller *et al*, 1989) and tyrosine phosphorylations (Brouet *et al*, 2001). For the $P2X_7$ receptor, geldanamycine an HSP90 inhibitor decreased the tyrosine phosphorylation of HSP90 and tripled the agonist evoked responses (Adinolfi *et al*,

2003). However, when the potential tyrosine phosphorylation site at the C-terminal was disrupted, this regulation of HSP90 increased and the mutated receptor exerted a much lower sensitivity to agonist that can be recovered by geldanamycine. Thus, the HSP90 was identified as a negative regulator for $P2X_7$ receptor. The proline-rich sequences at the $P2X_2$ receptor C-terminal constituted a range of protein-protein interaction motif including Src homology 3 (SH3), Enabled/VASP homology (EVH1) domains. Masin *et al* (Masin *et al*, 2006) adopt the yeast two-hybrid screening of rat brain cDNA library to investigate the interacting protein for $P2X_2$ receptor C-terminal. Consequently, Fe65 was isolated and a direct inhibitory regulation effect to $P2X_2$ receptor was revealed. The yeast two-hybrid screening could also be a practical way to identify the accessory protein at $P2X_1$ receptor. Alternatively, GST pull-down assay and co-immunoprecipitation methods can also be used for interacting protein identification.

Identification of the intracellular signaling regions

Roles of the intracellular domains in modulation were initially suggested by the concatemer generation and minigene strategy. The concatenated $P2X_1$ channels were generated at the first stage for investigating the roles of individual subunit for whole channel properties. However, the concatenated constructs showed dramatic reductions in the expression levels and significant channel internalization. The intracellular linkage sequence applied to this concatenation could be responsible for these decreased receptor expressions, and thus the intracellular domains were indicated as having essential roles in subunit interaction. Furthermore, the roles of the intracellular domains in channel regulation were revealed by the minigene study. The minigenes encoding the same sequences as amino and carboxy termini respectively abolished the PMA and GPCRs mediated potentiation effects to wild type $P2X_1$ receptor, and both of the intracellular domains were suggested to be involved in the intracellular regulatory mechanism.

The roles individual residues contribute to channel regulation subsequently became an interesting question, and the residues that are close to the transmembrane at amino and carboxy termini were further examined by point substitutions and electrophysiological studies with MTS modification. As a result, the YXTXR/K motif at the amino terminal and the region around the YXXXK motif at the carboxy terminal were highlighted for channel gating and protein trafficking. The intracellular residues lining around the channel pore were also demonstrated to have essential roles in ion conduction

regulation. These imply the interactions between the intracellular motifs and the regions next to channel pore. The functional residues to channel regulations were further studied by phober ester and GPCRs stimulations and further indicating the above assumption. The roles of the P2X$_1$ receptor intracellular residues involved in direct binding to the regulatory factor in the protein kinase regulations were investigated by co-expression of minigenes bearing equivalent mutations, and the channel pore neighboring domains were suggested to have roles in channel conformation and cooperate with the potential binding residues in this modulation pathway.

These current findings implicate the interactions between the proposed regulatory motifs and gating residues at the intracellular domains. Although the signal conduction mechanisms between these regions are still unclear, these regions may be close to each other in structure and react to the regulatory signaling together. At the amino terminus, the resides Asp[17], Thr[18] and Arg[20] that are around the conserved PKC motif were considered with the binding with the regulatory factor, while the residues clustered to the channel pore that also exhibited roles in phorbol ester mediated regulation showed no direct binding role in this modulation. The linkage between these two regions in P2X$_1$ receptor signaling cascades indicates an adjacency in topology. Structural model will aid to confirm this possibility.

Interaction between P2X$_1$ receptor amino and carboxyl termini

The interactions between the amino and carboxy terminus were also suggested in previous studies. The P2X$_1$ and P2X$_2$ chimeras were first generated by Werner *et al* (Werner *et al*, 1996), and the interactions between the two intracellular terminals are required for channel desensitizing. Subsequently, the amino terminal and carboxy termini demonstrated combined actions in channel desensitization at P2X$_5$ receptors. Le's group generated a chimera containing the amino acids 1-318 of human P2X$_5$ receptor and residue 318-455 of rat P2X$_5$ receptor by using a natural BamHI site (Le *et al*, 1997). The human-rat P2X$_5$ chimera made of the N-terminal domain of hP2X$_5$ linked to the C-terminal domain of rP2X$_5$ and expressed functionally in *Xenopus* oocytes. Both of the human and rat P2X$_5$ receptor exhibited little desensitization during the application of ATP. However, over 90% of the peak amplitudes of this artificial P2X$_5$ channel to 100 µM ATP ran down within 2 seconds application of ATP and cannot recover from desensitization after the 700 seconds washing off. Despite the high

sequence similarity with non-desensitizing wild type P2X$_5$ receptor, the chimeric channel displayed a unique property in desensitization. Therefore, this study suggested the contribution of the intracelluar domains of P2X$_5$ receptor to channel desensitizing and its kinetics is dependent on subtle changes in structure.

Cysteine substitution combining with the chemical cross-linking is practical way to investigate the interacting residues in proximity. The intersubunit cross-talk between the extracellular loops of neighboring subunits has been currently identified (Marquez-Klaka *et al*, 2007). Eight amino acids showed to be important for ATP sensitivity were substituted by cysteine residues, and intersubunit binding disulfide bonds between K68C/F291C and K68C/K309C were revealed. Thus these residues Lys^{68}, Phe^{291} and Lys^{309} from neighboring subunits showed proximity and contribute to the intersubunit ATP binding site together. Cysteines were individually introduced to the first and secondary transmembrane regions as well (Rassendren *et al*, 1997; Jiang *et al*, 2001). The residues Val^{48} at the TM1 and Ile^{328} at the TM2 were shown to be essential for channel gating respectively, and the formation of disulfide bonds revealed by cross-linking between the Val^{48} and Ile^{328} in adjacent subunits suggesting the possible intersubunit cross-talk for functional modulation (Jiang *et al*, 2003). These raise the possibilities of the intracellular residues close to the transmembrane segments of both amino and carboxy terminus may interact to modulate P2X$_1$ receptors in adjacency.

The locations of the functional residues to P2X receptor property maintaining and regulation were compared as showed in table 8.1 and 8.2. It is interesting that the regions for channel conformation changing during normal condition, the regions for channel gating during the regulation and the ones having direct interaction with regulatory factors are located at positions of similar distance from the transmembrane segments for both intracellular terminals (See figure 8.2). It raises the possibility of interactions between the intracellular domains of neighboring subunits. The cross talk between specific amino and carboxy terminal residues has been demonstrated at the P2X$_1$ receptor. The alanine replacement at either Thr^{18} of amino terminal or Lys^{367} of carboxy terminal produced non-functional receptors; however, co-expression of both mutants can partially rescue the amplitude of responses (Vial *et al*, 2006). This observation suggested the formation of heterotrimeric channels, and remained one pair

of wild type amino and carboxy terminal from adjacent subunits contribute to the recovered currents. Since both residues have similar distance to the transmembrane segments and contribute to the direct interacting with possible regulatory factor to the P2X$_1$ receptor responses modulation, the Thr^{18} and Lys^{367} and adjacent residues may comprise a potential intersubunit docking site (Figure 8.2). Moreover, the intersubunit interactions may be also required for the regions close to the TMs that contribute to the regulation via controlling the gating properties. As a further research direction, the potential interactions between the intracellular terminal transmembrane proximal regions can be estimated by chemical cross-linking approach to probe the potential linkages between the cysteine mutants in pairs, for instance from N26C to G30C for amino termini and from H355C to K359C for carboxy termini that have been generated in present study.
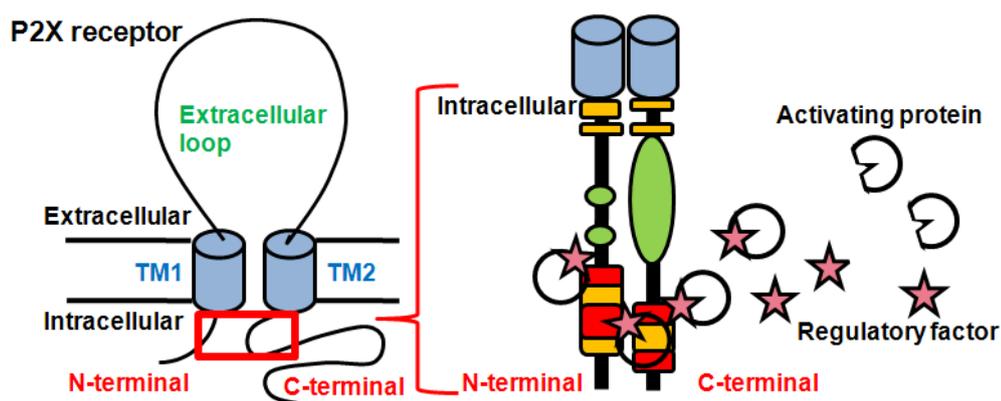

Figure 8.2 Schematic of possible interactions between amino and carboxyl termini
Both intracellular termini are involved in the P2X$_1$ receptor (left panel) regulation, and an intersubunit regulatory site may form between the amino and carboxy termini. The intracellular regions close to the TMs (right panel) were focused. Possible regulatory factor (pink star) activates by the activating protein (white) and acts on the P2X$_1$ receptor. Since the regions contribute to channel conformation changing in normal condition (green), ion conduction and channel conformation changing during regulation (yellow) and the direct interacting with the accessory regulatory factor (red) at both intracellular domains have similar distance to the transmemrbane segments, the regulation may via a cooperation of two intracellular termini and a potential intersubunit docking site for regulatory factor were proposed as shown.

The overall results suggested the involvement of intracellular regions in interactions with regulatory protein and subsequent channel regulation. To conclude, this research is expected to provide better understanding to the intracellular signaling regulatory pathway of P2X$_1$ receptors, and build up the directions for future studies.

References

ABBRACCHIO, M. P. & BURNSTOCK, G. (1994) Purinoceptors: are there families of P2X and P2Y purinoceptors? *Pharmacol Ther,* 64**,** 445-75.

ABBRACCHIO, M. P., BOEYNAEMS, J. M., BARNARD, E. A., BOYER, J. L., KENNEDY, C., MIRAS-PORTUGAL, M. T., KING, B. F., GACHET, C., JACOBSON, K. A., WEISMAN, G. A. & BURNSTOCK, G. (2003) Characterization of the UDP-glucose receptor (re-named here the P2Y14 receptor) adds diversity to the P2Y receptor family. *Trends Pharmacol Sci,* 24**,** 52-5.

ADINOLFI, E., KIM, M., YOUNG, M. T., DI VIRGILIO, F. & SURPRENANT, A. (2003) Tyrosine phosphorylation of HSP90 within the P2X7 receptor complex negatively regulates P2X7 receptors. *J Biol Chem,* 278**,** 37344-51.

AGBOH, K.C., WEBB, T.E.,EVANS, R.J. & ENNION, S.J. (2004) Functional characterization of a P2X receptor from Schistosoma mansoni. *J Biol Chem*, 297, 41650-57.

AKABAS, M. H., STAUFFER, D. A., XU, M. & KARLIN, A. (1992) Acetylcholine receptor channel structure probed in cysteine-substitution mutants. *Science,* 258**,** 307-10.

AKABAS, M. H., KAUFMANN, C., ARCHDEACON, P. & KARLIN, A. (1994) Identification of acetylcholine receptor channel-lining residues in the entire M2 segment of the alpha subunit. *Neuron,* 13**,** 919-27.

ARMSTRONG, N., MAYER, M. & GOUAUX, E. (2003) Tuning activation of the AMPA-sensitive GluR2 ion channel by genetic adjustment of agonist-induced conformational changes. *Proc Natl Acad Sci U S A,* 100**,** 5736-41.

ASE, A. R., RAOUF, R., BELANGER, D., HAMEL, E. & SEGUELA, P. (2005) Potentiation of P2X1 ATP-gated currents by 5-hydroxytryptamine 2A receptors involves diacylglycerol-dependent kinases and intracellular calcium. *J Pharmacol Exp Ther,* 315**,** 144-54.

BADDILEY, J., MICHELSON, A. M. & TODD, A.R. (1949) Nucleotides. Part II. A synthesis of adenosine triphosphate. *J Chem Soc,* 582-86.

BARRERA, N. P., ORMOND, S. J., HENDERSON, R. M., MURRELL-LAGNADO, R. D. & EDWARDSON, J. M. (2005) Atomic force microscopy imaging demonstrates that P2X2 receptors are trimers but that P2X6 receptor subunits do not oligomerize. *J Biol Chem,* 280**,** 10759-65.

BAUMANN, S. W., BAUR, R. & SIGEL, E. (2001) Subunit arrangement of gamma-aminobutyric acid type A receptors. *J Biol Chem,* 276**,** 36275-80.

BENHAM, C. D. & TSIEN, R. W. (1987) A novel receptor-operated Ca2+-permeable channel activated by ATP in smooth muscle. *Nature,* 328**,** 275-8.

BO, X., ZHANG, Y., NASSAR, M., BURNSTOCK, G. & SCHOEPFER, R. (1995) A P2X purinoceptor cDNA conferring a novel pharmacological profile. *FEBS Lett,* 375**,** 129-33.

BOBANOVIC, L. K., ROYLE, S. J. & MURRELL-LAGNADO, R. D. (2002) P2X receptor trafficking in neurons is subunit specific. *J Neurosci,* 22**,** 4814-24.

BODDEKE, H. W., HOFFMAN, B. J., PALACIOS, J. M. & HOYER, D. (1993) Calcineurin inhibits desensitization of cloned rat 5-HT1C receptors. *Naunyn Schmiedebergs Arch Pharmacol,* 348**,** 221-4.

BODIN, P. & BURNSTOCK, G. (2001) Purinergic signalling: ATP release. *Neurochem Res,* 26**,** 959-69.

BOUE-GRABOT, E., ARCHAMBAULT, V. & SEGUELA, P. (2000) A protein kinase C site highly conserved in P2X subunits controls the desensitization kinetics of P2X(2) ATP-gated channels. *J Biol Chem,* 275**,** 10190-5.

BOUE-GRABOT, E., BARAJAS-LOPEZ, C., CHAKFE, Y., BLAIS, D., BELANGER, D., EMERIT, M. B. & SEGUELA, P. (2003) Intracellular cross talk and physical interaction between two classes of neurotransmitter-gated channels. *J Neurosci,* 23**,** 1246-53.

BOUE-GRABOT, E., EMERIT, M. B., TOULME, E., SEGUELA, P. & GARRET, M. (2004) Cross-talk and co-trafficking between rho1/GABA receptors and ATP-gated channels. *J Biol Chem,* 279**,** 6967-75.

BOYD, G. W., LOW, P., DUNLOP, J. I., ROBERTSON, L. A., VARDY, A., LAMBERT, J. J., PETERS, J. A. & CONNOLLY, C. N. (2002) Assembly and cell surface expression of homomeric and heteromeric 5-HT3 receptors: the role of oligomerization and chaperone proteins. *Mol Cell Neurosci,* 21**,** 38-50.

BRAKE, A. J., WAGENBACH, M. J. & JULIUS, D. (1994) New structural motif for ligand-gated ion channels defined by an ionotropic ATP receptor. *Nature,* 371**,** 519-23.

BRANDLE, U., SPIELMANNS, P., OSTEROTH, R., SIM, J., SURPRENANT, A., BUELL, G., RUPPERSBERG, J. P., PLINKERT, P. K., ZENNER, H. P. & GLOWATZKI, E. (1997) Desensitization of the P2X(2) receptor controlled by alternative splicing. *FEBS Lett,* 404**,** 294-8.

BROUET, A., SONVEAUX, P., DESSY, C., BALLIGAND, J. L. & FERON, O. (2001) Hsp90 ensures the transition from the early Ca2+-dependent to the late phosphorylation-dependent activation of the endothelial nitric-oxide synthase in vascular endothelial growth factor-exposed endothelial cells. *J Biol Chem,* 276**,** 32663-9.

BROWN, S. G., TOWNSEND-NICHOLSON, A., JACOBSON, K. A., BURNSTOCK, G. & KING, B. F. (2002) Heteromultimeric P2X(1/2) receptors show a novel

sensitivity to extracellular pH. *J Pharmacol Exp Ther,* 300**,** 673-80.

BUELL, G., LEWIS, C., COLLO, G., NORTH, R. A. & SURPRENANT, A. (1996) An antagonist-insensitive P2X receptor expressed in epithelia and brain. *EMBO J,* 15**,** 55-62.

BURNSTOCK, G., CAMPBELL, G., SATCHELL, D. & SMYTHE, A. (1970) Evidence that adenosine triphosphate or a related nucleotide is the transmitter substance released by non-adrenergic inhibitory nerves in the gut. *Br J Pharmacol,* 40**,** 668-88.

BURNSTOCK, G., DUMSDAY, B. & SMYTHE, A. (1972) Atropine resistant excitation of the urinary bladder: the possibility of transmission via nerves releasing a purine nucleotide. *Br J Pharmacol,* 44**,** 451-61.

BURNSTOCK, G. (1978) *A basis for distinguishing two types of purinergic receptors,* New York, Raven Press.

BURNSTOCK, G. & KENNEDY, C. (1985) Is there a basis for distinguishing two types of P2-purinoceptor? *Gen Pharmacol,* 16**,** 433-40.

BURNSTOCK, G. (1996a) P2 purinoceptors: historical perspective and classification. *Ciba Found Symp,* 198**,** 1-28; discussion 29-34.

BURNSTOCK, G. & WOOD, J. N. (1996b) Purinergic receptors: their role in nociception and primary afferent neurotransmission. *Curr Opin Neurobiol,* 6**,** 526-32.

CALDWELL, P. C. & KEYNES, R. D. (1957) The utilization of phosphate bond energy for sodium extrusion from giant axons. *J Physiol,* 137**,** 12-3P.

CALVERT, J. A. & EVANS, R. J. (2004) Heterogeneity of P2X receptors in sympathetic neurons: contribution of neuronal P2X1 receptors revealed using knockout mice. *Mol Pharmacol,* 65**,** 139-48.

CAO, L., YOUNG, M. T., BROOMHEAD, H. E., FOUNTAIN, S. J. & NORTH, R. A. (2007) Thr339-to-serine substitution in rat P2X2 receptor second transmembrane domain causes constitutive opening and indicates a gating role for Lys308. *J Neurosci,* 27**,** 12916-23.

CHAMBERS, J. K., MACDONALD, L. E., SARAU, H. M., AMES, R. S., FREEMAN, K., FOLEY, J. J., ZHU, Y., MCLAUGHLIN, M. M., MURDOCK, P., MCMILLAN, L., TRILL, J., SWIFT, A., AIYAR, N., TAYLOR, P., VAWTER, L., NAHEED, S., SZEKERES, P., HERVIEU, G., SCOTT, C., WATSON, J. M., MURPHY, A. J., DUZIC, E., KLEIN, C., BERGSMA, D. J., WILSON, S. & LIVI, G. P. (2000) A G protein-coupled receptor for UDP-glucose. *J Biol Chem,* 275**,** 10767-71.

CHAUMONT, S., JIANG, L. H., PENNA, A., NORTH, R. A. & RASSENDREN, F. (2004) Identification of a trafficking motif involved in the stabilization and

polarization of P2X receptors. *J Biol Chem,* 279, 29628-38.

CHEN, C. C., AKOPIAN, A. N., SIVILOTTI, L., COLQUHOUN, D., BURNSTOCK, G. & WOOD, J. N. (1995) A P2X purinoceptor expressed by a subset of sensory neurons. *Nature,* 377, 428-31.

CHO, H. C., TSUSHIMA, R. G., NGUYEN, T. T., GUY, H. R. & BACKX, P. H. (2000) Two critical cysteine residues implicated in disulfide bond formation and proper folding of Kir2.1. *Biochemistry,* 39, 4649-57.

CHOMA, C., GRATKOWSKI, H., LEAR, J. D. & DEGRADO, W. F. (2000) Asparagine-mediated self-association of a model transmembrane helix. *Nat Struct Biol,* 7, 161-6.

CHOW, Y. W. & WANG, H. L. (1998) Functional modulation of P2X2 receptors by cyclic AMP-dependent protein kinase. *J Neurochem,* 70, 2606-12.

CHUNG, M. K., GULER, A. D. & CATERINA, M. J. (2008) TRPV1 shows dynamic ionic selectivity during agonist stimulation. *Nat Neurosci,* 11, 555-64.

CLYNE, J. D., WANG, L. F. & HUME, R. I. (2002a) Mutational analysis of the conserved cysteines of the rat P2X2 purinoceptor. *J Neurosci,* 22, 3873-80.

CLYNE, J. D., LAPOINTE, L. D. & HUME, R. I. (2002b) The role of histidine residues in modulation of the rat P2X(2) purinoceptor by zinc and pH. *J Physiol,* 539, 347-59.

COCKAYNE, D. A., HAMILTON, S. G., ZHU, Q. M., DUNN, P. M., ZHONG, Y., NOVAKOVIC, S., MALMBERG, A. B., CAIN, G., BERSON, A., KASSOTAKIS, L., HEDLEY, L., LACHNIT, W. G., BURNSTOCK, G., MCMAHON, S. B. & FORD, A. P. (2000) Urinary bladder hyporeflexia and reduced pain-related behaviour in P2X3-deficient mice. *Nature,* 407, 1011-5.

COLLO, G., NORTH, R. A., KAWASHIMA, E., MERLO-PICH, E., NEIDHART, S., SURPRENANT, A. & BUELL, G. (1996) Cloning OF P2X5 and P2X6 receptors and the distribution and properties of an extended family of ATP-gated ion channels. *J Neurosci,* 16, 2495-507.

COMMUNI, D., GONZALEZ, N. S., DETHEUX, M., BREZILLON, S., LANNOY, V., PARMENTIER, M. & BOEYNAEMS, J. M. (2001) Identification of a novel human ADP receptor coupled to G(i). *J Biol Chem,* 276, 41479-85.

CSERMELY, P., SCHNAIDER, T., SOTI, C., PROHASZKA, Z. & NARDAI, G. (1998) The 90-kDa molecular chaperone family: structure, function, and clinical applications. A comprehensive review. *Pharmacol Ther,* 79, 129-68.

DAVIES, R. E. (1963) A Molecular Theory of Muscle Contraction: Calcium-Dependent Contractions with Hydrogen Bond Formation Plus Atp-Dependent Extensions of Part of the Myosin-Actin Cross-Bridges. *Nature,* 199, 1068-74.

DAVIES, D. L., MACHU, T. K., GUO, Y. & ALKANA, R. L. (2002) Ethanol sensitivity in ATP-gated P2X receptors is subunit dependent. *Alcohol Clin Exp Res,* 26**,** 773-8.

DAVIES, D.L., KOCHEGAROV,A.A., KUO, S.T.,KULKARNI, A.A., WOODWARD, J.J. KING. B.F. & ALKANA, R.L. (2005) Ethanol differentially affects ATP-gated P2X$_3$ and P2X$_4$ receptor subtypes expressed in *Xenopus* oocytes. *J Neuropharm*, 49,243-53.

DEL GATTO, F., GESNEL, M. C. & BREATHNACH, R. (1996) The exon sequence TAGG can inhibit splicing. *Nucleic Acids Res,* 24**,** 2017-21.

DENLINGER, L. C., SOMMER, J. A., PARKER, K., GUDIPATY, L., FISETTE, P. L., WATTERS, J. W., PROCTOR, R. A., DUBYAK, G. R. & BERTICS, P. J. (2003) Mutation of a dibasic amino acid motif within the C terminus of the P2X7 nucleotide receptor results in trafficking defects and impaired function. *J Immunol,* 171**,** 1304-11.

DIGBY, H. R., ROBERTS, J. A., SUTCLIFFE, M. J. & EVANS, R. J. (2005) Contribution of conserved glycine residues to ATP action at human P2X1 receptors: mutagenesis indicates that the glycine at position 250 is important for channel function. *J Neurochem,* 95**,** 1746-54.

DING, S. & SACHS, F. (1999) Ion permeation and block of P2X(2) purinoceptors: single channel recordings. *J Membr Biol,* 172**,** 215-23.

DING, S. & SACHS, F. (2000) Inactivation of P2X2 purinoceptors by divalent cations. *J Physiol,* 522 Pt 2**,** 199-214.

DRURY, A. N. & SZENT-GYORGYI, A. (1929) The physiological activity of adenine compounds with especial reference to their action upon the mammalian heart. *J Physiol,* 68**,** 213-37.

EGAN, T. M., HAINES, W. R. & VOIGT, M. M. (1998) A domain contributing to the ion channel of ATP-gated P2X2 receptors identified by the substituted cysteine accessibility method. *J Neurosci,* 18**,** 2350-9.

EGAN, T. M. & KHAKH, B. S. (2004) Contribution of calcium ions to P2X channel responses. *J Neurosci,* 24**,** 3413-20.

EICKHORST, A. N., BERSON, A., COCKAYNE, D., LESTER, H. A. & KHAKH, B. S. (2002) Control of P2X(2) channel permeability by the cytosolic domain. *J Gen Physiol,* 120**,** 119-31.

EILLIOTT, W. H. EILLIOTT, D.C. (2005) *Biochemistry and molecular biology,* Italy, Oxford University press.

ENNION, S., HAGAN, S. & EVANS, R. J. (2000) The role of positively charged amino acids in ATP recognition by human P2X(1) receptors. *J Biol Chem,* 275**,** 29361-7.

ENNION, S. J., RITSON, J. & EVANS, R. J. (2001) Conserved negatively charged residues are not required for ATP action at P2X(1) receptors. *Biochem Biophys Res Commun,* 289**,** 700-4.

ENNION, S. J. & EVANS, R. J. (2002a) P2X(1) receptor subunit contribution to gating revealed by a dominant negative PKC mutant. *Biochem Biophys Res Commun,* 291**,** 611-6.

ENNION, S. J. & EVANS, R. J. (2002b) Conserved cysteine residues in the extracellular loop of the human P2X(1) receptor form disulfide bonds and are involved in receptor trafficking to the cell surface. *Mol Pharmacol,* 61**,** 303-11.

ERB, L., GARRAD, R., WANG, Y., QUINN, T., TURNER, J. T. & WEISMAN, G. A. (1995) Site-directed mutagenesis of P2U purinoceptors. Positively charged amino acids in transmembrane helices 6 and 7 affect agonist potency and specificity. *J Biol Chem,* 270**,** 4185-8.

EVANS, R. J. & KENNEDY, C. (1994) Characterization of P2-purinoceptors in the smooth muscle of the rat tail artery: a comparison between contractile and electrophysiological responses. *Br J Pharmacol,* 113**,** 853-60.

EVANS, R. J., LEWIS, C., BUELL, G., VALERA, S., NORTH, R. A. & SURPRENANT, A. (1995) Pharmacological characterization of heterologously expressed ATP-gated cation channels (P2x purinoceptors). *Mol Pharmacol,* 48**,** 178-83.

EVANS, R. J., LEWIS, C., VIRGINIO, C., LUNDSTROM, K., BUELL, G., SURPRENANT, A. & NORTH, R. A. (1996) Ionic permeability of, and divalent cation effects on, two ATP-gated cation channels (P2X receptors) expressed in mammalian cells. *J Physiol,* 497 (Pt 2)**,** 413-22.

EVANS, R. J. (2008) Orthosteric and allosteric binding sites of P2X receptors. *Eur Biophys J.*

FENG, Y. H., LI, X., WANG, L., ZHOU, L. & GORODESKI, G. I. (2006) A truncated P2X7 receptor variant (P2X7-j) endogenously expressed in cervical cancer cells antagonizes the full-length P2X7 receptor through hetero-oligomerization. *J Biol Chem,* 281**,** 17228-37.

FIRSOV, D., GAUTSCHI, I., MERILLAT, A. M., ROSSIER, B. C. & SCHILD, L. (1998) The heterotetrameric architecture of the epithelial sodium channel (ENaC). *EMBO J,* 17**,** 344-52.

FISKE, C. H. & SUBBAROW, Y. (1929) Phosphorus Compounds of Muscle and Liver. *Science,* 70**,** 381-382.

FOUNTAIN, S. J. & NORTH, R. A. (2006) A C-terminal lysine that controls human P2X4 receptor desensitization. *J Biol Chem,* 281**,** 15044-9.

FOUNTAIN, S. J., PARKINSON, K., YOUNG, M. T., CAO, L., THOMPSON, C. R. & NORTH, R. A. (2007) An intracellular P2X receptor required for osmoregulation in Dictyostelium discoideum. *Nature,* 448**,** 200-3.

FRANKLIN, C., BRAAM, U., EISELE, T., SCHMALZING, G. & HAUSMANN, R. (2007) Lack of evidence for direct phosphorylation of recombinantly expressed P2X(2) and P2X (3) receptors by protein kinase C. *Purinergic Signal,* 3**,** 377-88.

GITTERMAN, D. P. & EVANS, R. J. (2000) Properties of P2X and P2Y receptors are dependent on artery diameter in the rat mesenteric bed. *Br J Pharmacol,* 131**,** 1561-8.

GOLAN, D.E., TASHJIAN, A.H., ARMSTRONG, E.J. & GALANTER, J.M. (2005) *Principles of pharmacology: the pathophysiologic basis of drug therapy.* Philadelphia: Lippincott Williams&Wilkins.

GUO, C., MASIN, M., QURESHI, O. S. & MURRELL-LAGNADO, R. D. (2007) Evidence for functional P2X4/P2X7 heteromeric receptors. *Mol Pharmacol,* 72**,** 1447-56.

HAINES, W. R., MIGITA, K., COX, J. A., EGAN, T. M. & VOIGT, M. M. (2001) The first transmembrane domain of the P2X receptor subunit participates in the agonist-induced gating of the channel. *J Biol Chem,* 276**,** 32793-8.

HALL, A. C., TURCOTTE, C. M., BETTS, B. A., YEUNG, W. Y., AGYEMAN, A. S. & BURK, L. A. (2004) Modulation of human GABAA and glycine receptor currents by menthol and related monoterpenoids. *Eur J Pharmacol,* 506**,** 9-16.

HECHLER, B., LENAIN, N., MARCHESE, P., VIAL, C., HEIM, V., FREUND, M., CAZENAVE, J. P., CATTANEO, M., RUGGERI, Z. M., EVANS, R. & GACHET, C. (2003) A role of the fast ATP-gated P2X1 cation channel in thrombosis of small arteries in vivo. *J Exp Med,* 198**,** 661-7.

HECHLER, B., MAGNENAT, S., ZIGHETTI, M. L., KASSACK, M. U., ULLMANN, H., CAZENAVE, J. P., EVANS, R., CATTANEO, M. & GACHET, C. (2005) Inhibition of platelet functions and thrombosis through selective or nonselective inhibition of the platelet P2 receptors with increasing doses of NF449 [4,4',4",4'''-(carbonylbis(imino-5,1,3-benzenetriylbis-(carbonylimino)))t etrakis-benzene-1,3-disulfonic acid octasodium salt]. *J Pharmacol Exp Ther,* 314**,** 232-43.

HOLLOPETER, G., JANTZEN, H. M., VINCENT, D., LI, G., ENGLAND, L., RAMAKRISHNAN, V., YANG, R. B., NURDEN, P., NURDEN, A., JULIUS, D. & CONLEY, P. B. (2001) Identification of the platelet ADP receptor targeted by antithrombotic drugs. *Nature,* 409**,** 202-7.

HOLMGREN, M., LIU, Y., XU, Y. & YELLEN, G. (1996) On the use of thiol-modifying agents to determine channel topology. *Neuropharmacology,* 35**,** 797-804.

HOLTON, F. A. & HOLTON, P. (1954) The capillary dilator substances in dry powders of spinal roots; a possible role of adenosine triphosphate in chemical transmission from nerve endings. *J Physiol,* 126**,** 124-40.

HOLTON, P. (1959) The liberation of adenosine triphosphate on antidromic stimulation of sensory nerves. *J Physiol,* 145**,** 494-504.

HUANG, X. Y., MORIELLI, A. D. & PERALTA, E. G. (1993) Tyrosine kinase-dependent suppression of a potassium channel by the G protein-coupled m1 muscarinic acetylcholine receptor. *Cell,* 75**,** 1145-56.

HURST, R. S., NORTH, R. A. & ADELMAN, J. P. (1995) Potassium channel assembly from concatenated subunits: effects of proline substitutions in S4 segments. *Receptors Channels,* 3**,** 263-72.

ISACOFF, E. Y., JAN, Y. N. & JAN, L. Y. (1990) Evidence for the formation of heteromultimeric potassium channels in Xenopus oocytes. *Nature,* 345**,** 530-4.

JACOBSON, K. A., KIM, Y. C., WILDMAN, S. S., MOHANRAM, A., HARDEN, T. K., BOYER, J. L., KING, B. F. & BURNSTOCK, G. (1998) A pyridoxine cyclic phosphate and its 6-azoaryl derivative selectively potentiate and antagonize activation of P2X1 receptors. *J Med Chem,* 41**,** 2201-6.

JARVIS, M. F., BURGARD, E. C., MCGARAUGHTY, S., HONORE, P., LYNCH, K., BRENNAN, T. J., SUBIETA, A., VAN BIESEN, T., CARTMELL, J., BIANCHI, B., NIFORATOS, W., KAGE, K., YU, H., MIKUSA, J., WISMER, C. T., ZHU, C. Z., CHU, K., LEE, C. H., STEWART, A. O., POLAKOWSKI, J., COX, B. F., KOWALUK, E., WILLIAMS, M., SULLIVAN, J. & FALTYNEK, C. (2002) A-317491, a novel potent and selective non-nucleotide antagonist of P2X3 and P2X2/3 receptors, reduces chronic inflammatory and neuropathic pain in the rat. *Proc Natl Acad Sci U S A,* 99**,** 17179-84.

JIANG, Q., GUO, D., LEE, B. X., VAN RHEE, A. M., KIM, Y. C., NICHOLAS, R. A., SCHACHTER, J. B., HARDEN, T. K. & JACOBSON, K. A. (1997) A mutational analysis of residues essential for ligand recognition at the human P2Y1 receptor. *Mol Pharmacol,* 52**,** 499-507.

JIANG, L. H., RASSENDREN, F., SPELTA, V., SURPRENANT, A. & NORTH, R. A. (2001) Amino acid residues involved in gating identified in the first membrane-spanning domain of the rat P2X(2) receptor. *J Biol Chem,* 276**,** 14902-8.

JIANG, L. H., KIM, M., SPELTA, V., BO, X., SURPRENANT, A. & NORTH, R. A. (2003) Subunit arrangement in P2X receptors. *J Neurosci,* 23**,** 8903-10.

JO, Y. H. & SCHLICHTER, R. (1999) Synaptic corelease of ATP and GABA in cultured spinal neurons. *Nat Neurosci,* 2**,** 241-5.

JONES, C. A., VIAL, C., SELLERS, L. A., HUMPHREY, P. P., EVANS, R. J. & CHESSELL, I. P. (2004) Functional regulation of P2X6 receptors by N-linked glycosylation: identification of a novel alpha beta-methylene ATP-sensitive

phenotype. *Mol Pharmacol,* 65**,** 979-85.

KHAKH, B. S., HUMPHREY, P. P. & SURPRENANT, A. (1995) Electrophysiological properties of P2X-purinoceptors in rat superior cervical, nodose and guinea-pig coeliac neurones. *J Physiol,* 484 (Pt 2)**,** 385-95.

KHAKH, B. S., BAO, X. R., LABARCA, C. & LESTER, H. A. (1999) Neuronal P2X transmitter-gated cation channels change their ion selectivity in seconds. *Nat Neurosci,* 2**,** 322-30.

KHAKH, B. S., BURNSTOCK, G., KENNEDY, C., KING, B. F., NORTH, R. A., SEGUELA, P., VOIGT, M. & HUMPHREY, P. P. (2001) International union of pharmacology. XXIV. Current status of the nomenclature and properties of P2X receptors and their subunits. *Pharmacol Rev,* 53**,** 107-18.

KHAKH, B. S. & NORTH, R. A. (2006) P2X receptors as cell-surface ATP sensors in health and disease. *Nature,* 442**,** 527-32.

KIM, M.,SPELTA, V. SIM, J., NORTH, R.A.& SURPRENANT, A. (2001) Differential assembly of rat purinergic P2X7 receptor in immune cells of the brain and periphery. *J Biol Chem,* 276**,** 23262-7.

KING, B., CHEN, C. C., AKOPIAN, A. N., BURNSTOCK, G. & WOOD, J. N. (1997) A role for calcineurin in the desensitization of the P2X3 receptor. *Neuroreport,* 8**,** 1099-102.

KOSHIMIZU, T., TOMIC, M., KOSHIMIZU, M. & STOJILKOVIC, S. S. (1998) Identification of amino acid residues contributing to desensitization of the P2X2 receptor channel. *J Biol Chem,* 273**,** 12853-7.

KUGELGEN, I. (2005) Pharmacological profiles of cloned mammalian P2Y-receptor subtypes. *Pharmacol Therapeut*, 110, 415-32

KUNAPULI, S. P., DORSAM, R. T., KIM, S. & QUINTON, T. M. (2003) Platelet purinergic receptors. *Curr Opin Pharmacol,* 3**,** 175-80.

KUNER, T., WOLLMUTH, L. P., KARLIN, A., SEEBURG, P. H. & SAKMANN, B. (1996) Structure of the NMDA receptor channel M2 segment inferred from the accessibility of substituted cysteines. *Neuron,* 17**,** 343-52.

LA, M. & RAND, M. J. (1993) Endothelin-1 enhances vasoconstrictor responses to exogenously administered and neurogenically released ATP in rabbit isolated perfused arteries. *Eur J Pharmacol,* 249**,** 133-9.

LABASI, J. M., PETRUSHOVA, N., DONOVAN, C., MCCURDY, S., LIRA, P., PAYETTE, M. M., BRISSETTE, W., WICKS, J. R., AUDOLY, L. & GABEL, C. A. (2002) Absence of the P2X7 receptor alters leukocyte function and attenuates an inflammatory response. *J Immunol,* 168**,** 6436-45.

LANGLEY, J. N. (1878) On the Physiology of the Salivary Secretion: Part II. On the

Mutual Antagonism of Atropin and Pilocarpin, having especial reference to their relations in the Sub-maxillary Gland of the Cat. *J Physiol,* 1**,** 339-69.

LE, K. T., PAQUET, M., NOUEL, D., BABINSKI, K. & SEGUELA, P. (1997) Primary structure and expression of a naturally truncated human P2X ATP receptor subunit from brain and immune system. *FEBS Lett,* 418**,** 195-9.

LE, K. T., BABINSKI, K. & SEGUELA, P. (1998) Central P2X4 and P2X6 channel subunits coassemble into a novel heteromeric ATP receptor. *J Neurosci,* 18**,** 7152-9.

LE, K. T., BOUE-GRABOT, E., ARCHAMBAULT, V. & SEGUELA, P. (1999) Functional and biochemical evidence for heteromeric ATP-gated channels composed of P2X1 and P2X5 subunits. *J Biol Chem,* 274**,** 15415-9.

LEE, T. E., PHILIPSON, L. H., KUZNETSOV, A. & NELSON, D. J. (1994) Structural determinant for assembly of mammalian K+ channels. *Biophys J,* 66**,** 667-73.

LEES-MILLER, S. P. & ANDERSON, C. W. (1989) The human double-stranded DNA-activated protein kinase phosphorylates the 90-kDa heat-shock protein, hsp90 alpha at two NH2-terminal threonine residues. *J Biol Chem,* 264**,** 17275-80.

LESAGE, F., REYES, R., FINK, M., DUPRAT, F., GUILLEMARE, E. & LAZDUNSKI, M. (1996) Dimerization of TWIK-1 K+ channel subunits via a disulfide bridge. *EMBO J,* 15**,** 6400-7.

LEWIS, C., NEIDHART, S., HOLY, C., NORTH, R. A., BUELL, G. & SURPRENANT, A. (1995) Coexpression of P2X2 and P2X3 receptor subunits can account for ATP-gated currents in sensory neurons. *Nature,* 377**,** 432-5.

LI, M., CHANG, T. H., SILBERBERG, S. D. & SWARTZ, K. J. (2008) Gating the pore of P2X receptor channels. *Nat Neurosci,* 11**,** 883-7.

LI, Z., MIGITA, K., SAMWAYS, D. S., VOIGT, M. M. & EGAN, T. M. (2004) Gain and loss of channel function by alanine substitutions in the transmembrane segments of the rat ATP-gated P2X2 receptor. *J Neurosci,* 24**,** 7378-86.

LIMAN, E. R., TYTGAT, J. & HESS, P. (1992) Subunit stoichiometry of a mammalian K+ channel determined by construction of multimeric cDNAs. *Neuron,* 9**,** 861-71.

LIU, D. M. & ADAMS, D. J. (2001) Ionic selectivity of native ATP-activated (P2X) receptor channels in dissociated neurones from rat parasympathetic ganglia. *J Physiol,* 534**,** 423-35.

LIU, G. J., BROCKHAUSEN, J. & BENNETT, M. R. (2003) P2X1 receptor currents after disruption of the PKC site and its surroundings by dominant negative mutations in HEK293 cells. *Auton Neurosci,* 108**,** 12-6.

LOHMANN, K. (1929) On the phosohate fraction in muscle. *Naturwissenschaften,* 17**,** 624-625.

LUSTIG, K. D., SHIAU, A. K., BRAKE, A. J. & JULIUS, D. (1993) Expression cloning of an ATP receptor from mouse neuroblastoma cells. *Proc Natl Acad Sci U S A,* 90**,** 5113-7.

MARQUEZ-KLAKA, B., RETTINGER, J., BHARGAVA, Y., EISELE, T. & NICKE, A. (2007) Identification of an intersubunit cross-link between substituted cysteine residues located in the putative ATP binding site of the P2X1 receptor. *J Neurosci,* 27**,** 1456-66.

MARTINEZ, K. L., CORRINGER, P. J., EDELSTEIN, S. J., CHANGEUX, J. P. & MEROLA, F. (2000) Structural differences in the two agonist binding sites of the Torpedo nicotinic acetylcholine receptor revealed by time-resolved fluorescence spectroscopy. *Biochemistry,* 39**,** 6979-90.

MARTINY-BARON, G., KAZANIETZ, M. G., MISCHAK, H., BLUMBERG, P. M., KOCHS, G., HUG, H., MARME, D. & SCHACHTELE, C. (1993) Selective inhibition of protein kinase C isozymes by the indolocarbazole Go 6976. *J Biol Chem,* 268**,** 9194-7.

MASIN, M., KERSCHENSTEINER, D., DUMKE, K., RUBIO, M. E. & SOTO, F. (2006) Fe65 interacts with P2X2 subunits at excitatory synapses and modulates receptor function. *J Biol Chem,* 281**,** 4100-8.

MCGUFFIN, L. J., BRYSON, K. & JONES, D. T. (2000) The PSIPRED protein structure prediction server. *Bioinformatics,* 16**,** 404-5.

MIO, K., KUBO, Y., OGURA, T., YAMAMOTO, T. & SATO, C. (2005) Visualization of the trimeric P2X2 receptor with a crown-capped extracellular domain. *Biochem Biophys Res Commun,* 337**,** 998-1005.

MULRYAN, K., GITTERMAN, D. P., LEWIS, C. J., VIAL, C., LECKIE, B. J., COBB, A. L., BROWN, J. E., CONLEY, E. C., BUELL, G., PRITCHARD, C. A. & EVANS, R. J. (2000) Reduced vas deferens contraction and male infertility in mice lacking P2X1 receptors. *Nature,* 403**,** 86-9.

NAGAYA, N., TITTLE, R. K., SAAR, N., DELLAL, S. S. & HUME, R. I. (2005) An intersubunit zinc binding site in rat P2X2 receptors. *J Biol Chem,* 280**,** 25982-93.

NAKAZAWA, K., SAITO, H. & MATSUKI, N. (1987) Involvement of calcium in calcium-current inactivation in smooth muscle cells from rat vas deferens. *J Membr Biol,* 100**,** 13-9.

NAKAZAWA, K. & OHNO, Y. (1999) Neighboring glycine residues are essential for P2X2 receptor/channel function. *Eur J Pharmacol,* 370**,** R5-6.

NEWBOLT, A., STOOP, R., VIRGINIO, C., SURPRENANT, A., NORTH, R. A.,

BUELL, G. & RASSENDREN, F. (1998) Membrane topology of an ATP-gated ion channel (P2X receptor). *J Biol Chem,* 273**,** 15177-82.

NICKE, A., BAUMERT, H. G., RETTINGER, J., EICHELE, A., LAMBRECHT, G., MUTSCHLER, E. & SCHMALZING, G. (1998) P2X1 and P2X3 receptors form stable trimers: a novel structural motif of ligand-gated ion channels. *EMBO J,* 17**,** 3016-28.

NICKE, A., RETTINGER, J. & SCHMALZING, G. (2003) Monomeric and dimeric byproducts are the principal functional elements of higher order P2X1 concatamers. *Mol Pharmacol,* 63**,** 243-52.

NICKE, A., KERSCHENSTEINER, D. & SOTO, F. (2005) Biochemical and functional evidence for heteromeric assembly of P2X1 and P2X4 subunits. *J Neurochem,* 92**,** 925-33.

NORTH, R. A. (1996) P2X receptors: a third major class of ligand-gated ion channels. *Ciba Found Symp,* 198**,** 91-105; discussion 105-9.

NORTH, R. A. (2002) Molecular physiology of P2X receptors. *Physiol Rev,* 82**,** 1013-67.

OKKERI, J., LAAKKONEN, L. & HALTIA, T. (2004) The nucleotide-binding domain of the Zn2+-transporting P-type ATPase from Escherichia coli carries a glycine motif that may be involved in binding of ATP. *Biochem J,* 377**,** 95-105.

ORMOND, S. J., BARRERA, N. P., QURESHI, O. S., HENDERSON, R. M., EDWARDSON, J. M. & MURRELL-LAGNADO, R. D. (2006) An uncharged region within the N terminus of the P2X6 receptor inhibits its assembly and exit from the endoplasmic reticulum. *Mol Pharmacol,* 69**,** 1692-700.

PASCUAL, J. M., SHIEH, C. C., KIRSCH, G. E. & BROWN, A. M. (1995) K+ pore structure revealed by reporter cysteines at inner and outer surfaces. *Neuron,* 14**,** 1055-63.

PAUKERT, M., OSTEROTH, R., GEISLER, H. S., BRANDLE, U., GLOWATZKI, E., RUPPERSBERG, J. P. & GRUNDER, S. (2001) Inflammatory mediators potentiate ATP-gated channels through the P2X(3) subunit. *J Biol Chem,* 276**,** 21077-82.

PELEGRIN, P. & SURPRENANT, A. (2007) Pannexin-1 couples to maitotoxin- and nigericin-induced interleukin-1beta release through a dye uptake-independent pathway. *J Biol Chem,* 282**,** 2386-94.

PESSIA, M., TUCKER, S. J., LEE, K., BOND, C. T. & ADELMAN, J. P. (1996) Subunit positional effects revealed by novel heteromeric inwardly rectifying K+ channels. *EMBO J,* 15**,** 2980-7.

PREISIG-MULLER, R., SCHLICHTHORL, G., GOERGE, T., HEINEN, S., BRUGGEMANN, A., RAJAN, S., DERST, C., VEH, R. W. & DAUT, J. (2002)

Heteromerization of Kir2.x potassium channels contributes to the phenotype of Andersen's syndrome. *Proc Natl Acad Sci U S A,* 99**,** 7774-9.

RADFORD, K. M., VIRGINIO, C., SURPRENANT, A., NORTH, R. A. & KAWASHIMA, E. (1997) Baculovirus expression provides direct evidence for heteromeric assembly of P2X2 and P2X3 receptors. *J Neurosci,* 17**,** 6529-33.

RALEVIC, V. & BURNSTOCK, G. (1998) Receptors for purines and pyrimidines. *Pharmacol Rev,* 50**,** 413-92.

RANG, H. P. D., M.M.; RITTER, J.M. (1999) *Pharmacology,* London, Churchhill Livingstone.

RASSENDREN, F., BUELL, G., NEWBOLT, A., NORTH, R. A. & SURPRENANT, A. (1997) Identification of amino acid residues contributing to the pore of a P2X receptor. *EMBO J,* 16**,** 3446-54.

RETTINGER, J., ASCHRAFI, A. & SCHMALZING, G. (2000) Roles of individual N-glycans for ATP potency and expression of the rat P2X1 receptor. *J Biol Chem,* 275**,** 33542-7.

RETTINGER, J. & SCHMALZING, G. (2003) Activation and desensitization of the recombinant P2X1 receptor at nanomolar ATP concentrations. *J Gen Physiol,* 121**,** 451-61.

RETTINGER, J., BRAUN, K., HOCHMANN, H., KASSACK, M. U., ULLMANN, H., NICKEL, P., SCHMALZING, G. & LAMBRECHT, G. (2005) Profiling at recombinant homomeric and heteromeric rat P2X receptors identifies the suramin analogue NF449 as a highly potent P2X1 receptor antagonist. *Neuropharmacology,* 48**,** 461-8.

ROBERTS, J. A. & EVANS, R. J. (2004) ATP binding at human P2X1 receptors. Contribution of aromatic and basic amino acids revealed using mutagenesis and partial agonists. *J Biol Chem,* 279**,** 9043-55.

ROBERTS, J. A. & EVANS, R. J. (2005) Mutagenesis studies of conserved proline residues of human P2X receptors for ATP indicate that proline 272 contributes to channel function. *J Neurochem,* 92**,** 1256-64.

ROBERTS, J. A. & EVANS, R. J. (2006) Contribution of conserved polar glutamine, asparagine and threonine residues and glycosylation to agonist action at human P2X1 receptors for ATP. *J Neurochem,* 96**,** 843-52.

ROBERTS, J. A. & EVANS, R. J. (2007) Cysteine substitution mutants give structural insight and identify ATP binding and activation sites at P2X receptors. *J Neurosci,* 27**,** 4072-82.

ROBERTS, J. A., DIGBY, H. R., KARA, M., EL AJOUZ, S., SUTCLIFFE, M. J. & EVANS, R. J. (2008) Cysteine substitution mutagenesis and the effects of methanethiosulfonate reagents at P2X2 and P2X4 receptors support a core

common mode of ATP action at P2X receptors. *J Biol Chem,* 283**,** 20126-36.

ROSENMUND, C., STERN-BACH, Y. & STEVENS, C. F. (1998) The tetrameric structure of a glutamate receptor channel. *Science,* 280**,** 1596-9.

ROYLE, S. J., BOBANOVIC, L. K. & MURRELL-LAGNADO, R. D. (2002) Identification of a non-canonical tyrosine-based endocytic motif in an ionotropic receptor. *J Biol Chem,* 277**,** 35378-85.

SAGE, S. O., YAMOAH, E. H. & HEEMSKERK, J. W. (2000) The roles of P(2X1)and P(2T AC)receptors in ADP-evoked calcium signalling in human platelets. *Cell Calcium,* 28**,** 119-26.

SALGADO, A. I., CUNHA, R. A. & RIBEIRO, J. A. (2000) Facilitation by P(2) receptor activation of acetylcholine release from rat motor nerve terminals: interaction with presynaptic nicotinic receptors. *Brain Res,* 877**,** 245-50.

SATO, A., ARIMURA, Y., MANAGO, Y., NISHIKAWA, K., AOKI, K., WADA, E., SUZUKI, Y., OSAKA, H., SETSUIE, R., SAKURAI, M., AMANO, T., AOKI, S., WADA, K. & NODA, M. (2006) Parkin potentiates ATP-induced currents due to activation of P2X receptors in PC12 cells. *J Cell Physiol,* 209**,** 172-82.

SAVI, P. & HERBERT, J. M. (2005) Clopidogrel and ticlopidine: P2Y12 adenosine diphosphate-receptor antagonists for the prevention of atherothrombosis. *Semin Thromb Hemost,* 31**,** 174-83.

SCASE, T. J., HEATH, M. F., ALLEN, J. M., SAGE, S. O. & EVANS, R. J. (1998) Identification of a P2X1 purinoceptor expressed on human platelets. *Biochem Biophys Res Commun,* 242**,** 525-8.

SCHUMANN, H. J. (1958) [Noradrenalin and ATP content of sympathetic nerves.]. *Naunyn Schmiedebergs Arch Exp Pathol Pharmakol,* 233**,** 296-300.

SLADEK, C. D. & KAPOOR, J. R. (2001) Neurotransmitter/neuropeptide interactions in the regulation of neurohypophyseal hormone release. *Exp Neurol,* 171**,** 200-9.

SMITH, P. C., KARPOWICH, N., MILLEN, L., MOODY, J. E., ROSEN, J., THOMAS, P. J. & HUNT, J. F. (2002) ATP binding to the motor domain from an ABC transporter drives formation of a nucleotide sandwich dimer. *Mol Cell,* 10**,** 139-49.

SOLLE, M., LABASI, J., PERREGAUX, D. G., STAM, E., PETRUSHOVA, N., KOLLER, B. H., GRIFFITHS, R. J. & GABEL, C. A. (2001) Altered cytokine production in mice lacking P2X(7) receptors. *J Biol Chem,* 276**,** 125-32.

SOTO, F., GARCIA-GUZMAN, M., GOMEZ-HERNANDEZ, J. M., HOLLMANN, M., KARSCHIN, C. & STUHMER, W. (1996) P2X4: an ATP-activated ionotropic receptor cloned from rat brain. *Proc Natl Acad Sci U S A,* 93**,** 3684-8.

SOTO, F., GARCIA-GUZMAN, M. & STUHMER, W. (1997) Cloned ligand-gated channels activated by extracellular ATP (P2X receptors). *J Membr Biol,* 160**,**

91-100.

SOTO, F., LAMBRECHT, G., NICKEL, P., STUHMER, W. & BUSCH, A. E. (1999) Antagonistic properties of the suramin analogue NF023 at heterologously expressed P2X receptors. *Neuropharmacology,* 38**,** 141-9.

SOUSLOVA, V., CESARE, P., DING, Y., AKOPIAN, A. N., STANFA, L., SUZUKI, R., CARPENTER, K., DICKENSON, A., BOYCE, S., HILL, R., NEBENUIS-OOSTHUIZEN, D., SMITH, A. J., KIDD, E. J. & WOOD, J. N. (2000) Warm-coding deficits and aberrant inflammatory pain in mice lacking P2X3 receptors. *Nature,* 407**,** 1015-7.

SPELTA, V., JIANG, L. H., BAILEY, R. J., SURPRENANT, A. & NORTH, R. A. (2003) Interaction between cysteines introduced into each transmembrane domain of the rat P2X2 receptor. *Br J Pharmacol,* 138**,** 131-6.

SPERLAGH, B. & VIZI, E. S. (1991) Effect of presynaptic P2 receptor stimulation on transmitter release. *J Neurochem,* 56**,** 1466-70.

SPERLAGH, B. V., S.E. (1996) Neuronal synthesis, storage and release of ATP. *Seminars in Neuroscience,* 8**,** 11.

STOOP, R., SURPRENANT, A. & NORTH, R. A. (1997) Different sensitivities to pH of ATP-induced currents at four cloned P2X receptors. *J Neurophysiol,* 78**,** 1837-40.

STOOP, R., THOMAS, S., RASSENDREN, F., KAWASHIMA, E., BUELL, G., SURPRENANT, A. & NORTH, R. A. (1999) Contribution of individual subunits to the multimeric P2X(2) receptor: estimates based on methanethiosulfonate block at T336C. *Mol Pharmacol,* 56**,** 973-81.

SUN, H., HU, X. Q., MORADEL, E. M., WEIGHT, F. F. & ZHANG, L. (2003) Modulation of 5-HT3 receptor-mediated response and trafficking by activation of protein kinase C. *J Biol Chem,* 278**,** 34150-7.

SURPRENANT, A., RASSENDREN, F., KAWASHIMA, E., NORTH, R. A. & BUELL, G. (1996) The cytolytic P2Z receptor for extracellular ATP identified as a P2X receptor (P2X7). *Science,* 272**,** 735-8.

TONG, G., SHEPHERD, D. & JAHR, C. E. (1995) Synaptic desensitization of NMDA receptors by calcineurin. *Science,* 267**,** 1510-2.

TORRES, G. E., EGAN, T. M. & VOIGT, M. M. (1998a) Topological analysis of the ATP-gated ionotropic [correction of ionotrophic] P2X2 receptor subunit. *FEBS Lett,* 425**,** 19-23.

TORRES, G. E., HAINES, W. R., EGAN, T. M. & VOIGT, M. M. (1998b) Co-expression of P2X1 and P2X5 receptor subunits reveals a novel ATP-gated ion channel. *Mol Pharmacol,* 54**,** 989-93.

TORRES, G. E., EGAN, T. M. & VOIGT, M. M. (1999) Hetero-oligomeric assembly of P2X receptor subunits. Specificities exist with regard to possible partners. *J Biol Chem,* 274**,** 6653-9.

TOTH-ZSAMBOKI, E., OURY, C., WATANABE, H., NILIUS, B., VERMYLEN, J. & HOYLAERTS, M. F. (2002) The intracellular tyrosine residues of the ATP-gated P2X(1) ion channel are essential for its function. *FEBS Lett,* 524**,** 15-9.

TOULME, E., BLAIS, D., LEGER, C., LANDRY, M., GARRET, M., SEGUELA, P. & BOUE-GRABOT, E. (2007) An intracellular motif of P2X(3) receptors is required for functional cross-talk with GABA(A) receptors in nociceptive DRG neurons. *J Neurochem,* 102**,** 1357-68.

TREZISE, D. J., MICHEL, A. D., GRAHAMES, C. B., KHAKH, B. S., SURPRENANT, A. & HUMPHREY, P. P. (1995) The selective P2X purinoceptor agonist, beta,gamma-methylene-L-adenosine 5'-triphosphate, discriminates between smooth muscle and neuronal P2X purinoceptors. *Naunyn Schmiedebergs Arch Pharmacol,* 351**,** 603-9.

UNSWORTH, C. D. & JOHNSON, R. G. (1990) Acetylcholine and ATP are coreleased from the electromotor nerve terminals of Narcine brasiliensis by an exocytotic mechanism. *Proc Natl Acad Sci U S A,* 87**,** 553-7.

VALERA, S., HUSSY, N., EVANS, R. J., ADAMI, N., NORTH, R. A., SURPRENANT, A. & BUELL, G. (1994) A new class of ligand-gated ion channel defined by P2x receptor for extracellular ATP. *Nature,* 371**,** 516-9.

VIAL, C., HECHLER, B., LEON, C., CAZENAVE, J. P. & GACHET, C. (1997) Presence of P2X1 purinoceptors in human platelets and megakaryoblastic cell lines. *Thromb Haemost,* 78**,** 1500-4.

VIAL, C. & EVANS, R. J. (2000) P2X receptor expression in mouse urinary bladder and the requirement of P2X(1) receptors for functional P2X receptor responses in the mouse urinary bladder smooth muscle. *Br J Pharmacol,* 131**,** 1489-95.

VIAL, C., ROLF, M. G., MAHAUT-SMITH, M. P. & EVANS, R. J. (2002a) A study of P2X1 receptor function in murine megakaryocytes and human platelets reveals synergy with P2Y receptors. *Br J Pharmacol,* 135**,** 363-72.

VIAL, C. & EVANS, R. J. (2002b) P2X(1) receptor-deficient mice establish the native P2X receptor and a P2Y6-like receptor in arteries. *Mol Pharmacol,* 62**,** 1438-45.

VIAL, C., TOBIN, A. B. & EVANS, R. J. (2004a) G-protein-coupled receptor regulation of P2X1 receptors does not involve direct channel phosphorylation. *Biochem J,* 382**,** 101-10.

VIAL, C., ROBERTS, J. A. & EVANS, R. J. (2004b) Molecular properties of ATP-gated P2X receptor ion channels. *Trends Pharmacol Sci,* 25**,** 487-93.

VIAL, C., RIGBY, R. & EVANS, R. J. (2006) Contribution of P2X1 receptor intracellular basic residues to channel properties. *Biochem Biophys Res Commun,* 350**,** 244-8.

VIRGINIO, C., NORTH, R. A. & SURPRENANT, A. (1998) Calcium permeability and block at homomeric and heteromeric P2X2 and P2X3 receptors, and P2X receptors in rat nodose neurones. *J Physiol,* 510 (Pt 1)**,** 27-35.

VIRGINIO, C., MACKENZIE, A., RASSENDREN, F. A., NORTH, R. A. & SURPRENANT, A. (1999) Pore dilation of neuronal P2X receptor channels. *Nat Neurosci,* 2**,** 315-21.

VIZI, E. S., LIANG, S. D., SPERLAGH, B., KITTEL, A. & JURANYI, Z. (1997) Studies on the release and extracellular metabolism of endogenous ATP in rat superior cervical ganglion: support for neurotransmitter role of ATP. *Neuroscience,* 79**,** 893-903.

VIZI, E. S. & BURNSTOCK, G. (1988) Origin of ATP release in the rat vas deferens: concomitant measurement of [3H]noradrenaline and [14C]ATP. *Eur J Pharmacol,* 158**,** 69-77.

VIZI, E. S., SPERLAGH, B. & BARANYI, M. (1992) Evidence that ATP released from the postsynaptic site by noradrenaline, is involved in mechanical responses of guinea-pig vas deferens: cascade transmission. *Neuroscience,* 50**,** 455-65.

VULCHANOVA, L., RIEDL, M. S., SHUSTER, S. J., BUELL, G., SURPRENANT, A., NORTH, R. A. & ELDE, R. (1997) Immunohistochemical study of the P2X2 and P2X3 receptor subunits in rat and monkey sensory neurons and their central terminals. *Neuropharmacology,* 36**,** 1229-42.

WALKER, J. E., SARASTE, M., RUNSWICK, M. J. & GAY, N. J. (1982) Distantly related sequences in the alpha- and beta-subunits of ATP synthase, myosin, kinases and other ATP-requiring enzymes and a common nucleotide binding fold. *EMBO J,* 1**,** 945-51.

WATANO, T., CALVERT, J. A., VIAL, C., FORSYTHE, I. D. & EVANS, R. J. (2004) P2X receptor subtype-specific modulation of excitatory and inhibitory synaptic inputs in the rat brainstem. *J Physiol,* 558**,** 745-57.

WEBB, T. E., SIMON, J., KRISHEK, B. J., BATESON, A. N., SMART, T. G., KING, B. F., BURNSTOCK, G. & BARNARD, E. A. (1993) Cloning and functional expression of a brain G-protein-coupled ATP receptor. *FEBS Lett,* 324**,** 219-25.

WEN, H. & EVANS, R. J. (2009) Regions of the amino terminus of the P2X receptor required for modification by phorbol ester and mGluR1alpha receptors. *J Neurochem,* 108**,** 331-40.

WERNER, P., SEWARD, E. P., BUELL, G. N. & NORTH, R. A. (1996) Domains of P2X receptors involved in desensitization. *Proc Natl Acad Sci U S A,* 93**,** 15485-90.

WILDMAN, S. S., BROWN, S. G., KING, B. F. & BURNSTOCK, G. (1999) Selectivity of diadenosine polyphosphates for rat P2X receptor subunits. *Eur J Pharmacol,* 367**,** 119-23.

WILDMAN, S. S., BROWN, S. G., RAHMAN, M., NOEL, C. A., CHURCHILL, L., BURNSTOCK, G., UNWIN, R. J. & KING, B. F. (2002) Sensitization by extracellular Ca(2+) of rat P2X(5) receptor and its pharmacological properties compared with rat P2X(1). *Mol Pharmacol,* 62**,** 957-66.

WILEY, J. S., DAO-UNG, L. P., LI, C., SHEMON, A. N., GU, B. J., SMART, M. L., FULLER, S. J., BARDEN, J. A., PETROU, S. & SLUYTER, R. (2003) An Ile-568 to Asn polymorphism prevents normal trafficking and function of the human P2X7 receptor. *J Biol Chem,* 278**,** 17108-13.

WU, X., LIU, D., LEE, M. H. & GOLDEN, J. W. (2004) patS minigenes inhibit heterocyst development of Anabaena sp. strain PCC 7120. *J Bacteriol,* 186**,** 6422-9.

XIONG, K., PEOPLES, R. W., MONTGOMERY, J. P., CHIANG, Y., STEWART, R. R., WEIGHT, F. F. & LI, C. (1999) Differential modulation by copper and zinc of P2X2 and P2X4 receptor function. *J Neurophysiol,* 81**,** 2088-94.

XIONG, K., LI, C. & WEIGHT, F. F. (2000) Inhibition by ethanol of rat P2X(4) receptors expressed in Xenopus oocytes. *Br J Pharmacol,* 130**,** 1394-8.

XU, M. & AKABAS, M. H. (1993) Amino acids lining the channel of the gamma-aminobutyric acid type A receptor identified by cysteine substitution. *J Biol Chem,* 268**,** 21505-8.

YAMAMOTO, K., SOKABE, T., MATSUMOTO, T., YOSHIMURA, K., SHIBATA, M., OHURA, N., FUKUDA, T., SATO, T., SEKINE, K., KATO, S., ISSHIKI, M., FUJITA, T., KOBAYASHI, M., KAWAMURA, K., MASUDA, H., KAMIYA, A. & ANDO, J. (2006) Impaired flow-dependent control of vascular tone and remodeling in P2X4-deficient mice. *Nat Med,* 12**,** 133-7.

YOUNG, M. T., FISHER, J. A., FOUNTAIN, S. J., FORD, R. C., NORTH, R. A. & KHAKH, B. S. (2008) Molecular shape, architecture, and size of P2X4 receptors determined using fluorescence resonance energy transfer and electron microscopy. *J Biol Chem,* 283**,** 26241-51.